Role of sphingosine in fungal infection

Inaugural-Dissertation

zur

Erlangung des Doktorgrades

Dr. rer. nat.

der Fakultät für

Biologie

an der

Universität Duisburg-Essen

vorgelegt von

Fahimeh Hashemi Arani

aus

Aran, Iran

2023

Die der vorliegenden Arbeit zugrundeliegenden Experimente wurden am Institut für Molekularbiologie der Universität Duisburg-Essen durchgeführt.

1. Gutachter: Priv. Doz. Dr. med. Alexander Carpinteiro
2. Gutachter: Prof. Dr. Matthias Gunzer

Vorsitzender des Prüfungsausschusses: Prof. Dr. Astrid Westendorf

Tag der mündlichen Prüfung: 8. August 2023

DOI: 10.17185/duepublico/78864
URN: urn:nbn:de:hbz:465-20230825-064815-4

Abstract

Aspergillus and *Candida* species are opportunistic fungal pathogens that cause a wide variety of infections especially in immunocompromised patients. The high risk of invasive fungal infections within the raising population of immunocompromised individuals, along with the emergence of resistance to conventional antifungal agents, requires the development of new antifungal drugs.

Sphingosine has been implicated to play many roles in bacterial and viral infections. Thus, this study aims to identify the fungicidal activity of sphingosine and provide potential therapeutic strategies.

The killing rate of *C. glabrata* and *A. fumigatus* was investigated by kinetic growth assay, demonstrating that sphingosine kills 99.99% of the fungal cells in a time and dose dependent manner, representing the high efficiency of this new fungicidal agent. In hosts with a susceptible immune system, *Aspergillus* conidia initially infect lungs, invade epithelial cells and develop an invasive aspergillosis with high lethality. In high-risk patients, prophylaxis against *aspergillus* is a valuable clinical strategy. For *in vivo* infection, a novel inhalational murine model of invasive pulmonary aspergillosis was developed and disease progression was monitored by histology, analysis of chemokine and cytokine responses in mouse lung, colony forming unit (CFU) and galactomannan immunoassay in bronchoalveolar lavage.

The results showed a significant reduction in CFU and galactomannan index in sphingosine treated-infected mice as compared to infected untreated mice. The histological evidence supports the effectiveness of the sphingosine in the control of invasive aspergillosis without cytotoxicity. Prophylactic treatment with nebulized sphingosine starting 3 days before *Aspergillus* infection for up to 14 days resulted in 100% survival and in resolution of the infection, whilst placebo inhaled mice had a lethality/reaching of the dropout burden of 50%.

Mechanistic studies showed that treatment with sphingosine leads to the early depolarization of the mitochondrial membrane potential ($\Delta\Psi m$) and the generation of mitochondrial reactive oxygen species follow by release of cytochrome *c*, thereby initiating apoptosis.

Taken together, this study reveals the *in vitro* and *in vivo* efficacy of sphingosine and its mode of action against fungi via a direct effect on mitochondria. Moreover, because of its very good tolerability and ease of application, inhaled sphingosine should be

further developed as a possible prophylactic agent against pulmonary aspergillosis among severely immunocompromised patient.

Zusammenfassung

Aspergillus- und *Candida*-Arten sind opportunistische Pilzerreger, die insbesondere bei immungeschwächten Patienten eine Vielzahl von Infektionen verursachen. Das hohe Risiko invasiver Pilzinfektionen in der zunehmenden Population immungeschwächter Personen sowie das Auftreten von Resistenzen gegen herkömmliche Antimykotika machen die Entwicklung neuer Wirkstoffe erforderlich.

Sphingosin wird bei bakteriellen und viralen Infektionen eine wichtige Rolle zugeschrieben. Ziel dieser Studie ist es daher, die fungizide Wirkung von Sphingosin zu ermitteln und mögliche therapeutische Strategien zu entwickeln.

Die Abtötungsrate von *C. glabrata* und *A. fumigatus* wurde mittels eines kinetischen Wachstumstests untersucht. Dabei zeigte sich, dass Sphingosin 99.99% der Pilzzellen zeit- und dosisabhängig abtötet, was die hohe Effizienz dieses neuen fungiziden Wirkstoffs belegt.

In Wirten mit einem anfälligen Immunsystem infizieren *Aspergillus*-Konidien zunächst die Lunge, dringen in Epithelzellen ein und entwickeln eine invasive Aspergillose mit hoher Letalität. Bei Hochrisikopatienten ist die Prophylaxe gegen *Aspergillus* eine wertvolle klinische Strategie. Für die *In-vivo*-Infektion wurde ein neuartiges inhalatives Mausmodell der invasiven pulmonalen Aspergillose entwickelt und der Krankheitsverlauf durch Histologie, Analyse der Chemokin- und Zytokinreaktionen in der Mauslunge sowie *Colony-fomrming-units* (CFU) und Galaktomannan-Immunoassay in der bronchoalveolären Lavage überwacht.

Die Ergebnisse zeigten eine signifikante Verringerung der CFU und des Galaktomannan bei mit Sphingosin behandelten infizierten Mäusen im Vergleich zu infizierten unbehandelten Mäusen. Histoligische Untersuchungen untermauerten die Wirksamkeit von Sphingosin gegen invasive Aspergillose ohne Hinweise auf Toxizität.

Eine prophylaktische Behandlung mit inhalativem Sphingosin, die 3 Tage vor der *Aspergillus*-Infektion begann und bis zu 14 Tage andauerte, führte zu einer 100%igen Überlebensrate und zum Abklingen der Infektion, während bei Mäusen, die mit Placebo inhaliert wurden, die Letalität bzw. das Erreichen der Abbruchrate bei 50% lag.

Mechanistische Untersuchungen zeigten, dass die Behandlung mit Sphingosin zu einer frühen Depolarisierung des mitochondrialen Membranpotenzials ($\Delta\Psi m$) und zur Bildung mitochondrialer reaktiver Sauerstoffspezies führt, gefolgt von der Freisetzung von Cytochrom *c*, wodurch die Apoptose eingeleitet wird.

Insgesamt zeigt diese Studie die *In-vitro*- und *In-vivo*-Wirksamkeit von Sphingosin und seine Wirkungsweise gegen Pilze über eine direkte Wirkung auf Mitochondrien. Darüber hinaus sollte inhaliertes Sphingosin aufgrund seiner sehr guten Verträglichkeit und einfachen Anwendung als mögliches prophylaktisches Mittel gegen pulmonale Aspergillose bei stark immungeschwächten Patienten weiterentwickelt werden.

Contents

List of Abbreviations

°C	Degree Celsius
µg	Microgram
µL	Microliter
µm	Micrometer
µM	Micromolar
A	
A.	*Aspergillus*
Ab	Antibody
ABPA	Allergic Bronchopulmonary Aspergillosis
AEC	Alveolar epithelial cell
AFST	Antifungal susceptibility testing
AIDS	Acquired Immune Deficiency Syndrome
AIF	Apoptosis-inducing factors
AM	Alveolar macrophage
AMB	Amphotericin B
ANOVA	Analysis of variance
Asm	Acid sphingomyelinase
ATCC	American Type Culture Collection
ATP	Adenosine triphosphate
B	
BAL	Bronchoalveolar lavage
Bl6	C57BL/6
BSA	Bovine serum albumin
C	
C.	*Candida*
CARD	Caspase recruitment domain
CDase	Ceramidase
CERT	Ceramide transfer
CF	Cystic fibrosis
CFG	Caspofungin
CFU	Colony forming unit
CLSI	Clinical Laboratory Standards Institute

Conc.	Concentration
CV	Cristal violet
D	
DAPI	4',6-diamidino-2-phenylindole
dATP	Deoxy ATP
DCFHDA	Diacetyldichlorofluorescein
DCs	Dendritic cells
DED	Death-inducing domain
DF	Dilution factor
DISC	Death-inducing signal complex
DMEM	Dulbecco's Modified Eagle Medium
DMSO	Dimethyl sulfoxide
DNA	Deoxyribonucleic acid
DNase	Deoxyribonuclease
DSM	Deutsche Sammlung von Mikroorganismen
DTT	Dithiothreitol
E	
EUCAST	European Committee on Antimicrobial Susceptibility Testing
EDTA	Ethylenediaminetetraacetic acid
ELISA	Enzyme-linked immunosorbent assay
EPS	extracellular polymeric substances
ER	Endoplasmic reticulum
EtOH	Ethanol
F	
5-FC	Flucytosine
5-FU	5-fluorouracil
F12-K	Kaighn's Modification of Ham's F-12 Medium
FACS	Fluorescence-activated single cell sorting
FBS	Fetal Bovine Serum
FLC	Fluconazole
G	
G-CSF	Granulocyte-colony stimulating factor
GC	Growth control

GCase	Glucosylceramidas
GlcNAc	*N*-acetylglucosamine
GPI	Glycosylphosphatidylinositol
H	
h	Hours
H_2DCFDA	Cell-permeant 2',7'-dichlorodihydrofluorescein diacetate
HBSS	Hanks' Balanced Salt Solution
HCL	Hydrogen chloride
HEPES	4-(2-hydroxyethyl)-1-piperazineethanesulfonic acid
HIV	Human immunodeficiency virus
HPLC	High Performance Liquid Chromatography
HRP	Horseradish peroxidase
I	
IA	Invasive Aspergillosis
IFI	Invasive fungal infection
IFN-γ	Interferon-γ
IL	Interleukin
IP	Intraperitoneal
IPA	Invasive pulmonary aspergillosis
IPC	Inositol phosphoceramide
ITZ	Itraconazole
IV	Intravenous
K	
kg	Kilogram
KOH	Potassium hydroxide
L	
LCMS	Liquid chromatography mass spectrometry
LCB	Long-chain base
LL/2	Lewis lung carcinoma
Ln	Log base 10
LPS	Lipopolysaccharide
M	
M	Molar

m/z	Mass-to-charge ratio
mA	Milliampere
MBEC	Minimal biofilm eradication concentration
MCC	Mucociliary clearance
MEM	Minimum Essential Medium
MFC	Minimum fungicidal concentration
mg	Milligram
MIC	Minimal Inhibitory Concentration
MIPC	Mannose inositol phosphoceramide
mL	Milliliter
mM	Millimolar
MMP	Mitochondrial membrane potential
MOPS	3-(*N*-morpholino) propanesulfonic acid
MP	Multiphoton
MPO	Myeloperoxidase
MPT	Mitochondrial permeability transition
MTL	Mating type-like
MtOH	Methanol
MTT	3-(4,5-dimethylthiazol-2-yl)-2,5-diphenyltetrazolium bromide
MW	Molecular weight
N	
n. s	Not significant
NaN_3	Sodium azide
NaOH	Sodium hydroxide
NLRP	NACHT, LRR and PYD Domains-Containing Protein
nm	Nanometer
No.	Number
NOD	Nucleotide-binding oligomerization domain
O	
OGP	Octyl-beta-D-glucopyranoside
O_2	Oxygen
O_2^-	ROS superoxide
OD	Optical density

OD_C	Optical density cut-off
P	
PAMPs	Pathogen-associated molecular patterns
PAS	Periodic acid–Schiff
PBS	Phosphate Buffered Saline
PCR	Polymerase chain reaction
PE	Polyethylene
PFA	Paraformaldehyde
PI	Propidium iodide
PSI	Pounds per square inch
PVDF	Polyvinylidene difluoride
Q	
qPCR	Quantitative PCR
R	
RCF	Relative centrifugal force
Rh-123	Rhodamine 123
RNA	Ribonucleic acid
ROS	Reactive oxygen species
RP-HPLC	Reversed phase HPLC
RPM	Round per minute
RPMI	Roswell Park Memorial Institute medium
RT	Room temperature
S	
S1P	Sphingosine-1-phosphate
SD	Standard deviation
SDA	Sabouraud Dextrose Agar
SDS	Sodium dodecyl sulfate
SDS-PAGE	SDS polyacrylamide gel electrophoresis
SK	Sphingosine kinase
Smpd1	Sphingomyelin Phosphodiesterase 1, murine
SMPD3/Smpd3	Sphingomyelin Phosphodiesterase 3
SMS	Sphingomyelin synthase
SPH	Sphingosine

SphK	Sphingosine kinase
Spp.	Species
T	
t-test	Hypothesis test statistic
TBHP	Tert-butyl hydrogen peroxide
TBS	Tris-buffered saline
TBST	Tris-buffered saline with 0.1% Tween
TCR	T-cell receptor
TEMED	Tetraacetylethylenediamine
TFA	Trifluoroacetic acid
TLC	Thin-layer chromatography
TMB	3,3', 5,5; -tetramethylbenzidine
TNF-α	Tumor necrosis factor-alpha
TUNEL	Terminal deoxynucleotidyl transferase biotin-dUTP nick end labeling
U	
UDP	uridine diphosphate
UV	Ultraviolet
V	
v/v	Volume per volume
V	Volt
VLCFAs	Very long-chain fatty acids
vol.	Volume
W	
W	Watt
w/v	Weight in volume
w/w	Weight per weight
Wt.	Wild-type
X	
XTT	2,3-Bis-(2-Methoxy-4-Nitro-5-Sulfophenyl)-2H-Tetrazolium-5-Carboxanilide
Y	
YPD	Yeast extract peptone dextrose

List of Figures

List of Tables

1. Introduction

1.1 *Candida* spp.

Candida spp. are opportunistic fungal pathogens that colonize the gastrointestinal tract of healthy individuals in balance with different bacteria (e.g. *Lactobacillus acidophilus, Streptococcus faecalis, Escherichia coli*). Besides being a normal part of the gastrointestinal flora, *C. albicans* is able to colonize in nearly every human tissue and organ, causing serious, invasive infections susceptible, immunosuppressed patients. Therefore, it is the predominant isolated yeast species from blood cultures and tissue samples.

However, in the 1990s, an epidemiological transition to non-*albicans Candida* spp., such as *C. glabrata, C. dubliniensis, C. tropicalis, C. parapsilosis* and *C. krusei* has been seen (Hobson, 2003; Krcmery & Barnes, 2002; Zepelin et al., 2007) and was associated to the overuse of antimycotics especially triazoles (Girmenia et al., 1998).Among these non-*albicans Candida* spp. *C. glabrata* is considered as the most important pathogen. *C. glabrata* is an asexual, nondimorphic, haploid fungus, which reproduces exclusively by budding. It belongs to the ascomycetes and not to the deuteromycetes (without sexual state in their life cycle). This is, because *C. glabrata* has the genetic prerequisites to mate. It possesses three mating type-like (*MTL)* loci (*MTL1*, *MTL2*, and *MTL3*). The same configuration found at the mating type loci of *Saccharomyces cerevisiae* and it was shown that *C. glabrata* switches between the *MTL1a* and *MTL1α* genotypes *in vivo* (Haber, 2003).

C. glabrata cells can persist on environmental surfaces like rotten fruits for several months, but it can also grow on artificial surfaces like urinary and vascular catheters, prosthetic valves, and pacemakers and forms biofilms (Iraqui et al., 2005). On the other hand, *C. glabrata* is an opportunistic human fungal pathogen that causes superficial mucosal and life-threatening bloodstream infections in individuals with a compromised immune system. It is considered as a second most common cause of systemic candidiasis in immunocompromised patients after *C. albicans* (Pfaller et al., 1998; Vazquez et al., 1998). The most *C. glabrata* infections arise from the host's endogenous microflora. In Germany, epidemiological data on yeast cultures obtained from primarily sterile sites of patients displayed that *C. albicans* is the most frequently isolated species (58.5%), follow by *C. glabrata* (19.1%), *C. parapsilosis* (8.0%) and *C. tropicalis* (7.5%) (Zepelin et al., 2007).

As reviewed by Pfaller, *2012, C. glabrata* infections are especially difficult to treat due to a high intrinsic resistance against antifungals, particularly against azoles. Research in Germany has revealed that around 93% of *C. albicans* but only 23% of *C. glabrata* isolates are fully susceptible to treatment with Fluconazole. However, despite being the second leading cause of invasive candidiasis in humans, the underlying molecular bases of resistance mechanisms in *C. glabrata* are far less investigated. The difficulties in treating *C. glabrata* infections motivate the researchers to put effort into the molecular dissection of the pathogen. The identification of antifungal drug targets and resistance mechanisms together with a better understanding of its molecular structure and function (e.g. in respect to signal transduction pathways, transporter proteins, receptors and cell wall organization) might lead to successful strategies to treat *C. glabrata* infections (Pfaller, 2012).

1.1.1 Biofilm formation

One of the specific virulence factors of *Candida* species is their capacity to form biofilms on abiotic or biotic surfaces, which exhibit resistance to antifungals as well as host immune responses. Fungus cells in this form of community behave significantly differently from planktonic cells, exhibiting slower growth rates and higher resistance to antifungal treatment (Donlan, 2001). Fungal biofilms are communities of microorganisms attached to medical devices such as urinary and vascular catheters, dentures, prosthetic heart valves and joint replacements or different living tissues in the host, producing extracellular polymeric substances (EPS), known also as extracellular matrix (ECM) and hindering the eradication of *Candida* infections (Elving et al., 2016; Lewis, 2001; Potera, 1999). *Candida* biofilms are formed mostly in the mucosa or endothelium being involved in the development of common candidiasis, such as vaginal and oral candidiasis (Nett, 2016). Likewise, each *Candida* species exhibit differences in terms of biofilm formation, especially at the level of their morphology, characteristics of the extracellular matrix (ECM), ability to confer antifungal resistance, and in the dependency of surface and host niche. This biofilm variability rises the challenge of identifying an effective solution to tackle the threats of *Candida* biofilms as a unique issue. The comparative schematics the three stages of biofilm formation by *Candida albicans*, *Candida glabrata*, *Candida tropicalis,* and *Candida parapsilosis* are shown in Figure 1.

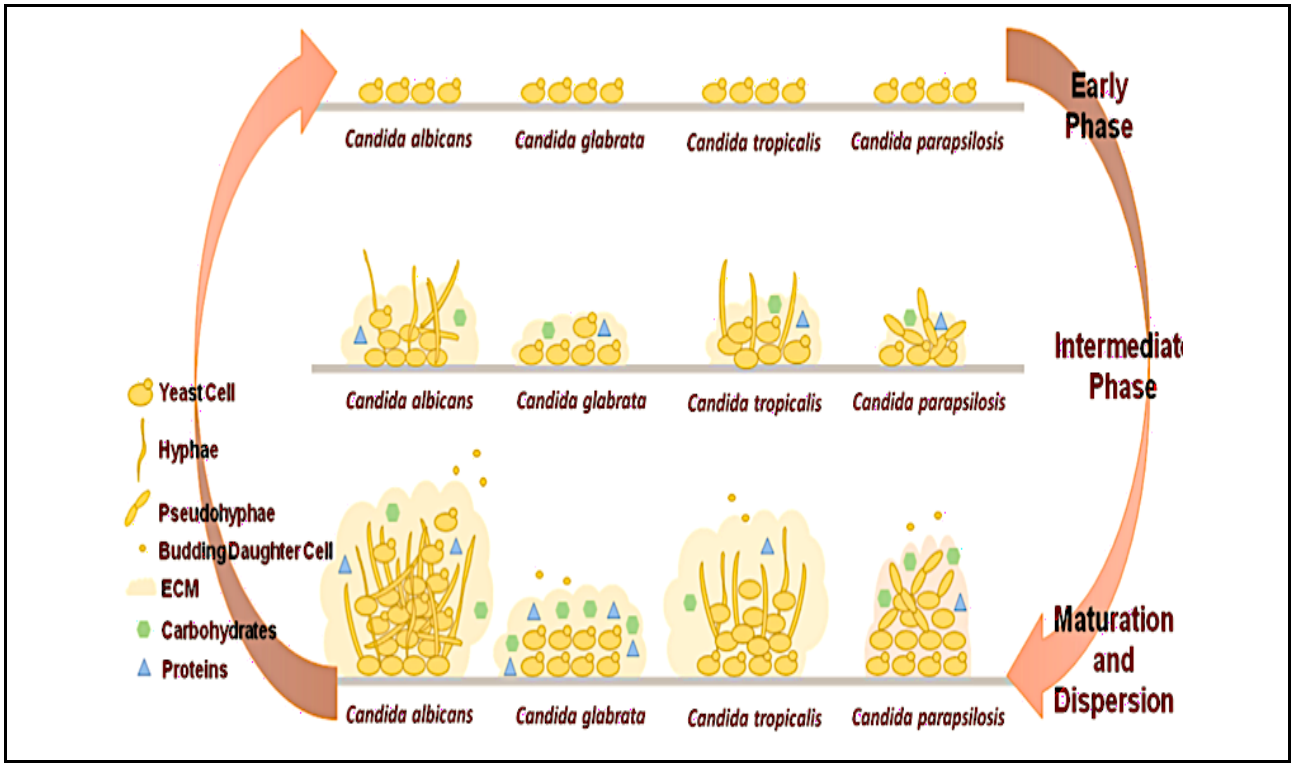

Figure 1. Comparative schematics the three stages of biofilm formation. *Candida albicans, Candida glabrata*, *Candida tropicalis*, and *Candida parapsilosis* show the variety of possible architectures, adhesion properties, cellular morphologies and extracellular matrix (ECM) composition. Adapted from Cavalheiro & Teixeira, 2018.

Biofilm formation of yeast occurs through specific steps which can be summarized as follow: initial adhesion, formation of microcolony, cell organization and production of extracellular polymeric substances and finally biofilm maturation and dispersion. Adhesion is the important initial stage in the development of biofilms. This process relies on a group of cell wall proteins known as adhesins that, by adhering to certain amino acid or sugar residues, facilitate the attachment to other cells—both epithelial and other microbial cells—or abiotic surfaces. Generally, adhesins are glycosyl-phosphatidylinositol-cell wall proteins (GPI-CWPs), comprising a GPI anchor, a serine/threonine domain and a carbohydrate or peptide binding domain (Verstrepen & Klis, 2006). The EPA (epithelial adhesion) family of adhesins is primarily responsible of adherence in *C. glabrata.* Following adhesion, biofilm formation continues through morphologic changes, an increase in cell population, and the generation of extracellular polymeric substances (EPS), which all have an impact on the final biofilm architecture. EPS components allow the maturation of a three-dimensional structure, forming the biofilm in the maturation phase. After biofilm maturation, there is still the possibility of dissemination of progeny biofilm cells that become detached spreading to other niches to form more biofilm (Chandra & Mukherjee, 2015). As shown in Figure 1 *C. albicans* mature biofilms are more

confluent than the ones of other *Candida* species and exhibit a more heterogenous structure, composed by oval budding, continuous septate hyphae and pseudo hyphae in infected tissues surrounded by a thick layer of ECM of polysaccharide material (Chandra et al., 2001; Douglas, 2003). The ECM acts as a barrier between the cells in the biofilm and the surrounding environment as well as a structural framework for attachment between cells and with other surfaces (Mitchell et al., 2016). *C. albicans* is also considered to be the strongest biofilm producer among the *Candida* spp. (Kuhn et al., 2002). When it comes to *C. glabrata*, the biofilm is exclusively composed by yeast form cells in multilayer structure that are closely packed and ECM with high levels of carbohydrates and proteins (S. Silva et al., 2009). These variations demonstrate the diversity of the biofilm development processes and possible architectures and the challenge of developing a novel method to completely eliminate all *Candida* biofilms. Several more extrinsic factors related to the biofilm surrounding environment also have an impact on the final biofilm formed, which increase the complexity of this challenge.

1.2 *Aspergillus* spp.

Aspergillus spp. as opportunistic fungi can cause a wide range of clinical syndromes, from allergic bronchopulmonary aspergillosis to fatal angioinvasive infections. There are about 180 species in the genus, but only 33 of them are associated with human disease (Hope et al., 2005). Colonies of aspergilli may be black, brown, yellow, red, white, green, or other colors depending on the species and the growth conditions.

A. fumigatus is the species of *Aspergillus* that causes human diseases most frequently and less commonly infections are due to *A. niger, A. terreus* and *A. flavus* (de Pauw et al., 2008). *A. fumigatus* is a common, ubiquitous, saprophytic fungus with its natural niche in soil that plays an important part in carbon and nitrogen recycling. The organism can be found widespread in nature (in soil, on decaying vegetation, in the air, and in water supplies). Conidia, the spores of *A. fumigatus,* have a diameter of 2 to 3.5 μm (Pasqualotto, 2009), which has a crucial role in pathogenicity. The small size of conidia in *A. fumigatus* helps it to reach the pulmonary alveoli easily via nose or mouth whereas other human fungal pathogens such as *A. niger* and *A. flavus* with larger conidia can be more easily removed by clearance in the upper respiratory tract. Once the conidia reach the alveoli, they germinate and produce hyphae-the vegetative form that has tropism for blood vessels (Lopes Bezerra & Filler, 2004) and trigger powerful immunological reactions.

A. fumigatus conidia have a very low weight and are hydrophobic (Pasqualotto, 2009), which is crucial for their diffusion in the environment as well as for protecting them from extreme environmental conditions like freezing and desiccation. According to surveys, each person is in contact with hundreds of these conidia every day (Chazalet et al., 1998), yet a healthy person's innate immune system can effectively keep them under control. Advances in medical treatment of many cancers and autoimmune diseases or receiving immunosuppressive drugs due to solid organ transplantation increase the patient population at risk for life threatening *Aspergillus* infections (Rogers, 1995). Initially, *A. fumigatus* was known as an important opportunistic fungal pathogen causing farmer's lung disease, which is an allergic reaction to conidia in case of unusually heavy contact with organic debris. Further studies have shown that it causes variety of diseases that fall into three categories: (1) chronic cavitary aspergillosis in individuals with normal immune systems, (2) invasive aspergillosis in patients with suppressed immune systems, (3) allergic reaction to inhaled conidia in persons with hyperactive immune responses (Daly & Kavanagh, 2001).

1.2.1 The life cycle of *Aspergillus*

Three processes of reproduction are recognized in *A. fumigatus*: asexual, sexual, and parasexual reproduction cycle (Verweij et al., 2016), which are summarized in Figure 2.

Asexual reproduction: The asexual cycle in *A. fumigatus* begins with the formation of a network of hyphae when single haploid conidia germinates under certain environmental conditions. Asexual reproduction and spore generation are borne on specialized stalks called conidiophores. These dormant spores are also produced sexually (ascospores) from asci (sac-like structures usually containing 2 to 8 ascospores and often formed within a fruiting body such as cleistothecium). The vegetative hyphal cells differentiate into aerial hyphae with a foot cell and eventually a specialized reproductive structure known as a conidiophore after a few days of germination. These conidiogenous cells undergo further mitosis, which results in a large number of unicellular, uninucleate, and asexual spores arranged in long chains called conidia. After couple of days, a single spore might produce up to 10^9 asexual spores in suitable conditions and spread over a large geographic region. Figure 2 (orange cycle) shows the infectious life cycle of *Aspergillus*, which starts with the production of conidia (Falvey & Streifel, 2007; Morris et al., 2000).

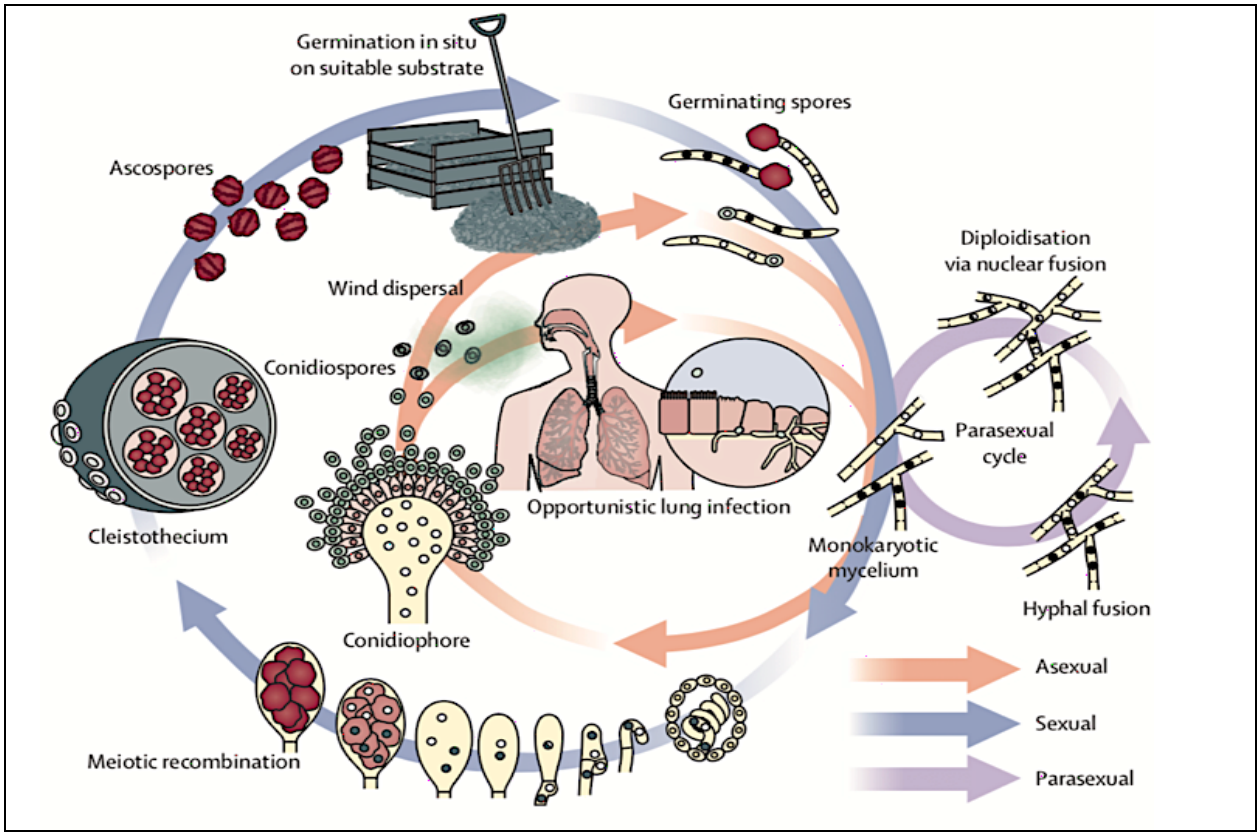

Figure 2. Schematic image of reproduction process in *A. fumigatus*. Asexual reproduction (orange line), sexual reproduction (blue line), and parasexual recombination (purple line). Adapted from Verweij et al., 2016.

Sexual reproduction*:* Sexual reproduction is a crucial strategy to enhance fungal genetic diversity and requires two parental strains of opposite mating type (*MAT1-1* and *MAT1-2*) (de Pauw et al., 2008). After fertilization, a fruiting body (cleistothecium) is generated. It contains around 10^4 sexual spores originated from the same zygote which have been hypothesized to enhance survival during adverse environmental conditions. The precise function of ascospores in the life cycle of *A. fumigatus* is still unknown. The sexual, in addition to the asexual reproduction is considered as a cycle which can facilitate adaptation to new or changing environments such as azole-containing environment (McDonald et al., 2016; Zhang, Snelders, et al., 2017; Zhang, van den Heuvel, et al., 2017) and it can take several months to complete under specific laboratory conditions.

1.3 Fungal cell wall composition

The fungal cell wall is located outside the plasma membrane. The cell wall is a dynamic structure that mediates all of the interactions between cell and environment since some of its proteins are adhesins and receptors(Garcia-Rubio et al., 2020). This organelle with

high plasticity is also essential for cell growth, cell division, and formation of hyphae or conidia during the fungal life cycle and protects fungi from osmotic pressure and other environmental stresses. Disruption of fungal cell walls make them very susceptible to lysis and death (Bowman & Free, 2006). The fact that almost one-fifth of the fungal genome is devoted to the biosynthesis of the cell wall, provides an indication of its importance. The basic components of the fungal cell wall are polysaccharides like chitin, glucan, mannan and glycoproteins which, when cross-linked together, create a complex network that provides the fungal cell wall's structural characteristics (Figure 3).

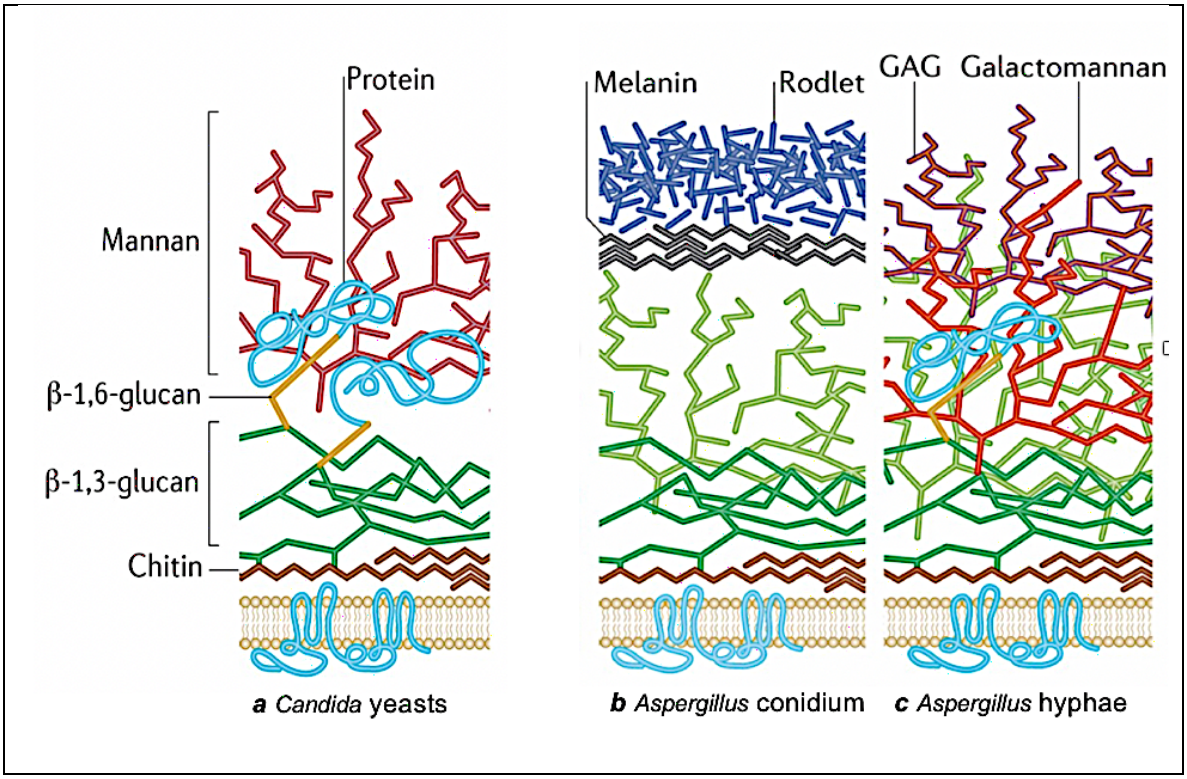

Figure 3. The structure of the fungal cell wall. The schematic images of the cell wall components and their interconnections are shown. The outer layer of cell wall in *Candida* spp. Consists of pro-inflammatory O-linked mannans, N-linked mannans and phosphorylated mannans (**a**). The cell wall in *Aspergillus* conidia comprises predominantly an immunologically inert outer hydrophobin rodlet layer and an inner melanin layer (**b**), whereas the hyphae of *A. fumigatus* have a typical inner cell wall composition along with α-1,3-glucan, galactomannan and galactosaminoglycan (GAG) in the outer cell wall (**c**). Adapted from Erwig & Gow, 2016.

1.4 Antifungal mechanisms

Current available antifungal candidates are divided into several groups according to their molecular targets. These targets are enzymes and other molecules involved in cell wall synthesis, plasma membrane synthesis, fungal DNA and protein synthesis, cellular

function-related, and virulence factors. Some mechanisms of action are explained below, and an overview is presented in Figure 4.

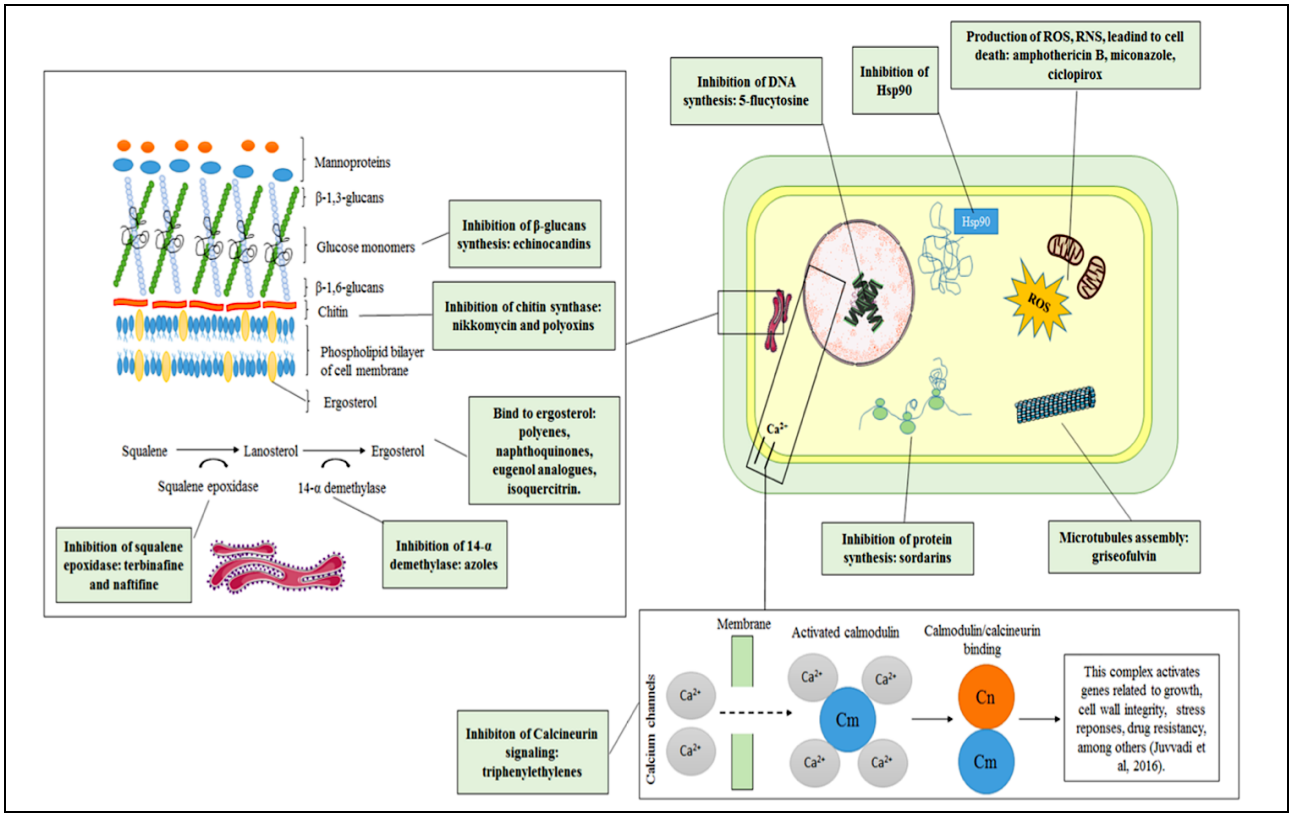

Figure 4. Old and new targets as antifungal candidates. Adapted from Scorzoni et al., 2017.

1.4.1 Cell wall

The components of fungal cell wall such as chitin, glucans, mannans, and glycoproteins are comprehensively described above (1.3). Inhibition of chitin and β-glucan synthesis are two main mechanisms of antifungal activities in the cell wall. The echinocandin class of drugs, represented by caspofungin target the protein complex responsible for the synthesis of β-1, 3 glucans by blocking the enzyme glucan synthase (Odds et al., 2003). This blockage causes a reduction in the integration of glucose residues binding β-1,3 and β-1,6 glucans, as a result weakening the cell wall and leading to fungal cell lysis (J. C. Song & Stevens, 2015). As explained before (section 1.3.1), Chitin as a β-1-4-linked *N*-acetylglucosamine polymer, is present in very small quantities in yeasts but in considerable amounts in filamentous fungi. Chitin synthase enzyme which is responsible for chitin synthesis and elongation is an attractive target for nikkomycin and polyoxins.

1.4.2 Ergosterol

Ergosterol (ergosta-5, 7, 22-trien-3β-ol), a sterol presented in cell membranes of fungi, is responsible for membrane fluidity as well as cell permeability. Furthermore, it is an essential molecule for the function of fungal integral membrane proteins and cell viability (Leber et al., 2003; J. Song et al., 2016; Tatsumi et al., 2013). Ergosterol is the target for several antifungal drugs. These antifungals either inhibit ergosterol biosynthesis or bind to it. As a result, pores are generated in the plasma membrane.

The mechanism of action of azole family such as imidazole and triazole, is based on the inhibition of ergosterol biosynthesis via the cytochrome P450 enzyme from family 51 (CYP51 or sterol 14*α*-demethylase), which catalyzes the conversion of lanosterol to ergosterol. Inhibition of fungal cytochrome P450 leads to blockage of ergosterol synthesis, sterol depletion from the membranes, and accumulation of 14α-methylated precursors. The allylamine class of antifungals includes terbinafine and naftifine, inhibits the enzyme squalene epoxidase, which results in a reduction in ergosterol and an elevation in squalene within the fungal cell membrane. Polyenes, such as nystatin and amphotericin B, bind to ergosterol, causing leakage of monovalent ions as well as other cytoplasmic contents (Baginski & Czub, 2009; Odds et al., 2003; Walsh et al., 2008). Polyene can also involve a cascade of oxidation reactions and interacts with lipoproteins in cytoplasmic membrane. This may impair membrane permeability through the release of free radicals (Mesa-Arango et al., 2014; Sangalli-Leite et al., 2011).

1.4.3 Nucleic acid, protein, and microtubule syntheses

Flucytosine (5-FC) is a synthetic antimycotic compound that inhibits nucleic acid synthesis. It is converted into 5-fluorouracil (5-FU) by the enzyme cytosine deaminase, and then further to 5-fluorouridylic acid by UMP pyrophosphorylase (Odds et al., 2003). This acid is incorporated into fungal RNA in place of uridylic acid, resulting in premature chain termination and inhibition of both RNA and DNA synthesis (Odds et al., 2003; Polak & Scholer, 1975). The combination of amphotericin B and 5-FC is used to treat severe systemic mycoses, such as candidiasis, chromoblastomycosis and aspergillosis. Griseofulvin which is used to treat skin infections such as jock itch and athlete's foot, inhibits nuclear acid synthesis as well as fungal cell mitosis by blocking the cell-cycle progression at G2/M and affecting the mitotic spindle microtubule (MT) function (Panda et al., 2005). The sordarins are the most important family of antifungal agents, which

suppress protein synthesis by stabilizing the ribosome/Elongation Factor 2 (eEF2) complex. The large ribosomal subunit protein rpP0 is another target of sordarins(Botet et al., 2008). Therefore, among other antifungals, sordarin has a highly specific binding site, which may also be the basis for the greater selectivity of these compounds in inhibiting fungal, but not the mammalian, protein synthesis.

1.4.4 Reactive oxygen species (ROS)

Reactive oxygen species (ROS) are generated during mitochondrial oxidative metabolism as well as in cellular response to xenobiotics, oxidants, UV light, bacterial invasion or other external stimuli, causing damage to proteins, lipids and DNA and leading to apoptosis and death. It is well known that some antifungal drugs, such as amphotericin B and itraconazole, can have multiple effects on fungus cells (Ferreira et al., 2013; Mesa-Arango et al., 2014). ROS production by amphotericin B is a crucial factor that is correlated with its fungicidal effect(Ferreira et al., 2013; Mesa-Arango et al., 2014).

1.5 Fungal diseases and host defense

1.5.1 Candidiasis

Candidiasis is a broad term that refers to cutaneous, mucosal and deep-seated organ infections caused by fungi of the *Candida* genus. It can occur most commonly as a superficial infection on skin and mucosa in immunocompromised hosts. Oral candidiasis, also known as oral thrush, is one of the most common fungal infections, affecting the oral mucosa. It appears as white or erythematous lesions (Millsop & Fazel, 2016).

Invasive candidiasis originates from the patient's own flora: when *Candida* introduced into bloodstream (that is, candidemia) or deep tissue (intra-abdominal abscess, peritonitis or osteomyelitis), it causes severe and life-threatening invasive candidiasis, especially in immunosuppressed hosts (Figure 5). The majority of invasive infections are caused by *C. albicans*, *C. glabrata*, *C. krusei*, *C. parapsilosis* and *C. tropicalis*.

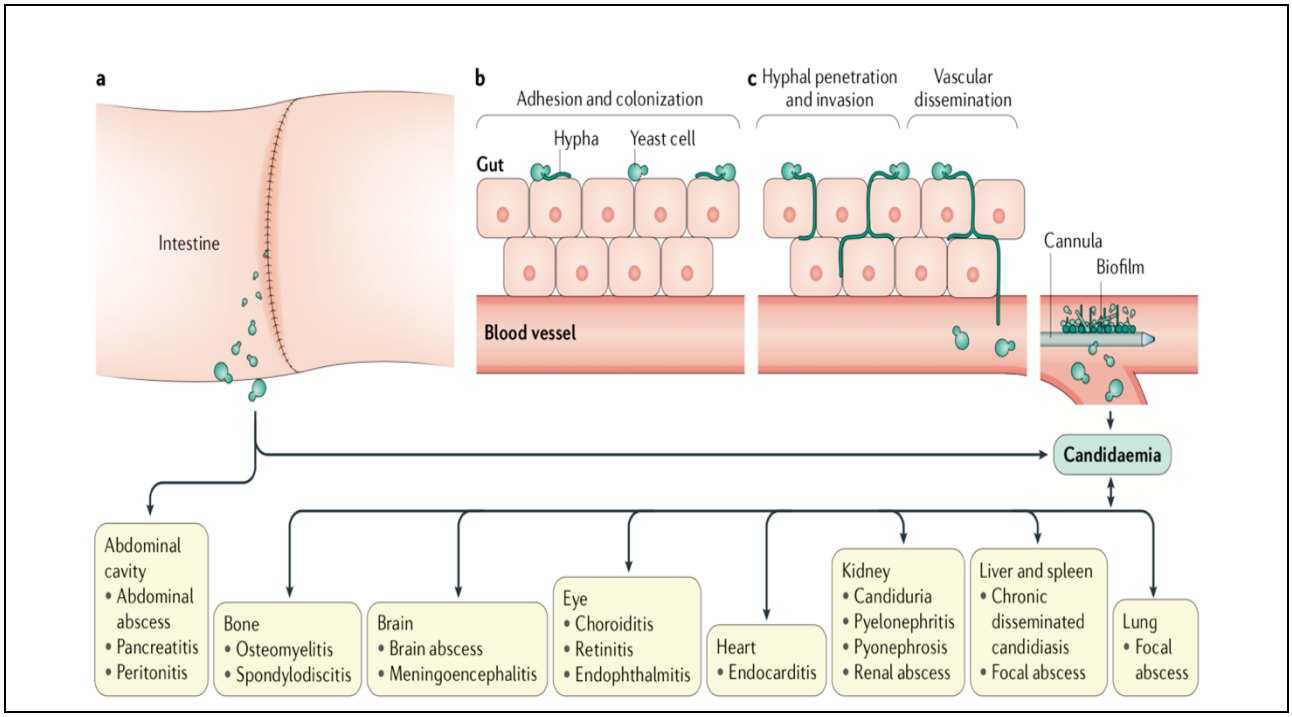

Figure 5. Pathogenesis of invasive candidiasis. (**a**) On the mucosal surface of 50-70% of healthy individuals, *Candida* spp. can be found after gastrointestinal surgery or other breaches in the intestinal barriers, *Candida* spp. can spread quickly to the abdominal cavity and invade the bloodstream (candidemia). (**b**) *Candida* spp. behave as a commensal organism without pathogenicity in healthy normal gastrointestinal tracts and/or skin. (**c**) Impaired immune system, between other factors, can lead to fungal overgrowth in the gut and candidemia. Consequently, *Candida* can get into the bloodstream and spreads to other organs (invasive candidiasis). Adapted from Pappas et al., 2018.

1.5.2 Host defense mechanisms against *Candida* infection

The human body is protected against pathogens and harmful substances through the immune system. To function properly, an immune system needs to distinguish the foreign antigens from its own healthy cells and respond to them. Some pathogens, especially viruses, can quickly evolve and adapt; thereby avoid immune sensing. However, several defense mechanisms have evolved to recognize the pathogens. These immune systems are made up two parts: the innate and adaptive responses. The innate immune system known as the "nonspecific" immune system, is the body's first line of human defense against foreign substances entering the body. The adaptive immune system takes over if the innate immune system is not able to destroy the pathogens. It is slower but more accurate than the innate immune system, because it first needs to identify the germ. It also creates an immunological memory after the initial response to the pathogen, so the next time the adaptive immune system can have a faster and stronger response to encounter with the known pathogen.

1.5.2.1 *Candida* spp. recognition

The initial stage in developing an effective anti-*Candida* immune response is recognition of extracellular or intracellular pathogen-associated molecular patterns (PAMPs) of fungal cell by the innate immune system. Membrane-bound pattern recognition receptors (PRRs) are proteins expressed, mainly, by cells of the innate immune system, such as myeloid phagocytes, to identify various PAMPs of *Candida* yeast and filamentous forms (G. D. Brown, 2011; Netea et al., 2006). Toll-like receptors (TLRs), mannose receptor, C-type lectin receptors (CLRs), nucleotide- binding oligomerization domain (NOD)-like receptors, retinoid-inducible gene 1 protein (RIG1, encoded by RARRES3)-like receptors, complement components and receptors are among the PRRs shown to recognize different fungal PAMPs including mannan, ß-glucan, RNA, and DNA (G. D. Brown, 2011; Hardison & Brown, 2012; LeibundGut-Landmann et al., 2012; Lionakis, 2014). *Candida* also activates the inflammasome; such as NLRP3 (NACHT, LRR and PYD domains-containing protein 3) and NLRP10, which are multiprotein intracellular complexes. Inflammasomes regulate activation of inflammatory responses and production of protective pro-inflammatory cytokines such as IL-1β, IFN-γ and IL-17(Gringhuis et al., 2012; Gross et al., 2009; Joly et al., 2012). Determining how *Candida* recognition is integrated by the variety of various PRRs *in vivo* will be challenging for future studies. In addition, more research is needed to find out how *Candida* influences its recognition *in vivo* by employing immune evasion strategies; for example, during infection of mice, β-glucan is masked initially but becomes exposed later in infected mouse tissue(Alexander et al., 2013), thus preventing CLR-mediated pathogen recognition during the early phase of invasive candidiasis, when recruitment of Cells of the adaptive immune system is important for survival (Vincent et al., 2009).

1.5.2.2 Neutrophils

Neutrophils represent the first line of innate immune defense against invasive candidiasis in mice, and low level of neutrophils (Neutropenia) increase the risk factor of infection and mortality in humans (Lionakis & Netea, 2013; Uzun et al., 2001). Some studies have shown that early neutrophil recruitment to the site of infection is of critical importance for *Candida* spp. clearance (Romani et al., 1997). In mouse tissues, such as the liver and spleen, that recruit large numbers of neutrophils within the first 24 hours post-infection, *Candida* spp. growth can be successfully controlled, whereas the delayed trafficking of neutrophils into the *Candida* spp.-infected organ is associated with increased fungal

evasion as well as ineffective renal host defense (Lionakis et al., 2011). Assembly of the NADPH oxidase complex at the phagosome membrane and reactive oxygen species (ROS) generated by NADPH oxidase play an important role in oxidative *Candida* spp. killing (Reeves et al., 2002; Segal et al., 2000). Indeed, impaired NADPH oxidase and myeloperoxidase activity in mice and human neutrophils can develop invasive candidiasis (Lehrer, 1970; Segal et al., 2000).

1.5.2.3 Mononuclear phagocytes

Besides neutrophils, mononuclear phagocytes including monocytes, macrophages and dendritic cells (DCs) play a crucial role in the response to invasive candidiasis (Lionakis et al., 2013; Ngo et al., 2014).

Monocytes and their derivatives, including tissue-resident macrophages exhibit marked efficiency in detecting and ensnaring *Candida* spp. and filamentous fungi within the first critical hours after infection. These immune cells produce pro-inflammatory cytokines and chemokines such as IL-1β, IL-6, and TNF-α, which recruit and activate neutrophils in infected site (Kanayama et al., 2015; Lionakis et al., 2013; Ngo et al., 2014). Monocytes/macrophages also provide lymphocyte-independent immune response following a subsequent occurrence of invasive candidiasis via epigenetic reprogramming, which result in enhanced responsiveness to subsequent triggers. This process has been termed 'trained immunity', or ‘innate memory’ that can mount resistance to reinfection (Quintin et al., 2012).

The role of other hematopoietic cells like dendritic cells in host defense against invasive candidiasis are investigated. DCs are requisite for host defense during invasive candidiasis. They are able to phagocytize plactonic cells and hyphae form in *Candida* yeasts and prime the production of inflammatory mediators and distinct cytokines (D’Ostiani et al., 2000). However, the *in vivo* role of different dendritic cell subsets remains unknown, partly owing to technical challenges in isolating specific dendritic cells.

1.5.3 Aspergillosis

Until the 1990s, *Candid*a spp. were the most common cause of invasive fungal infection (IFI) between immuno-compromised individuals (Koch et al., 2004). The epidemiology of invasive fungal infections has changed during1990s. Nowadays, *Aspergillus* spp. has overtaken *Candida* spp. as the main cause of IFI in advanced healthcare settings. As an

Example, between 1992 and 2001, *Aspergillus* spp. were responsible for 62% of IFIs, whereas *Candida* spp. caused only 35% of invasive infections (Lass-Flörl, 2009).
Although *A. fumigatus* can cause infection in the skin, peritoneum, eyes, bones, kidneys and gastrointestinal tract, the main sight of infection for this fungus is the respiratory tract. The inhalation of *Aspergillus* spores can have several consequences depending on host immune response ranging from aspergilloma and chronic necrotizing pulmonary aspergillosis (CNA) to invasive aspergillosis (IA) as shown in Figure 6 below.

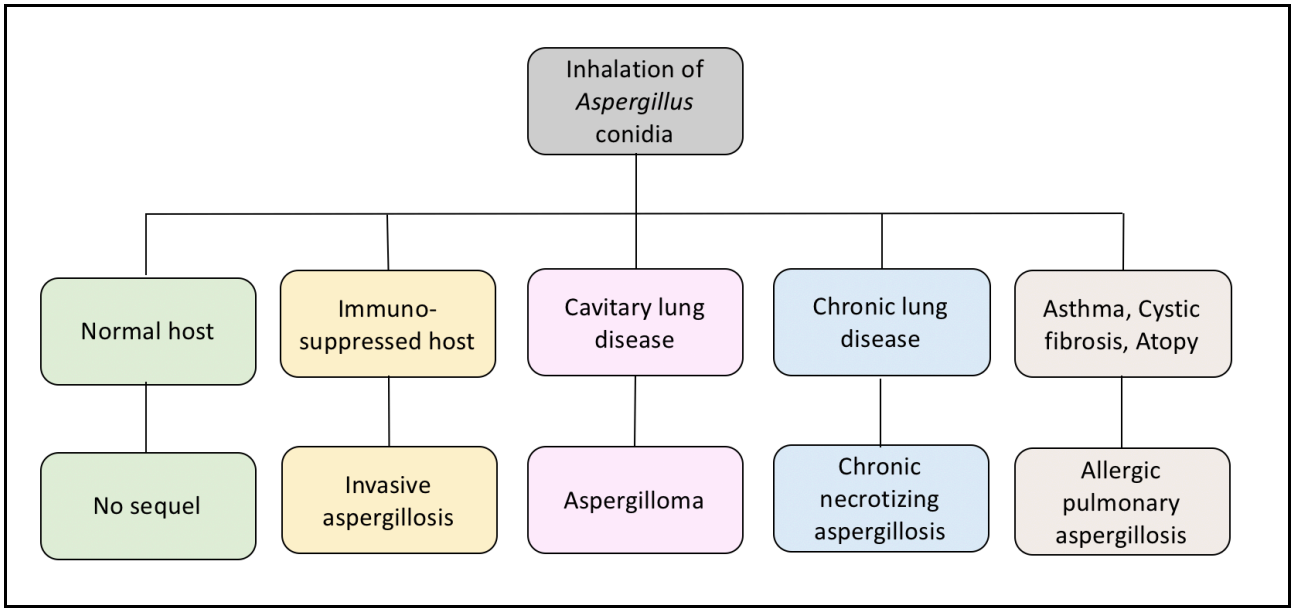

Figure 6. The clinical spectrum of conditions resulting from the inhalation of *Aspergillus* spores. Adapted from Kousha et al., 2011.

1.5.3.1 Aspergilloma

Aspergilloma (fungal ball) is the prevalent form of pulmonary aspergillosis. It is composed of masses of fungal hyphae, inflammatory cells, fibrin, mucus, and tissue debris and can move into the lung cavity but it is not able to invade the blood vessels and surrounding lung parenchyma (Rafferty et al., 1983; Tomee et al., 2012).
Although other fungi like *Mucorales, Zygomycetes* and *Fusarium* may develop the fungal balls, *Aspergillus* spp. (specifically, *A fumigatus*) are clearly the most common infectious agents (Soubani & Chandrasekar, 2002). The most common symptoms in patients with aspergilloma are mild hemoptysis and bleeding from bronchial blood vessels. Less commonly, patients may develop cough, fever and dyspnea. CT scan and chest radiography are useful methods for diagnosis of pulmonary aspergilloma.

1.5.3.2 Chronic necrotizing pulmonary aspergillosis

Chronic necrotizing aspergillosis (CNA), also called semi-invasive and sub-acute invasive aspergillosis, is an indolent, destructive process of the lung due to invasion by *Aspergillus* spp. (usually *A. fumigatus*) (Soubani & Chandrasekar, 2002). It usually occurs without vascular invasion or dissemination to other organs. CNA usually impacts middle-aged and elderly patients with weak immune systems or mild systemic immunosuppression, and is associated with chronic lung diseases such as cystic fibrosis, radiation therapy, pneumoconiosis, and lung infarction.

1.5.3.3 Invasive aspergillosis (IA)

Invasive aspergillosis (IA) is a highly lethal form of *Aspergillus* infection in immuno-suppressed patients, hematopoietic stem cell, solid-organ transplant patients, AIDS, cancer patients and in patients with acute leukemia (R. T. Brown et al., 1998). Among other pathogenic fungal strains, *A. fumigatus* is the most common cause of 90% of IA infections (Lopes Bezerra & Filler, 2004). Despite developing new antifungal drugs and improving the immunosuppression conditions, the mortality rate in immunocompromised patients with IA remains at around 50% overall.

There are four different forms of IAs in immunocompromised patients according to the area of the infection: 1) invasive pulmonary aspergillosis (IPA), 2) tracheobronchitis, 3) rhinosinusitis and 4) disseminated disease usually in the brain (Denning, 1998). Between these forms, invasive pulmonary aspergillosis (IPA) is the most common fungal infection. As mentioned before, the primary route of human infection is via inhalation of airborne conidia. Next, *A. fumigatus* conidia are deposited in the human bronchioles or alveoli. (Figure 7). In healthy individuals, inhaled conidia that are not removed by mucociliary clearance, come into contact with alveolar macrophages, which are the primary resident phagocytes of the lung. *Aspergillus* conidia are largely phagocytosed and killed by alveolar macrophages. In addition, alveolar macrophages regulate proinflammatory response and neutrophils recruitment (one type of polymorphonuclear cell [PMN]) to the site of infection. Neutrophils are able to destroy conidia and/or germinated hyphae that evade macrophage killing. Failure of host defense along with other specific features of this ubiquitous pathogen, that permit *A. fumigatus* survival and growth in this pulmonary environment, increase the risk of IA development (Schaffner et al., 1982).

The diagnosis of IPA is based on clinical, radiological, and mycological data. Up to now, tissue histopathological tests and CT scan are the most definite diagnostic method. Some

other approaches like nucleic acid detection in serum or in bronchoalveolar lavage (BAL) fluid by qPCR or quantification of galactomannan antigens by ELISA help to confirm the diagnosis (Denning, 1998; Horvath & Dummer, 1996; J P Latgé, 1995).

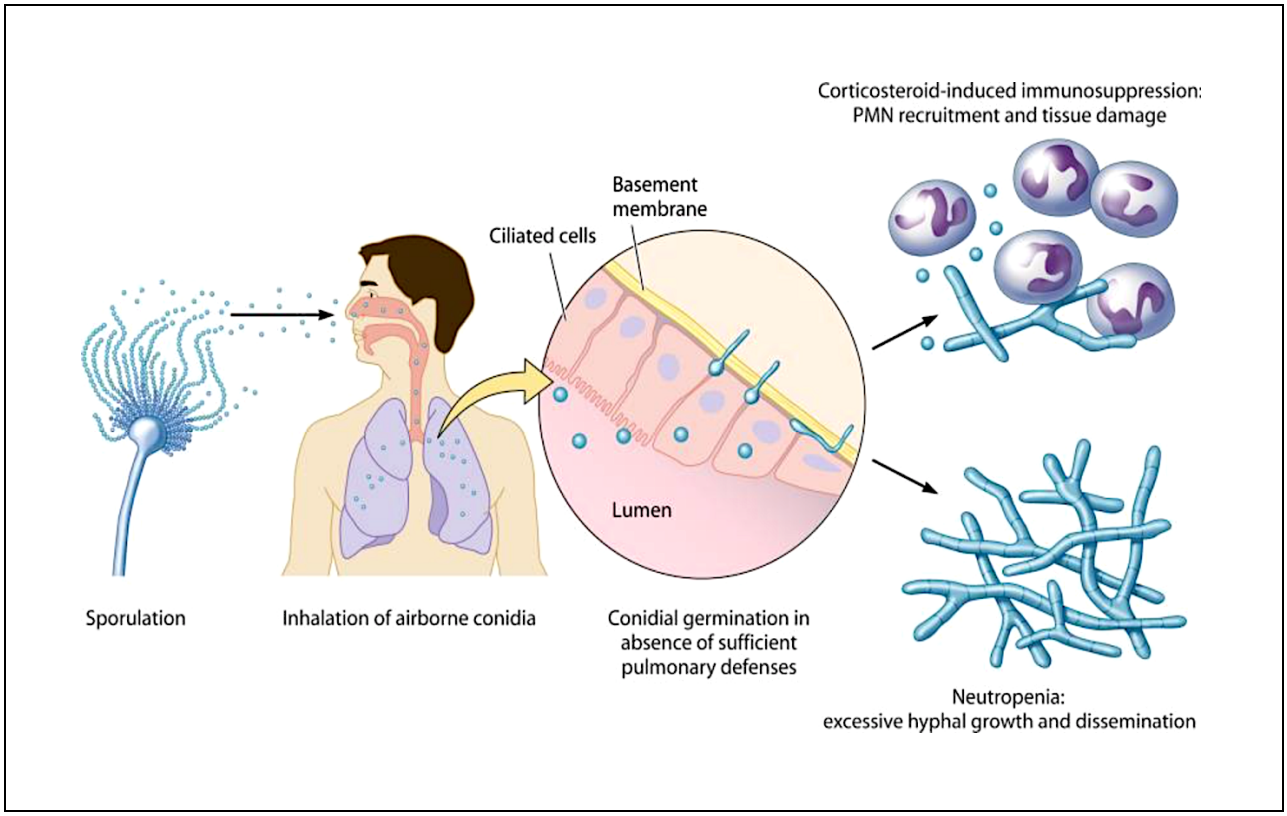

Figure 7. The infectious life cycle of *A. fumigatus* in the human lung. Inhalation by specific immunocompromised patients results in conidium penetration in the lung, germination, and either PMN-mediated fungal control with significant inflammation (corticosteroid therapy) or excessive hyphal growth with a lack of PMN infiltrates and, in the most severe cases, dissemination (neutropenia). Adapted from Dagenais & Keller, 2009.

1.5.4 Host defense mechanisms against *Aspergillus* infection

1.5.4.1 Airway colonization

Lung infections due to *A. fumigatus* are caused by inhalation of airborne conidia, which are present in in the environment; estimates suggest that each person may inhale up to 200 spores daily. In IA-susceptible populations like patients with weakened immune systems or lung diseases, the mucosal defenses of the lung are depressed and this leads to fungal colonization.

1.5.4.2 Interactions of *Aspergillus* with soluble lung components

A. fumigatus spores rapidly encounter with the airway mucosa, which is made up of the fluid lining the respiratory tract and airway epithelia, after inhalation. Mucus, proteins,

lipids, ions, water, and other cellular secretions make up this pulmonary fluid, which contribute to mucociliary clearance of inhaled conidia. PRRs, which are divided into two secreted PRRs and cell bound receptors, contribute to host defense within this fluid. *A. fumigatus* cell wall has a carbohydrate-rich structure that can be recognized by the most common PRRs like collectins, mannose-binding lectin (MBL) and the surfactant proteins SP-A and SP-D. MBL, SP-A, and SP-D have been shown *in vitro* to contribute in fungal clearance by binding and agglutinating *A. fumigatus* conidia. As a result, it aggravates the phagocytosis and killing of *A. fumigatus* conidia by alveolar macrophages and neutrophils (M. J. Allen et al., 1999, 2001. Several studies have shown that MBL and SP-D deficiency exhibit increased susceptibility to IA, revealing their important role in conidial clearance by enhancing complement activation, phagocytosis, and killing of conidia or aggregating conidia for other host defenses (Kaur et al., 2007; Madan et al., 2005). In brief, inhaled conidia bind to soluble receptors such as pentraxin-3, SP-A and SP-D and are swelled within alveolar macrophage phagosomes. It results in exposure of the β-glucan surface and triggers inflammatory responses. TLR-2 & TLR-4 contribute to host recognition of hyphae, where TLR-2 recognizes both spore and hyphal morphologies, TLR-4 is only able to detect the hyphal form (Netea et al., 2003). Recruited neutrophils and alveolar macrophages prevent conidial germination and development of IA in immunocompetent patients. This demonstrate that neutrophils mediate fungal killing with oxidative mechanisms and lactoferrin production (Hohl & Feldmesser, 2007).

1.5.4.3 Interaction of *Aspergillus* with respiratory epithelia

Airway epithelia are likely involved in the overall immune response to *A. fumigatus* as they are the first line that encounter by inhaled conidia. Epithelial cells with secretion of antimicrobial peptide such as defensin family, have a direct role in airway defense (Alekseeva et al., 2009). *In vitro*, host PRRs on epithelial cells are able to recognize *Aspergillus* germinating conidia and hyphae, but not resting conidia and induce the production of cytokines and chemokines such as IL-6, TNF-α, and IL-8 (Balloy et al., 2008; Bellanger et al., 2009). Administration of corticosteroid can eliminate this inflammatory response, raising concerns about the role of epithelial cells in corticosteroid-treated individuals who are at risk for IA (Bellanger et al., 2009). Numerous epithelial cells including tracheal epithelial cells, alveolar type II cells, human nasal epithelial cells, and the A549 lung epithelial cell line have been shown to bind and swallow *A. fumigatus* conidia (Filler & Sheppard, 2006; Paris et al., 1997; Wasylnka & Moore, 2003). Conidia

engulfed by A549 epithelia enter acidic phagolysosomes and can be digested, although some conidia are able to escape both the phagolysosome and pneumocyte and germinate without evidence of pneumocyte damage (Washburn et al., 1986; Wasylnka & Moore, 2003). There are several fungal derivatives which contribute to the ability of *A. fumigatus* to germinate, invade surrounding lung tissue and attach to the airway epithelium. These fungal products include proteases, gliotoxin, fumagillin, helvolic acid and sialic acid on the conidia's surface (Figure 8) (Amitani et al., 1995; Bromley & Donaldson, 1996. Interestingly, *A. fumigatus* and other pathogenic species of aspergilli have more conidial sialic acid than non-pathogenic aspergilli (Wasylnka et al., 2001). Sialic acid residues also mediate adhesion to fibrinogen and fibronectin (Annaix et al., 1992; Bouchara et al., 1997). *A. fumigatus* strains can also produce mycotoxins such as Gliotoxin with immunosuppressive properties. It may induce apoptosis in some immune cell types such as neutrophils, macrophages and epithelial cells. As a result, *A. fumigatus* binds to respiratory epithelial cells and membrane proteins and evades epithelial cells to escape host defenses and develop infection.

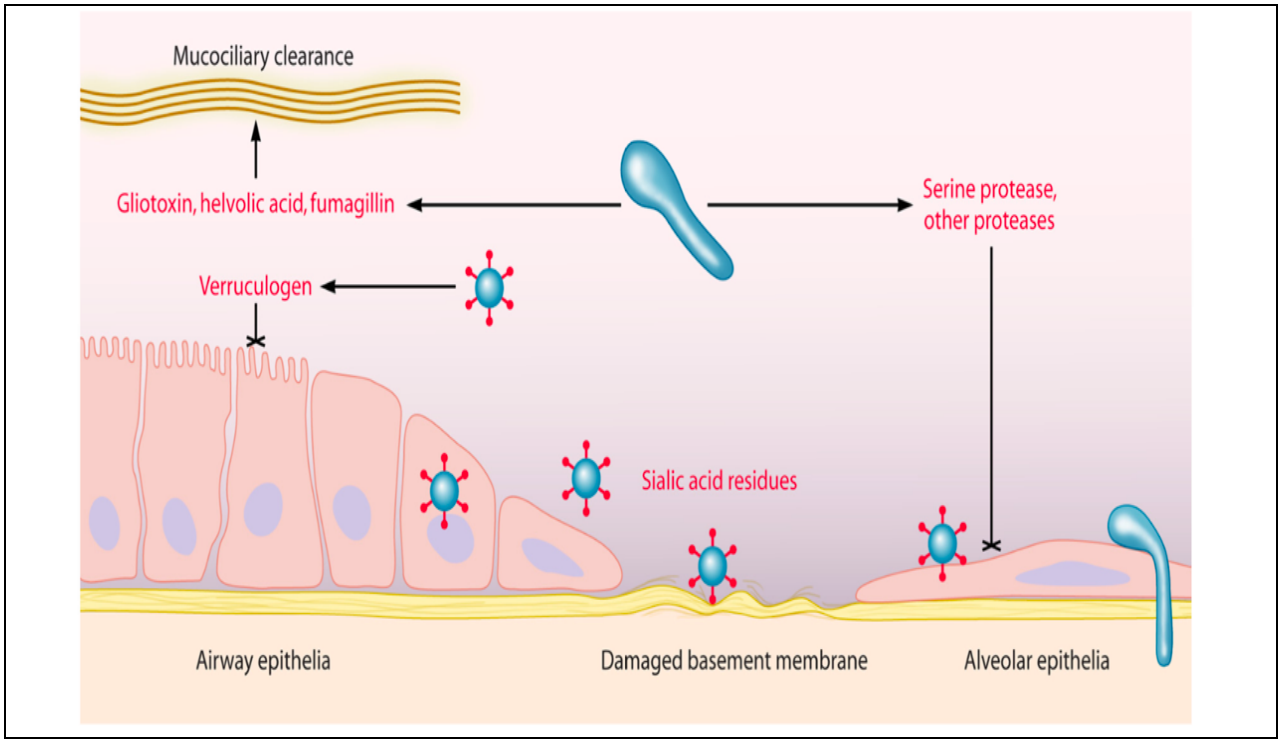

Figure 8. Interaction of *A. fumigatus* with respiratory epithelia. Inhaled *A. fumigatus* conidia encounters lining trachea, bronchi, and bronchioles, the mucus and fluid lining the upper respiratory tract, and, finally, the alveolar space. Fungal residues (shown in red) may enhance colonization through tissue injury (cross-haired line) and attachment to the airway epithelium or damaged basement membrane. Conidia may also germinate and invade the surrounding lung tissue via the basement membrane or following ingestion by epithelial cells. Adapted from Dagenais & Keller, 2009.

1.5.4.4 Interaction of *Aspergillus* with alveolar macrophages

Resident alveolar macrophages as the primary phagocytic cells of the respiratory tract play a significant role in the host's defense against *Aspergillus* conidia. Conidia of *A. fumigatus* are phagocytosed by alveolar macrophages in an actin-dependent manner, a process mediated by the recognition of pathogen-associated molecular patterns by host cell PRRs. This mechanism is mediated by binding of the host cell PRRs (mostly C-type lectin receptor dectin-1, TLR-2 and TLR-4) to *Aspergillus* PAMPs which generate a proinflammatory response characterized by the production of cytokines and chemokines including TNF-α, IL-1ß, IL-6, IL-8, macrophage inflammatory protein 1α, and monocyte chemoattractant protein 1 (Cenci et al., 2001).

It has been proved that alveolar macrophages can swallow conidia quickly and kill them by acidification and generation of reactive oxygen species (ROS) in phagolysosome (Figure 9) (Ibrahim-Granet et al., 2003; Philippe et al., 2003).

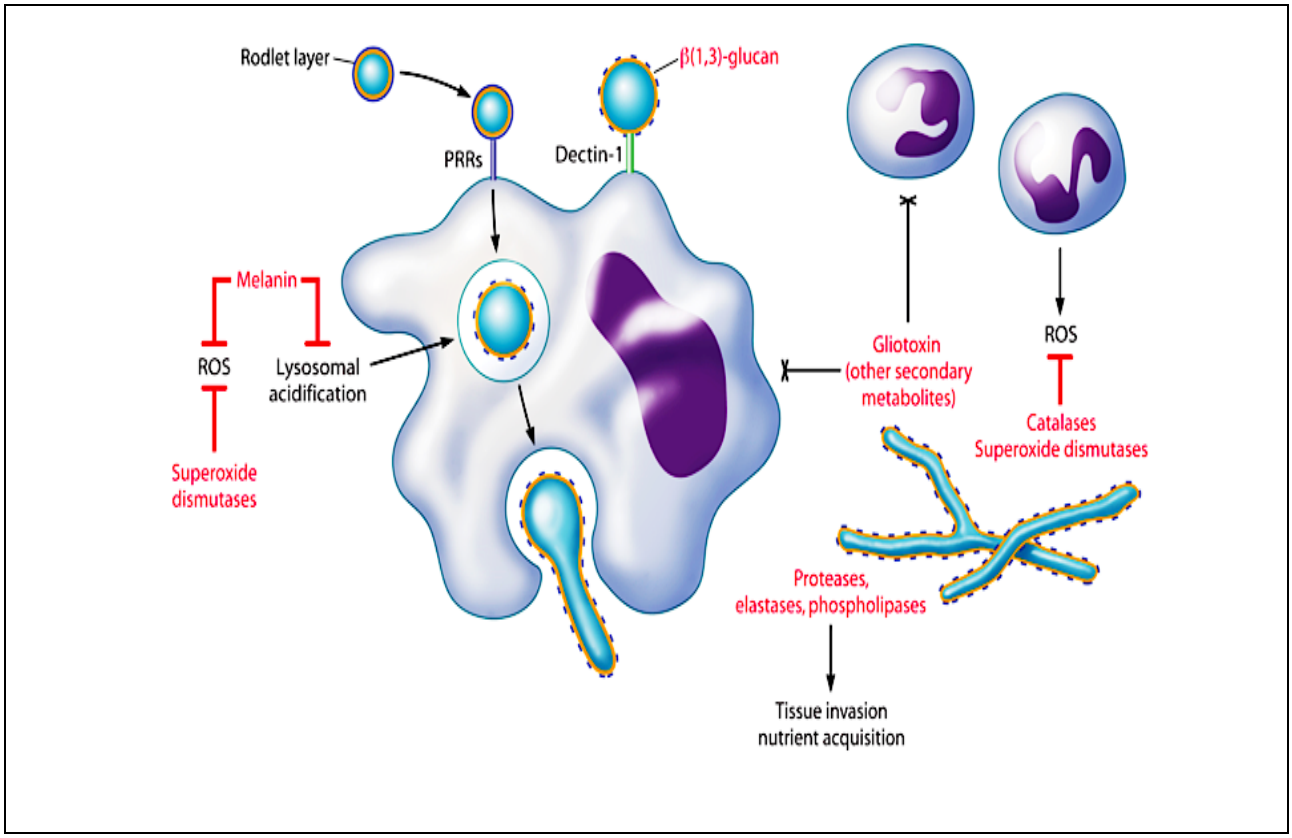

Figure 9. Interaction of *A. fumigatus* with phagocytic cells. Inhaled conidia are engulfed and attacked by alveolar macrophages via PRRs. Swollen conidia expose β-1, 3-glucans for recognition by dectin-1. Interaction of Dectin-1 and β-1, 3-glucans result in activation of macrophage proinflammatory response. Fungal products (shown in red) such as gliotoxin, catalases, proteases, elastases, phospholipases, superoxide dismutases, and melanin enhance *A. fumigatus* pathogenicity in immunocompromised individuals by evading or modulating host defenses. Adapted from Dagenais & Keller, 2009.

1.5.4.5 Interaction of *A. fumigatus* with other immune cells

Neutrophils employ distinct mechanisms for the killing of *A. fumigatus* hyphae as well as conidia, including the action of enzymes such as myeloperoxidase (MPO) or NADPH oxidase, production of reactive oxygen species (ROS) and the release of neutrophil extracellular traps (NETs), although their exact contribution has not been investigated in detail (Diamond & Clark, 1982; Levitz & Diamond, 1985; Schaffner et al., 1982). Neutropenic patients should be considered at high risk of developing IA. Neutrophils can bind to hyphae and induces the oxidative and non-oxidative mechanisms that mediate hyphal killing, although hyphae size constitute as a special challenge for the immune system, since they are too large to be phagocytosed by neutrophils (Diamond & Clark, 1982; Roilides et al., 1993a). Oxidative mechanisms involve the generation of ROS by activated neutrophils via multicomponent phagocyte NADPH oxidase, which generates superoxide and also myeloperoxidase, which catalyzes the conversion of hydrogen peroxide and chloride anions to hydrochories acid (Roos et al., 2003). In addition to these two processes, Neutrophils generate cytokine via neutrophil serine proteases activity and induce chemokine receptors in bronchial epithelial cells, thus enhancement of the inflammatory response (Roilides et al., 1993b). There is also evidence that neutrophils regulate fungal killing by non-oxidative mechanisms. As an example, they produce and localize lactoferrin and pentraxins when interacting with *Aspergillus* conidia to increase their fungal killing activity (Jaillon et al., 2007; Levitz & Diamond, 1985). It has been shown that in mouse with neutrophil depletion, the fungal burden increases within 3 hours. Neutrophils fail to inhibit hyphal development and hyphal tissue invasion after steroids treatment. This cause considerable tissue necrosis and inflammation (Ibrahim-Granet et al., 2010).

The major cells that produce IFN-γ in an *A. fumigatus*-infected neutropenic host are NK cells. NK cells were previously considered to have only anti-tumor and anti-virus activities, but more recent research has revealed that they act also against bacteria and fungi. The granule exocytosis pathway (perforin/granzymes) and the expression of death ligands are the primary and best characterized processes involved in NK cell-mediated cytotoxicity (Ramírez-Labrada et al., 2022; Schmidt et al., 2011). These mechanisms are recognized as activators of several cell death programs on the target cells especially fungal cells leading to their destruction. It has been demonstrated that NK cell depletion can decrease IFN-γ production and raise the incidence of pulmonary fungal infections. However, *A. fumigatus* can impair NK cell-derived immune functions by downregulating the levels of

GM-CSF and IFN-γ (Schmidt et al., 2011). Human investigations revealed that circulating monocytes, in addition to neutrophils and alveolar macrophages contribute to antifungal immunity. During lung inflammation, circulating monocytes leave the bloodstream and migrate into the pulmonary tissues, where following conditioning by local growth factors, pro-inflammatory cytokines and microbial products to differentiate into inflammatory macrophages or monocyte-derived dendritic cells. Flow cytometric phenotyping has revealed three different population of monocytes with different functions based on the relative expression level of CD14 [co-receptor for TLR4 and mediates lipopolysaccharide (LPS) signaling] and CD16 (Fc gamma receptor IIIa). These subunits are classified into classical ($CD14^{++}CD16^{-}$), intermediate ($CD14^{+}CD16^{+}$), and non-classical ($CD14^{+}CD16^{++}$), monocytes (Ziegler-Heitbrock et al., 2010). Beside phagocytosis activity and conidial germination, these subunits play an important role in increasing the inflammatory responses through production of TNF-α (Serbina et al., 2009).

Platelets, in addition to neutrophils, alveolar macrophages, NK, and monocyte cells, provide antifungal immunity by releasing of platelet microbial peptides (PMPs) or contact-dependent mechanisms (Tang et al., 2002). They act by binding to the hyphae cell wall and inhibiting hyphal elongation (Christin et al., 1998; Perkhofer et al., 2008). *Aspergillus* hyphae stimulate platelets and enhance IL-8 cytokine response in monocytes (Rødland et al., 2010). However, further research is required to fully understand how platelets contribute to *Aspergillus* infections.

1.6 Cell death

Understanding the various ways that cells potentially lose viability and finally die is essential for developing effective therapies for cancer and other diseases characterized by abnormalities in the regulation of cell death. The proceeding sections will provide an overview of the different definitions of cell death, Nevertheless, in general, cells are removed from the tissue within one of two directions: either in a controlled (programmed) manner involving a series of biochemical and molecular events, or alternatively in an uncontrolled manner, resulting in the spilling of the cellular contents into surrounding environment (Kerr et al., 1972).

1.6.1 Apoptosis (type I)

Apoptosis, which means "falling off" in Greek (as in leaves falling from a tree), is the most well-known and common type of programmed cell death (or more colloquially ‘cellular suicide’). Apoptosis is the process by which a cell stops dividing and growing and instead initiates a process that eventually leads to the controlled death without spillage of its contents into the surrounding tissues. The activation of a group of cysteine-aspartic proteases known as caspases is necessary for the initiation of apoptosis. Mammalian caspases are categorized into two functional groups, the initiator caspases and the executioner caspases. The initiator caspases (caspases 8 and 9) normally exist as inactive procaspase monomers. Once cell damage is detected, the initiator caspases are activated by dimerization and not by cleavage and go on to activate the executioner caspases (caspases 3, 6 and 7) (Boatright et al., 2003; D. W. Chang et al., 2003). The activation of the executioner caspases triggers a series of processes that lead to the destruction of the nuclear proteins and cytoskeleton, the expression of ligands for phagocytic cells, the development of apoptotic bodies, and DNA fragmentation (Martinvalet et al., 2005). The intrinsic and extrinsic pathways of apoptosis cooperate to eliminate defective cells from the body and preserve the health of multicellular organisms. Failure to regulate cell numbers through apoptosis can cause the pathologies seen in many diseases. For example, in Alzheimer’s as a neuro-degenerative disorder, accumulation of b-amyloids at lesion sites induces activation of caspases and excessive apoptosis of neurons. (D. W. Dickson, 2004). However, in cancer, lack of apoptosis can promote uncontrolled cell growth.

1.6.1.1 Intrinsic apoptosis

The intrinsic signaling pathways that initiate apoptosis involve a diverse array of non-receptor-mediated stimuli that produce intracellular signals that act directly on targets within the cell and are mitochondrial-initiated events. The intrinsic signaling pathways are mitochondrial-initiated events that can be initiated by the cell itself through intracellular signals (Oppenheim et al., 2001). Thus, it is known as the mitochondrial pathway of apoptosis involves a variety of stimuli that act directly on multiple targets within the cell. This type of apoptosis can proceed from either a positive or negative pathway and is dependent on compounds released by the mitochondria. The absence of cytokines, hormones, and growth factors in the cell's immediate environment results in negative

signals. Absence of these pro- survival signals activate pro-apoptotic molecules (normally are inhibited) within the cell, such as puma, noxa and bax and initiate apoptosis. Positive signals initiating apoptosis include exposure to hypoxia, toxins, radiation, reactive oxygen species, viruses and a variety of toxic agents (Brenner & Mak, 2009). The initiator caspase that controls the intrinsic signaling pathway is caspase 9, which can attach to adapter protein apoptotic protease activating factor 1 (APAF1) following exposure of its caspase recruitment domain (CARD).

After induction of apoptosis, the mitochondrial membrane undergoes alteration, resulting in the opening of the mitochondrial permeability transition (MPT) pore. Once the MPT pore is open, pro-apoptotic proteins (including cytochrome *c*, Smac/Diablo and HtrA2/Omi) efflux to the cytosol and activate apoptosis (Cain et al., 2002).

1.6.1.2 Extrinsic apoptosis

Apoptosis can also result from the interaction between an immune cell and a damaged cell, which is known as the extrinsic signaling or the death receptor (DR) pathway Oppenheim et al., 2001; Sica et al., 1990). This pathway is initiated by patrolling NK cells or macrophages when they generate death ligands, which upon attaching to DRs in the target cell membrane induce the extrinsic pathway via the activation of procaspase 8 to caspase 8 (J. H. Kim et al., 2004). For activation of caspase 8, a death ligand must attach to a DR, resulting in recruitment of monomeric procaspase 8 via its death-inducing (DED) domain to a death-inducing signal complex (DISC) located on the cytoplasmic domain of the ligand-bound DR. When numerous procaspase 8 monomers are recruited to the DISC, they get dimerized and activated, and this allows the resulting caspase 8 to trigger apoptosis by two different sub-pathways.

Whether or not apoptosis is triggered by the intrinsic or the extrinsic pathways, it should be tightly regulated and failure to regulate it effectively can have negative consequences.

1.6.1.3 Drug induced apoptosis in yeast

Similar to mammalian cells, yeasts typically undergo cell death and exhibit apoptotic markers such DNA fragmentation, chromatin condensation, and externalization of phosphatidylserine to the outer leaflet of the plasma membrane (Madeo et al., 1997). Several compounds, some of which have been demonstrated to work through mitochondrial pathways (Figure 10), have been utilized to trigger apoptosis in wild type

yeast cells (Madeo et al., 2004). The yeast genome codes for many proteins of the basic molecular apoptosis machinery, such as orthologues of caspases (Madeo et al., 2002) apoptosis inducing factor (Wissing et al., 2004), and inhibitor of apoptosis (IAP) proteins (Walter et al., 2006). The regulation of the programmed death and apoptosis in yeast required complex mitochondrial processes, such as cytochrome *c* and apoptosis-inducing factors (AIFs) release, channel opening upon human Bax expression, depolarization of mitochondrial membrane potential, and mitochondrial fragmentation.

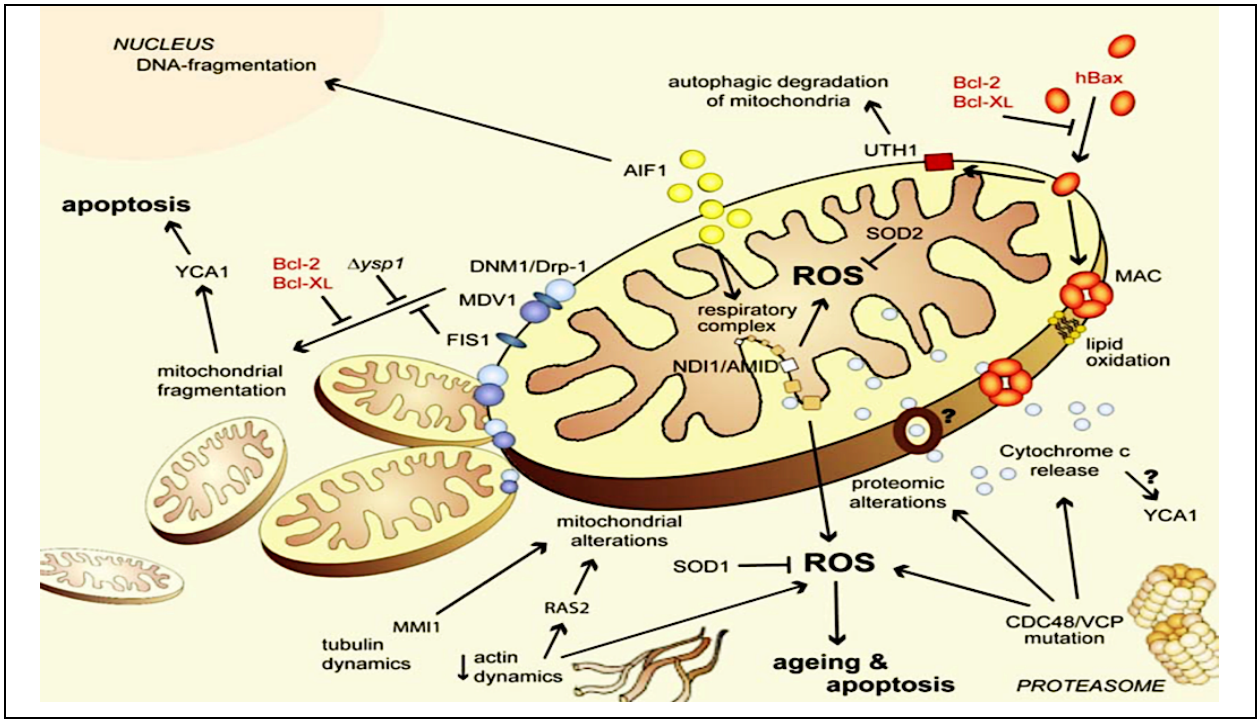

Figure 10. Mitochondrial pathways of yeast apoptosis and age induced programmed cell death. Shown are conserved substances and pathways that control yeast cell death. Red text color represents heterologous expression of mammalian proteins. Question marks shows interrelations that have been hypothesized but not completely proven. Adapted from Eisenberg et al., 2007.

Apoptosis induction by low doses of acetic acid, amiodarone, and α-factor has demonstrably been linked to hyperpolarization of the mitochondrial membrane potential, mitochondrial fragmentation, reduction of cytochrome *c* oxidase (COX) activity, mitochondrial ROS formation, cytochrome *c* release, and ultimately loss of mitochondrial membrane potential and cell death. However, the significant proportion of the upstream mechanisms are still unknown (Fannjiang et al., 2004; Ludovico et al., 2002; Pozniakovsky et al., 2005; Severin & Hyman, 2002). Recent studies have shown that hyperosmotic stress causes apoptosis induction in yeast through a caspase-dependent mitochondrial mechanism (R. D. Silva et al., 2005). High levels of glucose or sorbitol in

the media during incubation resulted in mitochondrial swelling and a decrease in the number of christae, which were followed by an elevation in caspase activation and cell death. These phenotypes were largely survived under hyperosmotic stress conditions in the mutant strains *cyc1Δ, cyc7Δ* and *cyc3Δ* compared to wild type (R. D. Silva et al., 2005). These results confirm the role of mitochondria and cytochrome *c* in yeast caspase activation. However, it is still unclear, whether the mechanisms following the release of cytochrome *c* is related to the development of an apoptosome-like structure and the subsequent activation of the yeast Yca1p caspase. Homologues of Apaf have not been detected and proteins with the same function have not been described in yeast so far. A timeline of events and mitochondrial death cascade in yeast has been proposed by Severin and colleagues (Pozniakovsky et al., 2005).

In brief, intracellular Ca^{2+} concentration increases while yeast cells are treated with α-factor or amiodarone. This leads to increasing the activity of respiratory enzymes and energy coupling, which is followed by hyperpolarization of the mitochondrial membrane potential (ΔΨm). Increased MMP enhances the generation of ROS, which then initiates the mitochondrial thread-grain transition (mitochondrial fragmentation) and de-energization (Pozniakovsky et al., 2005).

Mitochondrial depolarization accompanies cytochrome *c* release in yeast cells undergoing apoptosis. It should be noted that the mitochondrial death pathway suggested by Severin and colleagues goes in line with the results obtained through stimulation with various drugs. There is no doubt that many yeast apoptosis inducers acting through the mitochondrial pathway trigger a similar chain of events.

1.6.2 Autophagy (type II)

Autophagy is the natural, conserved degradation process in which cellular components such as macro proteins or even whole organelles are sequestered into a double-membrane vesicle, an autophagosome, and delivered into lysosomes for degradation and eventual converting to macromolecules (Mizushima et al., 2008; Shintani & Klionsky, 2004). These macromolecules can be recycled to create new cellular structures and/or organelles or alternatively can be further processed and used as a source of energy. Autophagy can be initiated by numerous stimuli, most notably by nutrient deprivation (caloric restriction) or may originate from signals present during cellular differentiation and embryogenesis and on the surface of damaged organelles (Mizushima et al., 2008).

The importance of autophagy for cell survival has long been appreciated, but more recently, its importance in both adaptive and innate immune system has been described, where it may degrade intracellular pathogens and deliver antigens to MHC class II holding compartments and initiate the transportation of viral nucleic acids to Toll-like receptors. Failure of autophagy has been associated to the accumulation of protein aggregates in the neurons and the development of neurological diseases like Alzheimer's disease (Nixon & Yang, 2011). The role of autophagy in cancer cells is rather controversial since it inhibits malignant transformation while, on the other hand, promoting tumor development.

1.6.3 Necrosis (type III)

Necrosis, which means "'to kill' in Greek is the uncontrolled form of cell death that is induced by external injury, such as hypoxia or inflammation. This process often involves upregulation of several pro-inflammatory proteins and substances including nuclear factor-κB which leads to the rupture of the cell membrane causing shrinkage of the cell contents into surrounding areas, resulting in a cascade of inflammation and tissue damage. Necrosis, in contrast to apoptosis, is an energy-independent type of cell death. Once the cell encounters a rapid shock including radiation, heat, chemicals, hypoxia and etc., it damages so severely that is not able to function resulting in necrosis. The cell usually responds by cytoplasmic swelling and karyolysis, (a process known as oncosis) as it fails to maintain homoeostasis with its internal environment.

1.7 Sphingolipids

Sphingolipids comprise a wide range of complex lipids consist of a long-chain base (LCB – the 18-carbon amino alcohol sphingosine, or one of its derivatives) attached to one long-chain fatty acid by an amide bond at C2, and, in most cases, to a polar head group (a phosphoalcohol or a sugar residue) at C1. Sphingolipids serve as membrane components of all eukaryotic cells; whose chemical features modulate the physical properties of lipid bilayers and membrane fluidity. Besides playing structural roles in cellular membranes, bioactive sphingolipids such as ceramide, sphingosine, and S1P are involved in cell death pathways (apoptosis, necrosis, autophagy, anoikis), cancer proliferation, migration, inflammation, and drug resistance (Hannun & Obeid, 2008). Figure 11 shows the general structure of sphingolipids. As reviewed in Ren & Hannun 2016, different species with

variations in head groups, acyl-chain length, location and number of hydroxyl groups, and degree of unsaturation of both the LCB and the acyl-chain result from variations to this fundamental structure. Sphingolipids do have several chiral centers, and only a certain arrangement of the stereoisomers may be found in natural sphingolipids. Each stereoisomer has been associated to certain biological characteristics (Ren & Hannun, 2016). The sphingolipid structure of yeast such as *Saccharomyces cerevisiae* is considerably simpler than that of human, making it a great model for research on sphingolipid metabolism and cellular functions. Studies in *S. cerevisiae* have pioneered the use of systems biology to dissect particular sphingolipid functions in addition to helping to clarify the role of individual genes in the sphingolipid metabolic pathways (Cowart et al., 2010; Montefusco et al., 2013).

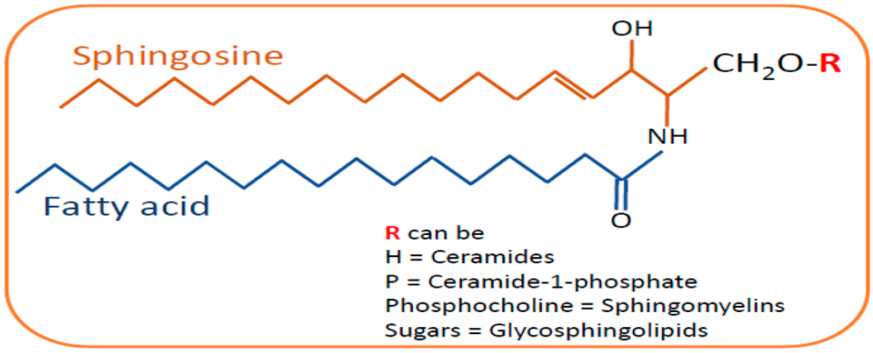

Figure 11. General structure of sphingolipids. Sphingosine is the backbone of the sphingolipid structure that is linked to fatty acids by an amide bond. Depending on the type of residue in the side chain, sphingolipids are categorized as ceramides, sphingomyelins and glycosphingolipids. Adapted from Mallela et al., 2022.

1.7.1 Biosynthesis of yeast sphingolipids

De novo sphingolipid synthesis starts at the cytosolic leaflet of the endoplasmic reticulum (ER), where yeast serine palmitoyl transferase (SPT) catalyzes the initial and rate-limiting step of condensation of serine with palmitoyl-CoA to form 3-ketodihydrosphingosine (R. C. Dickson & Lester, 1999) (Figure 12). SPT catalyzes the first condensation process, which results in the reduction of 3-ketodihydrosphingosine to dihydrosphingosine (DHS or sphinganine). Yeast hydroxylase Sur2p has the ability to hydroxylate the C4 position of DHS to produce phytosphingosine (PHS) (Grilley et al., 1998). SUR2 is not a crucial gene, and both DHS and PHS are available in yeast cell although it is not yet clear how the two vary functionally. However, several researches indicate that PHS is the more biologically

active LCBs in yeast and has particular inhibition activity on yeast growth and nutrient uptake (Chung et al., 2001).

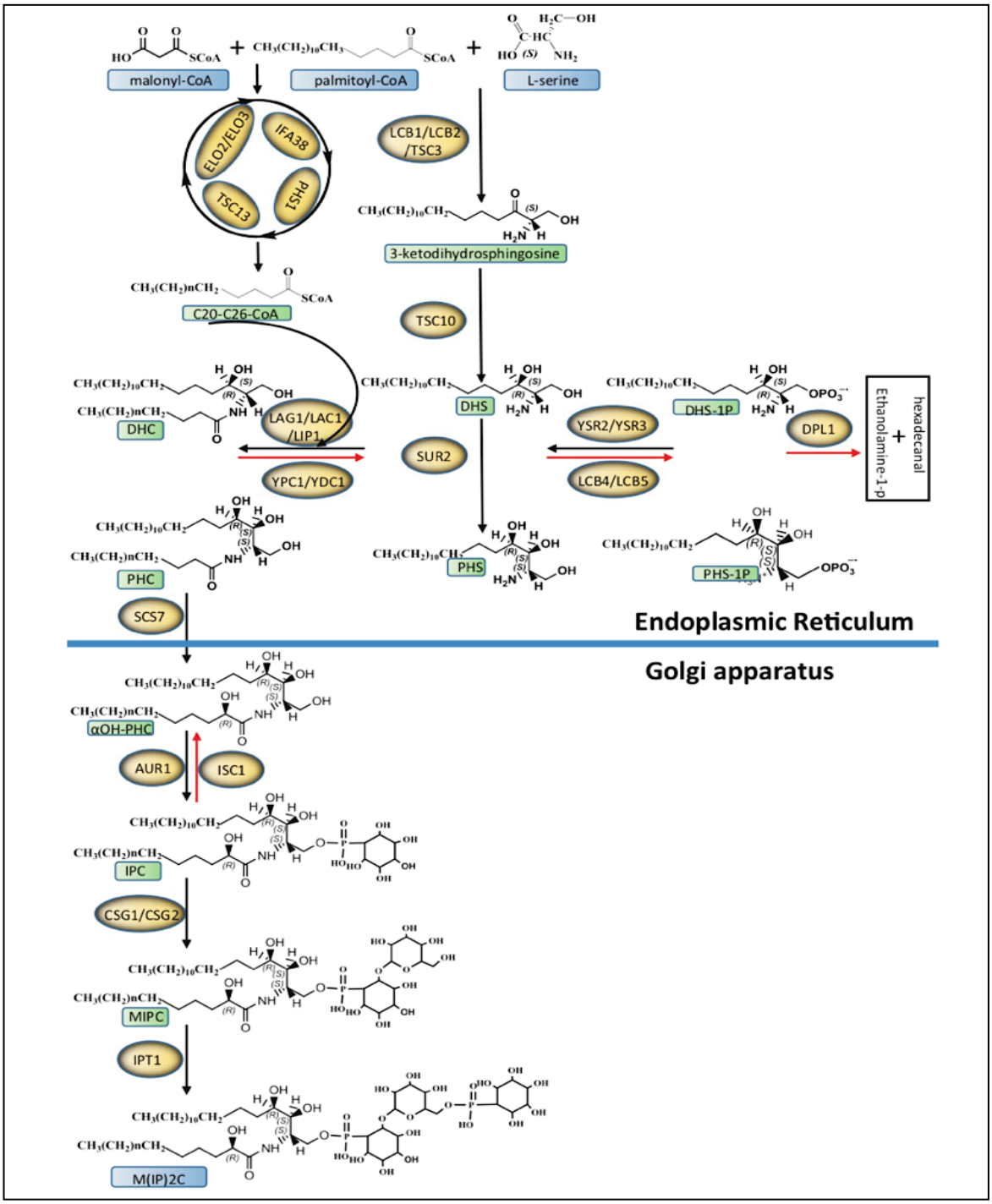

Figure 12. Overview of yeast sphingolipid metabolism. Blue rectangles indicate the initial substrates and final products of the sphingolipid biosynthesis pathway. Green rectangles highlight the intermediate products. Gold capsules indicate the genes, catalysing each step. The biosynthesis pathway's stages are indicated by black arrows, while the sphingolipid catabolism-causing processes are indicated by red arrows. Adapted from Ren & Hannun, 2016.

The next stage in the biosynthesis of yeast sphingolipids, is the N-acylation of LCBs to form dihydro- and phytoceramide. Lag1 and Lac1, two presumably redundant homologues that make up the main ceramide synthase activity, catalyze this reaction (Guillas et al., 2001; Schorling et al., 2001). Notably, ceramide in mammalian cells due to variations in hydroxylation and unsaturation as well as acyl chains of various lengths bound to the amino group of the LCB backbone exhibits more variety than it does in yeast. The preponderant incorporation of very long-chain fatty acids (VLCFAs) into ceramides—sphingolipids contain a substantial quantity of VLCFA of 26 carbons—is one of the distinctive features of yeast ceramides. Following the synthesis of dihydro-/phytoceramides, they are transferred from the ER to the Golgi network where they might undergo further processing to create complex sphingolipids. In yeast, this is accomplished via direct interaction between the ER and Golgi networks as well as by non-vesicular membrane transport (Funato & Riezman, 2001). In mammalian cells ceramide can also be transported by ceramide transfer (CERT) protein (Hanada et al., 2003; Kumagai et al., 2005). Ceramide could be converted into complex sphingolipids by altering the 1-OH head group of the sphingoid base. In mammals, this head group can be modified to create glycosphingolipids or sphingomyelin by adding sugar residues or phosphocholine. In contrast, in yeast mannose-(inositol-P) 2-ceramide (M (IP) 2C) is the final and most abundant sphingolipid product, which is transported to the plasma membrane (Figure 12). The respective genes of these steps do not exist in mammals and thus present great potential as antifungal drug targets (R. C. Dickson et al., 1997; Nagiec et al., 1997).

1.7.2 Functions of yeast sphingolipids

Sphingolipids, along with glycerophospholipids and cholesterol, are main components of cytoplasmic membranes. Beyond their structural function, sphingolipids have particular roles in a number of essential cellular processes, several of which are key contributors to human disorders like cancer, diabetes, inflammation, and degenerative diseases of the nervous system. The complex sphingolipids that are the final products of the sphingolipid biosynthesis pathway as well as important intermediate products like ceramide, LCBs, and their phosphorylated derivatives are all included in the category of bioactive sphingolipids. As reviewed in Hannun & Obeid, 2008, the most well-known and researched bioactive sphingolipids are ceramides and sphingosine-1-P, with ceramide primarily assumed to serve as an antiproliferative signal and sphingosine-1-P as a pro-growth signal Ceramide-mediated signaling pathway were initially shown in mammalian

cells, and later in the yeast *S. cerevisiae*. In yeast, both complex sphingolipids and LCBs have been associated with a variety of specific roles, which will be discussed below. In contrast, no DHS-1P or PHS-1-P receptors have been identified, and there is currently insufficient knowledge of the specific roles that these lipids play in yeast.

The following observations led to the discovery of ceramide as a bioactive chemical in mammalian cells: (1) activation of different cell types like HL-60 leukemic cells and MCF7 breast cancer cells by a number of extracellular components such as Vitamin D3, TNF-α, and α-interferon results in early accumulation of ceramide; (2) exogenous ceramide analogs specifically induce qualitatively same cell responses to those caused by ligands (Bezanilla et al., 1992; M. Y. Kim et al., 1991; Kolesnick, 1991; Obeid et al., 1993); (3) Furthermore, inhibiting ceramide synthesis frequently eliminates or reduces the effects of those extracellular agents. Following these findings, further study has found ceramide-mediated cell responses, such as the arrest of the cell cycle, activation of differentiation, and beginning of apoptosis (Hannun, 1994).

There are still many unanswered concerns regarding the particular processes, such as how ceramide is generated in response to certain stimuli or how it interacts with its immediate downstream effectors and what is the nature of the signaling pathways downstream of ceramide effectors. For three main reasons, the yeast *S. cerevisiae* is an effective model organism to research the mechanism of ceramide function. First, both yeast and human generate ceramide via the biosynthetic pathway as well as the hydrolytic pathway from complex sphingolipid breakdown. Second, several ceramide effectors, including CAPK and CAPP have been identified in yeast. Finally, a large number of important signaling pathways related to ceramide functions are conserved between yeast and mammalian systems. The initial investigation into the function of ceramide in yeast was the addition of C2-ceramide, a cell membrane permeable analogue of ceramide, which was discovered to inhibit yeast proliferation (Fishbein et al., 1993). The following data show that yeast ceramides are crucial regulators of mitochondrial function: (1) the translocation of ISC1 from the ER to the mitochondria during the diauxic shift from fermentation to respiration (de Avalos et al., 2004; Kitagaki et al., 2007); (2) lacking yeast ISC1 exhibits diauxic shift failure of growth, oxidative stress, diminished chronic life span, and disrupted mitochondrial dynamics (Almeida et al., 2008); and (3) Ceramide signaling via Sit4 and Hog1, also known as ceramide-responsive phosphatases and MAP kinases, mediates these phenotypes (Teixeira et al., 2015). Additionally, the transport of proteins

from the ER to the Golgi and the stable membrane association of proteins with glycosylphosphatidylinositol (GPI) anchors requires ceramide (Watanabe et al., 2002).
Complex sphingolipids in yeast include inositol phosphoceramide (IPC), mannose inositol phosphoceramide (MIPC) and mannose-(inositol-P) 2-ceramide (M (IP) 2C). They are the most abundant components of the cytoplasmic membrane where they constitute approximately 30% of the total phospholipid content (Patton & Lester, 1991). Surprisingly, none of the yeast complex sphingolipids have been shown to be essential for cell survival, as is demonstrated that csg1 and csg2 deletion mutants, which lack the ability to synthesis MIPC or its downstream product M (IP) 2C, continue to grow normally. With the help of this mutant strain, it has been shown that the regulation of cellular Ca^{2+} homeostasis is related to IPC accumulation (T. Beeler et al., 1994, 1998; T. J. Beeler et al., 1997). However, it is still unclear how IPC regulates Ca^{2+} homeostasis in yeast.
Long-chain sphingoid bases (LCBs), DHS and PHS in yeast, are necessary for appropriate actin organization, which is essential for the internalization step of endocytosis (Zanolari et al., 2000).
Sphingoid bases from de novo synthesis have also been considered as potential second messengers in the heat stress response, which allows yeast to adapt to growth at temperatures as high as 39°C. Complex physiological changes including gaining of thermo- tolerance through generation of trehalose, induction of heat shock proteins, decreased nutrient import, transient arrest of the cell cycle at G0/G1 and recovery of normal growth state even at the elevated temperature, occur during the yeast response to heat stress. Finally, the phenotypic expression of altered chronical life span (CLS) in a variety of mutants in the sphingolipid metabolic pathway demonstrates that sphingolipid metabolism has also been associated to yeast aging (Ren & Hannun, 2016).

1.7.3 Sphingosine and infection

Sphingosine (SPH) constitutes a class of natural products containing a long aliphatic chain with a polar 2-amino-1, 3-diol terminus (2-amino-4-trans-octadecene-1, 3-diol), that can be generated from the cleavage of ceramide into sphingosine and a free fatty acid via ceramidases in lysosomes. It is present in the cell membranes of all mammals and many plants, and it is essential for a variety of complex biological processes, including formation, differentiation, and autophagy (Hudlicky et al., 1994; Tommasino et al., 2015). Once sphingosine is released from complex sphingolipids, mostly reacylated by ceramide synthase or phosphorylated by sphingosine kinase to synthesize sphingosine-1-

phosphate (S1P) (Olivera et al., 1996). Sphingosine is associated with a wide range of cellular processes including regulation of actin cytoskeleton and endocytosis, inhibition of phosphokinase C (PKC), induction of cell cycle arrest and apoptosis by modulation of protein kinases and other signaling pathways (Hudlicky et al., 1994; Smith et al., 2000). In addition to its functions in cell signaling, sphingosine has broad-spectrum antimicrobial properties against Gram-positive and Gram-negative bacteria (Fischer et al., 2012), enveloped viruses (Sakamoto et al., 2005), and fungi (Bibel et al., 1993). The antimicrobial property of sphingosine is important in tissues such as the skin, respiratory epithelium, and the oral cavity. *In vivo* studies show that sphingosine is enriched in the epithelial cells of the trachea and large bronchi of healthy lungs and that it rapidly eliminates bacterial pathogens, whereas sphingosine concentrations decrease and ceramide accumulates in the respiratory tract of transgenic mice with cystic fibrosis (Grassmé et al., 2017; Pewzner-Jung et al., 2014). Therefore, exogenous sphingosine via inhalation may be a successful antimicrobial therapeutic. In multiple CF animal models, pneumonia has been effectively prevented and treated with inhaled nebulized sphingosine without severe toxicity effects on host (Carstens et al., 2019; Grassmé et al., 2017; Pewzner-Jung et al., 2014; Tavakoli Tabazavareh et al., 2016).

1.7.3.1 Sphingosine and Bactria

It has been demonstrated that sphingosine has remarkably effective against bacterial pathogens including *P. aeruginosa, S. aureus, A. baumannii, H. influenzae, B. cepacia, M. catarrhalis, E. coli, F. nucleatum, S. sanguinis, S. mitis, C. bovis, C. striatum, and C. jeikeiu*m (Arikawa et al., 2002; Bibel et al., 1993; Fischer et al., 2013; Grassmé et al., 2017; Martin et al., 2017; Pewzner-Jung et al., 2014; Tavakoli Tabazavareh et al., 2016). Mechanism of sphingosine-mediated bacterial killing has been clarified by recent research (Verhaegh et al., 2020). Sphingosine treatment resulted in bacterial membrane permeabilization, intracellular ATP release, decreased metabolic activity, and decreased bacterial survival. This antibacterial activity is reliant on the sphingosine NH2 group. Under neutral and slightly acidic conditions, NH_2 groups are positively charged and protonated (Muraglia et al., 2019), interacting with cardiolipin in pathogens and effectively kill bacteria, while this effect is profoundly reduced at alkaline condition or in bacteria that lack cardiolipin synthase. The interaction of sphingosine and bacterial cardiolipin disturb the original membrane structure and lead to membrane permeabilization and bacterial death. The following might be the killing mechanism mediated by the interaction between

sphingosine and cardiolipin: when cardiolipin, which is negatively charged, binds to sphingosine, it may aggregate and form rigid, gel-like membrane domains. These domains cause membrane permeabilization and bacterial mortality by disrupting the original membrane structure. This theory should be evaluated further (Verhaegh et al., 2020).

1.7.3.2 Sphingosine and viruses

Viruses are small obligate intracellular parasites: they exploit membranes and their components, such as sphingolipids, at all the steps of their replication cycle including attachment and membrane fusion, viral replication, and budding from host cells (Virgin, 2014; Yamauchi & Greber, 2016). Some of them including human immunodeficiency virus, measles virus, Ebola virus, Sindbis virus, and rhinovirus exhibit sphingolipid-dependent entry by activating sphingomyelinases and using of ceramides as adherence and signaling platforms (Avota et al., 2011; Grassmé et al., 2005; Ng & Griffin, 2006). The direct effect of sphingolipids on viruses has been rarely investigated. Lang et al. first reported that cellular acid ceramidase is required for the restriction of HSV-1 replication and the deficiency of acid ceramidase led to the uncontrolled replication of HSV-1 (Lang et al., 2020). They showed that treatment of macrophage with sphingosine blocked HSV-1 replication. This study was the first to demonstrate an endogenous sphingosine's direct antiviral effects (Lang et al., 2020). Recently, various reports have been published on the role of lipid rafts as functional membrane microdomains enriched with sphingolipids, including gangliosides, and cholesterol, in the infection of the severe acute respiratory syndrome coronavirus-2 (SARS-CoV-2) of host cells (Fantini et al., 2020, 2021; Sorice et al., 2021). SARS-CoV-2, which is characterized by a high mortality rate, is the causative agent of coronavirus disease 2019 (COVID-19) (Zhou et al., 2020). SARS-CoV-2 use its viral spike glycoprotein for infecting cells and interact with human epithelial cells via its cellular angiotensin-converting enzyme-2 (ACE2) receptors (M. Hoffmann et al., 2020; Wang et al., 2020). Lipid rafts serve as an ideal interface for concentrating the ACE2 receptor on epithelial cell membranes, so that the interaction with the viral spike proteins is facilitated (Fantini et al., 2020, 2021; Sorice et al., 2021). Some other studies revealed that sphingosine plays a protective role against infection with SARS-CoV-2 (Edwards et al., 2020). It is shown that pre-treating cells with exogenous sphingosine blocked the interaction between the viral spike protein and cell receptor ACE2, thus provides a potential defense strategy against SARS-CoV-2 infection (Edwards et al., 2020).

Although, the direct antiviral effects of sphingosine on SARS-CoV-2 or HSV-1 remain unknown as of today's writing.

1.7.3.3 Sphingosine and fungi

Sphingolipids are one of the components of the fungal eukaryotic cell membrane (Obeid et al., 2002). Various investigations have concentrated on the diverse strategies that could be used to block the synthesis or/and function of fungal sphingolipids for development of new antifungal drugs (McEvoy et al., 2020; Rollin-Pinheiro et al., 2016). A variety of natural and synthetic compounds such as fumonisin B1 as an inhibitor of ceramide synthase or FTY720 (fingolimod) as a sphingosine-1-phosphate antagonist, as well as antibodies, which can attenuate fungal sphingolipids, have been reported to act against the fungal sphingolipid biosynthetic pathway (McEvoy et al., 2020; Rollin-Pinheiro et al., 2016). It has been demonstrated that inositol phosphoryl ceramide synthase inhibitors are effective against *C. albicans* infection (Zhong et al., 2000), and glucosylceramide and galactosyl ceramide synthase inhibitor blocked the germination and hyphal growth of *A. nidulans* (Levery et al., 2002). Bible et al. demonstrated that sphingosine has fungistatic property against *C. albicans* and could prevent germination and delay thalli formation (Bibel et al., 1993). The treatment of sphingosine may influence the proliferation of fungi and disrupt the balance of eukaryotic sphingolipid metabolism. Because the therapeutic options for, e.g., IA and also some *Candida* infections are limited, and because of the development of resistance to azoles, echinocandin, and amphotericin B (Fakhim et al., 2022; Howard & Arendrup, 2011), new antifungal compounds with novel mechanisms of action are greatly needed.

1.8 Aim of the study

The aim of this study is to develop a safe antifungal agent which is effective against wide range of fungal cells. The need for novel antifungal drugs is prompted by the significant risk of invasive fungal infections among the rising population of immunocompromised patients and the emergence of antifungal drug resistance. Thus, the researches of fungal infections again gain attention to develop new antifungal agent and better prophylactic and therapeutic strategies.

Sphingosine, which is consumed from ceramide by activity of ceramidases, has remarkable antimicrobial activities against a wide range of bacteria including *P. aeruginosa* and *S. aureus* (Pewzner-Jung et al., 2014; Tavakoli Tabazavareh et al., 2016) as well as viruses by interfering with the interaction between the virus and its receptor (Edwards et al., 2020; Sakamoto et al., 2005). In the current study, *in vitro* and *in vivo* antifungal activity and mechanism of sphingosine against *Candida* and *Aspergillus* species was investigated.

The mechanism of action of sphingosine in fungal cell death is investigated using *C. glabrata* cells for detecting apoptotic and/or necrotic hallmarks after sphingosine treatment.

The main aim of *in vivo* study is to create a safe and cost-effective nebulized sphingosine treatment which could be given to patients before organ transplantation to prevent IA occurring post-transplantation. Although several antifungal prophylactic drugs have already been developed to decrease the incidence of invasive fungal infections, the utility of these drugs is limited because of safety concerns, loss of efficiency due to drug resistance mechanisms and cost. It has already been reported that inhalation of sphingosine normalized the susceptibility of CF mice to develop pulmonary infections (Pewzner-Jung et al., 2014), indicating the significance of sphingosine for the defense of the airways against pulmonary infections without any significant side effect.

To achieve these aims, it is necessary to: (1) test antifungal activity of sphingosine *in vitro* to detect MIC and MFC values; (2) determine the mechanism of yeast cell death trigger by SPH; (3) test SPH for its ability to protect C57Bl/6 mice immunosuppressed with steroids and infected with *A. fumigatus*. (4) Perform detailed kinetic studies of the effect of sphingosine inhalation on infected mice and identify potential adverse effects of sphingosine inhalation.

2. Material

2.1 Chemicals and enzymes

Chemicals, enzymes and beads are listed in table 1.

Table 1. Chemical, enzymes and beads

Name	Manufacturer
Acetic acid (100%)	Merck KGaA, Darmstadt, Germany
Acrylamide	Carl-Roth GmbH & Co KG, Karlsruhe, Germany
C12 ceramide	Avanti Polar Lipids, Alabaster, USA
C16 ceramide	Avanti Polar Lipids, Alabaster, USA
C6 ceramide	Avanti Polar Lipids, Alabaster, USA
Cyclophosphamide	Baxter Oncology, Halle, Germany
D (+)-Glucose	Carl-Roth GmbH & Co KG, Karlsruhe, Germany
Deoxy ribonuclease I	Sigma-Aldrich Chemie GmbH, Steinheim, Germany
Dimethylsulfoxid (DMSO)	Sigma-Aldrich Chemie GmbH, Steinheim, Germany
EDTA Disodium (Dihydrate)	Sigma-Aldrich Chemie GmbH, Steinheim, Germany
Ethanol (absolute, anhydrous)	Diagonal GmbH & Co. KG, Münster, Germany
Glycerol (≥ 99%)	Carl-Roth GmbH & Co KG, Karlsruhe, Germany
Glycine	Carl-Roth GmbH & Co KG, Karlsruhe, Germany
HEPES	Carl-Roth GmbH & Co KG, Karlsruhe, Germany
Hydrochloric acid (37%)	Sigma-Aldrich Chemie GmbH, Steinheim, Germany
Ketamine	Medistar, Ascheberg, Germany
Menadione	Sigma-Aldrich Chemie GmbH, Steinheim, Germany
Methanol (≥ 99.8%)	Diagonal GmbH & Co. KG, Münster, Germany
$MgCl_2$, hexyhydrate	Carl-Roth GmbH & Co KG, Karlsruhe, Germany
$MgSO_4$, heptahydrate	Sigma-Aldrich Chemie GmbH, Steinheim, Germany
MOPS	Sigma-Aldrich Chemie GmbH, Steinheim, Germany
Mowiol	Kuraray Specialities Europe, Frankfurt, Germany
Na_2HPO_4, Dihydrate	Carl-Roth GmbH & Co KG, Karlsruhe, Germany
N-acetylcysteine (NAC)	Merck KGaA, Darmstadt, Germany
OGP	Sigma-Aldrich Chemie GmbH, Steinheim, Germany
Paraformaldehyde (powder, 95%)	Sigma-Aldrich Chemie GmbH, Steinheim, Germany
Potassium chloride (≥ 99%)	Carl-Roth GmbH & Co KG, Karlsruhe, Germany
RPMI1640 Powder	Sigma-Aldrich Chemie GmbH, Steinheim, Germany
SDS	Carl-Roth GmbH & Co KG, Karlsruhe, Germany
Sodium bicarbonate	Carl-Roth GmbH & Co KG, Karlsruhe, Germany
Sodium chloride (≥ 99.5%)	Carl-Roth GmbH & Co KG, Karlsruhe, Germany

Sodium citrate (tribasic, dehydrate)	Sigma-Aldrich Chemie GmbH, Steinheim, Germany
Sorbitol	Sigma-Aldrich Chemie GmbH, Steinheim, Germany
Sphingosine 1 phosphate d18;1	Avanti Polar Lipids, Alabaster, USA
Sphingosine d18;1	Avanti Polar Lipids, Alabaster, USA
Sucrose	Carl-Roth GmbH & Co KG, Karlsruhe, Germany
Tween 20	Carl-Roth GmbH & Co KG, Karlsruhe, Germany
Urea	Sigma-Aldrich Chemie GmbH, Steinheim, Germany
XTT powder	Biotum, San Francisco, USA
Xylazine	Serumwerk Bernburg AG, Bernburg, Germany
Zymolyase20t	Carl-Roth GmbH & Co KG, Karlsruhe, Germany

2.2 Kits, dyes and antibodies

Kits, dyes and antibodies used for cellular and molecular experiments, such as western blot, flow cytometry and ELISA are listed in Table 2.

Table 2. Kits, dyes and antibodies

Name	Manufacturer
Anti-mouse IgG, HRP-linked Antibody	Cell Signaling Technology, USA
Bradford Protein Dye Reagent	Bio-Rad Laboratories, Redmond, WA, USA
Cell Proliferation Kit I (MTT)	Roche Diagnostics, Mannheim, Germany
Cell proliferation kit II	Roche Diagnostics, Mannheim, Germany
DCFDA-H2DCFDA-Cellular ROS Assay kit	Abcam PLC, Cambridge, UK
ELISA Mouse IFN-γ Immunoassay	R&D Systems, Mckinley, MN, USA
ELISA Mouse TNF-α Immunoassay	R&D Systems, Mckinley, MN, USA
In Situ cell Death detection kit, TMR red	Roche Diagnostics, Mannheim, Germany
LIVE/DEAD® Yeast Viability Kit	Thermo Fisher Scientific, Waltham, USA
MitoSOX RED	Thermo Fisher Scientific, Waltham, USA
Periodic Acid-Schiff (PAS) Kit	Merck KGaA, Darmstadt, Germany
PLATELIA *ASPERGILLUS* Ag	Bio-Rad Laboratories, Redmond, WA, USA
Prestained Protein Ladder	Thermo Fisher Scientific, Waltham, USA
Propidium iodide (95-98%)	Sigma-Aldrich GmbH, Steinheim, Germany
Purified Mouse Anti-Cytochrome *c*	BD GmbH, Heidelberg, Germany
Rhodamine 123	Biotium Inc., Fremont, CA, USA
ROTI®Lumin kit	Carl-Roth GmbH, Karlsruhe, Germany

2.3 Fungal and tissue culture materials

Cells and fungal culture mediums and materials are listed in Table 3.

Table 3. Cells and fungal culture mediums

Name	Manufacturer
DMEM	Thermo Fisher Scientific, Waltham, MA, USA
RPM1 1640	Thermo Fisher Scientific, Waltham, MA, USA
F-12K	Thermo Fisher Scientific, Waltham, MA, USA
FBS	Thermo Fisher Scientific, Waltham, MA, USA
L-Glutamine	Thermo Fisher Scientific, Waltham, MA, USA
Non-essential amino acids	Thermo Fisher Scientific, Waltham, MA, USA
PenStrep	Thermo Fisher Scientific, Waltham, MA, USA
Sodium pyruvate	Thermo Fisher Scientific, Waltham, MA, USA
SDA, 55 mm Plate	Oxoid, Wesel, Germany
YPD broth	Gibco, Grand Island, NY, USA
SDA dry powder	Oxoid, Wesel, Germany
RPM1 1640 powder	Sigma-Aldrich GmbH, Steinheim, Germany

2.4 Software and databases

Software and databases used in this work are listed in Table 4.

Table 4. Software and databases

Name	Manufacturer
BD FACS Diva (Ver.8)	Becton Dickinson, New Jersey, USA
FlowJo™ v10.8	FlowJo LLC, BD, Ashland, OR, USA
GraphPad Prism (Ver.9)	GraphPad Software, La Jolla, CA, USA
ImageJ (Fiji)	ImageJ, Bethesda, Maryland, USA
ImageQuant	GE Healthcare, Freiburg, Germany
Leica advanced F (Ver.2.61)	Leica Mikrosysteme Vertrieb, Wetzlar, Germany
MACSQuantify (Ver.2.6)	Miltenyi Biotec, Bergisch Gladbach, Germany
MassHunter Software (Ver.11.0)	Agilent Technologies, Waldbronn, Germany
Microsoft Office (2021)	Microsoft Corporation, Redmond, WA, USA

2.5 Prepared buffers and solutions

Buffers and solutions used in this work are listed in Table 5.

Table 5. Prepared buffer and solutions

Name	composition
Phosphate buffered saline (PBS) pH:7.4	NaCl 136.9 mM KCl 2.7 mM 10 mM Na_2HPO_4 • 2 H_2O 2.0 mM KH_2PO_4 pH adjusted with HCl and NaOH
RPMI 2% G medium	RPMI 1640 powder 20,8 g MOPS 69.06 g Glucose 36 g up to 1 liter with ddH_2O pH 7.0
Ketamine/Xylazine	Ketamine 1.2 mL (100 mg/mL) Xylazine 0.1 mL (20mg/mL) up to 4 mL with NaCl Solution (0.9%) or PBS
Western blot buffer A	1.5 M Tris-HCl pH 8.8 0.4% SDS
Western blot buffer B	Tris-HCl 0.5 M, pH 6.8 0.4% SDS
Western blot transfer buffer	25 mM Tris 192 mM Glycine 10% Methanol
Tris-buffered saline (TBS)	Tris 30 mM NaCl 150 mM pH 7.5
TBS-Tween	TBS 0.1% TWEEN 20
10×SDS electrophoresis running buffer	Glycine 1.92 M SDS 1% Tris-HCl 333 mM pH 8.1 – 8.5 adjusted with HCl 37%
SDS running buffer	Tris 21.2 g $C_3H_8O_3$ 100.8 g 10% SDS 70.0 mL
Paraformaldehyde (PFA), 4%	4% PFA 1×PBS pH 7.2 – 7.4 adjusted with HCl and NaOH

Mowiol	20-25% Mowiol-488 2.5% Dabco
Reducing SDS sample buffer (5×)	250 mM Tris pH 6.8 0.2% bromphenol blue 8% 2-mercaptoethanol 4% SDS 20% Glycerine
Trypsin	0.25% Trypsin 5 mM Glucose 1.3 mM EDTA
10 mM Na-HEPES 2% Glucose	0,238 g HEPES 2 g Glucose ddH_2O to 100 mL pH 7.2 adjusted with NaOH
Spheroplasting buffer	2.4 M sorbitol 50 mM KH_2PO_4 40mM 2-mercaptoethanol (0.3%) pH 7.2
DTT buffer [100 mM Tris/H2SO4 (pH 9.4) for mitochondria extraction	10 mM Dithiothreitol] (for 15 mL) 1.5 mL of 1 M Tris/H_2SO_4 buffer (pH 9.4) 150 µl of 1 M DTT Volume to 15 mL
Zymolyase buffer [20 mM potassium phosphate (pH 7.4) 1.2 M sorbitol]	2 mL of 1 M Potassium phosphate buffer (pH 7.4) 60 mL of 2 M Sorbitol Volume to 100 mL
Homogenization buffer [10 mM Tris/HCl (pH 7.4) 0.6 M sorbitol, 1 mM EDTA, 0.2% (w/v) BSA]	2.5 mL of 1 M Tris/HCl buffer (pH 7.4) 75 mL of 2 M Sorbitol 500 µl of 500 mM EDTA 0.5 g of BSA Volume to 250 mL
SEM buffer [10 mM MOPS/KOH (pH 7.2), 250 mM sucrose, 1 mM EDTA]	2.5 mL of 1 M MOPS/KOH buffer (pH 7.2) 31.25 mL of 2 M Sucrose 500 µL of 500 mM EDTA Volume to 250 mL
EM buffer [10 mM MOPS/KOH (pH 7.2), 1 mM EDTA]	2.5 mL of 1 M MOPS/KOH buffer (pH 7.2) 500 µL of 500 mM EDTA Volume to 250 mL
10% OGP solution	1 g OGP powder Volume to 10 mL

2.6 Consumables

Consumable materials used in this work are listed in Table 6.

Table 6. Consumables

Name	Manufacturer
10 cm Petri dish	VWR International, LLC, Germany
2 mL syringe	Terumo Europe NV, Leuven, Belgium
96 well flat bottom plate	Sarstedt AG & Co, Nümbrecht, Germany
96 well-rounded bottom plate	Carl-Roth, Karlsruhe, Germany
Cell culture, 6, 24 and 96 well plate	Corning Inc., NY, USA
Cell strainer (70 µm, 100 µm)	Corning Inc., New York, NY, USA
Coverglass (18×18 mm)	Engelbrecht GmbH, Wien, Austria
Coverslips (Ø 12 mm)	Carl-Roth GmbH & Co, Karlsruhe, Germany
Filcons filter (10 µm pore size)	Filcons, BD, Franklin Lakes, NJ, USA
Fine dosage syringe I mL syringe	B. Braun, Melsungen, Germany
gentleMACS™ C Tubes	Miltenyi Biotec, Bergisch Gladbach, Germany
HistoBond (Microscope slides)	Marienfeld, Lauda-Königshofen, Germany
Hypodermic needle	Becton Dickinson GmbH, Heidelberg, Germany
Insulin syringe (1 mL)	Becton Dickinson GmbH, Heidelberg, Germany
Intracan-W (Intravenous catheter)	B. Braun, Melsungen, Germany
Microscopic slides	Langenbringen, Emmendingen, Germany
Needles (different gauges)	Becton Dickinson GmbH, Heidelberg, Germany
PE tube 1.5 mL	Sarstedt AG & Co, Nümbrecht, Germany
PE tube 15 mL	Greiner Bio-One, Frickenhausen, Germany
PE tube 50 mL	Greiner Bio-One, Frickenhausen, Germany
Pipettes (5 mL, 10 mL, 25 mL)	Greiner Bio-One, Frickenhausen, Germany
Reaction tubes, 2 mL	Eppendorf AG, Hamburg, Germany
Reagent Reservoir (25 mL)	Stellar Scientific, Baltimore, MD, USA
Sterile Cotton Swab	neoLab Migge, Heidelberg, Germany
Syringe filters ROTILABO, 0,45 µm	Carl-Roth, Karlsruhe, Germany
Syringes (5 mL, 10 mL, 20 mL)	Becton Dickinson GmbH, Heidelberg, Germany

2.7 Equipment

Equipment and instruments are listed in Table 7.

Table 7. Lab equipment and instruments

Name	Manufacturer
5417 R Centrifuge	Eppendorf AG, Hamburg, Germany
Analytical balance (0.0001g)	Waagenet AF, Berlin, Germany
Attune NxT Flow Cytometer	Thermo Fisher, Waltham, MA, USA
Cell culture incubator	Thermo Fisher, Waltham, MA, USA
Confocal fluorescence (TCS-SP5)	Leica, Wetzlar, Germany
Developer machine	Thermo Fisher, Waltham, MA, USA
Fridge, 4°C, Premium BioFresh	Liebherr-International, Germany
gentleMACS Dissociator	Miltenyi, Bergisch Gladbach, Germany
Glasswares (beakers, cylinders, flasks)	DURAN Group, Wertheim, Germany
Inverted fluorescence microscope (DMIRE2)	Leica, Wetzlar, Germany
Laboratory scale(0.1g)	Waagenet AF, Berlin, Germany
Magnetic stirrer (M21)	Intern. Laborat, Dottingen, Germany
Mass spectrometer (6530/6490)	Agilent, Waldbronn, Germany
Mechanical shaker (Rotamax120)	Heidolph, Schwabach, Germany
Microbial incubator	Binder GmbH, Tuttlingen, Germany
Microplate reader (SpectraMax Gemini EM)	MD, Biberach an der Riß, Germany
Microtome	Thermo Fisher, Waltham, MA, USA
Minus 20°C, Premium NoFrost	Liebherr-International, Germany
PARI BOY SX inhalation device	PARI, Starnberg, Germany
pH Meter (HI9025)	Hanna, Woonsocket, RI, USA
Pipettes (different sizes)	Nichiryo CO., Ltd., Saitama, Japan
Pipettus (pipetus-akku)	Hirschmann, Eberstadt, Germany
Spectrophotometer	Eppendorf AG, Hamburg, Germany
Spin tissue processor	Thermo Fisher Waltham, MA, USA
SpotChem EZ chemistry analyser	Scil animal care, Viernheim, Germany
Typhoon FLA 9500	GE Healthcare, Freiburg, Germany
Ultrasonic bath (sonorex RK 102 H)	BANDELIN, Berlin, Germany
Vacuum concentrator (SpeedVac)	Bachofer GmbH, Reutlingen, Germany

3. Experimental methods

3.1 Yeast strain and culture conditions

A wide range of fungal strains were utilized in this study, these strains are outlined in Table 8. All strains were stored as a 50% glycerol stock at −80°C and grown in a liquid YPD (Gibco, Grand Island, NY, USA) media. Fungal strains were kindly provided by the institute of microbiology, university hospital Essen.

Table 8. *Candida* and *Aspergillus* strains used throughout this project

Strain	Reference	Strain	Reference
C. glabrata	DSM70614	*A. fumigatus*	ATCC204305
C. glabrata	195	*A. fumigatus*	ATCC46645
C. glabrata	196	*A. fumigatus*	2446
C. glabrata	160	*A. fumigatus*	2453
C. krusei	ATCC6258	*A. fumigatus*	2150
C. krusei	F31	*A. fumigatus*	2151
C. krusei	132	*A. fumigatus*	2040
C. krusei	126	*A. niger*	F19
C. krusei	201	*A. flavus*	CM-1813
C. albicans	ATCC90028	*A. flavus*	2476
C. albicans	197	*A. flavus*	2435
C. albicans	204	*A. flavus*	2412
C. albicans	205	*A. brasiliensis*	1988
C. albicans	207	*A. tubingensis*	1884
C. albicans	212	*A. tubingensis*	1885
C. albicans	223		
C. tropicalis	DSM1346		
C. parapsilosis	ATCC22019		

3.2 Planktonic susceptibility testing

3.2.1 Determination of MIC toward *Candida* and *Aspergillus* strains

Minimal inhibitory concentrations (MIC) for yeasts and conidia forming molds was carried out according to the EUCAST guidelines (EUCAST definitive document E.DEF 7.3.2 and E.DEF 9.4, respectively) with a slight modification (Arendrup et al., 2012; Rodriquez-Tudela et al., 2008).

3.2.1.1 Preparation of sphingosine stock solution

The amount of sphingosine powder (d18; 1) (Avanti Polar Lipids, Alabaster, USA) to prepare a standard solution was calculated as follows:

$$\text{Weight (g)} = \frac{\text{Volume (L)} \times \text{Concentration (mg/L)}}{\text{Potency (mg/g)}}$$

$$\text{Volume (L)} = \frac{\text{Weight (g)} \times \text{Potency (mg/g)}}{\text{Concentration (mg/L)}}$$

According to this formula, 6.4 mg sphingosine should be diluted in 1 mL OGP 10% (Sigma-Aldrich, St. Louis, MO, USA) to prepare 6.4mg/mL (= 6400mg/L) stock. Stock solution could be stored at -20°C without significant loss of activity.

3.2.1.2 Preparation of sphingosine working solution

For preparation of working solution, the stock solution was diluted with 10% OGP as described in Table 9 to produce a dilution series at 200-fold the final concentration (intermediate concentration).

Table 9. ISO Scheme for preparing sphingosine dilution series with a final concentration of 0.06-32 mg/L

Step	Conc. (mg/L)	Source	Vol. of SPH (µL)	Vol. of OGP 10% (µL)	Intermediate conc. (mg/L)	Conc. (mg/L) after 1:100 dilution with double strength RPMI 2%G	Final Conc. (mg/L) after 1:1 dilution with inoculum suspension
1	6400	Stock	200	0	6400	64	32
2	6400	Stock	100	100	3200	32	16
3	6400	Stock	50	150	1600	16	8
4	6400	Stock	50	350	800	8	4
5	800	Step4	100	100	400	4	2
6	800	Step4	50	150	200	2	1
7	800	Step4	50	350	100	1	0.5
8	100	Step7	100	100	50	0.5	0.25
9	100	Step7	50	150	25	0.25	0.125
10	100	Step7	25	175	12.5	0.125	0.06

Then; 9.9 mL of double strength RPMI 1640 (Sigma-Aldrich, St. Louis, MO, USA) + 2% glucose (Sigma-Aldrich, St. Louis, MO, USA) + MOPS (Sigma-Aldrich, St. Louis, MO, USA) at a final concentration of 0.165 mol/L (pH 7.0) medium were dispensed to ten tubes (Sarstedt, 60.540.012) and 100 µL of sphingosine intermediate concentrations were added to each specific tube (1:100 dilution).

The concentration of solvent in the culture medium tubes was 0.1% and the concentration of sphingosine was 2×final concentration (0,125-64 mg/L).

3.2.1.3 Preparation of microdilution plates

Sterile plastic 96 well microdilution plates (Sarstedt, Nümbrecht, Germany) with flat-bottom wells were used for microdilution assays. 100 µL from each of the tubes containing the corresponding concentration (2×final concentration) of sphingosine were dispensed into wells 1 to 10 of each column of the microdilution plate. To each well of column 11 and 12, 100 µL of double strength RPMI 2% G medium was added. Thus, each well in columns 1 to 10 contained 100 µL of twice the final sphingosine concentrations in double strength RPMI 2% G medium with 0.1% OGP. Columns 11 and 12 contained double-strength RPMI 2% G medium.

3.2.1.4 Preparation of inoculum

All *Candida* strains were grown on sabouraud glucose agar (OXOID, PO5001A) at 37°C for 24 h. Then five distinct colonies, ≥ 1 mm diameter from 24 h cultures were suspended in at least 3 mL of sterile distilled water. The suspension was homogenized for 15 seconds with a gyratory vortex mixer at approximately 2000 rpm.

Aspergillus strains were cultured on SDA agar plates at 37°C for 2-5 days. Colonies were covered with approximately 5 mL of sterile water supplemented with 0.1% Tween 20. Then, the conidia were carefully rubbed with a sterile cotton swab and transferred with a pipette to a sterile tube and filtered via 10µM syringe filter (BD, filcon, 340728) to separate conidia from hyphae and clumps.

Fungal cells were counted with a Neubauer chamber (Marienfeld, 0640710). Because of the small size of fungi compared to eukaryotic cells, only 4 of 25 medium square in the large central square of the Neubauer chamber were counted and CFU/mL was calculated as follow:

$$\text{CFU/mL} = 1000 \times \frac{\text{Average count of colonies in 4 medium square} \times \text{Dilution factor}}{\text{No. of small square}(16) \times \text{depth}(0.1\text{mm}) \times \text{surface } (0.0025\ \text{mm}^2)}$$

The fungal suspension was adjusted to 2-5×10^6 CFU/mL. A working suspension was prepared by a 1 in 10 dilution of the standardized suspension in sterile distilled water to yield 2-5×10^5 CFU/mL.

3.2.1.5 Inoculation, incubation and reading Results

100 µL of the 2-5×10^5 CFU/mL fungal suspension was added to column 1 to 10, without touching the contents of the well. This gave the required final drug concentration (final concentration = 0.06-32 mg/L) and inoculum density (final inoculum = 1-2.5×10^5 CFU/mL). Also, the growth control wells (column 11), containing 100 µL of sterile drug-free medium, was inoculated with 100 µL of the same inoculum suspension (growth control well). column 12 of the microdilution plate was filled with 100 µL of sterile distilled water (drug-free control). Plates were incubated at 35 ± 2ºC without agitation in ambient air for 24 ± 2 h. After incubation time, the absorbance of the plates was measured at 450 nm. The value of the blank (background) was subtracted from readings for the rest of the wells. The MIC of sphingosine is the lowest concentration giving rise to an ≥ 90% inhibition of growth relative to the drug-free control.

3.2.2 Determination of minimum fungicidal concentrations (MFC) of sphingosine

The minimum fungicidal concentration (MFC) was determined by spotting total volume (200 µL) aliquots from wells with no apparent growth onto SDA plates and incubating these at 37°C for 24-48 h. The lowest sphingosine concentration producing less than three colonies, which corresponds to killing ≥ 99.9% of the inoculum, was defined as the MFC.

3.3 Preformed biofilm studies

3.3.1 *In vitro* biofilm formation assay

Biofilms of *Candida* spp. were formed in flat-bottomed 96-well microplates as described by Stepanovic with some modifications (Stepanović et al., 2007). For each strain, a cell suspension in RPMI 1640 medium supplemented with 2% (w/v) glucose was adjusted to 1 × 10^6–5 × 10^6 CFU/mL as determined by cell counts using a hemocytometer Neubauer improved chamber. Plate wells were inoculated with 200 µL of standardized yeast suspension in triplicate and incubated at 37 °C for 90 minutes to allow cell adhesion. A negative control was prepared by inoculating 200 µL of a yeast suspension inactivated by

boiling. After the adhesion phase, non-adherent cells were removed by thoroughly washing the wells with 0.15 M sterile phosphate-buffered saline (PBS, pH 7.2). Each well was then filled with 200 µL of fresh RPMI 1640, and the plate was incubated at 37 °C for 24 h to allow biofilm formation.

To assess biofilm formation, the culture broth was gently aspirated, and each well was washed twice with PBS and dried at 60 °C for 30 minutes. The biofilm was stained by incubation for 30 min with 50 µL of a 1% (w/v) crystal violet solution. Any excess of crystal violet was removed by washing with PBS before adding 150 µL of absolute ethanol to release the dye from the biofilm. The absorbance was measured at 590 nm using a Microplate reader (SpectraMax Gemini EM) and was related to the amount of biofilm produced. The interpretation of obtained results requires definition of the cut-off value that separates biofilm-producing from non-biofilm-producing strains. The average OD values calculated for all tested strains and negative controls, since all tests were per-formed in triplicate and repeated three times. Second, the cut-off value (OD_C) should be established. It is defined as three standard deviations (SD) above the mean OD of the negative control: OD_C = average OD of negative control + (3×SD of negative control). Final OD value of a tested strain was expressed as average OD value of the strain reduced by OD_C value (OD = average OD of a strain - OD_C). OD_C value was calculated for each microtiter plate separately. If a negative value was obtained, it should be presented as zero, while any positive value indicates biofilm production. The easier interpretation of the results is listed in Table 10.

Table 10. Criteria of interpretation of biofilm production

Biofilm producer	OD Values
No biofilm producer	$OD < OD_C$
Weak biofilm producer	$OD_C < OD \leq 2\times OD_C$
Moderate biofilm producer	$2\times OD_C < OD \leq 4\times OD_C$
Strong biofilm producer	$4\times OD_C < OD$

According to this table, strains divided into the following categories, no biofilm producer ($OD \leq OD_C$), weak biofilm producer ($OD_C < OD \leq 2\times OD_C$), moderate biofilm producer ($2\times OD_C < OD \leq 4\times OD_C$) and strong biofilm producer ($4\times OD_C < OD$).

3.3.2 Antifungal susceptibility testing of 24 h-old *Candida* biofilms

Candida biofilms were produced as described above; upon mature biofilm formation, the medium was aspirated, and each well was washed twice gently with 200 µL of PBS to remove planktonic cells. Sphingosine aliquots (200 µL per well) ranging from 1–16 times the planktonic MICs were added, and the plate was incubated for 24 h. Sphingosine-free wells were included as positive controls. After 24 h incubation with different concertation of sphingosine, anti-biofilm activity of sphingosine was quantified with XTT assay using XTT cell proliferation Kit II (Roche, ≠11465015001). The anti-biofilm activity of antifungal drug was referred to as the minimum biofilm eradication concentration (MBEC), which is defined as the minimum sphingosine concentration resulting in 80% disruption of the biofilm compared to a peptide-free control culture.

3.4 Growth-inhibition kinetic studies for the *A. fumigatus*

3.4.1 Quantification of viable conidia using XTT

Before the tests were performed, *A. fumigatus* (ATCC46645) was grown for 48-72h at 35°C on SDA (Oxoid, Wesel, Germany) plates. Conidia were harvested with sterile water supplemented with 0.1% Tween 20. Different conidial concentrations (1×10^9, 5×10^8, 1×10^8, 5×10^7, 1×10^7, 5×10^6, 1×10^6, 5×10^5 and 1×10^5) were prepared in RPMI 1640 + MOPS + 2% glucose (pH 7.0). 200 µL of each concentration were added to the flat bottom 96 well plate and 50 µL of XTT (Santa Cruz Biotechnology, Dallas, TX, USA) (1 mg)/menadione (Sigma-Aldrich, St. Louis, MO, USA) (0.17 mg) solution was added to inoculated wells. Plates were incubated at 37°C for 2 h. Optical density of each inoculum concentration was measured at 450 nm. A standard calibration curve was plotted with log CFU/mL and the respective absorbance within the XTT reduction assay and used as reference for quantification of viable cells (Kiraz et al., 2011).

In addition, viability counts were performed for quality control purposes to ensure that test wells contain the correct amount of CFU/mL as follows. The conidial suspensions were homogenized with a gyratory vortex mixer at 2000 rpm. Then aliquots of prepared concentrations were serially diluted with sterile water and 100 µL spread out over the surface of a potato dextrose agar plate for colony forming unit determination.

3.4.2 Time kill kinetic studies with XTT reduction assay

XTT reduction assays were performed for time-kill kinetics as described previously with slight modifications(Öz et al., 2016). Separate 96 well microplates were used for different time-points of incubation (0, 1, 2, 4, 6, 8, 10, 24, 48h). Three different concentrations of sphingosine were prepared and 100 µL from each of the tubes containing the corresponding concentration (2×final concentration) of sphingosine were dispensed into wells 3 to 5 of each column of the microdilution plate. To each well of column 6 and 7, 100 µL of double strength RPMI 2% G medium without sphingosine were added. The inoculum was quantified using a hemocytometer and adjusted to 2×10^6 to 5×10^6 CFU/mL with sterile water. 100 µL of the fungal suspension was added to column 3 to 5, without touching the contents of the well. This gave the required final drug concentration (0.5×MIC, 1×MIC, 2×MIC) and inoculum density (final inoculum = $1\text{-}2.5\times10^6$ CFU/mL). Also, the growth control wells (column 6), containing 100 µL of sterile drug-free medium, was inoculated with 100 µL of the same inoculum suspension. Column 7 of the microdilution plate was filled with 100 µL of sterile distilled water (drug-free control). Plates were incubated at 35 ± 2 ºC without agitation in ambient air up to 24h. At the indicated time-points 2 h prior to the indicated incubation time, 50 µL of XTT–menadione solution was added to each well. After 2 h incubation the formazan absorbance was measured at 450 nm with a microplate reader (BMG Labtech, Midland, ON, Canada).

The number of colonies/mL was calculated according to the standard calibration curve. The procedure was performed in triplicate (three independent experiments) and a graph of the log CFU/mL was plotted against time.

3.5 Growth-inhibition kinetic studies for the *C. glabrata*

Prior to initiation of the growth-inhibition kinetic studies, the antifungal carryover effect was determined by the method described by Klepser, M.-E.et al. (Klepser et al., 1998). Additionally, all samples were plated as a single spot on Saboraud-dextrose agar plates and allowed to diffuse into the agar for 10 min before spreading. After the plate had dried, streaking was performed (Lignell et al., 2007).

After carry over determination, growth-inhibition kinetic studies were assessed (Cantón et al., 2004; Klepser et al., 1997).

Before the tests were performed, *C. glabrata* (DSM70614) was grown for 24 h at 35°C on SDA (Oxoid, Wesel, Germany) plates. The inoculum was quantified using a

hemocytometer and adjusted to 2×10^6 to 5×10^6 CFU/mL. The adjusted inoculum suspension was diluted 1:10 either in RPMI 1640 medium buffered with MOPS buffer and 2% Glucose (control) or in RPMI 1640 medium buffered with MOPS buffer and 2% Glucose containing the appropriate concentration of sphingosine (1×MIC, 2×MIC) and Cells were incubated at 35°C and 200 rpm. This procedure yielded an initial inoculum ranging 2×10^5 to 5×10^5 CFU/mL and sphingosine concentration of 0.5, 1, 2 and 4 µg/mL. at predetermined time points (0, 2, 4, 6, 8, 10, 12, 24h), a 1 mL aliquot from both the control tube (drug free) and each tube with a test solution and serially diluted in sterile water and streaked on a potato dextrose agar plate for colony forming unit determination. All experiments were run in triplicates.

3.6 Mechanism of action of sphingosine

3.6.1 Yeast strain and growth profile

C. glabrata DSM70614 was selected for further *in vitro* experiments. It grows in three main phases– the lag phase, the exponential phase and the stationary phase like other fungal strains. When a culture of yeast cells is inoculated in a fresh growth medium, they enter a brief lag phase where they are biochemically active but not dividing. The lag phase refers the initial growth phase, when number of cells remains relatively constant prior to rapid growth, also referred as adaptation time. During this phase the individual cells are actively metabolizing, in preparation for cell division. The cells usually activate the metabolic pathways to make enough of the essential nutrients to begin active growth. The third phase in growth of yeast is stationary phase when metabolism slows and the cells stop rapid cell division. To perform reliable and repeatable *in vitro* experiments, *Candida* cells should always be grown until the middle of the exponential phase.

5 mL *Candida* suspension (10^7 cells/mL) was dispensed into two sterile conical flasks, each containing 45 mL of fresh YPD broth. The flasks were incubated at 30°C and 37°C for 60 h in a shaking incubator to continuously agitate the suspension. Spectrophotometric assay, which was based on continuous monitoring of changes in the optical density of cell growth was employed. Cell growth was measured periodically at every one-hour interval over a period of 60 h at an on optical absorbance of 600 nm. The growth of *C. glabrata* can be distinguished by measuring the changes of specific growth rate (µ) and doubling time (g) following equations previously described (Nordin et al., 2013).

i) Specific-growth rate: $\mu = \frac{\log10(Nt/N0)}{t2-t1}$

ii) Doubling time: $g = \frac{\log10(Nt/N0)}{\log10(2)}$

Where, N_t represented the number of cells at log phase, N_0 represented the number of cells at zero time, t_2 was the time taken to reach plateau, and t_1 zero time when the cells enter the log phase (Meletiadis et al., 2001).

3.6.2 Cell wall staining

The effect of sphingosine on the cell wall of *Candida* was determined by calcofluor white (CFW) staining as previously describe (C. Allen et al., 2006; Essary & Marshall, 2009; H. S. Lee & Kim, 2020) with few modifications. *C. glabrata* DSM70614 were cultivated in YPD broth at 35°C up to the mid-exponential phase, 2-5×10^5 cells/mL were treated with two different concentrations of sphingosine at a final concentration equal to 1×MIC and 2×MIC for 4 h (37°C, 200 rpm). After incubation cells were harvested, washed with 2% D-(+)-glucose (Sigma-Aldrich, St. Louis, MO, USA) containing 10 mM Na-HEPES (Sigma-Aldrich, St. Louis, MO, USA), pH 7.2 and adjusted to a concentration of 5×10^7 cells/mL. Fungi incubated in 70% ethanol for 4h were used as positive control (Wenisch et al., 1997). Samples were stained with Molecular Probes' LIVE/DEAD® Yeast Viability Kit containing two fluorescent probes for yeast viability (FUN 1) and cell wall staining (Calcofluor White M2R) was performed according to the manufacturer's instructions. Concisely, 100 µL of the yeast suspension containing 10 µM FUN1 was mixed with 100 µL Calcofluor White M2R (final conc.: 25 µM). Cells were incubated at 30°C in the dark for 30 min and analyzed by confocal microscopy (Leica Microsystems, Wetzlar, Germany).

3.6.3 Plasma membrane disruption assay using propidium iodide

C. glabrata DSM70614 were cultivated and treated as mentioned above with different concentrations of sphingosine as indicated or 2 µg/mL amphotericin B as positive control. After incubation for the indicated time-points, cells were washed 3 times in PBS and then incubated with propidium iodide (1 µg/mL final concentration) for 5 min at room temperature. The mean fluorescence intensity values of 10,000 events were measured per sample using an Attune NxT Flow Cytometer (Pina-Vaz et al., 2001).

3.6.4 Intracellular ROS formation assay

Endogenous levels of ROS were assessed using 2', 7'dichlorodihydrofluorescein diacetate (H_2DCFDA; Molecular Probes) (W. Lee et al., 2019; Sun et al., 2017). Briefly, *C. glabrata* DSM70614 cells were cultivated and exposed to the indicated concentrations of sphingosine at 37°C, along with 50 µM tert- butyl hydrogen peroxide (TBHP) and 10 µg/mL antimycin A as positive control. At the indicated time-points aliquots were removed and stained with 10 µM DCFH-DA at 37°C for 30 min. After three times washing with PBS, the fluorescence intensities (excitation/emission at 485 nm/535 nm) of cells were measured using an Attune NxT Flow Cytometer.

3.6.5 Mitochondrial membrane potential determination (ΔΨm)

Disruption of mitochondrial membrane potential was assessed by staining with rhodamine (Rh)-123 as a fluorescent probe that is induced via mitochondrial energization(Britta et al., 2014; Ludovico et al., 2001; Shirazi & Kontoyiannis, 2015).

C. glabrata DSM70614 cells were cultivated and exposed to the indicated concentrations of sphingosine at 37°C and harvested after the indicated time-points and stained with Rh-123 (25µM for 10 min). Treatment with 20 mM sodium azide (NaN_3) was used as positive control. After staining with Rh-123, cells were washed three times with PBS, and the mean fluorescence intensity values of 10,000 events were measured per sample using an Attune NxT Flow Cytometer.

3.6.6 Measurement of mitochondrial ROS levels

In order to detect mitochondrial ROS of live cells MitoSOX Red dye was utilized (Molecular Probes) according to the manufacturer's instruction (Britta et al., 2014; C. K. Chang et al., 2021; W. Lee et al., 2019). *C. glabrata* DSM70614 cells were cultivated and exposed to the indicated concentrations of sphingosine at 37°C and harvested after the indicated time-points by centrifugation at 10,000 rpm for 5 min and incubated in 1×HBSS (Hank's Balanced Salt buffer without phenol red) containing 5 µM MitoSOX Red for 15 min at 37°C, protected from light. The cells were then washed three times with prewarmed buffer and the fluorescent cells were analyzed using a BD FACSCalibur flow cytometer.

3.6.7 Cytochrome *c* release from isolated mitochondria.

Isolated and functional mitochondria were used to investigate cytochrome *c* release as described with minor adjustments (Gregg et al., 2009; Wu et al., 2010; Wunder et al., 2004).

3.6.7.1 Purification of mitochondria

C. glabrata DSM70614 cells were cultured in YPD medium for 16 h at 30°C, collected by centrifugation at 3000 g, and washed twice with distilled water. The supernatant was discarded and the wet weight of cell pellet was determined, then the pelleted cells were resuspended in 2 mL DTT buffer (100 mM Tris/H_2SO_4 (pH 9.4), 10 mM Dithiothreitol) per gram wet weight. Cells were incubated for 20 min at 30°C and 70rpm and harvested by centrifugation for 5 min at 3000×g at room temperature. Pelleted cells were washed twice in zymolyase buffer without zymolyase [7 mL of 20 mM potassium phosphate (pH 7.4) 1.2 M sorbitol buffer/g (wet weight)]. The powder of Zymolyase-20T [5 mg of Zymolyase-20T/g (wet weight) cells] added to the cell suspension. Cells were then incubated for 30 min at 30°C with slight agitation in order to form spheroplasts. *Candida* spheroplasts were washed with 10 mM Tris/HCl (pH 7.4), 0.6 M sorbitol, 1 mM EDTA and 0.2% (w/v) BSA buffer and homogenized in a pre-chilled glass homogenizer.

Unbroken cells, nuclei, and large debris were pelleted by centrifuging for 5 min at 1500×g at 4°C and mitochondria were purified with sucrose density gradient centrifugation [60, 32, 23 and 15% (w/v) sucrose in 1 mM MOPS/KOH (pH 7.2), 1mM EDTA] at 134000 g for 1h.

3.6.7.2 Sphingosine treatment and sample preparation

Isolated mitochondria (0.9 mg of protein/mL) were incubated for 10, 30 and 60 min in presence and absence of sphingosine as indicated along with 1 mM H_2O_2 (positive control). After incubation, mitochondria were pelleted by centrifugation at 12000 *g* at 4°C for 15 min. After lysis and determination of protein concentration with Bradford assay, the supernatant and pellet fractions were subjected to SDS-polyacrylamide gel electrophoresis (PAGE) and analyzed by western blotting.

3.6.7.3 Western blot analysis

20 µg of each sample was run on a 10% SDS gel. Before, mitochondria and supernatants were added to 5×sodium dodecyl sulfate (SDS) sample buffer and boiled for 5 min at 95°C. Next, the samples were shortly mixed and centrifuged and loaded on the gel. 10 µL pre-stained protein standard was loaded on the first slot of the gel as ladder. The whole system was connected to a power supply. The gel was run for the first 10 minutes with 50 mA, so the samples in all the stacking gel slots settled. The remaining electrophoresis was performed at 70 mA for the separation. For blotting, while the SDS gel was running, a piece of PVDF membrane was incubated in methanol for 1 minute, then 5 minutes in ddH_2O and finally for 10 minutes in transfer buffer. When the gel was ready it was incubated for 10 minutes in transfer buffer at room temperature. Lastly, the blot was made using two pads and three Whatman papers, all pre-rinsed in transfer buffer on each side of the cassette and the nitrocellulose membrane (Amersham Protran Premium 0.2 µm, GE Healthcare) and gel were placed in the middle. The cassette was placed in a chamber filled with transfer buffer plus 10% methanol and was connected to a power supply with constant voltage of 80 V for 2 hours at 4°C.

After the transfer of the proteins from the gel to the nitrocellulose membrane, the membrane was incubated in 3% BSA in TBS-Tween (0.1%) for 1 hour at room temperature on a shaker for blocking to prevent nonspecific binding of the antibodies. The membrane was incubated with specific primary antibodies against cytochrome *c* (BD, 556433) (1:500) overnight at 4°C or 1 h at room temperature. After 5 washes in TBS/Tween, blots were incubated for 1 h at room temperature in TBS/Tween with Horseradish peroxidase-linked goat anti-rabbit immunoglobulin G (Santa Cruz, sc-2004, dilution:1/10000). After this step, the 5 washing steps just like before took place. Finally, for further development, ROTI®Lumin HRP substrate (Roth, P078.1) was used according to the manufacturer's protocol and the protein bands were visualized. The intensity of signals from western blot analysis were quantified using a Typhoon™FLA 9000 biomolecular imager.

3.7 Quantification of C16 ceramide, S1P and sphingosine

Ceramides, sphingosines, and S1Ps were quantified by Dr. Fabian Schumacher (Freie Universität Berlin, Germany) by rapid resolution liquid chromatography/mass spectrometry as recently described (Gulbins et al., 2018).

Briefly, sensitive (DSM70614) strain of *C. glabrata* was cultivated in YPD broth for 16h. Then, 10^6 cell/mL of strain was incubated with increasing concentrations of sphingosine

(2 µg/mL, 1 µg/mL and 0.5 µg/mL) in RPMI. Samples were washed 2-3 times with ice-cold PBS after predetermined timepoints, shock-frozen in liquid nitrogen and stored at -80° for further measurement.

For extracting lipid, cell pellets were sonicated on ice for 15 min. For saponification, the samples were then incubated with 150 µL methanolic KOH (1 M) for 2 h at 37°C with gentle shaking. Samples were then neutralized with 12 µL glacial acetic acid and centrifuged at 2200×g for 10 min at 4°C. The organic phase was dried in a Savant SpeedVac concentrator (Thermo Fisher Scientific). The dried samples were reconstituted in 200 µL of acetonitrile/methanol/water (47.5: 47.5: 1, v: v: v) and acidified with 0.1% formic acid. Samples were thoroughly vortexed for 10 min at 1500 rpm and centrifuged at 2200×g for 10 min at 4°C for mass spectrometric sphingolipid quantification. Ceramides were analyzed using a 6530-mass spectrometer (Agilent Technologies, Waldbronn, Germany). Sphingosine and S1P were analyzed with a 6490 triple quadrupole mass spectrometer (Agilent Technologies). Both instruments were interfaced with an electrospray ion source operating in the positive ion mode (ESI+). Ceramides, sphingosine, and S1P were analyzed in MS/MS mode utilizing the fragmentation of the precursor ions into the production m/z 264.3 (for S1P and all ceramides) or m/z 282.3 (for sphingosine). Quantification was performed using the MassHunter software (Agilent Technologies).

3.8 Infection and inhalation studies in laboratory murine model

3.8.1 Mice model

To test the efficacy of sphingosine *in vivo* a low-dose inhalational model of murine pulmonary aspergillosis was used. C57Bl/6 mice, weighing 18–20 g, were used in this study. Breeding and experimental procedures were approved by the State Agency for Nature, Environment and Consumer Protection (LANUV), approval number AZ 81-02.04. 2019. A153, NRW in Düsseldorf, Germany. Mice were immunosuppressed with 250 mg/kg of cyclophosphamide (Baxter Oncology, Halle, Germany) intraperitoneally and 200 mg/kg cortisone acetate (Sigma-Aldrich, St Louis, MO, USA) subcutaneously on day -2 relative to infection (day 0), followed by a second dose of cyclophosphamide (200 mg/kg) and cortisone acetate (200 mg/kg) on day +3.

3.8.2 Preparation of *A. fumigatus*

Wild type *A. fumigatus* strain ATCC46645 was used throughout the project. *Aspergillus* conidia were cultured on SDA plates at 37°C for 2-5 days. Colonies were covered with approximately 5 mL of sterile water supplemented with 0.1% Tween 20. Then, the conidia were carefully rubbed with a sterile cotton swab and transferred with a pipette to a sterile tube and filtered via 10 µM syringe filter (BD, filcon, 340728) to separate conidia from hyphae and clumps. Fungal conidia were counted with Neubauer chamber as described above and adjusted to 0.5-1×10^6CFU/mL with normal saline.

3.8.3 Intratracheal intubation

Immunosuppressed mice were infected intratracheally as described previously(Sheppard et al., 2006). C57Bl/6 mice were anesthetized with 87.5 µg/g Ketamine (medistar, Ascheberg, Germany) and 12.5 µg/g Xylazine (Serumwerk Bernburg AG, Bernburg, Germany). The mouse was fastened via the teeth on a special stage and the tongue was pulled aside by a laryngoscope. A 22 G Intravenous (IV) catheter (B. Braun medical Ltd, Sheffield, UK) was placed into the trachea and 50 µL *A. fumigatus* conidia with the concentration of 0.5-1×10^6 CFU/mL was instilled into the lung (2.5-5×10^4 conidia/50 µL) Control mice received normal saline only.

3.8.4 Sphingosine inhalation

For treatment studies, mice were immobilized in a restrainer and the clinically approved nebulizer (PARI BOY SX inhalation device, Starnberg, Germany) was used for nebulizing sphingosine/0.5% w/v OGP or 0.5% w/v OGP as control. Treatment started on day -3 and was inhaled daily in 1 mL volume over 10 minutes until the indicated time-point. On day 0 inhalation was applied 1 hour before infection with *A. fumigatus*.

3.8.5 Behavioral abnormalities and weight records

During the *in vivo* studies, burden of the mice was monitored twice per day using a scoring system that included body weight, pulmonary symptoms, general condition changes, and behavioral changes. In fact, burden was manifested by weight reduction and behavioral changes, so that a weight loss of 10-19% or more and self-isolation with lethargy was considered the end point of the analysis and the respective animal was immediately put to death using CO_2 fumigation.

3.9 Fungal burden in mouse lung

Mice were pre-treated with cyclophosphamide and cortisone acetate, infected with fungal forms, and, in case, inhaled with sphingosine as described above. Mice were put to death by CO_2 fumigation immediately post-infection (day 0) and at day 4 post-infection. At each time-point, two immunosuppressed but uninfected mice were included as negative controls (Sheppard et al., 2006; Shirkhani et al., 2015). The lungs were removed by sterile dissection, transferred to 2 mL of NaCl 0.85% w/v in a purple capped C-tube (Miltenyi Biotec, Bergisch Gladbach, Germany). The C-tube's lid was closed tightly and placed upside down into the gentleMACS dissociator (Miltenyi Biotec, Bergisch Gladbach, Germany). This instrument has two programs for dissociation of the lungs into single cells. Program one cuts the lung tissue into pieces by gentle rotation for 37 Seconds and program two turns the lung tissue pieces into a single cell suspension in 38 Seconds. After performing both programs one after the cell suspension was filtered through a 70 µM Falcon cell strainer (Fisher Scientific, Schwerte, Germany). At this point five PE 1.5 mL tubes numbered from 1 to 5 were filled with 900 µL PBS for the serial dilution of the single cell suspension. From the undiluted suspension, 100 µL was directly spread in a 10 cm SDA petri dish. Next, the single cell suspension was diluted 1:100 with PBS (100 µL undiluted suspension to 900 µL PBS in tube 1). From this tube 100 µL suspension was pipetted to tube number 2 with 900 µL PBS. With the same fashion, 5 dilutions were prepared and all of them got spread on SDA. The plates got incubated in 37°C. Right after 24 hours the grown colonies on the plates were counted if possible.

3.9.1 CFU calculation

The calculations were done as follow:

$\text{CFU}_{\text{Lung}} = \text{CFU}_{\text{counted}} \times \text{dilution factor}_{\text{plate}} \times \text{dilution factor}_{\text{suspension}}$

$\text{Dilution factor}_{\text{plate}}$ = Undiluted (1), 10, 100, 1000, 10000, 100000

$$\text{Dilution factor}_{\text{suspension}} = \frac{2000^{*}(\mu L) + \text{Volume}_{\text{plate}}}{\text{Volume plate}}$$

* 2000 µL indicates the amount of PBS in which the lung tissue was dissociated in the C-tube initially. This value can be variable from experiment to experiment.

The plates with less than 3 and more than 300 colonies were not included in the results. All counts were performed in triplicates.

3.10 Galactomannan enzyme immunoassay

Mice were pre-treated with cyclophosphamide and cortisone acetate, infected with fungal forms, and, in case, inhaled with sphingosine as described above. Mice were put to death by CO_2 fumigation immediately post-infection (day 0) and at day 4 post-infection. At each time-point, two immunosuppressed but uninfected mice were included as negative controls. In each time point (day 0 and day +4), the mice were fixed on a silicone pad on the bench top and the skin was cut opened. The salivary glands and the muscles around the tracheae were carefully removed. A 22 G IV catheter was placed into the trachea and 0.5 mL ice cold PBS was instilled into the lung with a 1 mL syringe and directly the PBS got aspirated and was collected in a 15 mL PE tube on ice. The same procedure was performed 3 times in order to collect as many cells as possible from the lung. In the first round of aspiration the amount of returned liquid is normally less than the following times and the fact is that the main portion of the washed cells are collected during the first couple of aspirations. Galactomannan was quantified in 300 µL aliquots of BAL fluid using Platelia Galactomannan EIA kits (Bio-Rad, Edmonds, WA, USA) according to the manufacturer's instructions. The assay uses rat EBA-2 monoclonal antibodies, which are directed against *Aspergillus* galactomannan, and have been characterized in previous studies(van Hoecke et al., 2017). The monoclonal antibodies were used, (1) to coat the wells of the microplate and bind the antigen, and (2) to detect the antigen bound to the sensitized microplate (conjugate reagent: peroxidase-linked monoclonal antibodies). Briefly, 300 µL BAL fluid samples were mixed with 100 µL Sample Treatment Solution, then were treated for 6 minutes in a heat block at 120°C in the presence of EDTA in order to dissociate immune complexes and to precipitate proteins that could possibly interfere with the test. Tubes were centrifuged at 10,000×g for 10 minutes and the supernatant was used for the detection of the galactomannan antigen. 50 µL of conjugate and 50 µL of treated BAL supernatant were added to the wells coated with monoclonal antibodies, and incubated for 90 ± 5 minutes at 37°C. A monoclonal antibody-galactomannan-monoclonal antibody/peroxidase complex was formed in the presence of galactomannan antigen. The strips were washed 5 times using 800 µL of working washing solution (available in the kit) to remove any unbound material. Next, 200 µL Chromogen TMB solution was added, which reacted with the complexes bound to the well to form a blue color reaction. The enzyme reaction was stopped by the addition of acid (100 µL of Stopping Solution), which changes the blue color to yellow. The absorbance (optical density) of specimens and

controls was determined with a spectrophotometer set at 450 nm (reference filter of 620/630 nm).

3.10.1 Validity criteria and calculations

Cut-off, negative and positive controls should pass the criteria as mentioned in the manufacturer protocol. OD cut off should be 0.3 < OD ≤ 0.8, positive control > 1.50 and negative control OD < 0.4. Failure of any of the controls to meet the validity criteria described above renders the assay invalid, and patient specimen results should not be reported. Then the average values of samples were calculated as below:

$$\text{Sample Index} = \frac{\text{OD sample}}{\text{Mean Cut-off Control OD}}$$

3.11 Cytokine detection

At designated time point, mice were sacrificed by CO_2 asphyxia. Lungs were then harvested for assessment of cytokine protein expression. The lungs were removed by sterile dissection, transferred to 1 mL of PBS in a purple capped C-tube (Miltenyi Biotec, Bergisch Gladbach, Germany). The C-tube's lid was closed tightly and placed upside down into the gentleMACS dissociator (Miltenyi Biotec, Bergisch Gladbach, Germany). The homogenates were centrifuged at 1400×*g* for 10 min and supernatants were collected, passed through a 0.45-µm-pore-size filter and then stored at −20°C for assessment of cytokine levels.

3.11.1 Cytokine immunoassay

Mouse IFN-γ and TNF-α were measured using the Quantikine® Mouse IFN-γ Immunoassay ELISA kit. For measuring IFN-γ, a dilution series of standard stock solution (3000 pg/mL) were prepared ranging from 600 pg/mL to 9.4 pg/mL. The appropriate calibrator diluent was served as the zero standard (0 pg/mL). 50 µL of Assay Diluent RD1-21 was added to each well, then 50 µL of prepared standards, control, and samples were added.

Plate was incubated for 2 hours at room temperature. After incubation time, wells were aspirated and washed 5 times with wash buffer (400 µL). After the last wash, any remaining wash buffer was removed by aspirating or decanting. 100 µL of mouse IFN-γ

conjugate was added to each well and incubated again for 2h at RT. After incubation time, each well was aspirated and washed 5 times with wash buffer (400 µL). Finally, 100 µL of stop solution was added and the ODs were read at 570 nm (Reference: 450 nm).
For quantitively measurement of TNF-α, a dilution series of standard stock solutions (7000 pg/mL) were prepared ranging from 700 pg/mL to 10.9 pg/mL. The appropriate calibrator diluent was served as the zero standard (0 pg/mL). 50 µL of assay diluent RD1-63 was added to each well, then 50 µL of prepared standards, control, and samples were added. Plate was incubated for 2 hours at room temperature. After incubation time, wells were aspirated and washed 5 times with wash buffer (400 µL). After the last wash, any remaining wash buffer was removed by aspirating or decanting. 100 µL of mouse TNF-α conjugate was added to each well and incubated again for 2h at RT. After incubation time, each well was aspirated and washed 5 times with wash buffer (400 µL). 100 µL of substrate solution was added to each well and incubated again for 30min at RT.
Finally, 100 µL of stop solution was added and the ODs were read at 570 nm (Reference: 450 nm).

3.12 Immunohistochemistry

C57/Bl6 mice were pre-treated with cyclophosphamide and cortisone acetate, infected with fungal forms, and, in case, inhaled with sphingosine as described above. Mice were put to death by CO_2 fumigation immediately post-infection (day 0) and at day 4 post-infection and the lung was collected for further studies. At each time-point, two immunosuppressed but uninfected mice were included as negative controls.

3.12.1 Paraffin embedding of lung

The lungs were perfused by ice cold PBS via the right ventricle of the heart. 1 mL 4% paraformaldehyde (PFA) was instilled into the lung with a 22G IV catheter through the tracheae and the tracheae were tied with a piece of yarn. The complete lungs with tracheae were cut and incubated with 2 mL 4% PFA overnight at 4°C for fixation. The next day, the tracheae were cut and the lung lobes were put in separate cassettes and in xylol and different ethanol gradients for dehydration. Thereafter, the fixed, dehydrated lung lobes were embedded in paraffin wax. Finally, the paraffin embedded lung lobes were cut into 5 µm sections with microtome on histobond slides (76×26×1 mm) (Marienfeld superior, Lauda-Königshofen).
Tissue section paraffinization and de-paraffinization steps are listed in Table 11.

Table 11. Paraffinization and de-paraffinization process and steps

Paraffinization	Incubation time	De-paraffinization	Incubation time
50% Ethanol	2 h	Xylol	15 min (3×)
60% Ethanol	2 h	100% Ethanol	5 min (2×)
70% Ethanol	Overnight (2×)	96% Ethanol	5 min (2×)
96% Ethanol	4 h (2×)	90% Ethanol	5 min (2×)
100% Ethanol	4 h (3×)		
Xylol	30 min	70% Ethanol	5 min
Xylol	30 min		
Paraffin	4 h	tap water	short incubation
Paraffin	overnight		
Paraffin	4 h	ddH_2O	2 min

3.13 PAS staining

Periodic Acid Schiff staining (PAS) (Carl Roth GmbH, Karlsruhe, Germany) is a staining method for detection of polysaccharides such as glycogen and other macromolecules like glycolipids, glycoproteins and mucins in tissues. PAS staining was performed according to Table 12 and the slides were visualized with wide field microscope Leica.

Table 12. PAS staining and dehydration steps

Pas staining	Incubation time	Dehydration	Incubation time
periodic acid solution	10 min	96% Ethanol	30 s
floating water	10 min	96% Ethanol	30 s
ddH_2O	2 min (2×)	100% Ethanol	3 min
Schiff´s reagent	10-20 min	100% Ethanol	5 min
Warm floating water (35°C)	5 min	Xylol	5 min
ddH_2O	1 min	Xylol	5 min
Hemalum solution acc. Mayer	5 min	Xylol	5 min
floating water	10-15 min	Xylol	1 min

After staining, a drop of mountant was placed in the center of the section. Then, the slide was inverted over a cover slip. Firm pressure was applied to the cover slip to get rid of air bubbles. The slides were stored long-term at room temperature.

3.13.1 Quantitation of lung inflammation

ImageJ is a public domain Java image processing program. It is a downloadable application on any computer with Java. It can display, edit, analyses, process, save and print 8-bit, 16-bit and 32-bit images. It can calculate area and pixel value statistics of user-defined selections. It can also measure distances and angles. The amount of inflammation was quantified in histopathological mouse lung tissue using ImageJ software (Shirkhani et al., 2015). Inflammation was determined by threshold particle analysis using this software. Herbst et al., (2013) reported that: “analysis of lung histopathological inflammation was performed using ImageJ software (rsb.info.nih.gov/ij/) (Herbst et al., 2013). Quantitative analysis of total lung area was performed by threshold particle analysis in ImageJ (http://rsbweb.nih.gov/ij/). Further thresholding procedures were performed within selective areas of inflammation that were visually identified and a subsequent percentage affected proportion calculated”. Mouse lungs were fixed and 3 PAS stained histology sections from each mouse were recorded with ImageJ software.

3.14 Evaluation of cytotoxic potential of sphingosine

3.14.1 *In vitro* MTT assay

For *in vitro* cytotoxicity assay, A549 (adherent) and LL/2 (Mixed: adherent and suspension) lung carcinoma cell lines were used. Upon receipt, LL/2 cells were cultured in DMEM medium (Dulbecco's Modified Eagle's Medium, Catalog No. 30-2002) supplemented with 10% FCS, 10 mM HEPES, 2 mM L-glutamine, 1 mM sodium pyruvate, 100 µM non-essential amino acids, 100 U/mL penicillin and 100 µg/mL streptomycin in a confluency of 70% for up to four passages, screened to confirm the absence of mycoplasma contamination by PCR and aliquots were frozen in liquid nitrogen to create a batch of authenticated stock lines. A549 cells were cultured in F-12K Medium, Catalog No. 30-2004 supplemented with 10% FCS; 100 U/mL penicillin and 100 µg/mL streptomycin.

Cell lines were defrosted and cultured to a limited passage (4-5) before implantation. Initially, the medium was discarded, and the cells were washed with PBS and treated with

0.25% trypsin, 0.53 mM EDTA solution to dissociate them from the surface of the flask for maximum 15 minutes at 37°C/5% CO_2. Later on, we added adequate medium with 10% FCS to neutralize trypsin activity, centrifuged at 300g for 5 minutes at 4°C, discarded the supernatant and washed the cells with PBS for three times (resuspending the pellet with PBS and centrifuge 300 g/5minutes/4°C). Cells were resuspended in 10 mL respective medium and counted with Neubauer counting chamber. Briefly, cells were diluted and mixed 1:1 with 0.4% Trypan blue solution and the number of live cells as well as the number of dead cells (blue) were counted inside the four large corner squares. The number of cells per unit volume (cells/mL) and the cell viability [%] were calculated using the following equations:

$$\text{Number of}\frac{\text{cells}}{\text{mL}} = \text{Average cell count} \times 10^4 \times \text{Dilution factor}$$

$$\text{Number of viable cells/mL} = \frac{\text{Number of live cells}}{4\ (\text{No. of large corner squares})} \times 10^4 \times \text{Dilution factor}$$

$$\text{Viability\%} = \frac{\text{Number of live cells}}{\text{Total no. of cells}} \times 100$$

To perform MTT assay, cells were seeded in a 96-well flat-bottom microtiter plate at a density of 1×10^4 cells/well and allowed to adhere for 24 hours at 37°C in a CO_2 incubator. After 24 hours of incubation, culture medium was replaced with a fresh medium. Cells were then treated with various concentrations of the sphingosine (0.06-32 µg/mL) for 24 hours at 37°C in a CO_2 incubator. After 24 hours of incubation, culture medium was replaced with a fresh medium. Subsequently, 10 µL of MTT working solution (5 mg/mL in phosphate buffer solution) was added to each well and the plate was incubated for 4 hours at 37°C in a CO_2 incubator. The medium was then aspirated, and the formed formazan crystals were solubilized by adding 50 µL of DMSO per well for 30 min at 37°C in a CO_2 incubator. Finally, the intensity of the dissolved formazan crystals (purple color) was quantified using the ELISA plate reader at 540 nm.

3.14.2 *In vivo* TUNEL assay

In situ terminal deoxynucleotidyl transferase dUTP nick-end labeling (TUNEL) assay was done using an *in-situ* cell death detection kit, TMR red (Roche, Mannheim, Germany). All steps were performed according to the supplier's instructions. Briefly, paraffin-embedded sections were dewaxed and rehydrated as above. Then they permeabilized in 0.1 M Na-citrate buffer pH 6.0 (Microwave irradiation: 5 min, 350 W). After, the slides were washed two times with PBS. The sections were then incubated with 50 µLTUNEL reaction mixture in a humidified chamber for 60 min at 37°C followed by two times washing with PBS and embedded with Mowiol (Carl Roth GmbH, Karlsruhe, Germany). Images were analyzed with Leica LCS software version 2.61 (Leica Microsystems, Mannheim, Germany). DNase I (Roche Diagnostics, Mannheim, Germany) treated tissue sections (1 mg/mL in Ca^{2+}/Mg^{2+} buffer) were used as positive control.

3.15 Statistical analysis

Data are expressed as arithmetic means ± standard deviation (SD) unless otherwise indicated. Statistical analysis was performed with Student's t-test for single comparisons or with analysis of variance (ANOVA) for multiple comparisons. Statistical significance was set at the level of $p \leq 0.05$ (*p<0.05, **p<0.01, ***p<0.001, ****p< 0.0001). All data were obtained from independent measurements. The GraphPad Prism statistical software program (GraphPad Software, La Jolla, CA, USA) was used for analysis.

4. Results

4.1 *In vitro* antifungal activity of sphingosine

4.1.1 Planktonic cells display susceptibility to sphingosine

Methods for susceptibility testing of yeasts and molds are developed and validated by the EUCAST subcommittee on antifungal susceptibility testing (AFST). The antifungal activity of sphingosine against 12 clinical and 3 reference isolates of *Aspergillus* spp. was determined after 48 h. The lowest concentration (MIC) of sphingosine (in µg/mL) that inhibits the growth of *Aspergillus* strains are listed in Table 13. All clinical and reference strains of *A. fumigatus* showed a MIC of 2 µg/mL, the one strain *A. niger* F19 showed a MIC of 4 µg/mL whereas all isolates of *A. flavus*, *A. brasiliensis* and *A. tubingensis* displayed a MIC > 8 µg/mL. Moreover, the lowest sphingosine concentration resulting in the death of 99.9% of the inoculum (MFC) was also determined. After spotting 200 µL aliquots from wells with no apparent growth onto SDA plates, it was found that nearly all MFCs were equal to MICs except two *A. fumigatus* clinical strains. *A. fumigatus* 2453 had an MFC of 4 µg/mL and *A. fumigatus* 2040 had an MFC of 8 µg/mL (Table 13).

We further investigated antifungal activity of sphingosine against 13 clinical isolates of Candida spp. as well of the reference strains of *C. albicans* ATCC90028, *C. glabrata* DMS70614, *C. tropicalis* DSM1346 and *C. parapsilosis* ATCC22019 (Table 13). Among them, the planktonic cell of the *C. glabrata* reference strain was the most susceptible to sphingosine (MIC = 1 µg/mL), followed by clinical strains of *C. glabrata* (MIC = 2 µg/mL) and *C. krusei* (MIC = 4 µg/mL), while *C. albicans*, *C. tropicalis* and *C. parapsilosis* planktonic cells were resistant, showing a MIC higher than 8 µg/mL. In addition, the activity of sphingosine toward sensitive strains was also investigated in terms of MFC. The values were equal to MIC for *C. glabrata* DSM70614, *C. glabrata* 196*, C. krusei* ATCC6258 and *C. krusei* 201. For the other strains MFC values were higher than the corresponding MICs (Table 13).

Table 13. MIC and MFC of sphingosine towards *Aspergillus* and *Candida* strains according to EUCAST. RPMI 1640. + MOPS + 2% glucose (pH 7.0) and 100 µL were mixed with 100 µL of cell suspensions in water (final working inoculum: 2-5×10^5 cells/mL) in 96-well plates. Plates were incubated without agitation at 37°C in ambient air for 24-48 h, the growth of *Aspergillus* strains was evaluated visually. To quantify *Candida* cells, absorbance was measured at 530 nm.

fungal strain	MIC µg/mL	MFC µg/mL
A. fumigatus ATCC204305	2	2
A. fumigatus ATCC46645	2	2
A. fumigatus 2446	2	2
A. fumigatus 2453	2	4
A. fumigatus 2150	2	2
A. fumigatus 2151	2	2
A. fumigatus 2040	2	> 8
A. niger F19	4	4
A. flavus CM-1813	> 8	-
A. flavus 2476	> 8	-
A. flavus 2435	> 8	-
A. flavus 2412	> 8	-
A. brasiliensis 1988	> 8	-
A. tubingensis 1884	> 8	-
A. tubingensis 1885	> 8	-
C. glabrata DSM70614	1	1
C. glabrata 195	2	4
C. glabrata 196	2	2
C. glabrata 160	2	4
C. krusei ATCC6258	4	4
C. krusei F31	8	> 8
C. krusei 132	4	8
C. krusei 126	4	> 8
C. krusei 201	4	4
C. albicans ATCC90028	> 8	-
C. albicans 197	> 8	-
C. albicans 204	> 8	-
C. albicans 205	> 8	-
C. albicans 207	> 8	-
C. albicans 212	> 8	-
C. albicans 223	> 8	-
C. tropicalis DSM1346	> 8	-
C. parapsilosis ATCC22019	> 8	-

4.1.2 Preformed biofilms show less susceptibility to sphingosine

In addition to evaluating the activity of sphingosine against planktonic cells, their activity against preformed biofilms were also evaluated. First, the biofilm-forming capacity of all strains was evaluated using the crystal violet staining method, and the results are shown in Figure 13. After 48h, all clinical and standard isolates were stained with crystal violet to determine the amount of biofilm. Crystal violet as a standard microbiological *in vitro* test, indirectly determines the amount of biofilm by measuring the optical density (OD) of the crystal violet-stained biofilm matrix and cells. Included were low (OD < 0.2), medium (OD ≥ 0.2 and ≤ 0.4), and high (OD > 0.4) biofilm performers as determined by the crystal violet test (OD_C = 0.2). In this experiment, all strains turned out to be biofilm producers. *C. glabrata* strains were weak and *C. Krusei* isolates were moderate producer according to crystal violet staining test. The strong biofilm producing *Candida* mainly belonged to the *C. albicans, C. tropicalis and C. parapsilosis* species. The biofilm matrix act as a protective barrier, making the yeast cells more resistant toward conventional antifungal therapeutics. Therefore, biofilm forming *Candida* are difficult to treat and the minimum biofilm eradication concentration (MBEC), which is defined as the minimum sphingosine concentration resulting in 80% disruption of the biofilm are often extremely higher that the MICs for planktonic cells. Because of this, the preformed biofilms of *C. krusei* strains were exposed to higher sphingosine concentrations (1–16 times the planktonic MICs equal to 4-64 µg/mL) for 24 h in 96 well plate. The MBEC of was measured using tetrazolium salt (XTT) reduction assay for quantitative measurement of *Candida* biofilm viability, as it is more sensitive techniques to study the antifungal activity. The results are summarized in Table 14. This data suggested that concentrations of 8-16 times the planktonic MICs were needed to achieve 80% reduction in metabolic activity of the biofilms. *C. krusei* ATCC6258 and *C. krusei* 132 showed a MBEC of 32 µg/mL (8×MIC) and *C. krusei* 126 and *C. krusei* 201 showed a MBEC of 64 µg/mL (16×MIC), whereas *C. krusei* F31 displayed a MBEC > 64 µg/mL. Taken together, these findings suggest that biofilm maturation includes the development of a thick layer of extracellular polymeric substances (EPS) that acts as a barrier and prevents the diffusion of sphingosine, leading to resistance when compared to the planktonic forms.

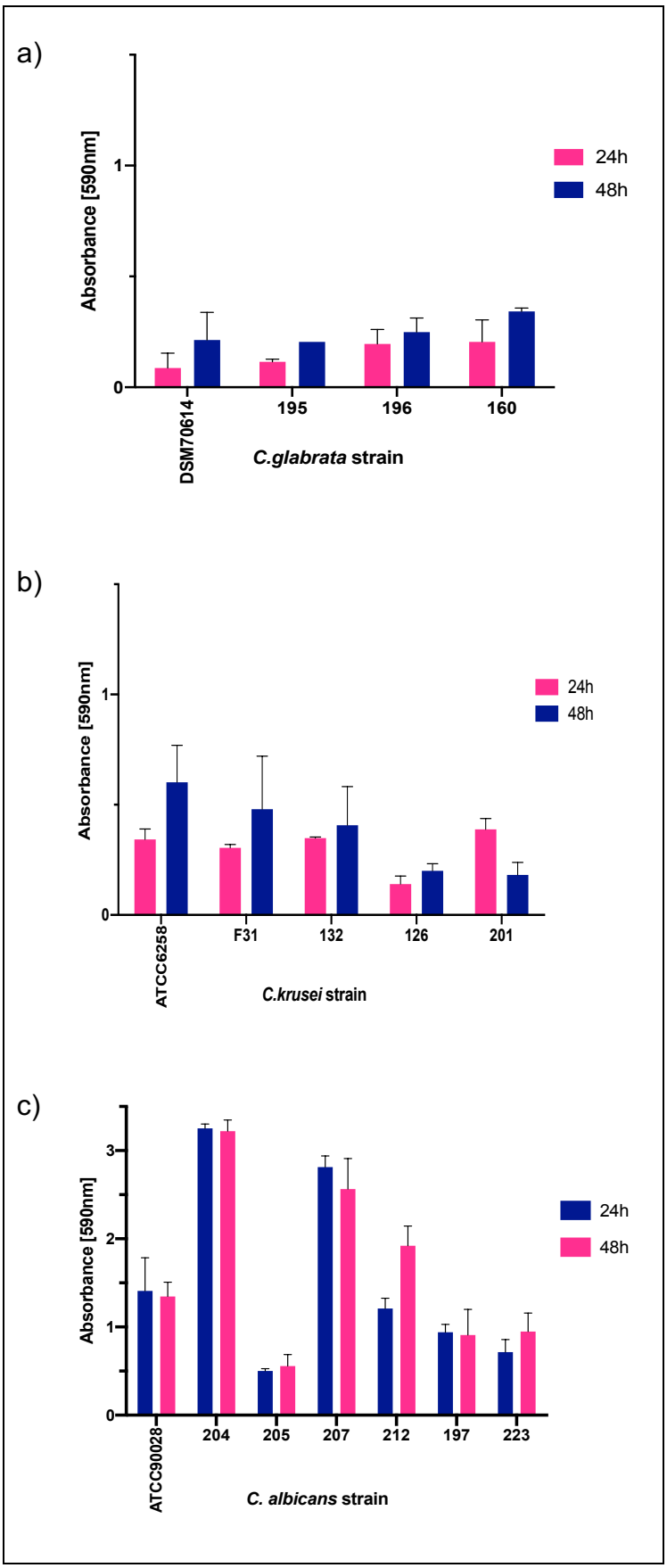

Figure 13. The ability of biofilm formation in different strains.

Table 14. Minimum biofilm eradication concentration (MBEC) toward pre-formed biofilm of *C. krusei* using XTT assay.

fungal strain	MBEC µg/mL
C. krusei ATCC6258	32
C. krusei F31	> 64
C. krusei 132	32
C. krusei 126	64
C. krusei 201	64

4.2 Sphingosine kills fungal cells in a time and dose dependent manner

4.2.1 Kinetic study against *C. glabrata*

Before the time-kill curve studies were initiated, antifungal carryover was evaluated using previously described methods. Significant antifungal carryover was defined as a reduction in the mean number of CFU per milliliter of > 25% compared with the colony count for the control (Cantón et al., 2004; Klepser et al., 1998). No antifungal carryover was observed at tested concentration (0.5-4×MIC). To illustrate the relationship between the concentration of sphingosine and the fungicidal effect over time, *C. glabrata* DSM70614 was exposed to different concentrations of sphingosine (vehicle control, 0.5×MIC, 1×MIC and 2×MIC) for different durations (0 to 24 hours). To determine the number of viable cells, diluted aliquots were plated on SDA and CFU/mL were calculated (Figure 14).

Sphingosine concentrations equal to 2×MIC and 1×MIC showed to be fungicidal (greater than 4 log unit reduction in number of colonies) after 6 and 10 hours respectively, while 0.5×MIC as non-inhibitory concentration showed no effect and the resultant curve was approximately comparable to those for the solvent treated vehicle control. These data demonstrated a dose- and time-dependent effect of sphingosine concentration on viability of *C. glabrata* cells(Klepser et al., 1998; Pearson et al., 1980).

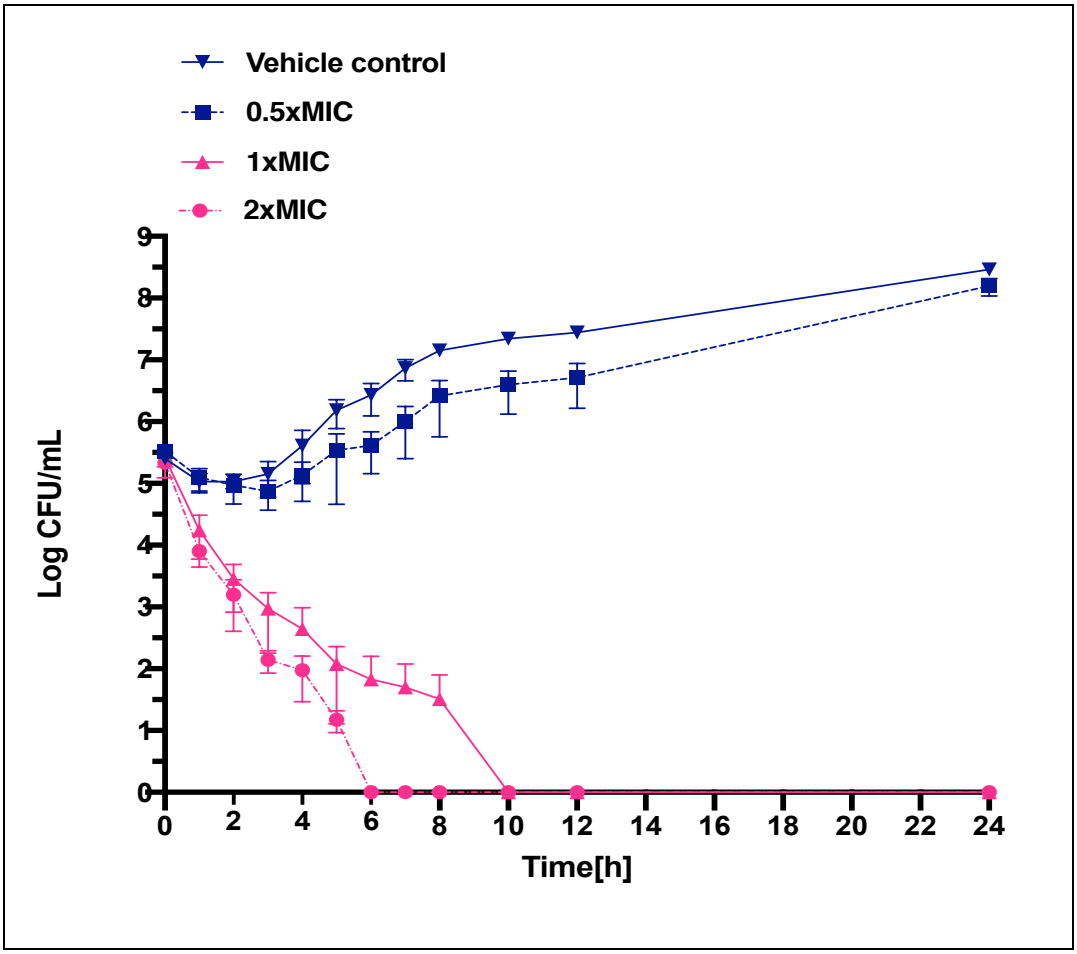

Figure 14. Time-kill plot demonstrating the effects of different concentration of sphingosine on *C. glabrata*. 1 to 5×10^5 CFU/mL *C. glabrata* DSM70614 were treated with 3 different concentrations of sphingosine (0.5, 1, 2×MIC) and a vehicle control. The log CFU/mL for all groups was determined at time 0 and at subsequent time points up to 24 hours as indicated.

4.2.2 Pattern of killing kinetic against *A. fumigatus*

Spores of filamentous fungi (for example, *Aspergillus* spp.) is able to germinate into branching hyphae. Due to this morphological changes, quantification of viable cells by CFU counting from agar medium are not applicable for multicellular filamentous fungi that may only grow as a single CFU when plated on agar. Therefore, XTT reduction assay was applied as an alternative to a CFU-based method for determining the kinetics of killing of *Aspergillus* strains.

In order to compare the cell viability values obtained by XTT assay with the number of colonies, a calibration curve was fitted (Figure 15). A linear relationship was confirmed between XTT value and initial inoculum size between 10^5 and 5×10^8 conidia/mL (R^2 = 0.8973). The effects of different concentrations of sphingosine over a 24-h period on *A. fumigatus* ATCC46645 conidia are shown (Figure 16). Addition of different concentrations

of sphingosine (1, 2 and 4×MIC) to culture medium containing 10^6 conidia reduced formazan absorbance, which was roughly equivalent to reduction in hyphal viability based on data generated from calibration curve (Figure 15). Within 10 hours, approximately 90% of the conidia were killed by sphingosine at 1×MIC (> 1 log reduction), while 2×MIC provided 99.9% killing (> 3 log reduction).

The maximum activity was observed at 4×MIC which provided 99.99% (> 4 log reduction) after 12 hours. As expected, with sub-inhibitory MIC concentration (0.5×MIC) no antifungal activity was detected. This data indicated that as the sphingosine concentration increases and as time passes, the killing activity of sphingosine elevates. Therefore, it can be concluded that a dynamic pharmacokinetic approach based on killing curves is directly depend of sphingosine concentration and exposure time.

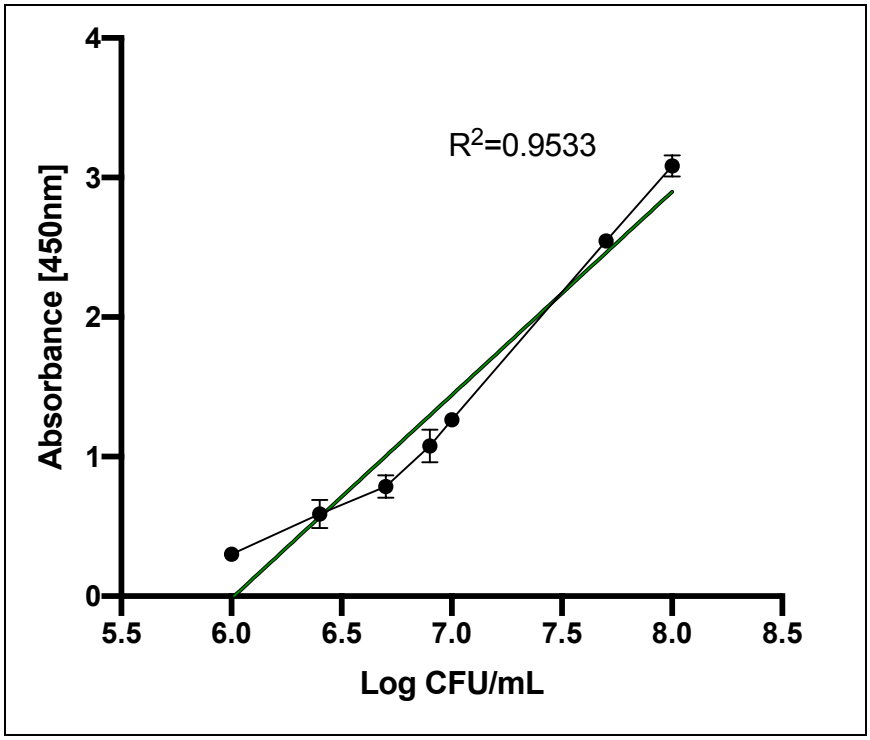

Figure 15. Graph of calibration curve of *A. fumigatus* conidia at 450nm. Serial dilutions of *A. fumigatus* conidia were prepared and XTT colorimetric intensity at 450 nm was measured after 2 h incubation. XTT activity was linearly associated with CFU counts more than 10^5 colonies/mL. A formula for a standard-curve and the correlation coefficient was calculated.

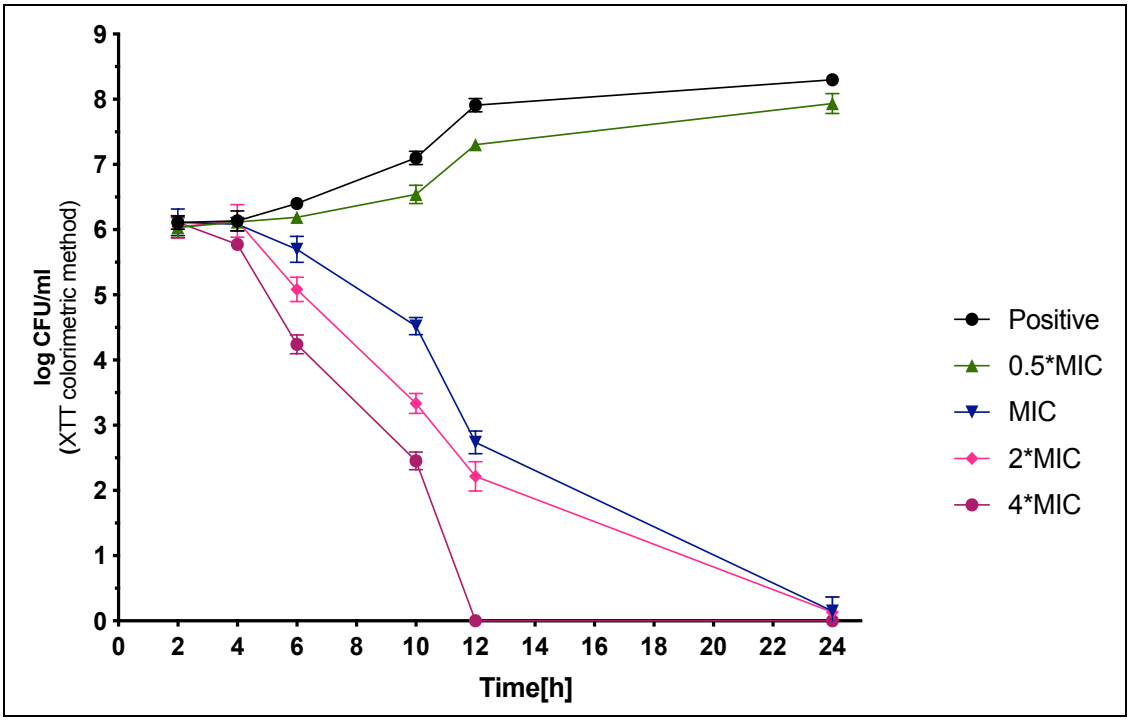

Figure 16. Time kill kinetic of *A. fumigatus*. 1-2.5×10^6 *A. fumigatus* (ATCC46645) conidia/mL where treated with different concentrations of sphingosine and viability was measured with XTT-menadione solution as indicated. CFU were calculated according to the standard-curve. Shown is the mean ± standard deviation, n = 3.

4.3 Sphingosine pre-exposure prophylaxis improves survival and prevents development of invasive aspergillosis in a murine model

4.3.1 Nebulized sphingosine prevents mortality

To study the efficacy of sphingosine as an antifungal agent in an *in vivo* model, a mouse model of invasive aspergillosis was used and sphingosine administered by inhalation. Groups of eight immunocompromised C57Bl/6 mice in three independent experiments were infected with *A. fumigatus* via an intratracheal tube. The test group received sphingosine via inhalation at a dose of 500 µM in 1 mL volume for the sequential 14 days treatment. As controls, immunosuppressed mice were inoculated with *A. fumigatus* and were inhaled with solvent/placebo. Behavioral Abnormalities and weights were recorded daily. As shown in Figure 17, the survival rate of sphingosine treated mice was markedly increased compared to that of placebo treated mice. *A. fumigatus* ATCC48846 infection resulted in a mortality of 50% within 4 days and weight loss (Figure 17, 18) in placebo-treated mice, whereas 100% of mice treated with sphingosine survived until the end of the observation-time, demonstrating that nebulized sphingosine prevents death caused by invasive aspergillosis in a mouse model.

Furthermore, the percentage weight loss was determined for both untreated and sphingosine treated mice (Figure 18). The untreated group lost much more weight than sphingosine treated whereas sphingosine treated mice slightly gained weight after infection. The mice were culled due to a ≥ 20% weight loss or 11-19% weight loss plus lethargy (n = 8 mice/group).

Loss of weight is indicative of an immuno-suppression related side effect or infection progression and could also be due to sphingosine toxicity. To sum up, the sphingosine dose that were tested in isolation did not result in weight loss and subsequently improved survival rate.

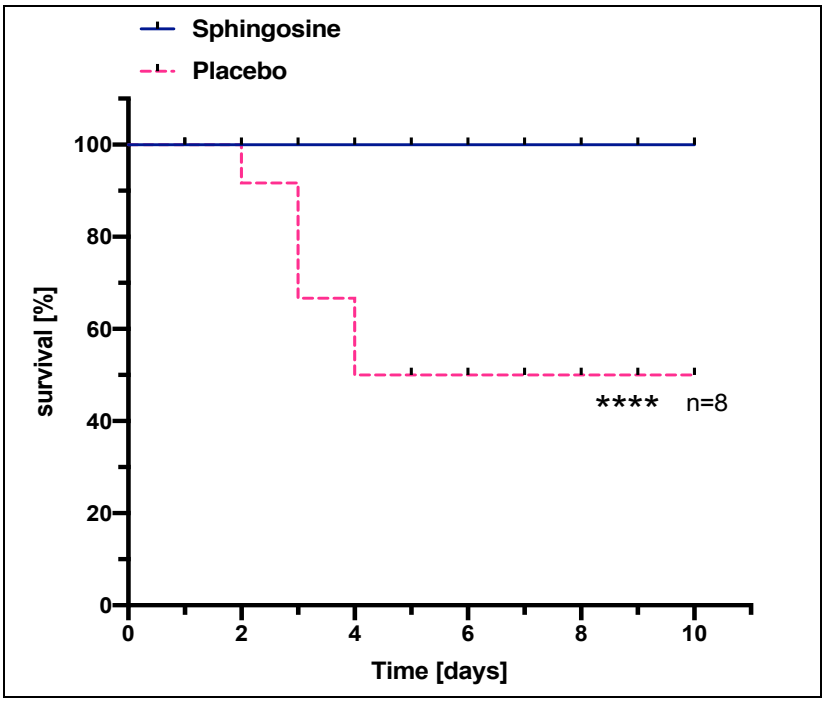

Figure 17. Kaplan-Meier survival curve. C57Bl/6 mice were immunosuppressed with 250mg/kg of cyclophosphamide intraperitoneally and 200mg/kg cortisone acetate subcutaneously on day -2 and day +3. For infection (day 0), mice were anesthetized and intubated, *A. fumigatus* (ATCC46645) forms were administered intratracheally (5×10^4 in 50 µL in 0.9% NaCl). For sphingosine inhalation, mice were immobilized in a restrainer and 1 mL 500 µM sphingosine/0.5% OGP was inhaled with a PARI BOY SX inhalation device daily, starting on day -3(*n = 8 per group, ** p < 0.01 (log-Rank test)*.

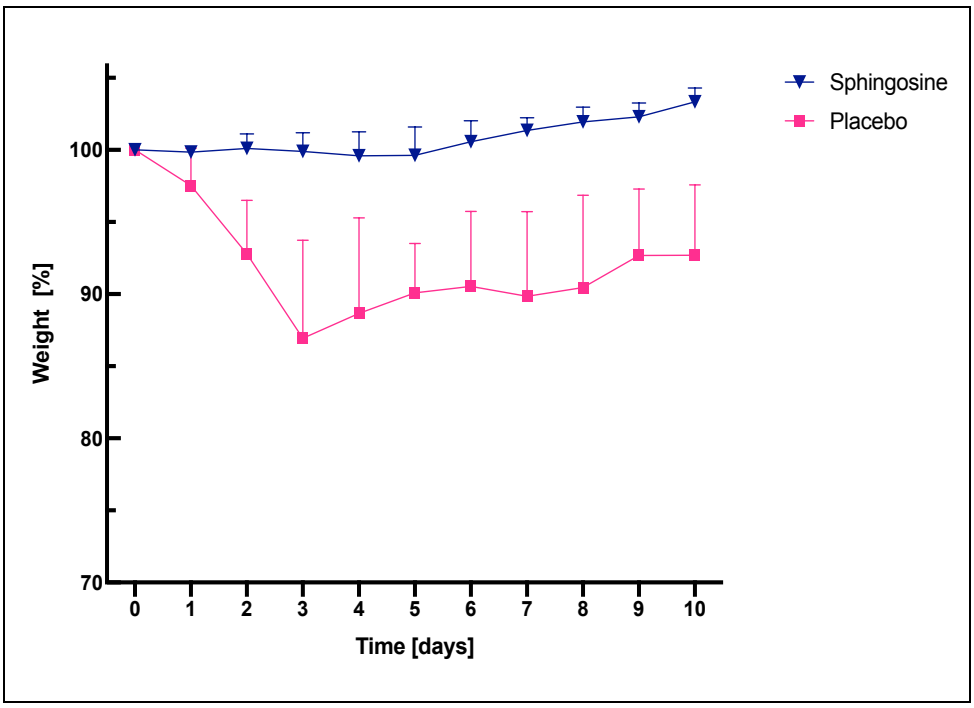

Figure 18. Percentage weight loss in immuno-suppressed and infected C57Bl/6 mice after sphingosine inhalation. Sphingosine treated mice gained weight after infection, whereas non-treated control lost about 10-20% weight. (n = 8 mice/group).

4.3.2 Reduction of fungal load in the infected lung after sphingosine treatment

To determine the fungal burden in the lung of C57Bl/6 mice, which were left untreated or treated with 500 µM sphingosine, CFU assays were performed. Two groups of immunosuppressed and infected mice (non-treated control and sphingosine treated) were sacrificed immediately after infection (day 0) and four days post infection. The fungal burden of organisms isolated from the lungs was analyzed by counting CFUs after serial dilutions and plating on SDA. *Aspergillus* conidia were detected and quantified in both treated and non-treated groups in a CFU-Assay (Figure 19). After 4 days of treatment with nebulized sphingosine, a significant reduction in fungal burden of nearly two log levels could be measured. In contrast, in placebo treated mice we could not see a significant reduction of fungal burden (Figure 19).

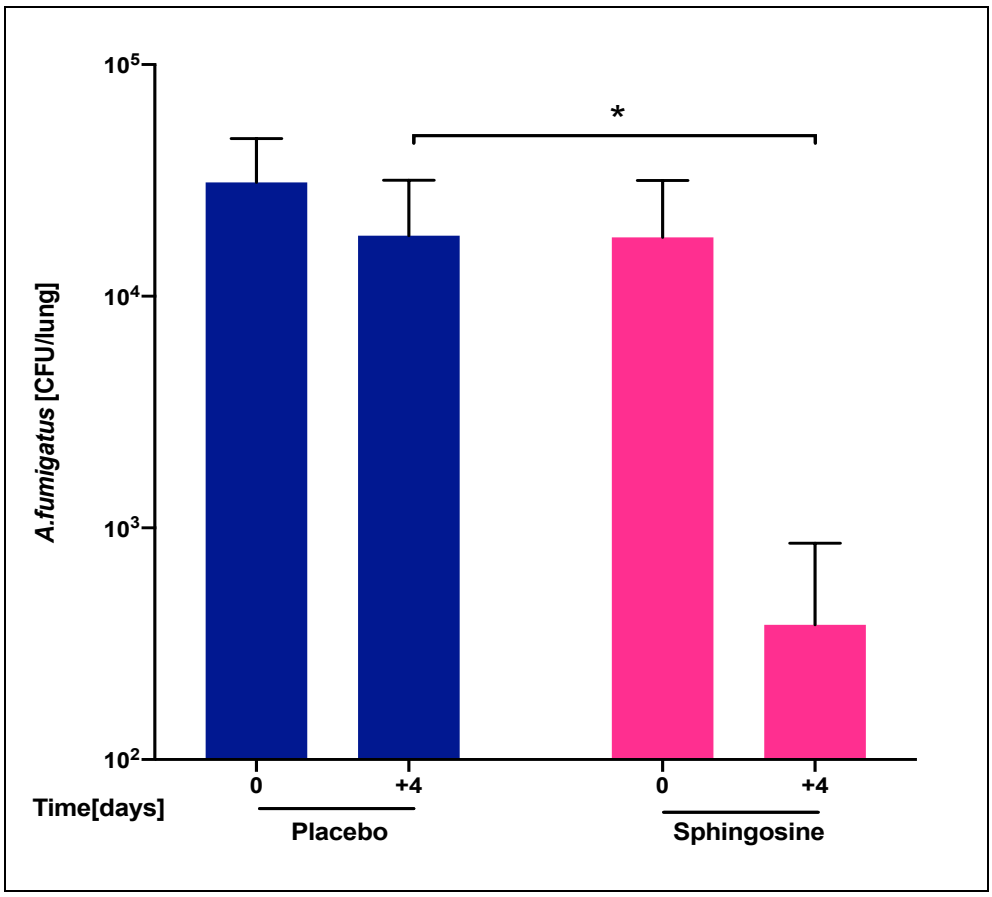

Figure 19. CFU counting after 4 days treatment with sphingosine. Immediately after infection (2×10^4 in 50 µL in 0.9% NaCl) (day 0) and 4 days post infection mice were put to death by CO_2 fumigation, lungs were removed by sterile dissection and homogenized. The amount of *A. fumigatus* CFU was counted after serial dilutions and spread on PDA plates. (Counts were performed in technical triplicates, n = 8 mice, shown is the mean ± standard deviation, *$p < 0.05$, student´s t-test).

4.3.3 Galactomannan depletion in bronchoalveolar lavage fluid

Because the CFU method suffers from limited sensitivity, galactomannan antigen assay was performed to monitor disease progression and to measure drug efficacy (Hoenigl et al., 2012). Galactomannan is a polysaccharide cell wall component of *Aspergillus* spp. that is released by fungal hyphae during invasive growth. Therefore, galactomannan antigen was quantified in bronchoalveolar lavage (BAL) fluid as a further index of fungal burden using PLATELIA™ *Aspergillus* Ag kit. Galactomannan positive and negative controls were available in the commercial kit.

The galactomannan level determined as optical density index (ODI) in BAL collected on day 4 post-infection was notably declined after inhalative treatment with sphingosine in comparison with the placebo treated control group (Figure 20). The average GM OD index values of sphingosine treated lung were equal to ODI of negative control, whereas ODI of no treated lung was higher than 1.6 (n = 8 per group).

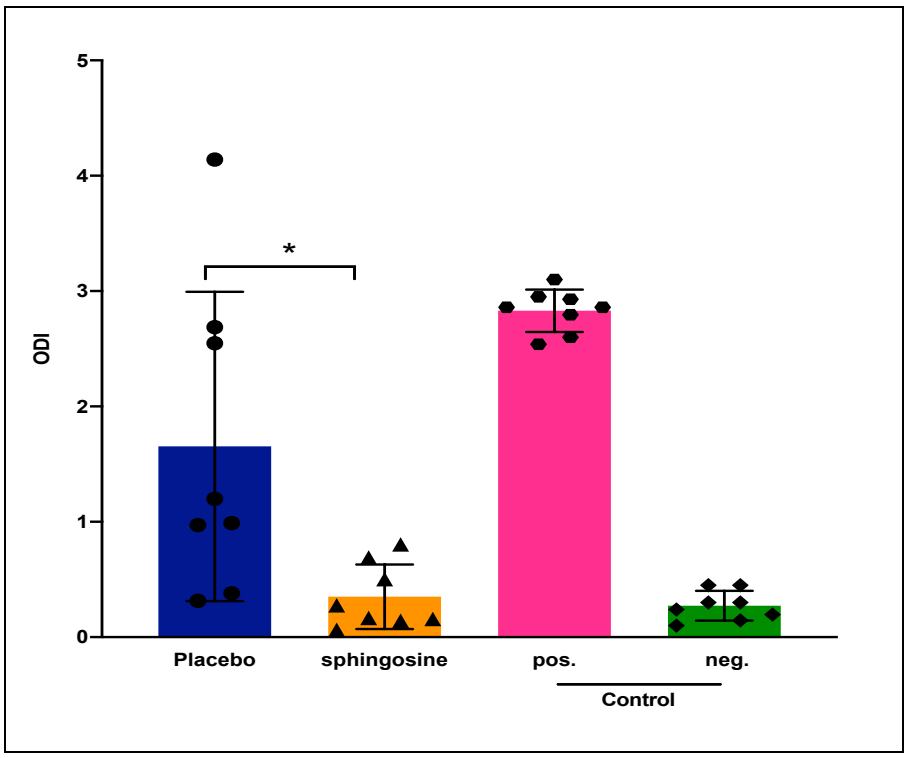

Figure 20. Galactomannan index after 4 days treatment with sphingosine. Bronchoalveolar lavage fluid was collected after 4 days inhalation of sphingosine/or solvent, galactomannan antigen detection in bronchoalveolar lavage fluid was done with Platelia Galactomannan EIA kits and expressed as optical density index (ODI) (n = 8, shown is the mean ± standard deviation, *$p < 0.05$, student´s t-test).

4.3.4 Sphingosine hinders hyphal growth and consequently less inflammation in the lung

After removing the lungs at day 4, the lungs of infected, sphingosine-treated mice already looked macroscopically like those of uninfected animals, whereas infected, placebo treated lungs had a distinct denser, inflammatory aspect. This was confirmed by histochemical examination of tissue sections. A noticeable difference was seen in the histology of BALB/c mice lung sections between untreated and sphingosine treated mice. At day 0, *Aspergillus* conidia were observed in the lungs of both groups (Figure 21) whereas at day +4, a large number of branching septate hyphal elements of *A. fumigatus* along with prominent tissue necrosis and inflammation was detected in infected, placebo treated mice, (Figure 22 a, b, c and d). In sphingosine treated mice, the lung was almost clear and no germinated fungi were seen after 4 days (Figure 22 e, f). *A. fumigatus* hyphae are visualized in pink (PAS stain-original magnification ×10 and ×40).

Inflammation was quantified by threshold particle analysis using ImageJ software at day +4. The inflammation in the lung with a dose of 500 µg sphingosine was similar to that

seen in normal non-infected C57Bl/6 mice. This was significantly less than the pronounced inflammation measured in infected mice/placebo-treated mice (Figure 23). The amount of inflammation increased the mass of focal pulmonary hyphae and necrosis in the lung of infected, placebo treated mice. The average percentage of inflammation was calculated as 58.4 ± 4.0% for six mice.

This data suggests that, 500 µg sphingosine is able to prevent conidia germination and consequently prevent invasive aspergillosis (IA) in the lung.

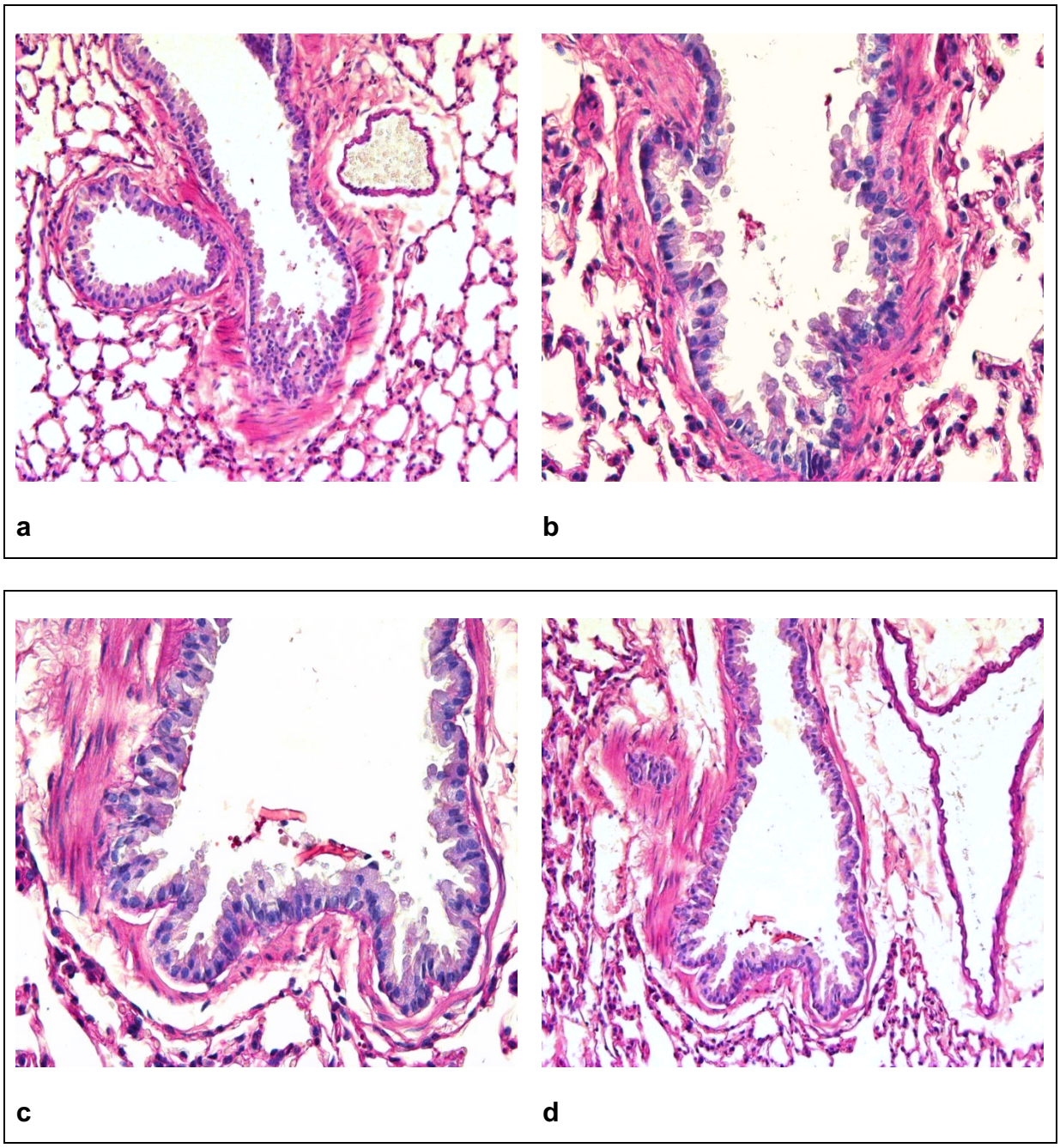

Figure 21. PAS stain of lung tissue of immuno-competent and infected C57Bl/6 mouse at day 0. Lungs were removed, fixed in 4% PFA dehydrated, embedded in paraffin, sectioned into 3-4 µm slices and stained with PAS reagent. *Aspergillus* conidia were observed in the lung of sphingosine treated (**a, b**) and placebo treated (**c, d**) at day 0. *A. fumigatus* conidia are seen in dark pink. Shown is one representative image from n = 6 mice.

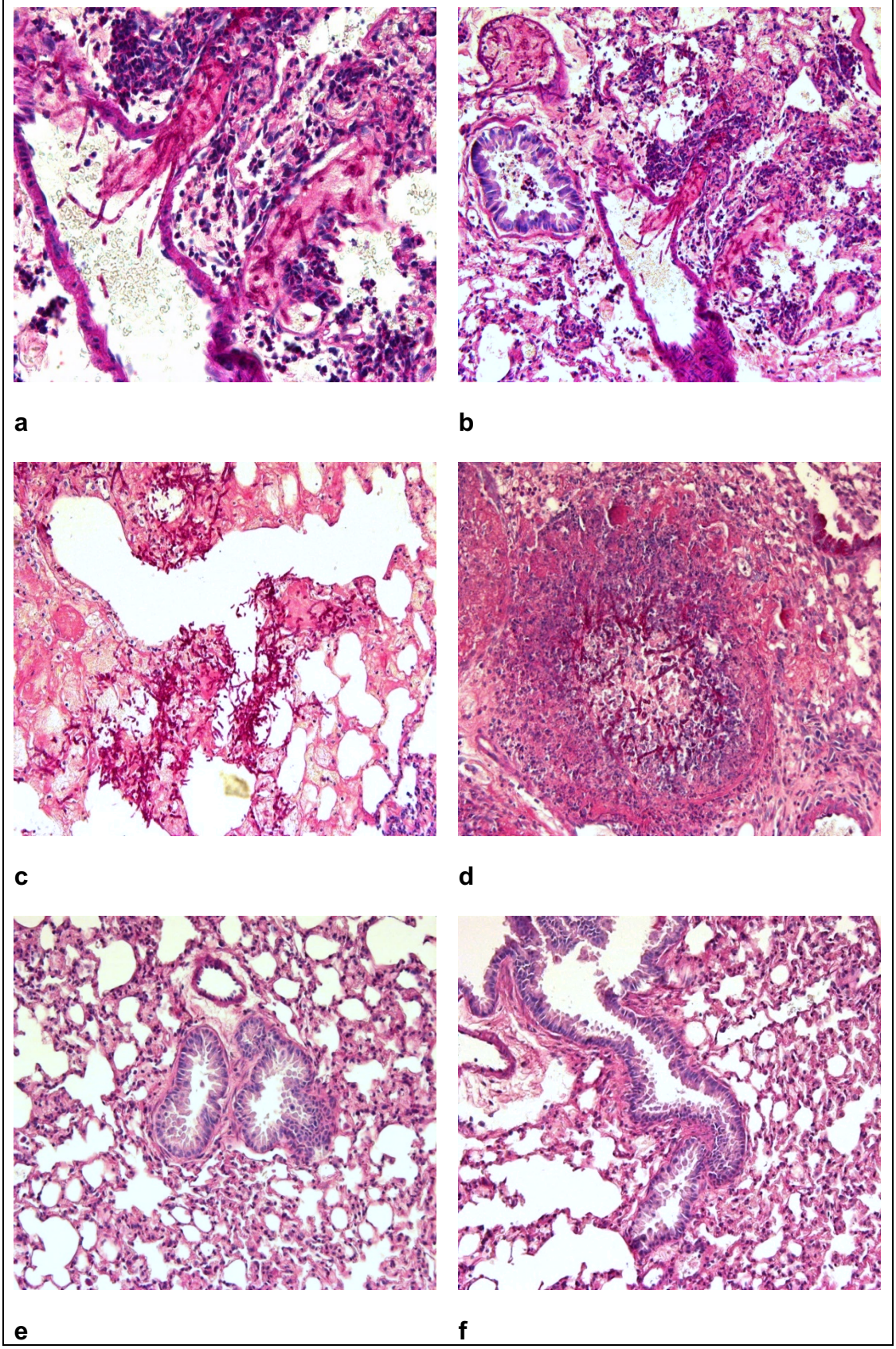

Figure 22. PAS stain of lung tissue of immuno-competent and infected C57Bl/6 mouse at day +4. Lungs from mice treated as indicated and removed at day 4, fixed in 4% PFA dehydrated, embedded in paraffin, sectioned into 3-4 µm slices and stained with PAS reagent. Hyphal invasion was observed in untreated mice (**a, b, c, d**). *A. fumigatus* hyphae are seen in dark pink. Sphingosine (500 µg) treated lung are clean, without conidia germination signs (**e, f**).

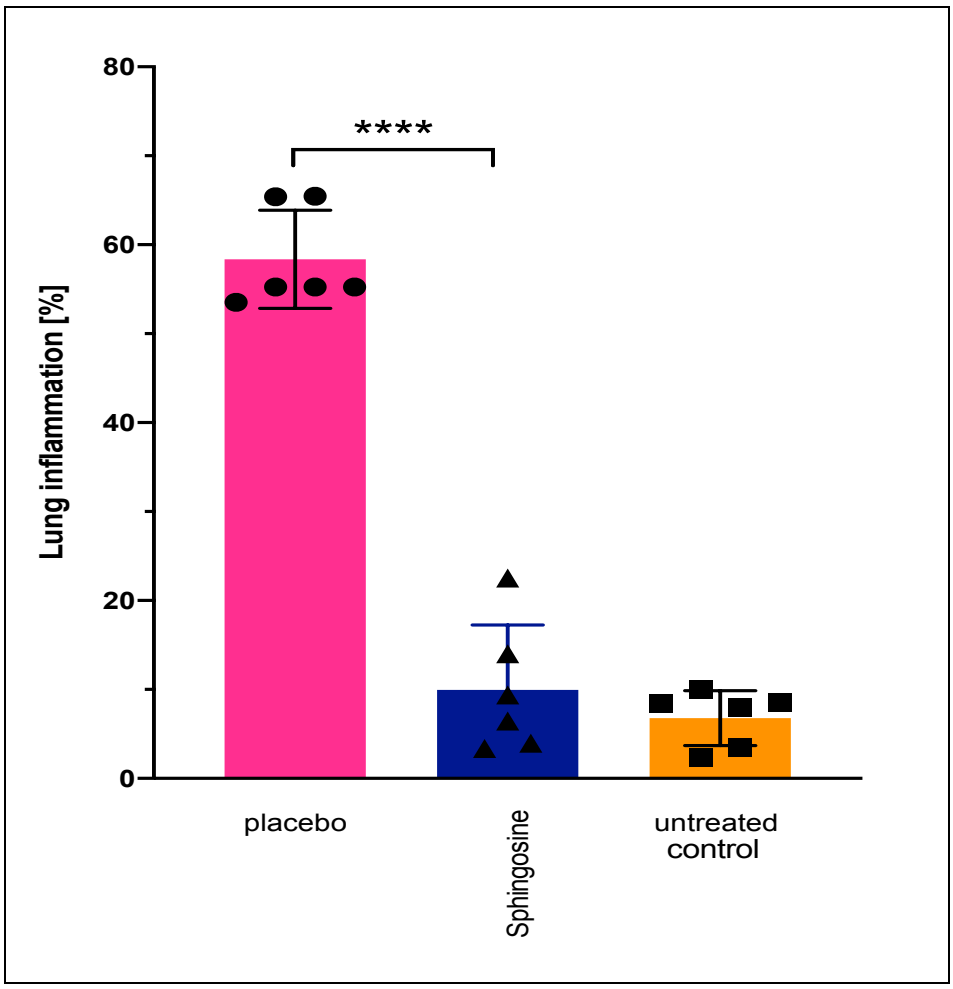

Figure 23. Lung Inflammation percentage after sphingosine treatment. Lungs from mice treated as indicated were removed at day 4, fixed in 4% PFA dehydrated, embedded in paraffin, sectioned into 3-4 µm slices and stained with periodic acid-Schiff reagent. ImageJ (http://rsbweb.nih.gov/ij/) was used to calculate the area and pixel value statistics of user-defined selections and thereby to quantitate lung inflammation in tissue sections (n = 6 for treated animals, n = 3 for untreated controls). Shown is the mean ± standard deviation. **** $p < 0.0001$, student´s t-test.

4.3.5 Measurement of cytokines responses from mouse lung after inhalation of sphingosine

Sphingosine prophylaxis was given to the mice from day -3 till day +4. At day 4 post-infection, mice were culled and lungs harvested for measurement of TNF-α and IFN-γ using Quantikine® Mouse Immunoassay ELISA kit. The standard curve for TNF-α and IFN-γ are shown in Figure 24 a and b respectively. The concentration of positive controls, sphingosine and placebo treated samples are listed in Table 15. No cytokine responses were detected in the tested samples.

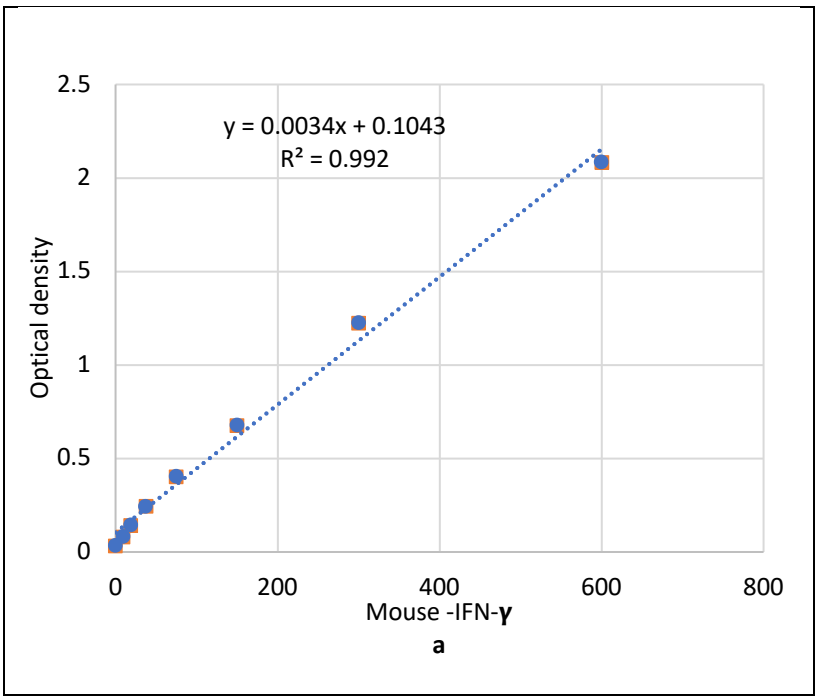

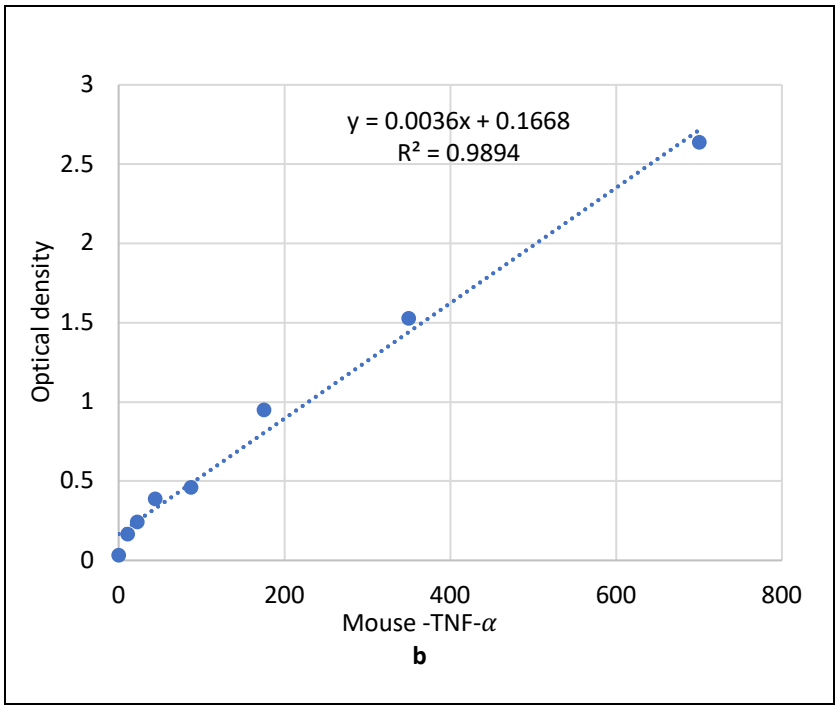

Figure 24. TNF-α and IFN-γ standard curves. (**a**) IFN-γ standard curves (**b**) TNF-α standard curve according to manufacturer protocol.

Table 15. Measurement of cytokines responses after inhalation of sphingosine.

	Sphingosine treated	Placebo treated	Positive control
IFN-γ Conc. (pg/mL)	9.2 ± 0.3	8.7 ± 0.5	193 ± 1.3
TNF-α Conc. (pg/mL)	10.1 ± 0.5	ND	120 ± 0.8

4.3.6 Nebulized sphingosine as a safe *in vivo* treatment

To examine whether treatment with inhalative sphingosine triggers apoptosis in mouse lung cells *in vivo*, we performed TUNEL assays on lung sections. We observed no increased apoptotic signals in non-infected sphingosine-treated (Figure 25a) and in infected but sphingosine treated mice (Figure 25b). In contrast, the lungs of *A. fumigatus* infected mice without treatment showed a dramatically increase in the number of TUNEL-positive cells (Figure 25c) due to cell death, caused by invasive aspergillosis. DNase I treated tissue was used as positive control (Figure 25d). These results clearly indicate that treatment with sphingosine neither mediated apoptosis nor toxicity in lung cells.

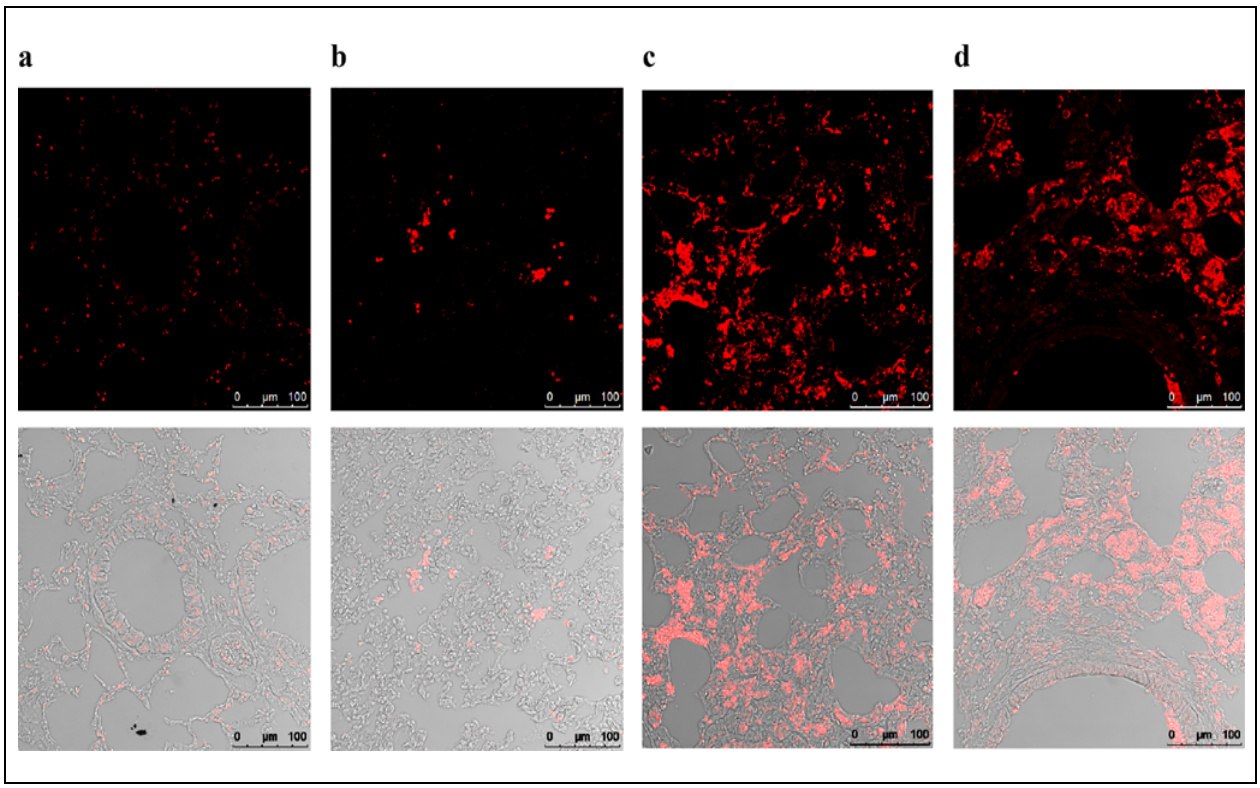

Figure 25. Lung TUNEL staining after sphingosine treatment. Inhalation of sphingosine does not affect normal lung tissue measured by Terminal deoxynucleotidyltransferase-mediated dUTP nick-end labeling (TUNEL) assay. Differentially treated mice as indicated were inhaled with 1 mL 500 µM daily over 7 days, mice were put to death using CO_2 fumigation at day 8. Lungs were fixed in 4% PFA dehydrated, embedded in paraffin, sectioned into 3-4 µm slices, and further processed for TUNEL-assay. (**a**) No pre-treatment. (**b**) Mice were immunosuppressed with 250mg/kg of cyclophosphamide intraperitoneally and 200mg/kg cortisone acetate subcutaneously on day 2 and day 6. At day 4 mice were anesthetized and intubated, *A. fumigatus* (ATCC46645) forms were administered intratracheally (2×10^4 in 50 µL 0.9% NaCl). For sphingosine inhalation, mice were immobilized in a restrainer and 1 mL 500 µM sphingosine/0.5% OGP was inhaled with a PARI BOY SX inhalation device daily, starting on day 1. (**c**) Mice treated like in **b**, but inhalation with placebo/0.5% OGP. (**d**) Untreated mouse, lung sections treated with DNase I to fragment the DNA as positive control. Shown is one representative lung section of n = 4 mice.

Beside the *in vivo* experiment, *in vitro* MTT assays were used to detect the effect of sphingosine on A549 and LL/2 cell proliferation. A549 and LL/2 cells were treated with different concentration of sphingosine (0.125-32 μg/mL) for 24 hours, and cell proliferation suppression rate was detected by MTT (thiazolyl blue tetrazolium bromide) assay and half maximal inhibitory concentration (IC_{50}) sphingosine to lung cancer cells was calculated. The results (Figure 26) demonstrated that the IC_{50} of sphingosine to LL/2 cells was lower than A549 cells. The value of IC_{50} in LL/2 cells (4 μg/mL) is 4 times higher than MIC value in *C. glabrata* (1 μg/mL) and 2 times higher than MIC value in *A. fumigatus* (2 μg/mL). Moreover, as it is shown in Figure 26 the IC_{50} value in A549 cells (8 μg/mL) is 8 times higher than MIC value in *C. glabrata* and 4 times higher than MIC value in *A. fumigatus* strains.

Taken together, these results suggest that, sphingosine is a safe treatment particularly for *in vivo* inhalation.

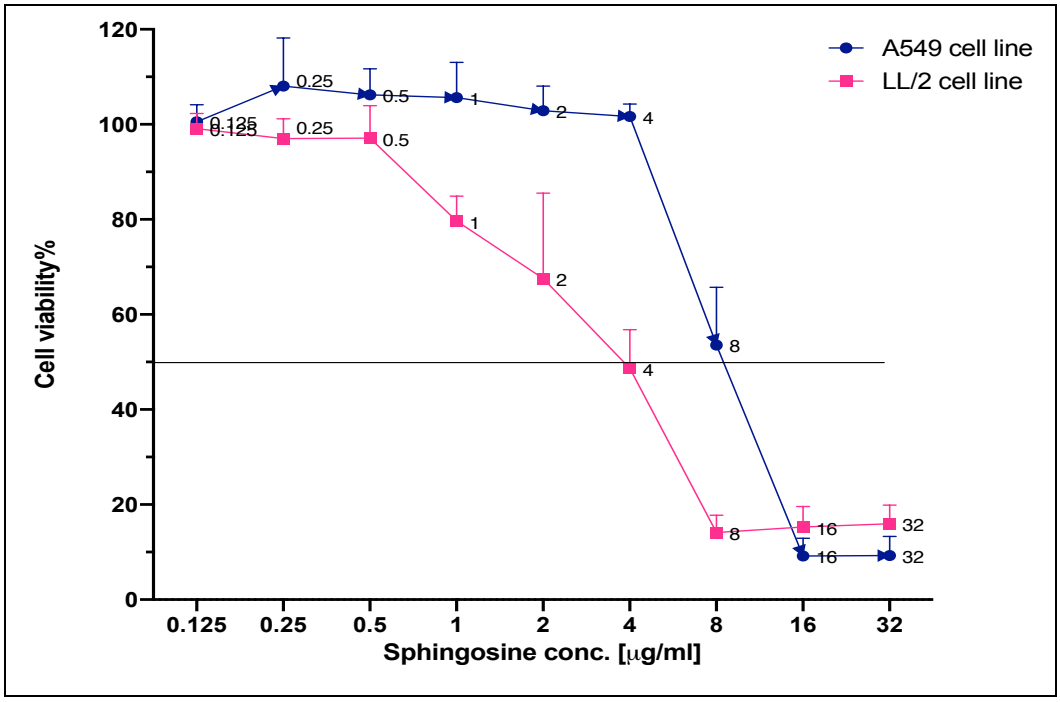

Figure 26. In vitro cytotoxicity assay of sphingosine. A549 and LL/2 cells were treated with different concentration of sphingosine (0.125-32 μg/mL) for 24 hours, and cell viability was measured by MTT assay.

4.4 Sphingosine triggers a mitochondria-mediated cell death

4.4.1 Intact cell wall through sphingosine treatment

Aspergillus spp. grow in hyphae in liquid culture, therefore single cell analysis to investigate the mechanism of sphingosine toxicity are difficult. Therefore, we selected the reference strain of *C. glabrata* DSM70614 for further experiments to elucidate the mode of action of sphingosine. Before performing further *in vitro* research, it is important to understand and track rates of *C. glabrata* growth within a sample. Growth curve measurement based on optical density (OD) is one of the most commonly used methods in microbiology for monitoring the proliferation of microbes in time, which provides a simple, reliable and routine way to understand various aspects of the microbes. It is particularly important for sampling, because it should always be done at a certain time and phase to ensure the repeatability of the *in vitro* experiments.

Because of this reason, *C. glabrata* growth curve was plotted as explained in method part and doubling time (g) was calculated. The curve was sigmoidal, with clear exhibition of the lag, log and stationary phases. In general, about 4 to 6 h was required by the cells to adapt to the normal growth environment before they were ready to proliferate and enter the log phase. According to the formula which explained above, the doubling time was about 5.530 ± 0.106 h and after 15 h incubation (Figure 27), yeast culture was in the middle of logarithmic phase. Mid-log phase was the time that the cells were harvested for further analysis.

To determine the effect of sphingosine on cell wall integrity, cells were stained with calcofluor white and FUN1 (LIVE/DEAD® Yeast Viability Kit, Molecular probes). Calcofluor is a fluorescent dye that binds polysaccharides of the fungal cell wall, while FUN 1 is a two-color fluorescent viability probe for yeasts. Metabolically active cells are able to compact the dye into orange-red cylindrical intravacuolar structures (CIVS) while dead cells or cells with intact membranes but with no metabolic activity exhibit bright green cytoplasmic fluorescence in absence of fluorescent intravacuolar bodies. Non-treated control cells were oval and calcofluor dye uniformly distributed on the cell wall. Orange-red FUN1 dye was compacted in CIVS indicating the intact metabolic activity of the controls, as expected (Figure 28a). *C. glabrata* DSM70614 cells treated with sphingosine (2×MIC) for 4 hours did not form orange-red dye compacted in CIVS, indicating that they were metabolically inactive (Figure 28b) whereas cell wall integrity remained intact.

Treatment of the cells with 70% v/v ethanol as negative control led to a loss of calcofluor signal and to a lack of formation of orange-red dye compacted in CIVS, as expected (Figure 28c).

These data suggest that although sphingosine is able to kill or to suppress the metabolic activity, respectively, it has no effect on the cell wall integrity, indicating that the killing mechanism of sphingosine is not through a direct effect on the cell wall.

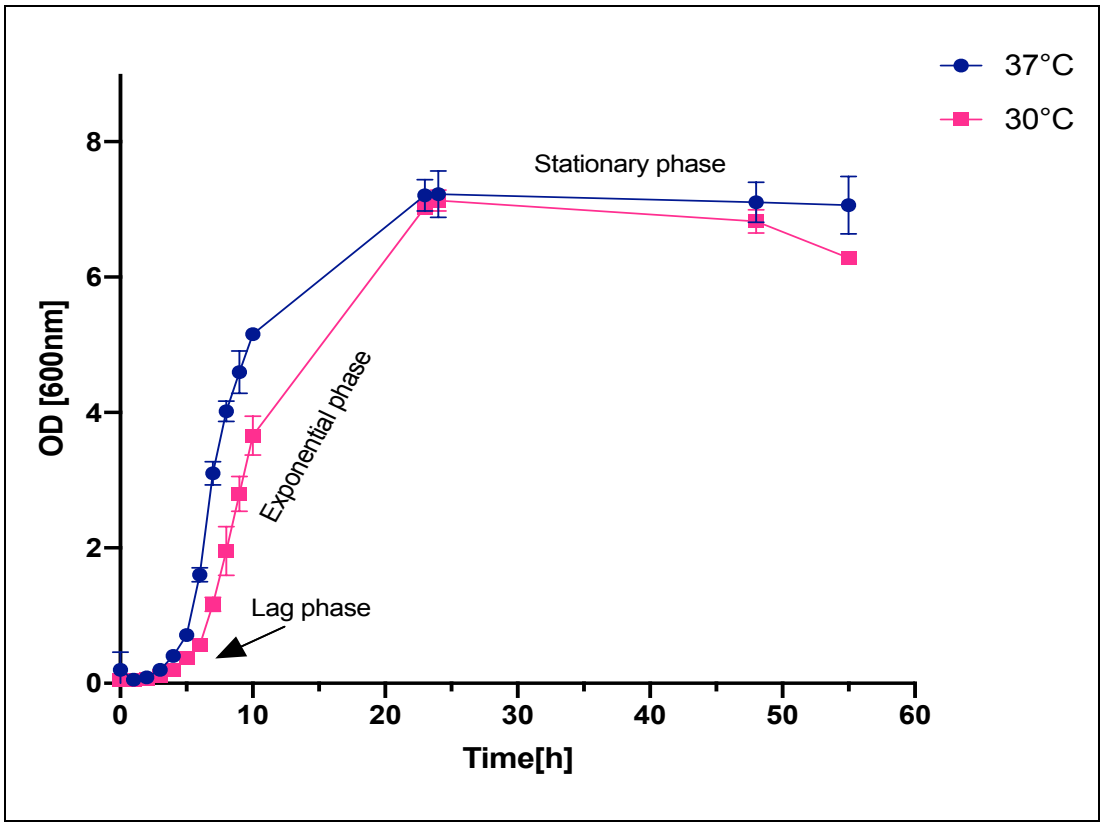

Figure 27. *C. glabrata* growth curve. Cells are cultivated in YPD broth medium. The cell growth signified by the sigmoidal growth pattern indicating an orderly increase in cell mass and size. The values are expressed mean ± SD from three independent experiments.

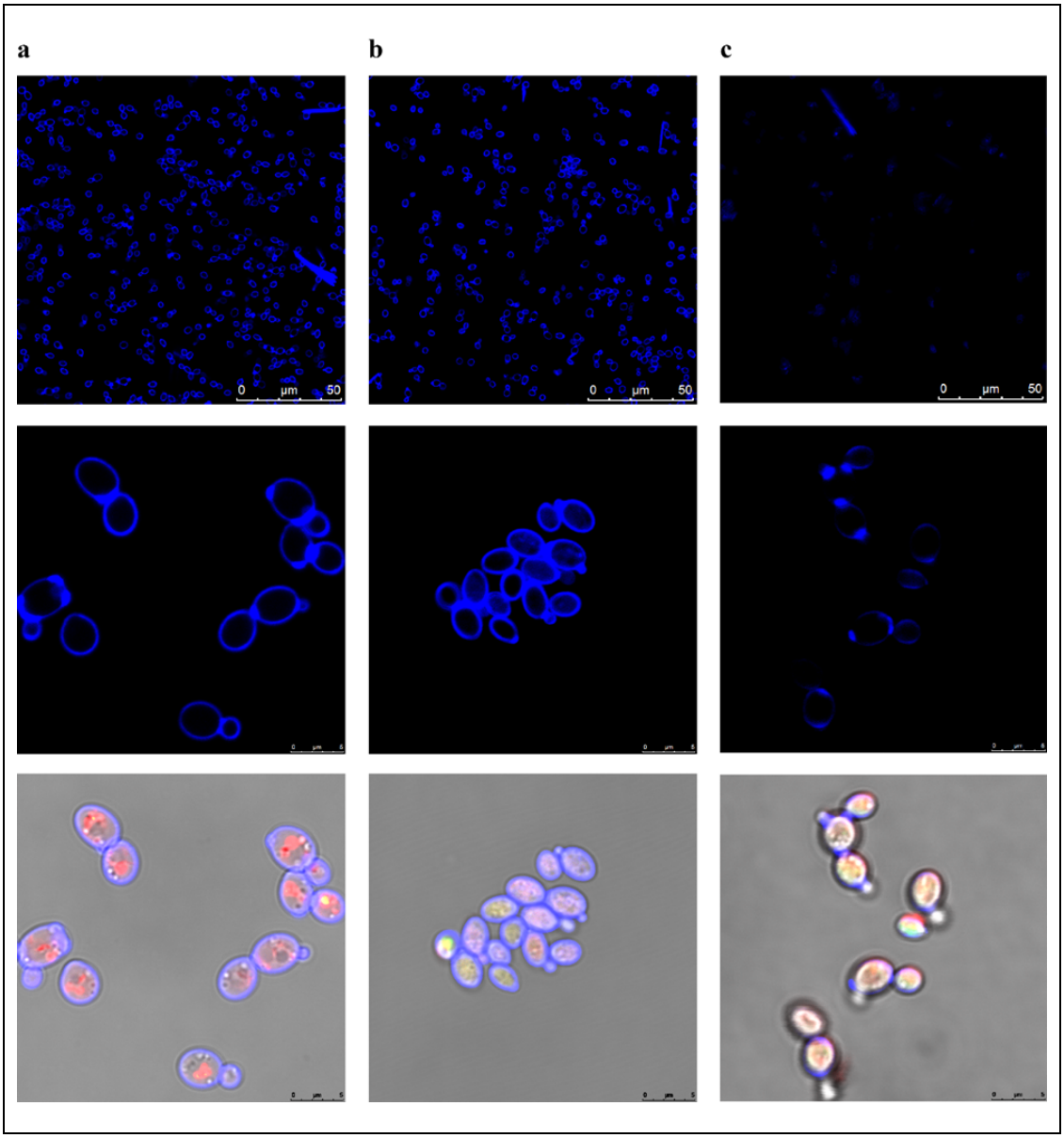

Figure 28. General overview of stained cell wall with calcofluor white and FUN1. Cell wall integrity is not affected by treatment with sphingosine. *C. glabrata* DSM70614 cells were treated with sphingosine at a concentration of 2×MIC at 37℃ for 4 hours, washed with PBS (pH 7.4), stained with 25 µM Calcofluor White (upper row), 10 µM FUN1 (middle row) for 30 min in the dark, and examined by fluorescence microscopy (lower row). (**a**) No treatment. (**b**) Sphingosine treated (2×MIC). (**c**) 70% v/w Ethanol treated (positive control). Displayed are representative results of n = 3 independent experiments.

4.4.2 Plasma membrane damage in a time dependent manner

After cell wall investigation, the second target for sphingosine may be plasma membrane. Therefore, membrane integrity was investigated using PI probe. Propidium iodide (PI) is a nucleic acid-binding fluorescent probe that only enters cells with compromised plasma membrane (Pina-Vaz et al., 2001).

In this study, *C. glabrata* DSM70614 cells were treated with increasing concentrations of sphingosine for different durations and the PI influx was assessed by flow cytometry. We

found a time and dose dependent effect of sphingosine on the cell membrane integrity. Sphingosine treated cells showed a strong increase in permeability to PI (Figure 29). The PI-stained subpopulation after exposure to 1×MIC for 4h and 6h was 69.5% and 78.3%, respectively. The maximum PI influx percentage was observed after 6h treatment in 2×MIC (82.3%). However, treatment in sub MIC (0.5×MIC) concentration did not increase PI fluorescence, indicating that sub-MIC do not affect cell membrane integrity. Similar patterns of PI staining and death were recorded for amphotericin B-treated cells as positive control (Figure 29). Figure 30 shows a control and three sphingosine concentration histograms (0.5, 1 and 2×MIC) after 4h and the gating strategy applied for these single parameter histograms.

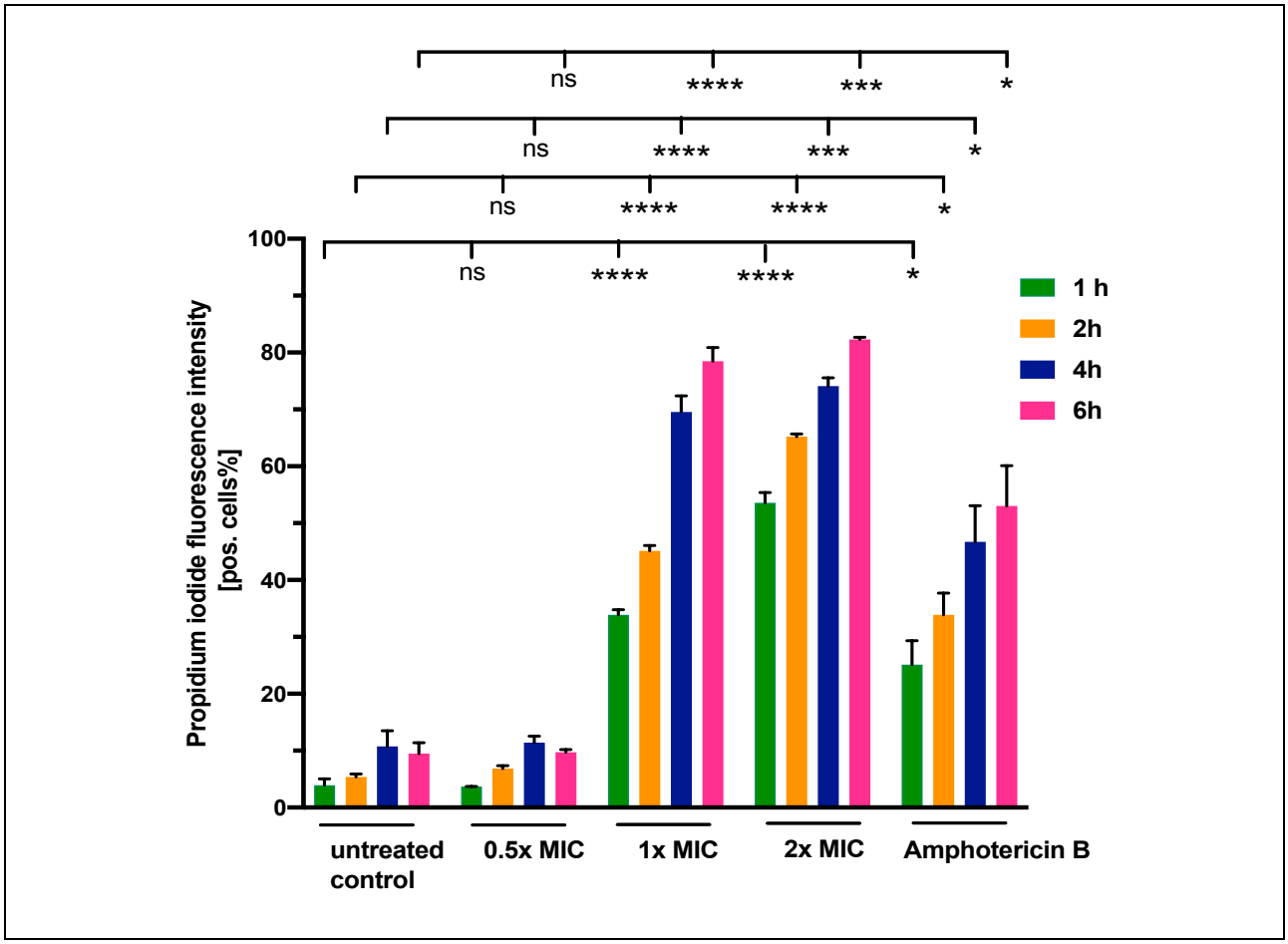

Figure 29. PI influx after sphingosine treatment. Treatment with sphingosine results in rapid disruption of the cell membrane. *C. glabrata* DSM70614 cells were treated with 0.5×MIC, 1×MIC and 2×MIC for 1, 2, 4 and 6 hours as indicated, washed with PBS and stained with 1 µg/mL propidium iodide and fluorescence measured with an Attune NXT flow cytometer. Shown is the mean ± standard deviation, n = 3. $^{**}p < 0.01$; $^{***}p < 0.001$. Dunnett´s multiple comparisons test.

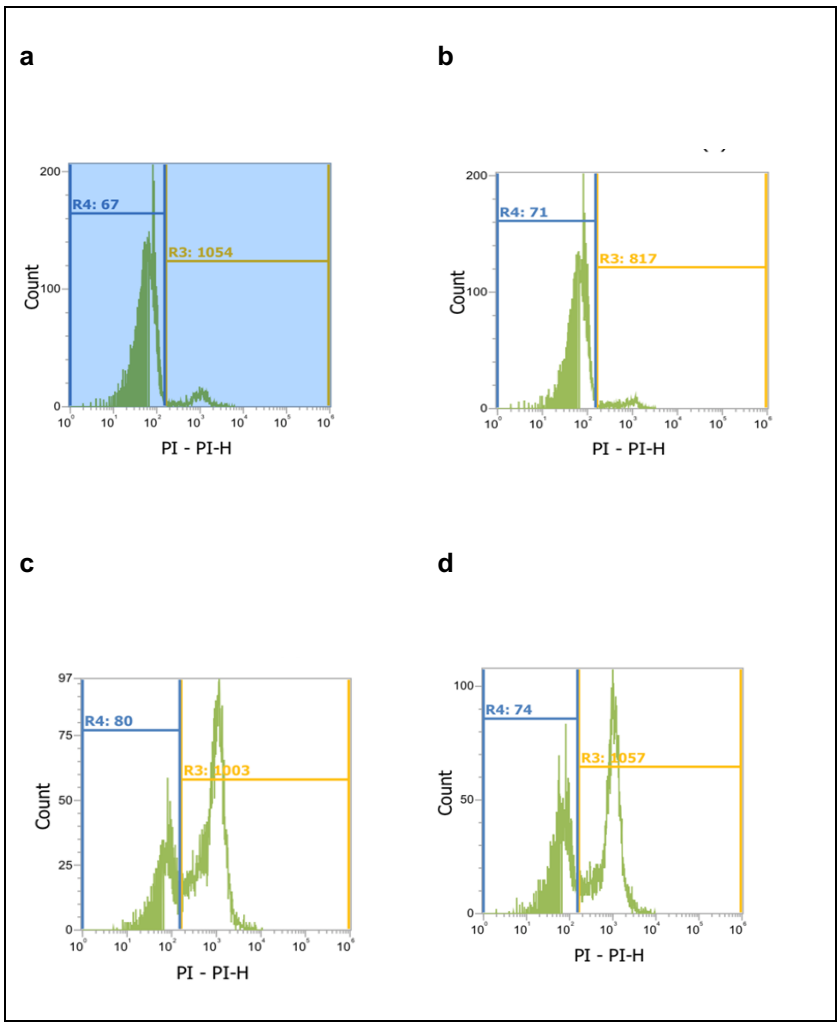

Figure 30. Flow cytometry histogram of PI stained cells. (**a**) Control non-treated (**b**) 0.5×MIC after 1 h (**c**) 1×MIC after 1h (**d**) 2×MIC after 1h. The applied gating strategy was equivalent.

4.4.3 Cellular and mitochondrial ROS generation

Numerous studies have suggested that ROS are generated by the cellular disruption that occurs during apoptosis and that ROS overproduction triggers cell death. It acts as a potent intrinsic stimulus in yeasts and other filamentous fungi and regulates the expression of various apoptosis-regulatory proteins (Azad et al., 2008).

This raises the question of whether ROS produces via sphingosine treatment in yeast cells. To address this question, ROS production was assessed in sphingosine treated cells using a general oxidative stress indicator. In the presence of ROS, the non-fluorescent H_2DCFDA is rapidly converted to highly fluorescent 2′, 7′-dichlorofluorescein (DCF) and detected with flow cytometry (Jin et al., 2005).

C. glabrata DSM70614 exposed to different concentrations of sphingosine for different durations and detected fluorescence by flow cytometry (Figure 31). These results show

that the fluorescence intensity in cells dramatically increased after 30- and 60-minutes treatment with 1×MIC and even more with 2×MIC compared to untreated control. The cells treated with 1×MIC and 2×MIC showed dramatic increases in the H_2DCFDA fluorescent intensity (347 ± SD and 615 ± SD, respectively) in comparison with untreated cells (31 ± SD). When Antimycin A and TBHP were applied, the fluorescence intensity increased to 136 ± SD and 145 ± SD, respectively (Figure 31a).

Figure 31b shows a stained vehicle treated dataset in yellow, overlaid onto the stained 2×MIC, in red, and 1×MIC dataset, in blue allowing the positive cells to be accurately identified.

We next wanted to determine the source of ROS production. Mitochondria are the most likely source of ROS generation and, as such, mitochondrial superoxide was evaluated using the MitoSOX™ Red reagent. Oxidation of MitoSOX Red by ROS, especially superoxide produces red fluorescence, which can be detected by flow cytometric analysis and is corresponded to the amount of ROS present in the mitochondria. It was found that sphingosine treatment leads to an elevation in the mitochondrial superoxide levels indicated by a significant shift in the fluorescence signal peak toward higher ROS levels as compared with untreated control (Figure 32). This effect was time and dosage dependent.

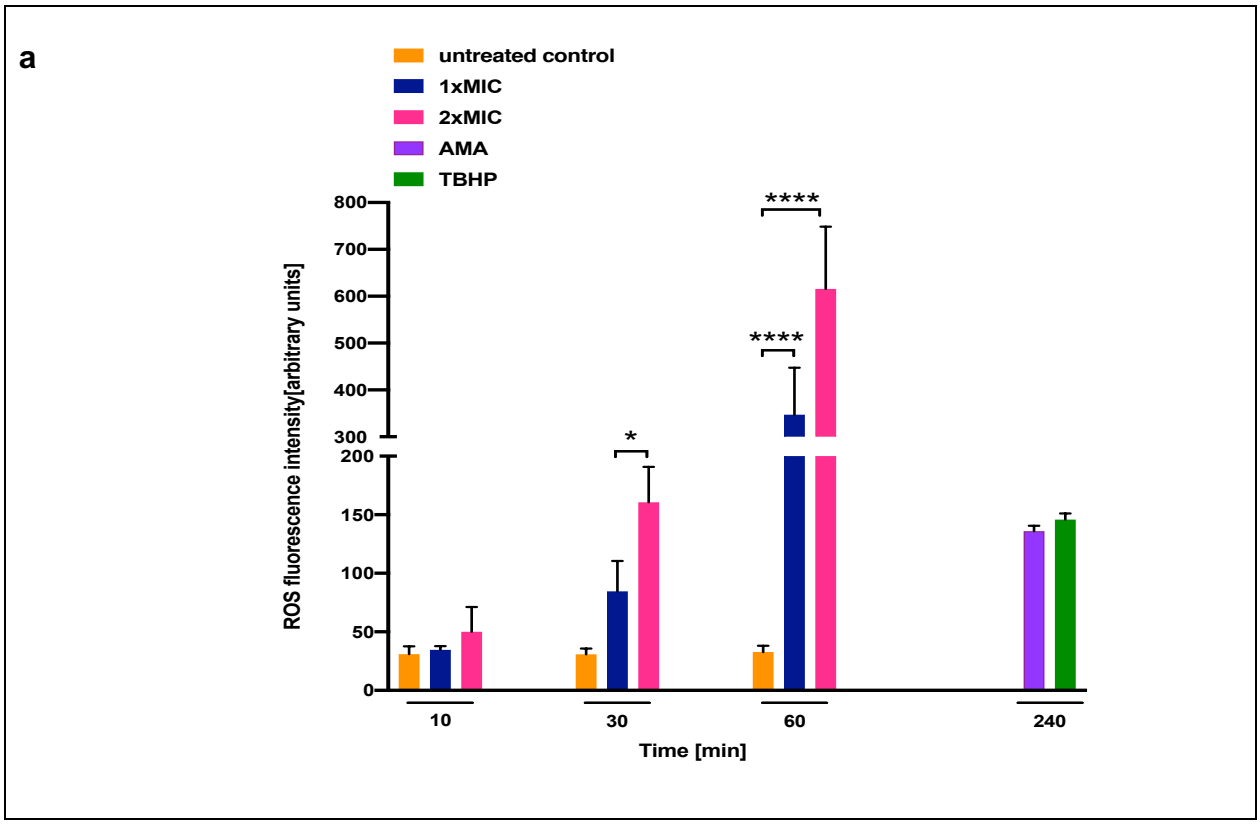

b

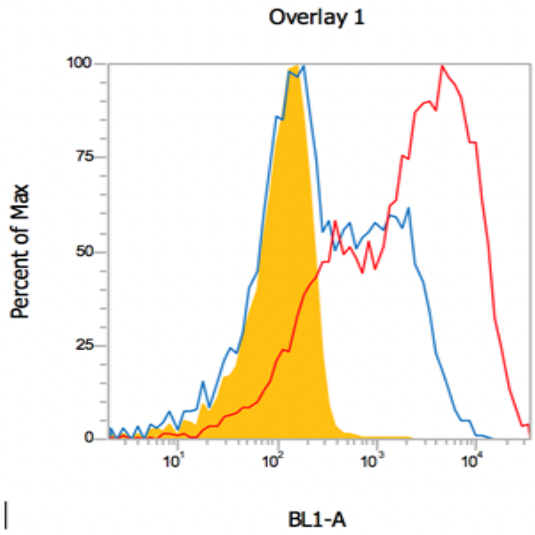

Figure 31. Assessment of ROS accumulation after sphingosine treatment. (**a**) ROS accumulation in *C. glabrata* was evaluated by H_2DCFDA and analysed by flow cytometry. Cells were exposed to different concentrations (1×MIC, 2×MIC) of sphingosine at 37°C for 10, 30, 60 min, along with 50 µM tertbutyl hydrogen peroxide (TBHP) and 10 µg/mL antimycin A (AMA) for 240 min as positive controls. Cellular production of ROS was detected 60 min after treatment with sphingosine. (**b**) Overlay histogram of vehicle treated dataset in yellow, stained 2×MIC, in red, and 1×MIC dataset, in blue. The x-axis shows the H_2DCFDA fluorescence and the y-axis shows the cell counts. Shown is the mean ± standard deviation, n = 3. *$p < 0.05$; ****$p < 0.0001$, Dunnett´s multiple comparisons test.

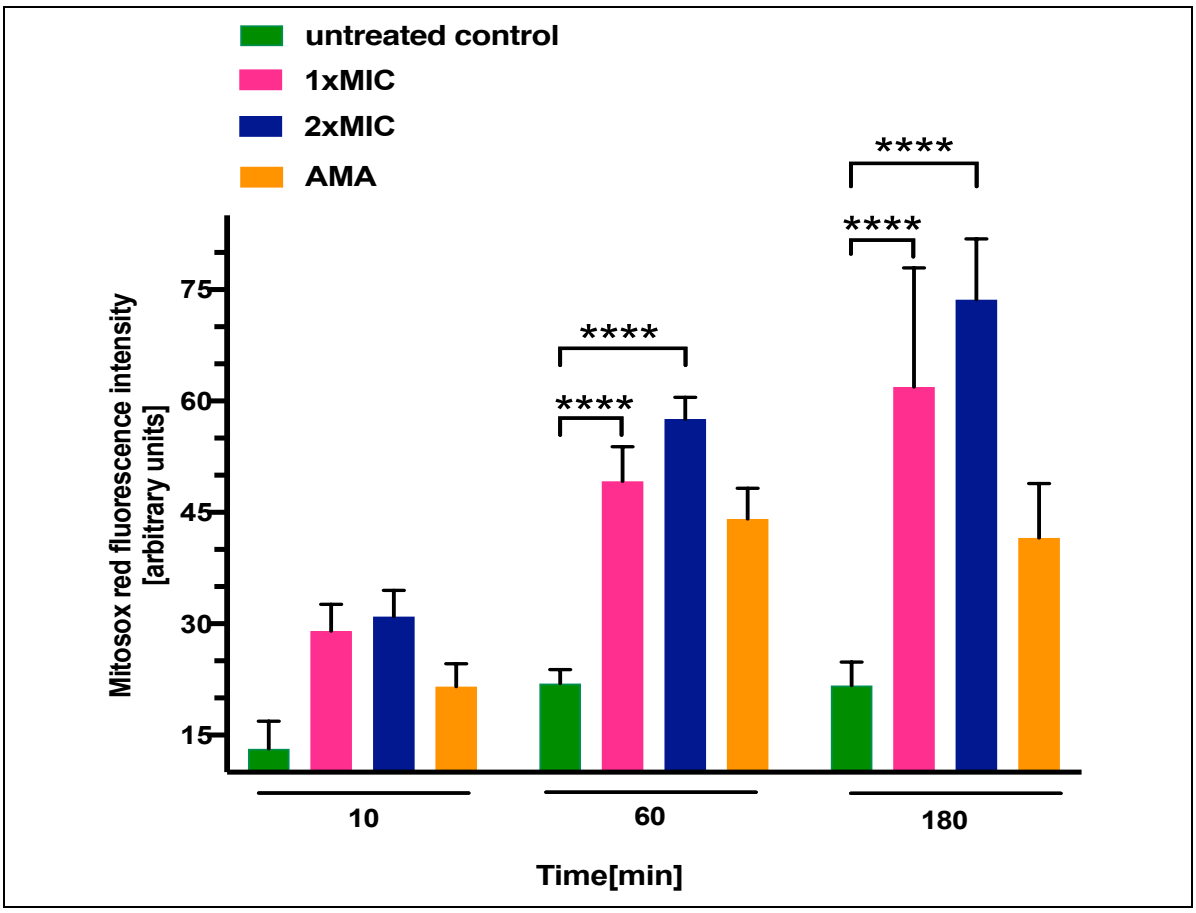

Figure 32. Flow cytometry analysis of mitochondrial ROS accumulation. 10 µM antimycin A (AMA)-treated cells were used as positive control. All samples were stained with 5 µM MitoSOX Red for 15 min. The x-axis shows the MitoSOX Red fluorescence and the y-axis shows the cell counts. Shown is the mean ± standard deviation, n = 3. ****$p < 0.0001$. Dunnett´s multiple comparisons test.

4.4.3 Depolarization of the mitochondrial membrane potential (Δψm)

The maintenance of appropriate Δψm is crucial for cells to survive as disorder of Δψm triggers a series of events like cytochrome *c* release, alteration in mitochondrial morphology and mitochondria-mediated apoptosis (Ganta et al., 2017). Occurrence of mitochondrial outer membrane permeabilization (MOMP) is considered as 'point of no return' due to the leakage mitochondrial inner membrane proteins in to the cytosol (Chipuk et al., 2006). We therefore evaluated the alteration in Δψm as a function of sphingosine treatment using Rhodamine 123 probe. Rh123 is a lipophilic cationic fluorescent dye known to accumulate into the respiring mitochondria and distributes according to the negative membrane potential across the mitochondrial inner membrane. Loss of potential will result in loss of the dye and, therefore, the fluorescence intensity (J. A. Brown & Catley, 1992; Johnson et al., 1980).

C. glabrata DSM70614 cells were subjected to 10, 60 and 120 minute-treatment of sphingosine with different concentrations and stained with Rh123, which accumulates within energized mitochondria with intact membrane potential. These results reveal a significant reduction in total fluorescence intensity (Figure 33) already after 10 minutes treatment with 1×MIC indicating mitochondrial membrane depolarization as an early event in killing by sphingosine. Further increase of the dosage of sphingosine to 2×MIC or increasing the duration of the treatment up to 120 minutes does not significantly increase the effect. NaN_3 as an apoptosis inducer via increasing the permeability potential of the mitochondrial membrane and inhibition of cytochrome oxidase in the mitochondrial electron transport chain (Leary et al., 2002; van Laar et al., 2015) was used as positive control.

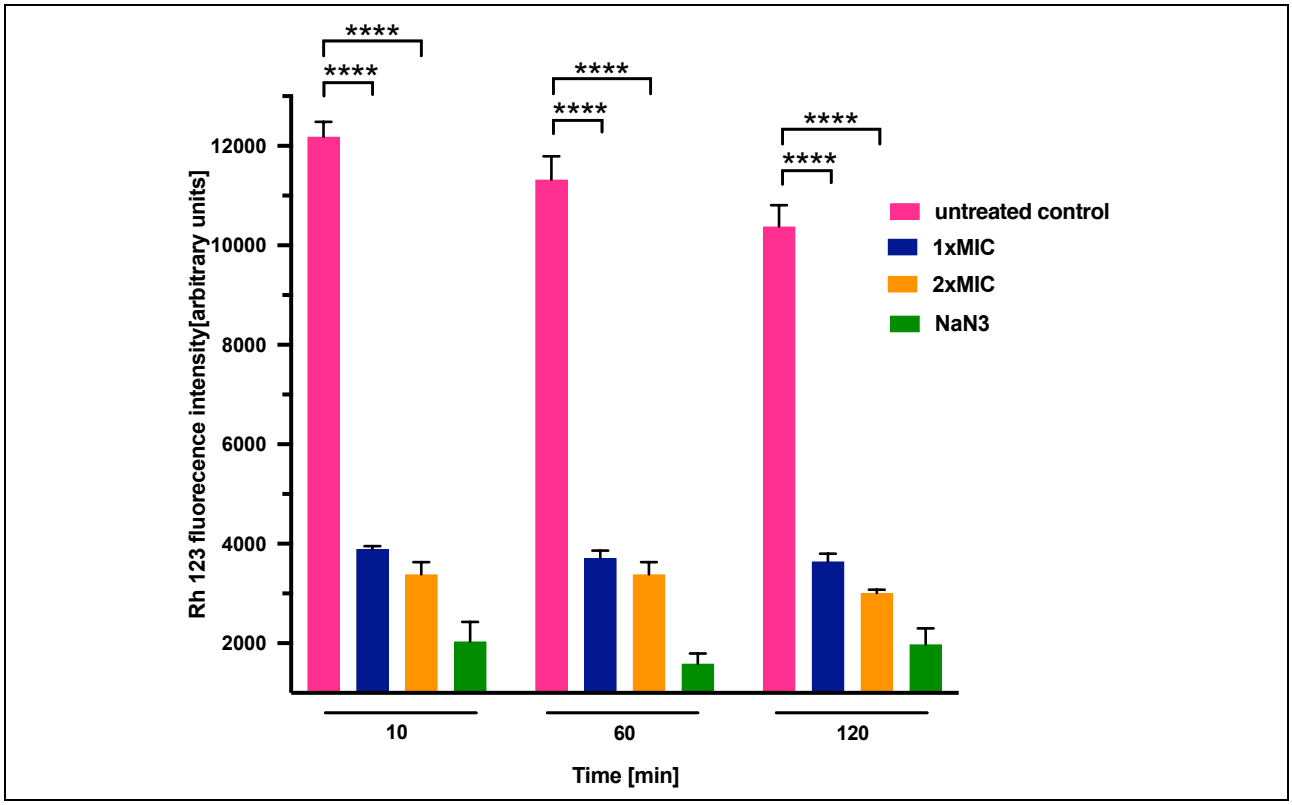

Figure 33. Mitochondrial membrane potential (Δψm) depolarization detected by FCM.
Treatment with sphingosine leads to early depolarization of the mitochondrial membrane potential (Δψm), mitochondrial ROS generation and directly to a release of cytochrome *c*. *C. glabrata* DSM70614 cells were exposed to sphingosine (1×MIC, 2×MIC), harvested after 10, 60- and 120-min incubation. Rh-123 was added at a final concentration of 25 µM for 10 min. Shown is the mean ± standard deviation, n = 3. ****$p < 0.0001$. Dunnett´s multiple comparisons test.

4.4.4 Release of cytochrome *c* from mitochondria

Loss of Δψm during apoptosis initiates opening of permeability transition pores for release of cytochrome *c* which further enhances upon caspase activation (Ricci et al., 2003). Release of cytochrome *c* leading to intrinsic apoptotic pathway is one of the regular phenomena resulting due to stress caused by different drugs that may be initiated by ROS (Atlante et al., 2000). To determine the release of cytochrome *c* we freshly isolated mitochondria from *C. glabrata* and incubated them with different concentrations of sphingosine for 10, 30 and 60 minutes. Cytochrome *c* release into the supernatant was detected by western blotting (Figure 34). It is shown that treatment with sphingosine results in the release of cytochrome *c* to the cytosol in a dose and time dependent manner. Treatment with 1 mM H_2O_2 was used as positive control. This experiment shows that the action of sphingosine directly on mitochondria induces the release of cytochrome *c in vitro,* supporting the notion that a direct effect on mitochondria may be the main mechanism of the fungicidal effect of sphingosine. Overall, these data indicate that dissipation of Δψm is an early event during sphingosine treatment followed by cytochrome *c* release. During early events of apoptosis, loss of Δψm causes detachment and release of cytochrome *c* from mitochondria (Heiskanen et al. 1999; Gottlieb et al. 2003).

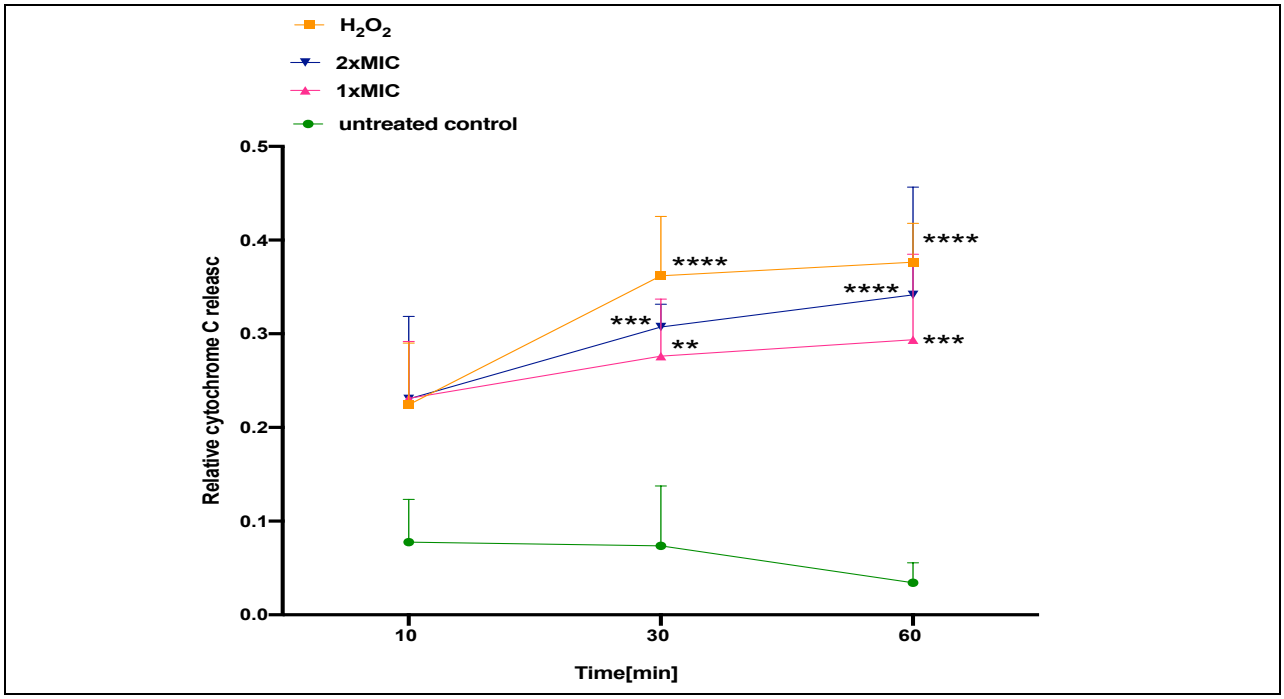

Figure 34. Mitochondrial cytochrome c release. Mitochondria from *C. glabrata* cells were freshly isolated, suspended in osmotic buffer, and incubated either with or without sphingosine (1×MIC, 2×MIC) for 10, 30 or 60 min at 25°C. Mitochondria were centrifuged, and both the pellet and the supernatant were subjected to SDS–15% PAGE and western blotting using anti-cytochrome *c* antibodies. The intensity of signals from western blot analysis were quantified using a Typhoon™FLA 9000 biomolecular imager. Shown is the mean ± standard deviation, n = 3. $^{**}p < 0.01$, $^{***}p < 0.001$, $^{****}p < 0.0001$, Dunnett´s multiple comparisons test.

4.4.5 Structural characterization of sphingosine metabolites shows no significant conversion

To determine whether sphingosine is converted to metabolites including S1P, C16 ceramide, a rapid resolution liquid chromatography/mass spectrometry analysis was performed according to previous study (Gulbins et al., 2018). In brief, *Candida* cells were cultivated in YPD broth for 16 h. Then, 10^6 cell/mL was incubated with increasing concentrations of sphingosine (2 µg/mL, 1 µg/mL and 0.5 µg/mL) in RPMI. Samples were washed 2-3 times with ice-cold PBS after predetermined timepoints, shock-frozen in liquid nitrogen and stored at -80° for lipid extraction. It was shown that cells accumulate SPH within a minute in a dose-dependent manner (Figure 35b) and form substantial amounts of S1P. Although S1P has no antifungal activity, it is probably produced due to yeast SK activity in the cytosol. The amount of traces of C16 Cer upon incubation with SPH were lower than the detection limit. The mass spectrometer results are shown in Figure 35.

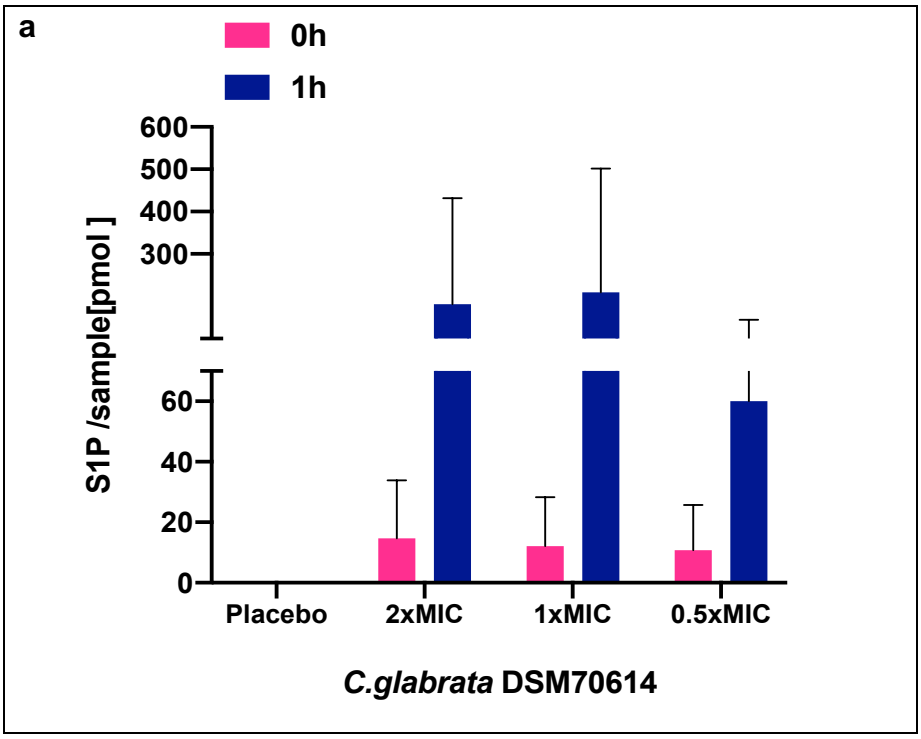

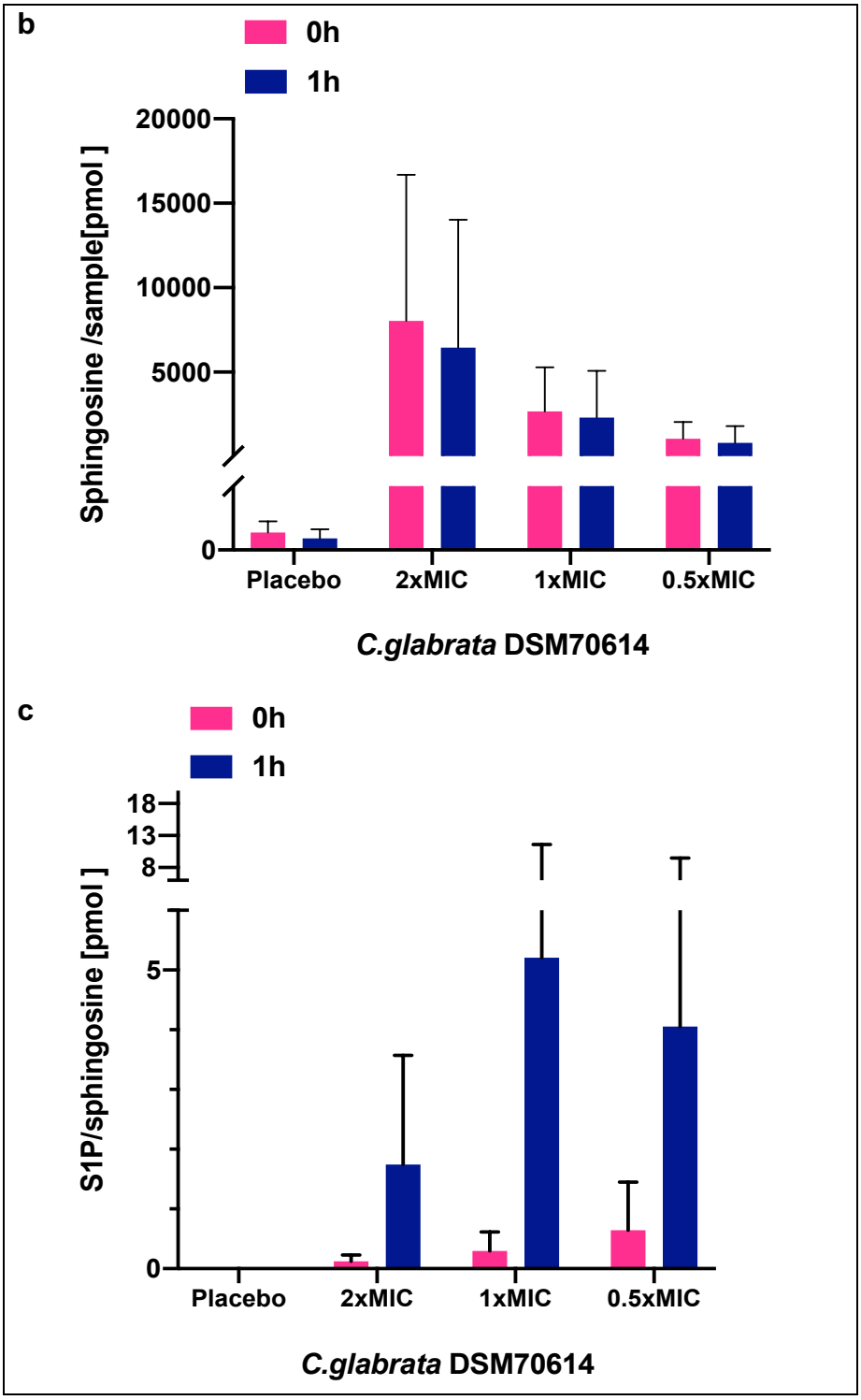

Figure 35. Mass spectrometric analysis of sphingosine metabolites. 10^6 cell/mL was incubated with increasing concentrations of sphingosine (2 µg/mL, 1 µg/mL and 0.5 µg/mL) in RPMI. Cells washed with ice-cold PBS after predetermined timepoints, shock-frozen in liquid nitrogen and lipids were extracted (**a**) Cells form S1P after sphingosine treatment (**b**) cells accumulate SPH within a minute in a dose-dependent manner (**c**) S1P/SPH ratio shows conversion of SPH to S1P.

5. Discussion

5.1 Part 1: Sphingosine and fungal cells

Sphingolipids have been shown to play a central role in many viral and bacterial infections. Sphingosine, which is consumed from ceramide by activity of ceramidases, has remarkable antimicrobial activities against a wide range of Gram-positive and Gram-negative bacteria (Azuma et al., 2018; Bibel et al., 1992; Fischer et al., 2013; Grassmé et al., 2017; LaBauve & Wargo, 2014; Pewzner-Jung et al., 2014; Tavakoli Tabazavareh et al., 2016). Inhaled nebulized sphingosine can also eliminate *P. aeruginosa* and *S. aureus* in pulmonary infected cystic fibrosis mice without producing severe toxic side effects (Pewzner-Jung et al., 2014; Sakamoto et al., 2005; Tavakoli Tabazavareh et al., 2016). Sphingosine even seems to positively influence several significant viral infections, such as HCV and SARS-CoV-2, by interfering with the interaction between the virus and its receptor (Edwards et al., 2020; Sakamoto et al., 2005).

It has been shown that sphingosine may be useful as a coating for plastic surfaces and orthopedic implants, thereby preventing bacteria-induced wound infections (Seitz et al., 2019). Biofilm formation contributes to the chronicity of an infection, which is really difficult to manage. Coating implant samples (titanium, steel, and polymethylmethacrylate) with sphingosine prevented implant contamination and resulted in a significant reduction in biofilm formation on the implant surfaces (Beck et al., 2020). These promising data provide evidence that sphingosine may be a novel antimicrobial agent that can prevent bacterial adherence and induce the killing of pathogens and it might be helpful as an antifungal agent. As a result, it may contribute to defensive barrier functions and has the potential in prophylactic application or therapeutic interventions in infection.

The high risk of invasive fungal infections within the raising population of immunocompromised individuals, along with the emergence of resistance to conventional antifungal agents, also due to biofilm formation, requires the development of new antifungal drugs. For this purpose, examinations of sphingosine are warranted to evaluate its potential use as a prophylactic or early treatment for fungal infections.

In the present study, we demonstrate that sphingosine has not only inhibitory but also fungicidal activity against a wide range of standard and clinical strains of fungi, especially *C. glabrata* and *A. fumigatus.* The antifungal activity of sphingosine against *Aspergillus* spp. and *Candida* spp. (Table 13) was determined according to the European Committee for Antimicrobial Susceptibility Testing (EUCAST) protocol for yeasts and conidia forming

molds and MIC and MFC values were calculated. Whilst *C. glabrata and C. krusei* are rather sensitive to sphingosine treatment, *C. albicans*, *C. tropicalis* and *C. parapsilosis* strains were resistant (Table 13).

Interestingly, we found marked differences in the sensitivity to sphingosine between *Aspergillus* species: Whilst *A. fumigatus* is rather sensitive to sphingosine treatment, *A. niger*, *A. flavus* and *A. brasiliensis* and *A. tubingnesis* are more resistant (Table 13). The mechanisms of resistance in fungal strains are beyond the focus of this work and were not further investigated but it could be due to increasing expression of conventional resistance genes, such as those coding for efflux pumps, increasing/decreasing expression of proteins involved in cell wall modulation and oxidative stress (Mathé & van Dijck, 2013; Shishodia et al., 2019). Another strategy of antifungal drug resistance is the ability of biofilm formation, which allows adhesion of fungal cells to epithelial or endothelial surfaces, as well as to implanted medical devices (Shishodia et al., 2019).

This ability is an important virulence trait that promotes the persistence of the infection. Compared with planktonic cells, *Candida* biofilms are characterized by increased resistance to the most common antifungal drugs, in particular to amphotericin B and fluconazole (Fernandes et al., 2015; Fonseca et al., 2014; Ramage et al., 2001). We have shown that sensitive strains of *C. glabrata* are weak producer of biofilm, semi-sensitive strains of *C. krusei* are intermediate and resistant strains including *C. albicans*, *C. tropicalis* and *C. parapsilosis* are strong biofilm-producers, which was consistent with the data of previous studies in this field (Brilhante et al., 2016; Roscetto et al., 2018). The ability to produce biofilm seems to correlate inversely to the sensitivity to sphingosine. Although, our main experiments were performed according to the EUCAST protocol on planktonic cells, the effect of sphingosine on the preformed *C. krusei* biofilm was also investigated. Sphingosine was able to penetrate biofilm at a concentration way higher than the MIC value. In fact, the drug concentrations reaching the distal edges of the biofilms always substantially exceeded the MIC. As explained before, fungal biofilms are less susceptible to antifungal drugs than are planktonic yeast cells, because cells are surrounded by an extracellular impenetrable matrix (ECM).

Time-kill assay has the ability to evaluate the efficacy of antifungal agents and the rate of killing a fixed inoculum fungus, determined by comparing control group (no drug) and test group (antifungal agent-containing). Time-kill assays may prove to be helpful in understanding the differences in rates of kill of *A. fumigatus* and *C. glabrata.* Therefore, the killing rate of *C. glabrata* and *A. fumigatus* were further investigated by kinetic growth

assay. We reported that sphingosine is able to kill 99.99% of the cells in couple of hours, which shows the high efficiency of this fungicidal agent. Although numerous factors influence the activity of an agent *in vivo*, our data suggest that the rate and extent of fungicidal activity exhibited by sphingosine *in vitro* are enhanced by increasing the concentration of drug present in solution.

Consideration should be given to the *in vivo* study of optimization of sphingosine dosing regimens based the antifungal properties described for this agent.

5.2 Part 2: Inhaled sphingosine and invasive aspergillosis

The aim of the second part of this thesis was to determine the efficacy of sphingosine as an antifungal agent in an *in vivo* model of invasive aspergillosis in immunosuppressed mice. Invasive aspergillosis (IA) has become the most serious infection in transplant recipient on immunosuppressive therapy and *A. fumigatus* is responsible for most of the invasive fungal infections. According to data from US TRANSNET, patients who received solid organ transplantation have an overall risk of 3.1% per annum for invasive fungal infections, and this risk lasts for at least 3 years after transplantation (Pappas et al., 2010). To address the problems of poor responses to antifungal therapy, effective prophylactic treatments are being developed. Atkins & Crowder (2004) reported that pulmonary infections may not often respond effectively to systemic treatment due to insufficient drug diffusion into pulmonary tissue and dose-limiting toxicities (Crowder & Atkins, 2003). In the last few decades, aerosol delivery of antifungal agents has received more attention. Avoiding the systemic side-effects by direct deposition of antifungal drugs in the lungs is the main advantage of inhalation of antifungal agents.

Immunosuppression and prophylaxis studies: In this research, mice were rendered susceptible to infection with *A. fumigatus* by immunosuppression with a combination of cyclophosphamide and cortisone acetate on day -2 relative to infection (day 0), followed by a second dose of cyclophosphamide and cortisone acetate on day +3. This regimen extended the duration of leukopenia to 9 to 10 days, providing 7 to 8 days of leukopenia after infection and permitting the development of lethal infection (Sheppard et al., 2004). In fact, immunosuppressed C57BL/6 mice were susceptible to pulmonary fungal infections and they could not eliminate or control fungal growth. This is believed to be due to down- regulation of the Th1 immune response after steroid treatment. In addition, the

presence of a Th2 response that involves the up-regulation of IL-10 inhibits fungal clearance in the lung (Elenkov, 2004).

Due to the increased occurrence of IA in high-risk populations, prophylactic treatments against IA are important. There are three potential antifungal prophylactic strategies. One strategy is the use of nonabsorbable antifungal agents to decrease the colonization of the patient ‘s gastrointestinal tract. The second is to give systemic antifungal drugs to patients during or following organ transplantation. The third is to aerosolize antifungal drugs directly into the lung (Perfect et al., 2004). It has been shown that inhaled antifungals such as amphotericin B are able to decrease the incidence of IA in solid organ transplant populations and neutropenic patients (Arthur et al., 2004).

Recently it was proven that *in vivo* and *ex vivo* inhalation of sphingosine has no local side effects in mice and minipig lungs as well as does not induce cell death in bronchi (Carstens et al., 2019, 2021). It was demonstrated that the daily administration of sphingosine did not have any obvious effect of the health status, loss of activity or reduced food intake. No local signs of inflammation in the upper airway were observed, thus it can be used as an effective treatment prior to lung re-implantation by reducing bacterial counts and improving outcome after lung transplantation (Carstens et al., 2021). Additional data supports the use of inhaled sphingosine *against* bacterial infection in a cystic fibrosis (CF) mouse model Pewzner-Jung et al., 2014).

Sphingosine is a long chain base that abundantly expressed on the luminal side of nasal to bronchial epithelial cells in wild-type mice, while sphingosine is greatly reduced in epithelial cells of CF patients and mice, due to reduced activity of the acid ceramidase in CF epithelial cells (Grassmé et al., 2017; Pewzner-Jung et al., 2014; Tavakoli Tabazavareh et al., 2016). These mice showed an increased susceptibility for pulmonary infections, which was corrected by inhalation of sphingosine (Rice et al., 2017; Tavakoli Tabazavareh et al., 2016). Sphingosine inhalation leads to an increase of sphingosine concentrations in the luminal plasma membrane of tracheal and bronchial epithelial cells of CF mice and normalized the susceptibility of CF mice to develop pulmonary infections (Pewzner-Jung et al., 2014), indicating the significance of sphingosine for the defense of the airways against pulmonary infections. Therefore, high efficiency, broad spectrum activity, the lack of adverse effects and good tolerability are big benefits of using inhaled sphingosine as prophylaxis treatment. Furthermore, the correct administration is an important factor in determining the efficacy of sphingosine by inhalation. Therefore, the types of nebulizer and compressor need to be considered. An appropriate nebulizer

producing aerosol particles that are 2-5 μm in diameter. Different nebulizers have been used in the several published reports for nebulizing antifungals. Some factors including design, operating conditions and ancillary equipment are pivotal for final delivered dose and product stability delivered by nebulizer (Drew, 2006). Sphingosine (0.3 kDa) was administrated to the mouse lung using a PARI BOY SX nebulizer.

In this study, the optimized inhalative SPH was tested for its efficacy as prophylaxis against pulmonary aspergillosis in a new immunosuppression mouse model. As explained earlier, a suitable therapeutic antifungal drug for treating IA should have no relevant toxicity and require a simple method of administration. After examining the different concentration of inhaled sphingosine, it was shown that nebulization of 1 mL normal saline solution containing 500 μg SPH prevented the germination of *Aspergillus* spores into mycelia. Therefore, it could be a safe and effective prophylactic dose that gives rise to good efficacy *in vivo* with no inflammation and no side-effects. Specifically, it was evaluated for its prophylaxis properties in reducing the fungal load and inhibiting the invasion of hyphae into lung tissue. The efficacy of sphingosine inhalation on disease progression was assessed by counting CFU, estimating of the rate of mortality and analysis of galactomannan index, inflammation and cytokine responses in the mouse lung.

Estimating the burden of IA: Mice were infected with *A. fumigatus* ATCC46645 conidia. Sphingosine was applied by daily inhalation for 10 min, inhalation started 3 days before infection. Therefore, our translational model mimics closer a prophylactical setting. Prophylactic treatment with inhalative sphingosine starting 3 days before *Aspergillus* infection for up to 14 days resulted in 100% survival and in resolution of the infection, whilst placebo inhaled mice had a lethality/reaching of the dropout burden of 50% (Figure 17). Pulmonary disease development was accompanied by marked weight loss, with the animals reaching a critical threshold for survival when they had lost 20% of their body weight on day 0. In this study placebo treated mice display clinical signs while alive (20% weight loss with respect to weight on D0 and lethargic behavior) had histological signs of invasive aspergillosis (Figure 18), whereas weight loss in SPH treated mice was not significant.

We further quantified *Aspergillus* burden 1 hour after infection and 4 days after infection in sphingosine and placebo-treated mice. While one hour after infection the number of detectable conidia in treated and placebo-treated animals was about the same, 4 days

after infection, there was already a clear difference with a reduction of detectable *Aspergillus* by 99% in the CFU assay, indicating a marked effect of sphingosine (Figure 19). The BAL galactomannan levels also paralleled the microbiologic decline in pulmonary tissue burden of *A. fumigatus* as a surrogate parameter for a therapeutic response (Figure 20). Galactomannan makes up a major part of the cell wall of *Aspergillus* spp. (Latge et al., 1994) and are secreted *in vivo* by the fungus during invasive growth. In recent years, the detection of glucofuranose-containing antigens, including GM, has been used for diagnosing invasive aspergillosis (IA) (Mercier et al., 2018). This assay could potentially also be useful for the early evaluation of the efficacy of antifungal therapy and for predicting the outcome in terms of response and survival. GM monitoring can be continued after antifungal therapy has been initiated. The significant decrease in the GM index after SPH treatment is completely consistent with the previous data, indicating the absence of infection (Figure 20).

In additional experiments we started sphingosine treatment 3 days after infection. Here we could not detect any protective effect improving survival. The infection of the mice was caused by application of conidia. It is therefore possible that the effect of sphingosine is essentially limited to the killing of conidia. A therapeutic effect of sphingosine after later application from day 3 of infection showed no measurable survival advantage compared to placebo. This may be because the mice in the selected setting may have been already too sick and the disease too much advanced having passed a point of no return. On the other hand, one speculates that the ineffective therapeutic effect might be due to the formation of hyphae with their invasive growth and possibly inhalative sphingosine may not have reached the area of severe infection due the associated aeration disturbance.

However, it must be assumed that there are more limitations in our mouse model of invasive aspergillosis compared to the human setting; i. the spontaneous course of the disease is very short, we find 50% lethality/reaching of the dropout burden in placebo-treated mice after 4 days. In humans, an invasive aspergillosis, even in immunosuppressed, develops over several weeks to months. ii. due to the direct intratracheal application/nebulization the lung is affected in very short time; in the human situation invasive aspergillosis in the many most times does not affect the whole lung. Future studies are required to establish a curative model.

Cytokine responses: Although, IFN-γ and TNF-α are the most important cytokines responsible for host resistance against *A. fumigatus* infection (Cortez et al., 2006),

surprisingly no cytokine response was observed in both sphingosine and placebo treated groups. It is likely that the steroid treatment required to make the mouse susceptible and suppresses cytokine production in the lung. Cortisone acetate, which is used in this study, is the C21 acetate ester of cortisone and acts as a prodrug of cortisone in the body (Løvås & Husebye, 2003). This group of immunosuppressive agents are known to affect T cell-mediated inflammation by the inhibition of proliferation and cytokine production (de Jong et al., 1999). Previously, it has been demonstrated that corticosteroids down-regulate the production of the pro-inflammatory cytokines IL-1 beta, IL-6, TNF-α and IFN-γ (Breuninger et al., 1993; Hu et al., 2003; Linden & Brattsand, 1994; Steer et al., 1997; Wilckens & de Rijk, 1997).

However, to prove this hypothesis in this study, more accurate experiments such as measuring the chemokine and cytokine levels using RT-PCR of lung tissue homogenates at different time points post-infection are needed.

Histological studies: The effects of sphingosine treatment and the progress of the disease was also studied using tissue histology. It is an essential tool to further demonstrate the impact of SPH on pathology and fungal load. This method is commonly used to recognize the differences in tissue morphology of experimental animal models after infection with *A. fumigatus*. PAS stained lung tissue sections is also very useful in visualizing the differences between SPH treated and untreated mice. Histological slides of immunosuppressed infected and placebo treated mouse lung showed mycelia with dichotomous branching and septate hyphae with extensive necrosis of the lung tissue (Figure 22 a, b, c and d). In contrast, no necrosis and invasive fungal hyphae were seen in SPH treated slides at day +4 (Figure 22 e, f).

The effect of SPH treatment and progress of the disease was also studied using tissue inflammation as readout. The percentage inflammation surface was increased almost six times in immunosuppressed and infected C57Bl/6 mice (58.4 ± 4.0%) as compared to immuno-suppressed + infected and SPH treated mice with 500 µg SPH (Figure 23). The histological evidence supports the effectiveness of the sphingosine in the control of invasive aspergillosis. This was seen as a reduction in fungal load, inflammation and cellular infiltrate in sphingosine treated mice lungs.

Cytotoxicity of SPH: The biological properties of the different concentrations of SPH were determined *in vitro*. LL2 and A549 cell lines were used for these biological studies.

Toxicity was assessed using an MTT assay. We have shown that the IC_{50} value in LL/2 cells is 4 times and in A549 is 8 times higher than MIC value in *C. glabrata.* In addition, the effect of SPH was also tested in the lung tissue. Our treatment protocol was very well tolerated, the mice did not have any visible side effects that would have been attributable to the inhalation treatment with sphingosine. In TUNEL assays performed with lung tissue sections after 7 days of sphingosine inhalation no cell death could be detected (Figure 25). The results showed no evidence for any induction of cell death by sphingosine. These data are in line with previous work in mini-pig and mouse models with sphingosine-inhalation in other contexts which explained earlier (Carstens et al., 2019; Martin et al., 2017; Seitz et al., 2019). From the above study it is concluded that sphingosine is a promising compound with potential use in the treatment of fungal infection.

In conclusion, sphingosine is effective in a mouse model of pulmonary aspergillosis, at least in a prophylactic setting, and the therapy is well tolerated without so far detectable side effects. Given its potent antifungal activity, excellent safety profile, and favorable pharmacokinetic parameters, sphingosine presents the potential for administration as a prophylactic treatment in the prevention of invasive pulmonary aspergillosis. These *in vivo* findings provide a foundation for understanding the antifungal activity, safety, and pharmacokinetics of sphingosine in immunocompromised patients and form a foundation for developing clinical trials for the prevention and treatment of invasive pulmonary aspergillosis.

5.3 Part 3: Fungal cell death pathway

The commonly used antifungal drugs can be classified into different classes based on their site of action. The fungistatic azoles inhibit ergosterol biosynthesis via the cytochrome P450 enzyme 14-α demethylase, which is involved in conversion of lanosterol to ergosterol. Depletion of membrane ergosterol due to the use of azoles causes' cell membrane disruption and growth inhibition (Tatsumi et al., 2013). Polyenes mainly include amphotericin B, natamycin and nystatin exhibit fungicidal activity primarily by binding to ergosterol and formation of pores in plasma membrane that promote leakage of intracellular ions and cell death (Baginski & Czub, 2009; Odds et al., 2003; Sanglard et al., 2009). Inhibition of DNA and RNA synthesis is related to the action of pyrimidine analogues such as 5-flucytosine (5-FC) via converting to 5-fluorouracil and then to 5-fluorouridylic acid by UMP pyrophosphorylase (Odds et al., 2003; Sanglard et al., 2009). The fungal cell wall containing chitin and β-glucan is another target of many antifungal

drugs. It is known that treatment with echinocandins family which include caspofungin, micafungin and anidulafungin can cause inhibition of cell wall synthesis by acting as non-competitive inhibitors of -1, 3 glucan synthases required for glucan synthesis.

It was somewhat challenging to choose the appropriate specie to perform the experiments related to the mechanism of action of sphingosine. The limited range of molecular and synthetic biology tools, probes and high-throughput technologies, which are designed for filamentous fungi delays research and the identification of antifungal targets. In addition, development of these filamentous fungi to multinucleated hyphal structure in liquid medium was an extra challenge. Therefore, we selected the reference strain of *C. glabrata* DSM70614 due to its simplicity and its close relatedness to higher eukaryotes as experimental system to elucidate the mode of action of sphingosine.

Previous studies in our group have shown that sphingosine is able to kill bacteria by binding to cardiolipin. Cardiolipin (CL) consists of two molecules of phosphatidate linked by one molecule of glycerol. The lipid differs from all other phosphoglycerates in that it carries four fatty acids instead of two. Cardiolipin is found in the inner membrane of mitochondria as well as in bacterial membranes, but not in eukaryotic cell membranes. It has been shown that the presence of the protonated NH_2 group in sphingosine, which is an amino-alcohol, is required for sphingosine's bactericidal activity(Verhaegh et al., 2020). The protonated NH_2 group of sphingosine binds to the highly negatively–charged lipid cardiolipin in bacterial plasma membranes. *E. coli* or *P. aeruginosa* strains that lack cardiolipin synthase were resistant to sphingosine, finally indicating that the binding of sphingosine and cardiolipin is required for sphingosine toxicity(Verhaegh et al., 2020). Presumably, this clustering results in rapid permeabilization of the plasma membrane and bacterial cell death.

It should be mentioned that similar to mammalian cells, yeasts typically undergo cell death and exhibit apoptotic markers(Madeo et al., 1997). Several compounds, some of which have been demonstrated to work through mitochondrial pathways, have been utilized to trigger apoptosis in wild type yeast cells (Madeo et al., 2004). The regulation of yeast programmed cell death required complex mitochondrial processes, such as cytochrome *c* release, channel opening upon human Bax expression, depolarization of mitochondrial membrane potential, and mitochondrial fragmentation (Eisenberg et al., 2007; Madeo et al., 2004). Cardiolipin (CL), the signature lipid of yeast mitochondria, roles in many mitochondrial processes as well as apoptosis (Joshi et al., 2009). In response to apoptosis-inducing stimuli, cells lacking CL exhibit accelerated entry into apoptosis (Choi

et al., 2006). In normal cells, CL is necessary for the loose binding of cytochrome *c* to the mitochondrial inner membrane by electrostatic interactions (Iverson & Orrenius, 2004) and for the function of the adenine nucleotide translocase, which is a component of the mitochondrial permeability transition pore (Crompton, 2000; Halestrap, 1999; B. Hoffmann et al., 1994). A considerable increase in the cytochrome *c* released into the cytoplasm during apoptosis is mediated by CL peroxidation and a decline in total CL levels (Choi et al., 2006; Iverson & Orrenius, 2004; Ostrander et al., 2001; Ott et al., 2002; Shidoji et al., 1999). Furthermore, the loss of CL leads into respiration defects that may contribute to the generation of ROS. Increased ROS, which is related to mitochondrial dysfunction, triggers apoptosis (Büttner et al., 2006; Iverson & Orrenius, 2004; Osiewacz & Scheckhuber, 2006).

In this study, we also found a direct effect of sphingosine on mitochondria. Incubation of yeast cells with sphingosine leads to early depolarization of the mitochondrial membrane potential (Δψm) and mitochondrial ROS generation within minutes. Mitochondrial depolarization accompanies cytochrome *c* release in yeast cells undergoing apoptosis. Cardiolipins are also present in the inner mitochondrial membrane (IMM), so that the data on the mechanism of action generated in bacteria may be transferable to mitochondria. This is supported by the fact that we already see clear effects which indicate the permeabilization of the inner mitochondrial membrane and mitochondrial depolarization within a few minutes of sphingosine treatment. CL is particularly susceptible to ROS attack because of its location in the mitochondrial inner membrane close to the site of ROS generation, and due to its high content of unsaturated fatty acids that are highly vulnerable to oxidative damage (Petrosillo et al., 2001; Shidoji et al., 1999).

In line with our findings, previously has been proven that the oxidation of CL, in fact, generates CL hydroperoxides, compounds that, having a low affinity for cytochrome *c*, favor the permeabilization of the mitochondrial membrane, and the release of cytochrome *c* together with other pro-apoptotic factors into the cytosol (Chertkova et al., 2021; Dadsena et al., 2021). Although further research is needed, but apparently sphingosine via binding to cardiolipin in the IMM induce program cell death. The schematic diagram of this molecular mechanism is shown in Figure 36.

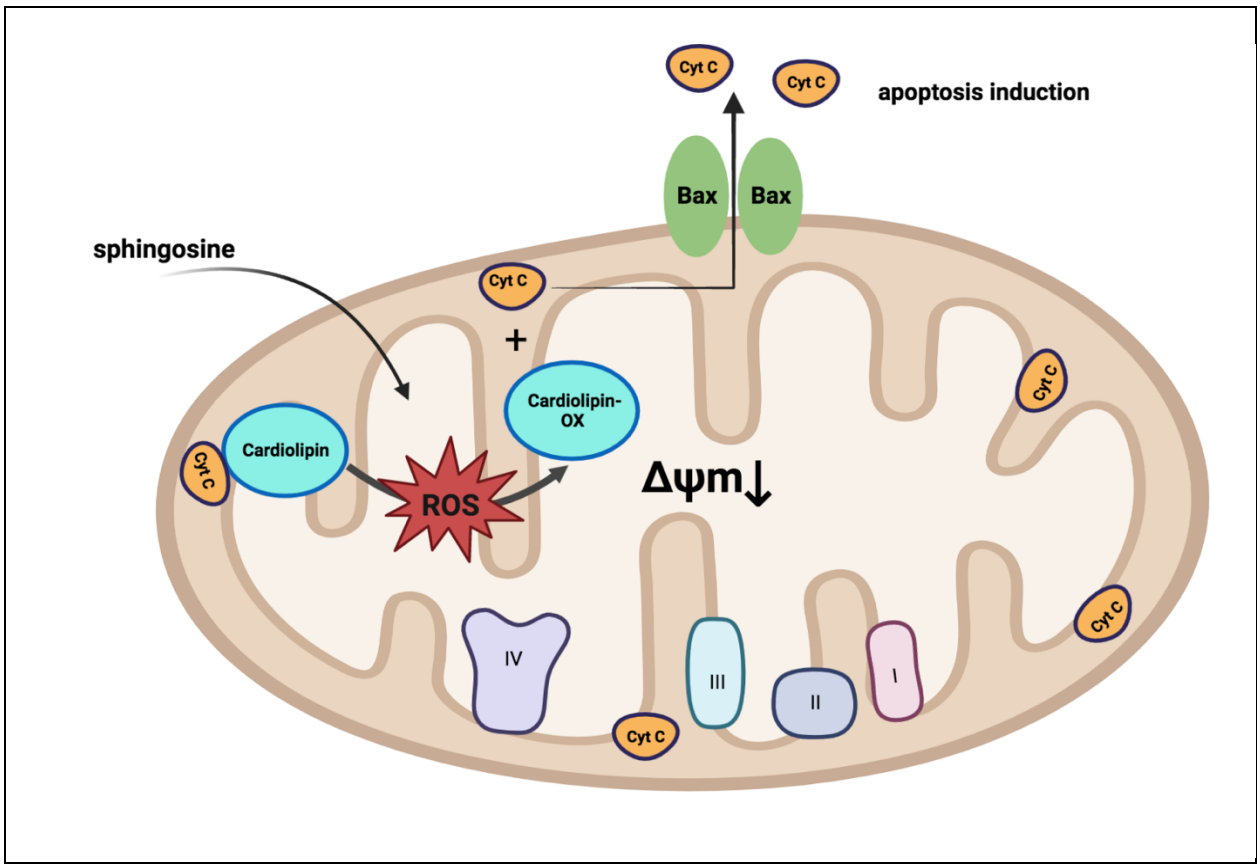

Figure 36. Schematic representation of apoptosis mechanism after sphingosine treatment. Incubation of yeast cells with sphingosine leads to early depolarization of the mitochondrial membrane potential (Δψm) and mitochondrial ROS generation within minutes. CL is particularly susceptible to ROS attack and converted to cardiolipin hydroperoxides with low affinity for cytochrome *c* and favor the permeabilization of the mitochondrial membrane. Cytochrome *c* is detached from oxidized CL and released into the cytosol. Created with Biorender.com.

We further detected disruption of the cell membrane by staining with propidium iodide which substantially increased during incubation within 6 hours, indicating that this effect has to be seen as secondary consequence of the effects of sphingosine on mitochondria in the frame of apoptosis. Direct fluorescence imaging of the cell wall revealed that sphingosine has no interaction with cell wall polysaccharides, where its structure remained apparently intact.

Our data suggest that the mode of action of sphingosine in fungi is due to a direct effect on mitochondria. It should be noted that the mitochondrial death pathway suggested by us in this study goes in line with the results obtained through stimulation with various drugs. It is certainly many yeast apoptosis inducers acting through the mitochondrial pathway trigger a similar chain of events.

If the toxicity of sphingosine is due to its effect on cardiolipins of the inner mitochondrial membrane, the question naturally arises as to how the specificity of the effect could be achieved in the mouse model. As explained in discussion part 2, no toxicity was detected

in normal lung tissue after SPH treatment. In line with our results, also in previous studies no relevant increase in bronchial epithelium was observed after inhalation of up to 1000 µM sphingosine (Carstens et al., 2019). The exact reason for this is not known, but it might be that inhalation amounts of sphingosine micelles are trapped in the mucus and able to kill pathogens, but do not penetrate the epithelium itself. In accordance, it has been shown that large portion of sphingosine remains in the mucus on top of the epithelial cell layer and is not uptake (Seitz et al., 2019). Furthermore, it is possible that bronchial cells can rapidly metabolize sphingosine through increased expression of sphingosine kinases, therefore reducing its toxicity. However, the reason for sphingosine-resistance of normal bronchial cells requires further definition.

In summary, the results of the present study show that sphingosine is effective against fungal infection. Using a murine model of pulmonary aspergillosis, we found that prophylactically applied inhaled sphingosine protects against the lethal course of pulmonary aspergillosis. Our findings suggest that the mechanism of action is a direct effect on mitochondria, but to better understand the complex molecular mechanisms of the effect of SPH in fungal infections and to develop antifungal therapies, especially for aspergillosis, further studies are needed.

6. Summary

The presented thesis studied the role of sphingosine in fungal infection, focusing on pulmonary aspergillosis causing by *A. fumigatus*. The work also employed *C. glabrata* as experimental system to elucidate the mode of action of sphingosine due to its simplicity and its close relatedness to higher eukaryotes.

The major findings are:

- Sphingosine is effective against yeast and conidia forming moulds according to EUCAST methods.
- Fungicidal activity of sphingosine is time and dose dependent.
- Prophylactically applied sphingosine as inhalation protects against the lethal course of pulmonary aspergillosis in immunocompromised mice.
- Lung fungal load as well as galactomannan index and inflammation percentage decrease after sphingosine inhalation.
- Inhaled sphingosine has no adverse side effects in the mice lungs.
- Sphingosine permeabilizes the inner mitochondrial membrane and causes mitochondrial depolarization and ROS generation, follow by cytochrome *c* release.
- Sphingosine causes fungal cell death via direct effect on yeast mitochondria.
- Cell membrane disruption is considered as secondary consequence of the effects of sphingosine on mitochondria in the frame of apoptosis.

The present data regarding the role of sphingosine in fungal infection provide a novel prophylactic strategy against pulmonary infections in susceptible patients.

7. References

Alekseeva, L., Huet, D., Féménia, F., Mouyna, I., Abdelouahab, M., Cagna, A., Guerrier, D., Tichanné-Seltzer, V., Baeza-Squiban, A., Chermette, R., Latgé, J. P., & Berkova, N. (2009). Inducible expression of beta defensins by human respiratory epithelial cells exposed to Aspergillus fumigatus organisms. *BMC Microbiology*, *9*(1), 1–21. https://doi.org/10.1186/1471-2180-9-33/TABLES/2

Alexander, B. D., Johnson, M. D., Pfeiffer, C. D., Jiménez-Ortigosa, C., Catania, J., Booker, R., Castanheira, M., Messer, S. A., Perlin, D. S., & Pfaller, M. A. (2013). Increasing Echinocandin Resistance in Candida glabrata: Clinical Failure Correlates with Presence of FKS Mutations and Elevated Minimum Inhibitory Concentrations. *Clinical Infectious Diseases*, *56*(12), 1724–1732. https://doi.org/10.1093/CID/CIT136

Allen, C., Büttner, S., Aragon, A. D., Thomas, J. A., Meirelles, O., Jaetao, J. E., Benn, D., Ruby, S. W., Veenhuis, M., Madeo, F., & Werner-Washburne, M. (2006). Isolation of quiescent and nonquiescent cells from yeast stationary-phase cultures. *The Journal of Cell Biology*, *174*(1), 89. https://doi.org/10.1083/JCB.200604072

Allen, M. J., Harbeck, R., Smith, B., Voelker, D. R., & Mason, R. J. (1999). Binding of Rat and Human Surfactant Proteins A and D to Aspergillus fumigatus Conidia. *Infection and Immunity*, *67*(9), 4563. https://doi.org/10.1128/IAI.67.9.4563-4569.1999

Allen, M. J., Voelker, D. R., & Mason, R. J. (2001). Interactions of Surfactant Proteins A and D with Saccharomyces cerevisiae and Aspergillus fumigatus. *Infection and Immunity*, *69*(4), 2037. https://doi.org/10.1128/IAI.69.4.2037-2044.2001

Almeida, T., Marques, M., Mojzita, D., Amorim, M. A., Silva, R. D., Almeida, B., Rodrigues, P., Ludovico, P., Hohmann, S., Moradas-Ferreira, P., Côrte-Real, M., & Costa, V. (2008). Isc1p plays a key role in hydrogen peroxide resistance and chronological lifespan through modulation of iron levels and apoptosis. *Molecular Biology of the Cell*, *19*(3), 865–876. https://doi.org/10.1091/MBC.E07-06-0604/ASSET/IMAGES/LARGE/ZMK0030884400011.JPEG

Amitani, R., Taylor, G., Elezis, E. N., Llewellyn-Jones, C., Mitchell, J., Kuze, F., Cole, P. J., & Wilson, R. (1995). Purification and characterization of factors produced by Aspergillus fumigatus which affect human ciliated respiratory epithelium. *Infection and Immunity*, *63*(9), 3266. https://doi.org/10.1128/IAI.63.9.3266-3271.1995

Annaix, V., Bouchara, J. P., Larcher, G., Chabasse, D., & Tronchin, G. (1992). Specific binding of human fibrinogen fragment D to Aspergillus fumigatus conidia. *Infection and Immunity*, *60*(5), 1747. https://doi.org/10.1128/IAI.60.5.1747-1755.1992

Arendrup, M. C., Cuenca-Estrella, M., Lass-Flörl, C., Hope, W., Arendrup, M. C., Hope, W. W., Flörl, C., Cuenca-Estrella, M., Arikan, S., Barchiesi, F., Bille, J., Chryssanthou, E., Groll, A., Gaustad, P., Järv, H., Klimko, N., Lortholary, O., Matos, T., Moore, C., … Verweij, P. (2012). EUCAST technical note on the EUCAST definitive document EDef 7.2: method for the determination of broth dilution minimum inhibitory concentrations of antifungal agents for yeasts EDef 7.2 (EUCAST-AFST). *Clinical Microbiology and Infection: The Official Publication of the European Society of Clinical Microbiology and Infectious Diseases*, *18*(7). https://doi.org/10.1111/J.1469-0691.2012.03880.X

Arikawa, J., Ishibashi, M., Kawashima, M., Takagi, Y., Ichikawa, Y., & Imokawa, G. (2002). Decreased Levels of Sphingosine, a Natural Antimicrobial Agent, may be Associated with Vulnerability of the Stratum Corneum from Patients with Atopic Dermatitis to Colonization by Staphylococcus aureus. *Journal of Investigative Dermatology*, *119*(2), 433–439. https://doi.org/10.1046/J.1523-1747.2002.01846.X

Arthur, R. R., Drew, R. H., & Perfect, J. R. (2004). Novel modes of antifungal drug administration. *Expert Opinion on Investigational Drugs*, *13*(8), 903–932. https://doi.org/10.1517/13543784.13.8.903

Atlante, A., Calissano, P., Bobba, A., Azzariti, A., Marra, E., & Passarella, S. (2000). Cytochrome c is released from mitochondria in a reactive oxygen species (ROS)-dependent fashion and can operate as a ROS scavenger and as a respiratory substrate in cerebellar neurons undergoing excitotoxic death. *The Journal of Biological Chemistry*, *275*(47), 37159–37166. https://doi.org/10.1074/JBC.M002361200

Avota, E., Gulbins, E., & Schneider-Schaulies, S. (2011). DC-SIGN Mediated Sphingomyelinase-Activation and Ceramide Generation Is Essential for Enhancement of Viral Uptake in Dendritic Cells. *PLOS Pathogens*, *7*(2), e1001290. https://doi.org/10.1371/JOURNAL.PPAT.1001290

Azad, N., Iyer, A. K. v., Manosroi, A., Wang, L., & Rojanasakul, Y. (2008). Superoxide-mediated proteasomal degradation of Bcl-2 determines cell susceptibility to Cr (VI)-induced apoptosis. *Carcinogenesis*, *29*(8), 1538–1545. https://doi.org/10.1093/CARCIN/BGN137

Azuma, M. M., Balani, P., Boisvert, H., Gil, M., Egashira, K., Yamaguchi, T., Hasturk, H., Duncan, M., Kawai, T., & Movila, A. (2018). Endogenous acid ceramidase protects epithelial cells from Porphyromonas gingivalis-induced inflammation in vitro. *Biochemical and Biophysical Research Communications*, *495*(4), 2383–2389. https://doi.org/10.1016/J.BBRC.2017.12.137

Baginski, M., & Czub, J. (2009). Amphotericin B and Its New Derivatives – Mode of Action. *Current Drug Metabolism*, *10*(5), 459–469. https://doi.org/10.2174/138920009788898019

Balloy, V., Sallenave, J. M., Wu, Y., Touqui, L., Latgé, J. P., Si-Tahar, M., & Chignard, M. (2008). Aspergillus fumigatus-induced Interleukin-8 Synthesis by Respiratory Epithelial Cells Is Controlled by the Phosphatidylinositol 3-Kinase, p38 MAPK, and ERK1/2 Pathways and Not by the Toll-like Receptor-MyD88 Pathway. *Journal of Biological Chemistry*, *283*(45), 30513–30521. https://doi.org/10.1074/JBC.M803149200

Beck, S., Sehl, C., Voortmann, S., Verhasselt, H. L., Edwards, M. J., Buer, J., Hasenberg, M., Gulbins, E., & Becker, K. A. (2020). Sphingosine is able to prevent and eliminate Staphylococcus epidermidis biofilm formation on different orthopedic implant materials in vitro. *Journal of Molecular Medicine (Berlin, Germany)*, *98*(2), 209–219. https://doi.org/10.1007/S00109-019-01858-X

Beeler, T., Bacikova, D., Gable, K., Hopkins, L., Johnson, C., Slife, H., & Dunn, T. (1998). The Saccharomyces cerevisiae TSC10/YBR265w Gene Encoding 3-Ketosphinganine Reductase Is Identified in a Screen for Temperature-sensitive Suppressors of the Ca2+-sensitive csg2Δ Mutant. *Journal of Biological Chemistry*, *273*(46), 30688–30694. https://doi.org/10.1074/JBC.273.46.30688

Beeler, T., Gable, K., Zhao, C., & Dunn, T. (1994). A novel protein, CSG2p, is required for Ca2+ regulation in Saccharomyces cerevisiae. *Journal of Biological Chemistry*, *269*(10), 7279–7284. https://doi.org/10.1016/S0021-9258(17)37280-0

Beeler, T. J., Fu, D., Rivera, J., Monaghan, E., Gable, K., & Dunn, T. M. (1997). SUR1 (CSG1/BCL21), a gene necessary for growth of Saccharomyces cerevisiae in the presence of high Ca2+ concentrations at 37°C, is required for mannosylation of inositolphosphorylceramide. *Molecular and General Genetics*, *255*(6), 570–579. https://doi.org/10.1007/S004380050530/METRICS

Bellanger, A. P., Millon, L., Khoufache, K., Rivollet, D., Bièche, I., Laurendeau, I., Vidaud, M., Botterel, F., & Bretagne, S. (2009). Aspergillus fumigatus germ tube growth and

not conidia ingestion induces expression of inflammatory mediator genes in the human lung epithelial cell line A549. *Journal of Medical Microbiology*, *58*(2), 174–179. https://doi.org/10.1099/JMM.0.005488-0/CITE/REFWORKS

Bezanilla, F., Perozo, E., Papazian, D. M., Stefani, E., Lucchesi, K., Ravindran, A., Young, H., Moczyd-lowski, E., Membr Biol, J., Dressler, K. A., Mathias, S., & Kolesnick, R. N. (1992). Tumor Necrosis Factor-α Activates the Sphingomyelin Signal Transduction Pathway in a Cell-Free System. *Science*, *255*(5052), 1715–1718. https://doi.org/10.1126/SCIENCE.1313189

Bibel, D. J., Aly, R., Shah, S., & Shinefield, H. R. (1993). Sphingosines: antimicrobial barriers of the skin. *Acta Dermato-Venereologica*, *73*(6), 407–411. https://doi.org/10.2340/0001555573407411

Bibel, D. J., Aly, R., & Shinefield, H. R. (1992). Antimicrobial activity of sphingosines. *The Journal of Investigative Dermatology*, *98*(3), 269–273. https://doi.org/10.1111/1523-1747.EP12497842

Boatright, K. M., Renatus, M., Scott, F. L., Sperandio, S., Shin, H., Pedersen, I. M., Ricci, J. E., Edris, W. A., Sutherlin, D. P., Green, D. R., & Salvesen, G. S. (2003). A unified model for apical caspase activation. *Molecular Cell*, *11*(2), 529–541. https://doi.org/10.1016/S1097-2765(03)00051-0

Botet, J., Rodríguez-Mateos, M., Ballesta, J. P. G., Revuelta, J. L., & Remacha, M. (2008). A Chemical Genomic Screen in Saccharomyces cerevisiae Reveals a Role for Diphthamidation of Translation Elongation Factor 2 in Inhibition of Protein Synthesis by Sordarin. *Antimicrobial Agents and Chemotherapy*, *52*(5), 1623. https://doi.org/10.1128/AAC.01603-07

Bouchara, J. P., Sanchez, M., Chevailler, A., Marot-Leblond, A., Lissitzky, J. C., Tronchin, G., & Chabasse, D. (1997). Sialic acid-dependent recognition of laminin and fibrinogen by Aspergillus fumigatus conidia. *Infection and Immunity*, *65*(7), 2717. https://doi.org/10.1128/IAI.65.7.2717-2724.1997

Bowman, S. M., & Free, S. J. (2006). The structure and synthesis of the fungal cell wall. *BioEssays*, *28*(8), 799–808. https://doi.org/10.1002/BIES.20441

Brenner, D., & Mak, T. W. (2009). Mitochondrial cell death effectors. *Current Opinion in Cell Biology*, *21*(6), 871–877. https://doi.org/10.1016/J.CEB.2009.09.004

Breuninger, L. M., Dempsey, W. L., Uhl, J., & Murasko, D. M. (1993). Hydrocortisone regulation of interleukin-6 protein production by a purified population of human peripheral blood monocytes. *Clinical Immunology and Immunopathology*, *69*(2), 205–214. https://doi.org/10.1006/clin.1993.1171

Brilhante, R. S. N., Oliveira, J. S. de, Evangelista, A. J. de J., Serpa, R., Silva, A. L. da, Aguiar, F. R. M. de, Pereira, V. S., Castelo-Branco, D. de S. C. M., Pereira-Neto, W. A., Cordeiro, R. de A., Sidrim, J. J. C., & Rocha, M. F. G. (2016). Candida tropicalis from veterinary and human sources shows similar in vitro hemolytic activity, antifungal biofilm susceptibility and pathogenesis against Caenorhabditis elegans. *Veterinary Microbiology*, *192*, 213–219. https://doi.org/10.1016/J.VETMIC.2016.07.022

Britta, E. A., Scariot, D. B., Falzirolli, H., Ueda-Nakamura, T., Silva, C. C., Filho, B. P. D., Borsali, R., & Nakamura, C. V. (2014). Cell death and ultrastructural alterations in Leishmania amazonensis caused by new compound 4-Nitrobenzaldehyde thiosemicarbazone derived from S-limonene. *BMC Microbiology*, *14*(1), 1–12. https://doi.org/10.1186/S12866-014-0236-0/FIGURES/10

Bromley, I. M. J., & Donaldson, K. (1996). Binding of Aspergillus fumigatus spores to lung epithelial cells and basement membrane proteins: relevance to the asthmatic lung. *Thorax*, *51*(12), 1203–1209. https://doi.org/10.1136/THX.51.12.1203

Brown, G. D. (2011). Innate Antifungal Immunity: The Key Role of Phagocytes. *Https://Doi.Org/10.1146/Annurev-Immunol-030409-101229*, *29*, 1–21. https://doi.org/10.1146/ANNUREV-IMMUNOL-030409-101229

Brown, J. A., & Catley, B. J. (1992). Monitoring polysaccharide synthesis in Candida albicans. *Carbohydrate Research*, *227*(C), 195–202. https://doi.org/10.1016/0008-6215(92)85071-7

Brown, R. T., Madan-Swain, A., Walco, G. A., Cherrick, I., Ievers, C. E., Conte, P. M., Vega, R., Bell, B., & Lauer, S. J. (1998). Cognitive and academic late effects among children previously treated for acute lymphocytic leukemia receiving chemotherapy as CNS prophylaxis. *Journal of Pediatric Psychology*, *23*(5), 333–340. https://doi.org/10.1093/JPEPSY/23.5.333

Büttner, S., Eisenberg, T., Herker, E., Carmona-Gutierrez, D., Kroemer, G., & Madeo, F. (2006). Why yeast cells can undergo apoptosis: death in times of peace, love, and war. *The Journal of Cell Biology*, *175*(4), 521–525. https://doi.org/10.1083/JCB.200608098

Cain, K., Bratton, S. B., & Cohen, G. M. (2002). The Apaf-1 apoptosome: a large caspase-activating complex. *Biochimie*, *84*(2–3), 203–214. https://doi.org/10.1016/S0300-9084(02)01376-7

Cantón, E., Pemán, J., Gobernado, M., Viudes, A., & Espinel-Ingroff, A. (2004). Patterns of Amphotericin B Killing Kinetics against Seven Candida Species. *Antimicrobial Agents and Chemotherapy*, *48*(7), 2477. https://doi.org/10.1128/AAC.48.7.2477-2482.2004

Carstens, H., Kalka, K., Verhaegh, R., Schumacher, F., Soddemann, M., Wilker, B., Keitsch, S., Sehl, C., Kleuser, B., Wahlers, T., Reiner, G., Koch, A., Rauen, U., Gulbins, E., & Kamler, M. (2021). Inhaled sphingosine has no adverse side effects in isolated ventilated and perfused pig lungs. *Scientific Reports 2021 11:1*, *11*(1), 1–10. https://doi.org/10.1038/s41598-021-97708-3

Carstens, H., Schumacher, F., Keitsch, S., Kramer, M., Kühn, C., Sehl, C., Soddemann, M., Wilker, B., Herrmann, D., Swaidan, A., Kleuser, B., Verhaegh, R., Hilken, G., Edwards, M. J., Dubicanac, M., Carpinteiro, A., Wissmann, A., Becker, K. A., Kamler, M., & Gulbins, E. (2019). Clinical development of sphingosine as anti-bacterial drug: Inhalation of sphingosine in mini pigs has no adverse side effects. *Cellular Physiology & Biochemistry*, *53*(6), 1015–1028. https://doi.org/10.33594/000000194

Cavalheiro, M., & Teixeira, M. C. (2018). Candida Biofilms: Threats, Challenges, and Promising Strategies. *Frontiers in Medicine*, *5*(FEB). https://doi.org/10.3389/FMED.2018.00028

Cenci, E., Mencacci, A., Casagrande, A., Mosci, P., Bistoni, F., & Romani, L. (2001). Impaired Antifungal Effector Activity but Not Inflammatory Cell Recruitment in Interleukin-6-Deficient Mice with Invasive Pulmonary Aspergillosis. *The Journal of Infectious Diseases*, *184*(5), 610–617. https://doi.org/10.1086/322793

Chandra, J., Kuhn, D. M., Mukherjee, P. K., Hoyer, L. L., McCormick, T., & Ghannoum, M. A. (2001). Biofilm formation by the fungal pathogen Candida albicans: Development, architecture, and drug resistance. *Journal of Bacteriology*, *183*(18), 5385–5394. https://doi.org/10.1128/JB.183.18.5385-5394.2001/ASSET/7682BA16-1CB1-4757-B4AC-81291C643CA8/ASSETS/GRAPHIC/JB1810569007.JPEG

Chandra, J., & Mukherjee, P. K. (2015). Candida Biofilms: Development, Architecture, and Resistance. *Microbiology Spectrum*, *3*(4). https://doi.org/10.1128/MICROBIOLSPEC.MB-0020-2015

Chang, C. K., Kao, M. C., & Lan, C. Y. (2021). Antimicrobial Activity of the Peptide LfcinB15 against Candida albicans. *Journal of Fungi (Basel, Switzerland)*, *7*(7). https://doi.org/10.3390/JOF7070519

Chang, D. W., Xing, Z., Capacio, V. L., Peter, M. E., & Yang, X. (2003). Interdimer processing mechanism of procaspase-8 activation. *The EMBO Journal*, *22*(16), 4132–4142. https://doi.org/10.1093/EMBOJ/CDG414

Chazalet, V., Debeaupuis, J. P., Sarfati, J., Lortholary, J., Ribaud, P., Shah, P., Cornet, M., Vu Thien, H., Gluckman, E., Brücker, G., & Latgé, J. P. (1998). Molecular Typing of Environmental and Patient Isolates of Aspergillus fumigatus from Various Hospital Settings. *Journal of Clinical Microbiology*, *36*(6), 1494. https://doi.org/10.1128/JCM.36.6.1494-1500.1998

Chertkova, R. v., Firsov, A. M., Kotova, E. A., Gusev, I. D., Dolgikh, D. A., Kirpichnikov, M. P., & Antonenko, Y. N. (2021). Lysine 72 substitutions differently affect lipid membrane permeabilizing and proapoptotic activities of horse heart cytochrome c. *Biochemical and Biophysical Research Communications*, *548*, 74–77. https://doi.org/10.1016/J.BBRC.2021.02.023

Chipuk, J. E., Bouchier-Hayes, L., & Green, D. R. (2006). Mitochondrial outer membrane permeabilization during apoptosis: the innocent bystander scenario. *Cell Death & Differentiation 2006 13:8*, *13*(8), 1396–1402. https://doi.org/10.1038/sj.cdd.4401963

Choi, S. Y., Gonzalvez, F., Jenkins, G. M., Slomianny, C., Chretien, D., Arnoult, D., Petit, P. X., & Frohman, M. A. (2006). Cardiolipin deficiency releases cytochrome c from the inner mitochondrial membrane and accelerates stimuli-elicited apoptosis. *Cell Death & Differentiation 2007 14:3*, *14*(3), 597–606. https://doi.org/10.1038/sj.cdd.4402020

Christin, L., Wysong, D. R., Meshulam, T., Hastey, R., Simons, E. R., & Diamond, R. D. (1998). Human platelets damage Aspergillus fumigatus hyphae and may supplement killing by neutrophils. *Infection and Immunity*, *66*(3), 1181–1189. https://doi.org/10.1128/IAI.66.3.1181-1189.1998/ASSET/BBAB4DC8-C57E-4003-A275-94E1C4698441/ASSETS/GRAPHIC/II0380504006.JPEG

Chung, N., Mao, C., Heitman, J., Hannun, Y. A., & Obeid, L. M. (2001). Phytosphingosine as a Specific Inhibitor of Growth and Nutrient Import in Saccharomyces cerevisiae. *Journal of Biological Chemistry*, *276*(38), 35614–35621. https://doi.org/10.1074/JBC.M105653200

Cortez, K. J., Lyman, C. A., Kottilil, S., Kim, H. S., Roilides, E., Yang, J., Fullmer, B., Lempicki, R., & Walsh, T. J. (2006). Functional Genomics of Innate Host Defense Molecules in Normal Human Monocytes in Response to Aspergillus fumigatus. *Infection and Immunity*, *74*(4), 2353. https://doi.org/10.1128/IAI.74.4.2353-2365.2006

Cowart, L. A., Shotwell, M., Worley, M. L., Richards, A. J., Montefusco, D. J., Hannun, Y. A., & Lu, X. (2010). Revealing a signaling role of phytosphingosine-1-phosphate in yeast. *Molecular Systems Biology*, *6*(1), 349. https://doi.org/10.1038/MSB.2010.3

Crompton, M. (2000). Mitochondrial intermembrane junctional complexes and their role in cell death. *The Journal of Physiology*, *529*(Pt 1), 11. https://doi.org/10.1111/J.1469-7793.2000.00011.X

Crowder, T., & Atkins, P. (2003). *The Design and Development of Inhalation Drug Delivery Systems*. https://doi.org/10.1201/9780203912898.CH9

Dadsena, S., Zollo, C., & García-Sáez, A. J. (2021). Mechanisms of mitochondrial cell death. *Biochemical Society Transactions*, *49*(2), 663–674. https://doi.org/10.1042/BST20200522

Dagenais, T. R. T., & Keller, N. P. (2009). Pathogenesis of Aspergillus fumigatus in invasive aspergillosis. *Clinical Microbiology Reviews*, *22*(3), 447–465. https://doi.org/10.1128/CMR.00055-08/ASSET/60DDB4B5-4B4D-4C08-9AEA-B23F84EADC19/ASSETS/GRAPHIC/ZCM0030922850003.JPEG

Daly, P., & Kavanagh, K. (2001). Pulmonary aspergillosis: clinical presentation, diagnosis and therapy. *British Journal of Biomedical Science*, *58*(3), 197–205. https://pubmed.ncbi.nlm.nih.gov/11575744/

de Avalos, S. V., Okamoto, Y., & Hannun, Y. A. (2004). Activation and Localization of Inositol Phosphosphingolipid Phospholipase C, Isc1p, to the Mitochondria during Growth of Saccharomyces cerevisiae. *Journal of Biological Chemistry*, *279*(12), 11537–11545. https://doi.org/10.1074/JBC.M309586200

de Jong, E. C., Vieira, P. L., Kalinski, P., & Kapsenberg, M. L. (1999). Corticosteroids inhibit the production of inflammatory mediators in immature monocyte-derived DC and induce the development of tolerogenic DC3. *Journal of Leukocyte Biology*, *66*(2), 201–204. https://doi.org/10.1002/JLB.66.2.201

de Pauw, B., Walsh, T. J., Donnelly, J. P., Stevens, D. A., Edwards, J. E., Calandra, T., Pappas, P. G., Maertens, J., Lortholary, O., Kauffman, C. A., Denning, D. W., Patterson, T. F., Maschmeyer, G., Bille, J., Dismukes, W. E., Herbrecht, R., Hope, W. W., Kibbler, C. C., Kullberg, B. J., … Bennett, J. E. (2008). Revised definitions of invasive fungal disease from the European Organization for Research and Treatment of Cancer/Invasive Fungal Infections Cooperative Group and the National Institute of Allergy and Infectious Diseases Mycoses Study Group (EORTC/MSG) Consensus Group. *Clinical Infectious Diseases: An Official Publication of the Infectious Diseases Society of America*, *46*(12), 1813–1821. https://doi.org/10.1086/588660

Denning, D. W. (1998). Invasive aspergillosis. *Clinical Infectious Diseases: An Official Publication of the Infectious Diseases Society of America*, *26*(4), 781–805. https://doi.org/10.1086/513943

Diamond, R. D., & Clark, R. A. (1982). Damage to Aspergillus fumigatus and Rhizopus oryzae hyphae by oxidative and nonoxidative microbicidal products of human neutrophils in vitro. *Infection and Immunity*, *38*(2), 487–495. https://doi.org/10.1128/IAI.38.2.487-495.1982

Dickson, D. W. (2004). Apoptotic mechanisms in Alzheimer neurofibrillary degeneration: cause or effect? *The Journal of Clinical Investigation*, *114*(1), 23–27. https://doi.org/10.1172/JCI22317

Dickson, R. C., & Lester, R. L. (1999). Yeast sphingolipids. *Biochimica et Biophysica Acta (BBA) - General Subjects*, *1426*(2), 347–357. https://doi.org/10.1016/S0304-4165(98)00135-4

Dickson, R. C., Nagiec, E. E., Wells, G. B., Nagiec, M. M., & Lester, R. L. (1997). Synthesis of Mannose-(inositol-P)2-ceramide, the Major Sphingolipid in Saccharomyces cerevisiae, Requires the IPT1 (YDR072c) Gene. *Journal of Biological Chemistry*, *272*(47), 29620–29625. https://doi.org/10.1074/JBC.272.47.29620

Donlan, R. M. (2001). Biofilms and device-associated infections. *Emerging Infectious Diseases*, *7*(2), 277–281. https://doi.org/10.3201/EID0702.010226

D'Ostiani, C. F., del Sero, G. del, Bacci, A., Montagnoli, C., Spreca, A., Mencacci, A., Ricciardi-Castagnoli, P., & Romani, L. (2000). Dendritic cells discriminate between yeasts and hyphae of the fungus Candida albicans. Implications for initiation of T helper cell immunity in vitro and in vivo. *The Journal of Experimental Medicine*, *191*(10), 1661–1673. https://doi.org/10.1084/JEM.191.10.1661

Douglas, L. J. (2003). Candida biofilms and their role in infection. *Trends in Microbiology*, *11*(1), 30–36. https://doi.org/10.1016/S0966-842X(02)00002-1

Drew, R. (2006). Potential role of aerosolized amphotericin B formulations in the prevention and adjunctive treatment of invasive fungal infections. *International Journal of Antimicrobial Agents*, *27 Suppl 1*(SUPPL. 1), 36–44. https://doi.org/10.1016/J.IJANTIMICAG.2006.03.018

Edwards, M. J., Becker, K. A., Gripp, B., Hoffmann, M., Keitsch, S., Wilker, B., Soddemann, M., Gulbins, A., Carpinteiro, E., Patel, S. H., Wilson, G. C., Pöhlmann, S., Walter, S., Fassbender, K., Ahmad, S. A., Carpinteiro, A., & Gulbins, E. (2020). Sphingosine prevents binding of SARS–CoV-2 spike to its cellular receptor ACE2. *Journal of Biological Chemistry*, *295*(45), 15174–15182. https://doi.org/10.1074/JBC.RA120.015249

Eisenberg, T., Büttner, S., Kroemer, G., & Madeo, F. (2007). The mitochondrial pathway in yeast apoptosis. *Apoptosis: An International Journal on Programmed Cell Death*, *12*(5), 1011–1023. https://doi.org/10.1007/S10495-007-0758-0

Elenkov, I. J. (2004). Glucocorticoids and the Th1/Th2 balance. *Annals of the New York Academy of Sciences*, *1024*, 138–146. https://doi.org/10.1196/ANNALS.1321.010

Elving, G. J., van der Mei, H. C., Busscher, H. J., van Weissenbruch, R., & Albers, F. W. J. (2016). Comparison of the Microbial Composition of Voice Prosthesis Biofilms from Patients Requiring Frequent versus Infrequent Replacement. *Https://Doi.Org/10.1177/000348940211100302*, *111*(3), 200–203. https://doi.org/10.1177/000348940211100302

Erwig, L. P., & Gow, N. A. R. (2016). Interactions of fungal pathogens with phagocytes. *Nature Reviews Microbiology 2016 14:3*, *14*(3), 163–176. https://doi.org/10.1038/nrmicro.2015.21

Essary, B. D., & Marshall, P. A. (2009). Assessment of FUN-1 vital dye staining: Yeast with a block in the vacuolar sorting pathway have impaired ability to form CIVS when stained with FUN-1 fluorescent dye. *Journal of Microbiological Methods*, *78*(2), 208–212. https://doi.org/10.1016/J.MIMET.2009.05.018

Fakhim, H., Badali, H., Dannaoui, E., Nasirian, M., Jahangiri, F., Raei, M., Vaseghi, N., Ahmadikia, K., & Vaezi, A. (2022). Trends in the Prevalence of Amphotericin B-Resistance (AmBR) among Clinical Isolates of Aspergillus Species. *Journal of Medical Mycology*, *32*(4), 101310. https://doi.org/10.1016/J.MYCMED.2022.101310

Falvey, D. G., & Streifel, A. J. (2007). Ten-year air sample analysis of Aspergillus prevalence in a university hospital. *Journal of Hospital Infection*, *67*(1), 35–41. https://doi.org/10.1016/j.jhin.2007.06.008

Fannjiang, Y., Cheng, W. C., Lee, S. J., Qi, B., Pevsner, J., McCaffery, J. M., Hill, R. B., Basañez, G., & Hardwick, J. M. (2004). Mitochondrial fission proteins regulate programmed cell death in yeast. *Genes & Development*, *18*(22), 2785. https://doi.org/10.1101/GAD.1247904

Fantini, J., Chahinian, H., & Yahi, N. (2021). Leveraging coronavirus binding to gangliosides for innovative vaccine and therapeutic strategies against COVID-19. *Biochemical and Biophysical Research Communications*, *538*, 132–136. https://doi.org/10.1016/J.BBRC.2020.10.015

Fantini, J., di Scala, C., Chahinian, H., & Yahi, N. (2020). Structural and molecular modelling studies reveal a new mechanism of action of chloroquine and hydroxychloroquine against SARS-CoV-2 infection. *International Journal of Antimicrobial Agents*, *55*(5), 105960. https://doi.org/10.1016/J.IJANTIMICAG.2020.105960

Fernandes, T., Silva, S., & Henriques, M. (2015). Candida tropicalis biofilm's matrix--involvement on its resistance to amphotericin B. *Diagnostic Microbiology and Infectious Disease*, *83*(2), 165–169. https://doi.org/10.1016/J.DIAGMICROBIO.2015.06.015

Ferreira, G. F., Baltazar, L. de M., Alves Santos, J. R., Monteiro, A. S., Fraga, L. A. de O., Resende-Stoianoff, M. A., & Santos, D. A. (2013). The role of oxidative and nitrosative bursts caused by azoles and amphotericin B against the fungal pathogen Cryptococcus gattii. *Journal of Antimicrobial Chemotherapy*, *68*(8), 1801–1811. https://doi.org/10.1093/JAC/DKT114

Filler, S. G., & Sheppard, D. C. (2006). Fungal Invasion of Normally Non-Phagocytic Host Cells. *PLOS Pathogens*, *2*(12), e129. https://doi.org/10.1371/JOURNAL.PPAT.0020129

Fischer, C. L., Drake, D. R., Dawson, D. v., Blanchette, D. R., Brogden, K. A., & Wertz, P. W. (2012). Antibacterial activity of sphingoid bases and fatty acids against gram-positive and gram-negative bacteria. *Antimicrobial Agents and Chemotherapy*, *56*(3), 1157–1161. https://doi.org/10.1128/AAC.05151-11/SUPPL_FILE/FIGS1LEGEND.DOC

Fischer, C. L., Walters, K. S., Drake, D. R., Blanchette, D. R., Dawson, D. v., Brogden, K. A., & Wertz, P. W. (2013). Sphingoid Bases Are Taken Up by Escherichia coli and Staphylococcus aureus and Induce Ultrastructural Damage. *Skin Pharmacology and Physiology*, *26*(1), 36–44. https://doi.org/10.1159/000343175

Fishbein, J. D., Dobrowsky, R. T., Bielawska, A., Garrett, S., & Hannun, Y. A. (1993). Ceramide-mediated growth inhibition and CAPP are conserved in Saccharomyces cerevisiae. *Journal of Biological Chemistry*, *268*(13), 9255–9261. https://doi.org/10.1016/S0021-9258(18)98343-2

Fonseca, E., Silva, S., Rodrigues, C. F., Alves, C. T., Azeredo, J., & Henriques, M. (2014). Effects of fluconazole on Candida glabrata biofilms and its relationship with ABC transporter gene expression. *Biofouling*, *30*(4), 447–457. https://doi.org/10.1080/08927014.2014.886108

Funato, K., & Riezman, H. (2001). Vesicular and nonvesicular transport of ceramide from ER to the Golgi apparatus in yeast. *The Journal of Cell Biology*, *155*(6), 949. https://doi.org/10.1083/JCB.200105033

Ganta, K. K., Mandal, A., & Chaubey, B. (2017). Depolarization of mitochondrial membrane potential is the initial event in non-nucleoside reverse transcriptase inhibitor efavirenz induced cytotoxicity. *Cell Biology and Toxicology*, *33*(1), 69–82. https://doi.org/10.1007/S10565-016-9362-9

Garcia-Rubio, R., de Oliveira, H. C., Rivera, J., & Trevijano-Contador, N. (2020). The Fungal Cell Wall: Candida, Cryptococcus, and Aspergillus Species. *Frontiers in Microbiology*, *10*, 2993. https://doi.org/10.3389/FMICB.2019.02993/BIBTEX

Girmenia, C., Martino, P., & White, M. H. (1998). Fluconazole and the changing epidemiology of candidemia [6] (multiple letters). *Clinical Infectious Diseases*, *27*(1), 232–233. https://doi.org/10.1086/517694/2/27-1-232.PDF.GIF

Grassmé, H., Henry, B., Ziobro, R., Becker, K. A., Riethmüller, J., Gardner, A., Seitz, A. P., Steinmann, J., Lang, S., Ward, C., Schuchman, E. H., Caldwell, C. C., Kamler, M., Edwards, M. J., Brodlie, M., & Gulbins, E. (2017). β1-Integrin Accumulates in Cystic Fibrosis Luminal Airway Epithelial Membranes and Decreases Sphingosine, Promoting Bacterial Infections. *Cell Host & Microbe*, *21*(6), 707-718.e8. https://doi.org/10.1016/J.CHOM.2017.05.001

Grassmé, H., Riehle, A., Wilker, B., & Gulbins, E. (2005). Rhinoviruses Infect Human Epithelial Cells via Ceramide-enriched Membrane Platforms. *Journal of Biological Chemistry*, *280*(28), 26256–26262. https://doi.org/10.1074/JBC.M500835200

Gregg, C., Kyryakov, P., & Titorenko, V. I. (2009). Purification of Mitochondria from Yeast Cells. *Journal of Visualized Experiments: JoVE*, *30*(30). https://doi.org/10.3791/1417

Grilley, M. M., Stock, S. D., Dickson, R. C., Lester, R. L., & Takemoto, J. Y. (1998). Syringomycin Action Gene SYR2 Is Essential for Sphingolipid 4-Hydroxylation in Saccharomyces cerevisiae. *Journal of Biological Chemistry*, *273*(18), 11062–11068. https://doi.org/10.1074/JBC.273.18.11062

Gringhuis, S. I., Kaptein, T. M., Wevers, B. A., Theelen, B., van der Vlist, M., Boekhout, T., & Geijtenbeek, T. B. H. (2012). Dectin-1 is an extracellular pathogen sensor for the induction and processing of IL-1β via a noncanonical caspase-8 inflammasome. *Nature Immunology 2012 13:3*, *13*(3), 246–254. https://doi.org/10.1038/ni.2222

Gross, O., Poeck, H., Bscheider, M., Dostert, C., Hannesschläger, N., Endres, S., Hartmann, G., Tardivel, A., Schweighoffer, E., Tybulewicz, V., Mocsai, A., Tschopp, J., & Ruland, J. (2009). Syk kinase signalling couples to the Nlrp3 inflammasome for anti-fungal host defence. *Nature 2009 459:7245*, *459*(7245), 433–436. https://doi.org/10.1038/nature07965

Guillas, I., Kirchman, P. A., Chuard, R., Pfefferli, M., Jiang, J. C., Jazwinski, S. M., & Conzelmann, A. (2001). C26-CoA-dependent ceramide synthesis of Saccharomyces cerevisiae is operated by Lag1p and Lac1p. *The EMBO Journal*, *20*(11), 2655–2665. https://doi.org/10.1093/EMBOJ/20.11.2655

Gulbins, A., Schumacher, F., Becker, K. A., Wilker, B., Soddemann, M., Boldrin, F., Müller, C. P., Edwards, M. J., Goodman, M., Caldwell, C. C., Kleuser, B., Kornhuber, J., Szabo, I., & Gulbins, E. (2018). Antidepressants act by inducing autophagy controlled by sphingomyelin-ceramide. *Molecular Psychiatry*, *23*(12), 2324–2346. https://doi.org/10.1038/S41380-018-0090-9

Haber, J. E. (2003). MATING-TYPE GENE SWITCHING IN SACCHAROMYCES CEREVISIAE. *Https://Doi.Org/10.1146/Annurev.Genet.32.1.561*, *32*, 561–599. https://doi.org/10.1146/ANNUREV.GENET.32.1.561

Halestrap, A. P. (1999). The mitochondrial permeability transition: its molecular mechanism and role in reperfusion injury. *Biochemical Society Symposium*, *66*, 181–203. https://doi.org/10.1042/BSS0660181

Hanada, K., Kumagai, K., Yasuda, S., Miura, Y., Kawano, M., Fukasawa, M., & Nishijima, M. (2003). Molecular machinery for non-vesicular trafficking of ceramide. *Nature 2004 426:6968*, *426*(6968), 803–809. https://doi.org/10.1038/nature02188

Hannun, Y. A. (1994). The sphingomyelin cycle and the second messenger function of ceramide. *Journal of Biological Chemistry*, *269*(5), 3125–3128. https://doi.org/10.1016/S0021-9258(17)41834-5

Hannun, Y. A., & Obeid, L. M. (2008). Principles of bioactive lipid signalling: lessons from sphingolipids. *Nature Reviews Molecular Cell Biology 2008 9:2*, *9*(2), 139–150. https://doi.org/10.1038/nrm2329

Hardison, S. E., & Brown, G. D. (2012). C-type lectin receptors orchestrate antifungal immunity. *Nature Immunology 2012 13:9*, *13*(9), 817–822. https://doi.org/10.1038/ni.2369

Herbst, S., Shah, A., Carby, M., Chusney, G., Kikkeri, N., Dorling, A., Bignell, E., Shaunak, S., & Armstrong-James, D. (2013). A new and clinically relevant murine model of solid-organ transplant aspergillosis. *Disease Models & Mechanisms*, *6*(3), 643–651. https://doi.org/10.1242/DMM.010330

Hobson, R. P. (2003). The global epidemiology of invasive Candida infections - Is the tide turning? *Journal of Hospital Infection*, *55*(3), 159–168. https://doi.org/10.1016/j.jhin.2003.08.012

Hoenigl, M., Salzer, H. J. F., Raggam, R. B., Valentin, T., Rohn, A., Woelfler, A., Seeber, K., Linkesch, W., & Krause, R. (2012). Impact of galactomannan testing on the prevalence of invasive aspergillosis in patients with hematological malignancies. *Medical Mycology*, *50*(3), 266–269. https://doi.org/10.3109/13693786.2011.603102

Hoffmann, B., Stöckl, A., Schlame, M., Beyer, K., & Klingenberg, M. (1994). The reconstituted ADP/ATP carrier activity has an absolute requirement for cardiolipin as shown in cysteine mutants. *Journal of Biological Chemistry*, *269*(3), 1940–1944. https://doi.org/10.1016/S0021-9258(17)42117-X

Hoffmann, M., Kleine-Weber, H., Schroeder, S., Krüger, N., Herrler, T., Erichsen, S., Schiergens, T. S., Herrler, G., Wu, N. H., Nitsche, A., Müller, M. A., Drosten, C., & Pöhlmann, S. (2020). SARS-CoV-2 Cell Entry Depends on ACE2 and TMPRSS2 and Is Blocked by a Clinically Proven Protease Inhibitor. *Cell*, *181*(2), 271-280.e8. https://doi.org/10.1016/J.CELL.2020.02.052

Hohl, T. M., & Feldmesser, M. (2007). Aspergillus fumigatus: Principles of Pathogenesis and Host Defense. *Eukaryotic Cell*, *6*(11), 1953. https://doi.org/10.1128/EC.00274-07

Hope, W. W., Walsh, T. J., & Denning, D. W. (2005). Laboratory diagnosis of invasive aspergillosis. *The Lancet Infectious Diseases*, *5*(10), 609–622. https://doi.org/10.1016/S1473-3099(05)70238-3

Horvath, J. A., & Dummer, S. (1996). The use of respiratory-tract cultures in the diagnosis of invasive pulmonary aspergillosis. *American Journal of Medicine*, *100*(2), 171–178. https://doi.org/10.1016/S0002-9343(97)89455-7

Howard, S. J., & Arendrup, M. C. (2011). Acquired antifungal drug resistance in Aspergillus fumigatus: epidemiology and detection. *Medical Mycology*, *49*(Supplement_1), S90–S95. https://doi.org/10.3109/13693786.2010.508469

Hu, X., Li, W.-P., Meng, C., & Ivashkiv, L. B. (2003). Inhibition of IFN-gamma signaling by glucocorticoids. *Journal of Immunology (Baltimore, Md.: 1950)*, *170*(9), 4833–4839. https://doi.org/10.4049/JIMMUNOL.170.9.4833

Hudlicky, T., Rouden, J., Luna, H., & Allen, S. (1994). Microbial Oxidation of Aromatics in Enantiocontrolled Synthesis. 2.1 Rational Design of Aza Sugars (endo-Nitrogenous). Total Synthesis of (+)-Kifunensine, Mannojirimycin, and Other Glycosidase Inhibitors. *Journal of the American Chemical Society*, *116*(12), 5099–5107. https://doi.org/10.1021/JA00091A011/SUPPL_FILE/JA5099.PDF

Ibrahim-Granet, O., Jouvion, G., Hohl, T. M., Droin-Bergère, S., Philippart, F., Kim, O. Y., Adib-Conquy, M., Schwendener, R., Cavaillon, J. M., & Brock, M. (2010). In vivo bioluminescence imaging and histopathopathologic analysis reveal distinct roles for resident and recruited immune effector cells in defense against invasive aspergillosis. *BMC Microbiology*, *10*, 105. https://doi.org/10.1186/1471-2180-10-105

Ibrahim-Granet, O., Philippe, B., Boleti, H., Boisvieux-Ulrich, E., Grenet, D., Stern, M., & Latgé, J. P. (2003). Phagocytosis and intracellular fate of Aspergillus fumigatus conidia in alveolar macrophages. *Infection and Immunity*, *71*(2), 891–903. https://doi.org/10.1128/IAI.71.2.891-903.2003/ASSET/8DB21237-CF8F-4889-A0D8-442AB1740C99/ASSETS/GRAPHIC/II0230978009.JPEG

Iraqui, I., Garcia-Sanchez, S., Aubert, S., Dromer, F., Ghigo, J. M., D'Enfert, C., & Janbon, G. (2005). The Yak1p kinase controls expression of adhesins and biofilm formation in Candida glabrata in a Sir4p-dependent pathway. *Molecular Microbiology*, *55*(4), 1259–1271. https://doi.org/10.1111/J.1365-2958.2004.04475.X

Iverson, S. L., & Orrenius, S. (2004). The cardiolipin-cytochrome c interaction and the mitochondrial regulation of apoptosis. *Archives of Biochemistry and Biophysics*, *423*(1), 37–46. https://doi.org/10.1016/J.ABB.2003.12.002

J P Latgé. (1995). Tools and trends in the detection of Aspergillus fumigatus. *Curr Top Med Mycol*, *6*, 285–295.

Jaillon, S., Peri, G., Delneste, Y., Frémaux, I., Doni, A., Moalli, F., Garlanda, C., Romani, L., Gascan, H., Bellocchio, S., Bozza, S., Cassatella, M. A., Jeannin, P., & Mantovani, A. (2007). The humoral pattern recognition receptor PTX3 is stored in neutrophil granules and localizes in extracellular traps. *The Journal of Experimental Medicine*, *204*(4), 793. https://doi.org/10.1084/JEM.20061301

Jin, M. L., Yaung, J., Kannan, R., He, S., Ryan, S. J., & Hinton, D. R. (2005). Hepatocyte Growth Factor Protects RPE Cells from Apoptosis Induced by Glutathione Depletion. *Investigative Ophthalmology & Visual Science*, *46*(11), 4311–4319. https://doi.org/10.1167/IOVS.05-0353

Johnson, L. v., Walsh, M. L., & Chen, L. B. (1980). Localization of mitochondria in living cells with rhodamine 123. *Proceedings of the National Academy of Sciences*, *77*(2), 990–994. https://doi.org/10.1073/PNAS.77.2.990

Joly, S., Eisenbarth, S. C., Olivier, A. K., Williams, A., Kaplan, D. H., Cassel, S. L., Flavell, R. A., & Sutterwala, F. S. (2012). Cutting Edge: Nlrp10 Is Essential for Protective Antifungal Adaptive Immunity against Candida albicans. *The Journal of Immunology*, *189*(10), 4713–4717. https://doi.org/10.4049/JIMMUNOL.1201715

Joshi, A. S., Zhou, J., Gohil, V. M., Chen, S., & Greenberg, M. L. (2009). Cellular functions of cardiolipin in yeast. *Biochimica et Biophysica Acta*, *1793*(1), 212–218. https://doi.org/10.1016/J.BBAMCR.2008.07.024

Kanayama, M., Inoue, M., Danzaki, K., Hammer, G., He, Y. W., & Shinohara, M. L. (2015). Autophagy enhances NFκB activity in specific tissue macrophages by sequestering A20 to boost antifungal immunity. *Nature Communications 2015 6:1*, *6*(1), 1–14. https://doi.org/10.1038/ncomms6779

Kaur, S., Gupta, V. K., Thiel, S., Sarma, P. U., & Madan, T. (2007). Protective role of mannan-binding lectin in a murine model of invasive pulmonary aspergillosis. *Clinical and Experimental Immunology*, *148*(2), 382. https://doi.org/10.1111/J.1365-2249.2007.03351.X

Kerr, J. F. R., Wyllie, A. H., & Currie, A. R. (1972). Apoptosis: A Basic Biological Phenomenon with Wideranging Implications in Tissue Kinetics. *British Journal of Cancer 1972 26:4*, *26*(4), 239–257. https://doi.org/10.1038/bjc.1972.33

Kim, J. H., Lee, S. Y., Oh, S. Y., Han, S. I., Park, H. G., Yoo, M. A., & Kang, H. S. (2004). Methyl jasmonate induces apoptosis through induction of Bax/Bcl-X sand activation of caspase-3 via ROS production in A549 cells. *Oncology Reports*, *12*(6), 1233–1238. https://doi.org/10.3892/OR.12.6.1233/HTML

Kim, M. Y., Linardic, C., Obeid, L., & Hannun, Y. (1991). Identification of sphingomyelin turnover as an effector mechanism for the action of tumor necrosis factor alpha and gamma-interferon. Specific role in cell differentiation. *Journal of Biological Chemistry*, *266*(1), 484–489. https://doi.org/10.1016/S0021-9258(18)52461-3

Kiraz, N., Oz, Y., & Dag, I. (2011). The evaluation of in vitro pharmacodynamic properties of amphotericin B, voriconazole and caspofungin against A. fumigatus isolates by the conventional and colorimetric time-kill assays. *Medical Mycology*, *49*(6), 594–601. https://doi.org/10.3109/13693786.2011.555847

Kitagaki, H., Cowart, L. A., Matmati, N., Vaena de Avalos, S., Novgorodov, S. A., Zeidan, Y. H., Bielawski, J., Obeid, L. M., & Hannun, Y. A. (2007). Isc1 regulates sphingolipid metabolism in yeast mitochondria. *Biochimica et Biophysica Acta (BBA)* -

Biomembranes, *1768*(11), 2849–2861. https://doi.org/10.1016/J.BBAMEM.2007.07.019

Klepser, M. E., Wolfe, E. J., Jones, R. N., Nightingale, C. H., & Pfaller, M. A. (1997). Antifungal pharmacodynamic characteristics of fluconazole and amphotericin B tested against Candida albicans. *Antimicrobial Agents and Chemotherapy*, *41*(6), 1392–1395. https://doi.org/10.1128/AAC.41.6.1392

Klepser, M. E., Wolfe, E. J., & Pfaller, M. A. (1998). Antifungal pharmacodynamic characteristics of fluconazole and amphotericin B against Cryptococcus neoformans. *The Journal of Antimicrobial Chemotherapy*, *41*(3), 397–401. https://doi.org/10.1093/JAC/41.3.397

Koch, S., Höhne, F. M., & Tietz, H. J. (2004). Incidence of systemic mycoses in autopsy material. *Mycoses*, *47*(1–2), 40–46. https://doi.org/10.1046/J.0933-7407.2003.00937.X

Kolesnick, R. N. (1991). Sphingomyelin and derivatives as cellular signals. *Progress in Lipid Research*, *30*(1), 1–38. https://doi.org/10.1016/0163-7827(91)90005-P

Kousha, M., Tadi, R., & Soubani, A. O. (2011). Pulmonary aspergillosis: a clinical review. *European Respiratory Review*, *20*(121), 156–174. https://doi.org/10.1183/09059180.00001011

Krcmery, V., & Barnes, A. J. (2002). Non-albicans Candida spp. causing fungaemia: pathogenicity and antifungal resistance. *Journal of Hospital Infection*, *50*(4), 243–260. https://doi.org/10.1053/JHIN.2001.1151

Kuhn, D. M., Chandra, J., Mukherjee, P. K., & Ghannoum, M. A. (2002). Comparison of Biofilms Formed by Candida albicans and Candida parapsilosis on Bioprosthetic Surfaces. *Infection and Immunity*, *70*(2), 878. https://doi.org/10.1128/IAI.70.2.878-888.2002

Kumagai, K., Yasuda, S., Okemoto, K., Nishijima, M., Kobayashi, S., & Hanada, K. (2005). CERT Mediates Intermembrane Transfer of Various Molecular Species of Ceramides. *Journal of Biological Chemistry*, *280*(8), 6488–6495. https://doi.org/10.1074/JBC.M409290200

LaBauve, A. E., & Wargo, M. J. (2014). Detection of Host-Derived Sphingosine by Pseudomonas aeruginosa Is Important for Survival in the Murine Lung. *PLOS Pathogens*, *10*(1), e1003889. https://doi.org/10.1371/JOURNAL.PPAT.1003889

Lang, J., Bohn, P., Bhat, H., Jastrow, H., Walkenfort, B., Cansiz, F., Fink, J., Bauer, M., Olszewski, D., Ramos-Nascimento, A., Duhan, V., Friedrich, S. K., Becker, K. A., Krawczyk, A., Edwards, M. J., Burchert, A., Huber, M., Friebus-Kardash, J., Göthert, J. R., … Lang, K. S. (2020). Acid ceramidase of macrophages traps herpes simplex virus in multivesicular bodies and protects from severe disease. *Nature Communications 2020 11:1*, *11*(1), 1–15. https://doi.org/10.1038/s41467-020-15072-8

Lass-Flörl, C. (2009). The changing face of epidemiology of invasive fungal disease in Europe. *Mycoses*, *52*(3), 197–205. https://doi.org/10.1111/J.1439-0507.2009.01691.X

Latge, J. P., Kobayashi, H., Debeaupuis, J. P., Diaquin, M., Sarfati, J., Wieruszeski, J. M., Parra, E., Bouchara, J. P., & Fournet, B. (1994). Chemical and immunological characterization of the extracellular galactomannan of Aspergillus fumigatus. *Infection and Immunity*, *62*(12), 5424. https://doi.org/10.1128/IAI.62.12.5424-5433.1994

Leary, S. C., Hill, B. C., Lyons, C. N., Carlson, C. G., Michaud, D., Kraft, C. S., Ko, K., Moira Glerum, D., & Moyes, C. D. (2002). Chronic treatment with azide in situ leads to an irreversible loss of cytochrome c oxidase activity via holoenzyme dissociation.

The Journal of Biological Chemistry, *277*(13), 11321–11328. https://doi.org/10.1074/JBC.M112303200

Leber, R., Fuchsbichler, S., Klobučníková, V., Schweighofer, N., Pitters, E., Wohlfarter, K., Lederer, M., Landl, K., Ruckenstuhl, C., Hapala, I., & Turnowsky, F. (2003). Molecular Mechanism of Terbinafine Resistance in Saccharomyces cerevisiae. *Antimicrobial Agents and Chemotherapy*, *47*(12), 3890. https://doi.org/10.1128/AAC.47.12.3890-3900.2003

Lee, H. S., & Kim, Y. (2020). Aucklandia lappa Causes Cell Wall Damage in Candida albicans by Reducing Chitin and (1,3)-β-D-Glucan. *Journal of Microbiology and Biotechnology*, *30*(7), 967–973. https://doi.org/10.4014/JMB.2002.02025

Lee, W., Woo, E. R., & Lee, D. G. (2019). Effect of apigenin isolated from Aster yomena against Candida albicans: apigenin-triggered apoptotic pathway regulated by mitochondrial calcium signaling. *Journal of Ethnopharmacology*, *231*, 19–28. https://doi.org/10.1016/J.JEP.2018.11.005

Lehrer, R. I. (1970). Measurement of Candidacidal Activity of Specific Leukocyte Types in Mixed Cell Populations I. Normal, Myeloperoxidase-Deficient, and Chronic Granulomatous Disease Neutrophils. *Infection and Immunity*, *2*(1), 42–47. https://doi.org/10.1128/IAI.2.1.42-47.1970

LeibundGut-Landmann, S., Wüthrich, M., & Hohl, T. M. (2012). Immunity to fungi. *Current Opinion in Immunology*, *24*(4), 449–458. https://doi.org/10.1016/J.COI.2012.04.007

Levery, S. B., Momany, M., Lindsey, R., Toledo, M. S., Shayman, J. A., Fuller, M., Brooks, K., Doong, R. lou, Straus, A. H., & Takahashi, H. K. (2002). Disruption of the glucosylceramide biosynthetic pathway in Aspergillus nidulans and Aspergillus fumigatus by inhibitors of UDP-Glc:ceramide glucosyltransferase strongly affects spore germination, cell cycle, and hyphal growth. *FEBS Letters*, *525*(1–3), 59–64. https://doi.org/10.1016/S0014-5793(02)03067-3

Levitz, S. M., & Diamond, R. D. (1985). Mechanisms of Resistance of Aspergillus fumigatus Conidia to Killing by Neutrophils in Vitro. *The Journal of Infectious Diseases*, *152*(1), 33–42. https://doi.org/10.1093/INFDIS/152.1.33

Lewis, K. (2001). Riddle of biofilm resistance. *Antimicrobial Agents and Chemotherapy*, *45*(4), 999–1007. https://doi.org/10.1128/AAC.45.4.999-1007.2001/ASSET/99371851-3C0C-448B-8407-3C959FBF409F/ASSETS/GRAPHIC/AC0410819002.JPEG

Lignell, A., Johansson, A., Löwdin, E., Cars, O., & Sjölin, J. (2007). A new in-vitro kinetic model to study the pharmacodynamics of antifungal agents: inhibition of the fungicidal activity of amphotericin B against Candida albicans by voriconazole. *Clinical Microbiology and Infection: The Official Publication of the European Society of Clinical Microbiology and Infectious Diseases*, *13*(6), 613–619. https://doi.org/10.1111/J.1469-0691.2007.01710.X

Linden, M., & Brattsand, R. (1994). Effects of a corticosteroid, budesonide, on alveolar macrophage and blood monocyte secretion of cytokines: differential sensitivity of GM-CSF, IL-1 beta, and IL-6. *Pulmonary Pharmacology*, *7*(1), 43–47. https://doi.org/10.1006/PULP.1994.1004

Lionakis, M. S. (2014). New insights into innate immune control of systemic candidiasis. *Medical Mycology*, *52*(6), 555–564. https://doi.org/10.1093/MMY/MYU029

Lionakis, M. S., Lim, J. K., Lee, C. C. R., & Murphy, P. M. (2011). Organ-Specific Innate Immune Responses in a Mouse Model of Invasive Candidiasis. *Journal of Innate Immunity*, *3*(2), 180–199. https://doi.org/10.1159/000321157

Lionakis, M. S., & Netea, M. G. (2013). Candida and Host Determinants of Susceptibility to Invasive Candidiasis. *PLOS Pathogens*, *9*(1), e1003079. https://doi.org/10.1371/JOURNAL.PPAT.1003079

Lionakis, M. S., Swamydas, M., Fischer, B. G., Plantinga, T. S., Johnson, M. D., Jaeger, M., Green, N. M., Masedunskas, A., Weigert, R., Mikelis, C., Wan, W., Lee, C. C. R., Lim, J. K., Rivollier, A., Yang, J. C., Laird, G. M., Wheeler, R. T., Alexander, B. D., Perfect, J. R., … Murphy, P. M. (2013). CX3CR1-dependent renal macrophage survival promotes Candida control and host survival. *The Journal of Clinical Investigation*, *123*(12), 5035. https://doi.org/10.1172/JCI71307

Lopes Bezerra, L. M., & Filler, S. G. (2004). Interactions of Aspergillus fumigatus with endothelial cells: internalization, injury, and stimulation of tissue factor activity. *Blood*, *103*(6), 2143–2149. https://doi.org/10.1182/BLOOD-2003-06-2186

Løvås, K., & Husebye, E. (2003). Replacement therapy in Addison's disease. *Expert Opinion on Pharmacotherapy*, *4*(12), 2145–2149. https://doi.org/10.1517/14656566.4.12.2145

Ludovico, P., Rodrigues, F., Almeida, A., Silva, M. T., Barrientos, A., & Côrte-Real, M. (2002). Cytochrome c release and mitochondria involvement in programmed cell death induced by acetic acid in Saccharomyces cerevisiae. *Molecular Biology of the Cell*, *13*(8), 2598–2606. https://doi.org/10.1091/MBC.E01-12-0161

Ludovico, P., Sansonetty, F., & Côrte-Real, M. (2001). Assessment of mitochondrial membrane potential in yeast cell populations by flow cytometry. *Microbiology (Reading, England)*, *147*(Pt 12), 3335–3343. https://doi.org/10.1099/00221287-147-12-3335

Madan, T., Reid, K. B. M., Singh, M., Sarma, P. U., & Kishore, U. (2005). Susceptibility of Mice Genetically Deficient in the Surfactant Protein (SP)-A or SP-D Gene to Pulmonary Hypersensitivity Induced by Antigens and Allergens of Aspergillus fumigatus. *The Journal of Immunology*, *174*(11), 6943–6954. https://doi.org/10.4049/JIMMUNOL.174.11.6943

Madeo, F., Fröhlich, E., & Fröhlich, K. U. (1997). A Yeast Mutant Showing Diagnostic Markers of Early and Late Apoptosis. *The Journal of Cell Biology*, *139*(3), 729. https://doi.org/10.1083/JCB.139.3.729

Madeo, F., Herker, E., Maldener, C., Wissing, S., Lächelt, S., Herlan, M., Fehr, M., Lauber, K., Sigrist, S. J., Wesselborg, S., & Fröhlich, K. U. (2002). A caspase-related protease regulates apoptosis in yeast. *Molecular Cell*, *9*(4), 911–917. https://doi.org/10.1016/S1097-2765(02)00501-4

Madeo, F., Herker, E., Wissing, S., Jungwirth, H., Eisenberg, T., & Fröhlich, K. U. (2004). Apoptosis in yeast. *Current Opinion in Microbiology*, *7*(6), 655–660. https://doi.org/10.1016/J.MIB.2004.10.012

Mallela, S. K., Merscher, S., & Fornoni, A. (2022). Implications of Sphingolipid Metabolites in Kidney Diseases. *International Journal of Molecular Sciences 2022, Vol. 23, Page 4244*, *23*(8), 4244. https://doi.org/10.3390/IJMS23084244

Martin, G. E., Boudreau, R. M., Couch, C., Becker, K. A., Edwards, M. J., Caldwell, C. C., Gulbins, E., & Seitz, A. (2017). Sphingosine's role in epithelial host defense: A natural antimicrobial and novel therapeutic. *Biochimie*, *141*, 91–96. https://doi.org/10.1016/J.BIOCHI.2017.03.014

Martinvalet, D., Zhu, P., & Lieberman, J. (2005). Granzyme A Induces Caspase-Independent Mitochondrial Damage, a Required First Step for Apoptosis. *Immunity*, *22*(3), 355–370. https://doi.org/10.1016/J.IMMUNI.2005.02.004

Mathé, L., & van Dijck, P. (2013). Recent insights into Candida albicans biofilm resistance mechanisms. *Current Genetics*, *59*(4), 251–264. https://doi.org/10.1007/S00294-013-0400-3

McDonald, M. J., Rice, D. P., & Desai, M. M. (2016). Sex speeds adaptation by altering the dynamics of molecular evolution. *Nature 2016 531:7593*, *531*(7593), 233–236. https://doi.org/10.1038/nature17143

McEvoy, K., Normile, T. G., & del Poeta, M. (2020). Antifungal Drug Development: Targeting the Fungal Sphingolipid Pathway. *Journal of Fungi (Basel, Switzerland)*, *6*(3), 1–13. https://doi.org/10.3390/JOF6030142

Mehrad, B., Strieter, R. M., & Standiford, T. J. (1999). Role of TNF-α in Pulmonary Host Defense in Murine Invasive Aspergillosis. *The Journal of Immunology*, *162*(3), 1633–1640. https://doi.org/10.4049/JIMMUNOL.162.3.1633

Meletiadis, J., Meis, J. F. G. M., Mouton, J. W., & Verweij, P. E. (2001). Analysis of growth characteristics of filamentous fungi in different nutrient media. *Journal of Clinical Microbiology*, *39*(2), 478–484. https://doi.org/10.1128/JCM.39.2.478-484.2001/ASSET/FFD29659-95C7-464D-A935-217C784506BB/ASSETS/GRAPHIC/JM0211054003.JPEG

Mercier, T., Guldentops, E., Lagrou, K., & Maertens, J. (2018). Galactomannan, a surrogate marker for outcome in invasive aspergillosis: Finally coming of age. *Frontiers in Microbiology*, *9*(APR), 661. https://doi.org/10.3389/FMICB.2018.00661/BIBTEX

Mesa-Arango, A. C., Trevijano-Contador, N., Román, E., Sánchez-Fresneda, R., Casas, C., Herrero, E., Argüelles, J. C., Pla, J., Cuenca-Estrella, M., & Zaragoza, O. (2014). The production of reactive oxygen species is a universal action mechanism of amphotericin B against pathogenic yeasts and contributes to the fungicidal effect of this drug. *Antimicrobial Agents and Chemotherapy*, *58*(11), 6627–6638. https://doi.org/10.1128/AAC.03570-14/SUPPL_FILE/ZAC011143393SO1.PDF

Millsop, J. W., & Fazel, N. (2016). Oral candidiasis. *Clinics in Dermatology*, *34*(4), 487–494. https://doi.org/10.1016/J.CLINDERMATOL.2016.02.022

Mitchell, K. F., Zarnowski, R., & Andes, D. R. (2016). The extracellular matrix of fungal biofilms. *Advances in Experimental Medicine and Biology*, *931*, 21–35. https://doi.org/10.1007/5584_2016_6/TABLES/1

Mizushima, N., Levine, B., Cuervo, A. M., & Klionsky, D. J. (2008). Autophagy fights disease through cellular self-digestion. *Nature 2008 451:7182*, *451*(7182), 1069–1075. https://doi.org/10.1038/nature06639

Montefusco, D. J., Chen, L., Matmati, N., Lu, S., Newcomb, B., Cooper, G. F., Hannun, Y. A., & Lu, X. (2013). Distinct signaling roles of ceramide species in yeast revealed through systematic perturbation and systems biology analyses. *Science Signaling*, *6*(299). https://doi.org/10.1126/SCISIGNAL.2004515/SUPPL_FILE/6_RS14_TABLES_S1_S3_TO_S6.ZIP

Morris, G., Kokki, M. H., Anderson, K., & Richardson, M. D. (2000). Sampling of Aspergillus spores in air. *Journal of Hospital Infection*, *44*(2), 81–92. https://doi.org/10.1053/JHIN.1999.0688

Muraglia, K. A., Chorghade, R. S., Kim, B. R., Tang, X. X., Shah, V. S., Grillo, A. S., Daniels, P. N., Cioffi, A. G., Karp, P. H., Zhu, L., Welsh, M. J., & Burke, M. D. (2019). Small-molecule ion channels increase host defences in cystic fibrosis airway epithelia. *Nature 2019 567:7748*, *567*(7748), 405–408. https://doi.org/10.1038/s41586-019-1018-5

Nagiec, M. M., Nagiec, E. E., Baltisberger, J. A., Wells, G. B., Lester, R. L., & Dickson, R. C. (1997). Sphingolipid Synthesis as a Target for Antifungal Drugs: COMPLEMENTATION OF THE INOSITOL PHOSPHORYLCERAMIDE SYNTHASE DEFECT IN A MUTANT STRAIN OF SACCHAROMYCES

CEREVISIAE BY THE AUR1 GENE. *Journal of Biological Chemistry*, *272*(15), 9809–9817. https://doi.org/10.1074/JBC.272.15.9809

Netea, M. G., Gow, N. A. R., Munro, C. A., Bates, S., Collins, C., Ferwerda, G., Hobson, R. P., Bertram, G., Hughes, H. B., Jansen, T., Jacobs, L., Buurman, E. T., Gijzen, K., Williams, D. L., Torensma, R., McKinnon, A., MacCallum, D. M., Odds, F. C., van der Meer, J. W. M., … Kullberg, B. J. (2006). Immune sensing of Candida albicans requires cooperative recognition of mannans and glucans by lectin and Toll-like receptors. *The Journal of Clinical Investigation*, *116*(6), 1642–1650. https://doi.org/10.1172/JCI27114

Netea, M. G., Warris, A., van der Meer, J. W. M., Fenton, M. J., Verver-Janssen, T. J. G., Jacobs, L. E. H., Andresen, T., Verweij, P. E., & Kullberg, B. J. (2003). Aspergillus fumigatus Evades Immune Recognition during Germination through Loss of Toll-Like Receptor-4-Mediated Signal Transduction. *The Journal of Infectious Diseases*, *188*(2), 320–326. https://doi.org/10.1086/376456

Nett, J. E. (2016). The Host's Reply to Candida Biofilm. *Pathogens 2016, Vol. 5, Page 33*, *5*(1), 33. https://doi.org/10.3390/PATHOGENS5010033

Ng, C. G., & Griffin, D. E. (2006). Acid Sphingomyelinase Deficiency Increases Susceptibility to Fatal Alphavirus Encephalomyelitis. *Journal of Virology*, *80*(22), 10989–10999. https://doi.org/10.1128/JVI.01154-06/ASSET/80EF7862-BFBD-48F4-9E1A-064FCFC3368B/ASSETS/GRAPHIC/ZJV0220684040008.JPEG

Ngo, L. Y., Kasahara, S., Kumasaka, D. K., Knoblaugh, S. E., Jhingran, A., & Hohl, T. M. (2014). Inflammatory Monocytes Mediate Early and Organ-Specific Innate Defense During Systemic Candidiasis. *The Journal of Infectious Diseases*, *209*(1), 109–119. https://doi.org/10.1093/INFDIS/JIT413

Nixon, R. A., & Yang, D. S. (2011). Autophagy failure in Alzheimer's disease—locating the primary defect. *Neurobiology of Disease*, *43*(1), 38–45. https://doi.org/10.1016/J.NBD.2011.01.021

Nordin, M. A. F., Himratul-Aznita, W. H., & Abdul Razak, F. (2013). Antifungal susceptibility and growth inhibitory response of oral Candida species to Brucea javanica Linn. extract. *BMC Complementary and Alternative Medicine*, *13*. https://doi.org/10.1186/1472-6882-13-342

Obeid, L. M., Linardic, C. M., Karolak, L. A., & Hannun, Y. A. (1993). Programmed Cell Death Induced by Ceramide. *Science*, *259*(5102), 1769–1771. https://doi.org/10.1126/SCIENCE.8456305

Obeid, L. M., Okamoto, Y., & Mao, C. (2002). Yeast sphingolipids: metabolism and biology. *Biochimica et Biophysica Acta (BBA) - Molecular and Cell Biology of Lipids*, *1585*(2–3), 163–171. https://doi.org/10.1016/S1388-1981(02)00337-2

Odds, F. C., Brown, A. J. P., & Gow, N. A. R. (2003). Antifungal agents: mechanisms of action. *Trends in Microbiology*, *11*(6), 272–279. https://doi.org/10.1016/S0966-842X(03)00117-3

Olivera, A., Rosenthal, J., & Spiegel, S. (1996). Effect of Acidic Phospholipids on Sphingosine Kinase. *Journal of Cellular Biochemistry*, *60*(4), 529–537. https://doi.org/10.1002/(SICI)1097-4644(19960315)60:4

Oppenheim, R. W., Flavell, R. A., Vinsant, S., Prevette, D., Kuan, C. Y., & Rakic, P. (2001). Programmed Cell Death of Developing Mammalian Neurons after Genetic Deletion of Caspases. *The Journal of Neuroscience*, *21*(13), 4752. https://doi.org/10.1523/JNEUROSCI.21-13-04752.2001

Osiewacz, H. D., & Scheckhuber, C. Q. (2006). Impact of ROS on ageing of two fungal model systems: Saccharomyces cerevisiae and Podospora anserina. *Free Radical Research*, *40*(12), 1350–1358. https://doi.org/10.1080/10715760600921153

Ostrander, D. B., Sparagna, G. C., Amoscato, A. A., McMillin, J. B., & Dowhan, W. (2001). Decreased cardiolipin synthesis corresponds with cytochrome c release in palmitate-induced cardiomyocyte apoptosis. *The Journal of Biological Chemistry*, *276*(41), 38061–38067. https://doi.org/10.1074/JBC.M107067200

Ott, M., Robertson, J. D., Gogvadze, V., Zhivotovsky, B., & Orrenius, S. (2002). Cytochrome c release from mitochondria proceeds by a two-step process. *Proceedings of the National Academy of Sciences of the United States of America*, *99*(3), 1259–1263. https://doi.org/10.1073/PNAS.241655498

Öz, Y., Özdemir, H. G., Gökbolat, E., Kiraz, N., Ilkit, M., & Seyedmousavi, S. (2016). Time-Kill Kinetics and In Vitro Antifungal Susceptibility of Non-fumigatus Aspergillus Species Isolated from Patients with Ocular Mycoses. *Mycopathologia*, *181*(3–4), 225–233. https://doi.org/10.1007/S11046-015-9969-Z

Panda, D., Rathinasamy, K., Santra, M. K., & Wilson, L. (2005). Kinetic suppression of microtubule dynamic instability by griseofulvin: Implications for its possible use in the treatment of cancer. *Proceedings of the National Academy of Sciences of the United States of America*, *102*(28), 9878–9883. https://doi.org/10.1073/PNAS.0501821102/ASSET/B430E4F5-1507-4387-B1C8-AAAC8986288C/ASSETS/GRAPHIC/ZPQ0270587280005.JPEG

Pappas, P. G., Alexander, B. D., Andes, D. R., Hadley, S., Kauffman, C. A., Freifeld, A., Anaissie, E. J., Brumble, L. M., Herwaldt, L., Lto, J., Kontoyiannis, D. P., Marshall Lyon, G., Marr, K. A., Morrison, V. A., Park, B. J., Patterson, T. F., Perl, T. M., Oster, R. A., Schuster, M. G., … Chiller, T. M. (2010). Invasive fungal infections among organ transplant recipients: results of the Transplant-Associated Infection Surveillance Network (TRANSNET). *Clinical Infectious Diseases: An Official Publication of the Infectious Diseases Society of America*, *50*(8), 1101–1111. https://doi.org/10.1086/651262

Pappas, P. G., Lionakis, M. S., Arendrup, M. C., Ostrosky-Zeichner, L., & Kullberg, B. J. (2018). Invasive candidiasis. *Nature Reviews Disease Primers 2018 4:1*, *4*(1), 1–20. https://doi.org/10.1038/nrdp.2018.26

Paris, S., Boisvieux-Ulrich, E., Crestani, B., Houcine, O., Taramelli, D., Lombardi, L., & Latge, J. P. (1997). Internalization of Aspergillus fumigatus conidia by epithelial and endothelial cells. *Infection and Immunity*, *65*(4), 1510–1514. https://doi.org/10.1128/IAI.65.4.1510-1514.1997

Pasqualotto, A. C. (2009). Differences in pathogenicity and clinical syndromes due to Aspergillus fumigatus and Aspergillus flavus. *Medical Mycology*, *47*(SUPPL. 1), S261–S270. https://doi.org/10.1080/13693780802247702/2/13693780802247702F0002G.GIF

Patton, J. L., & Lester, R. L. (1991). The phosphoinositol sphingolipids of Saccharomyces cerevisiae are highly localized in the plasma membrane. *Journal of Bacteriology*, *173*(10), 3101. https://doi.org/10.1128/JB.173.10.3101-3108.1991

Pearson, R. D., Steigbigel, R. T., Davis, H. T., & Chapman, S. W. (1980). Method of reliable determination of minimal lethal antibiotic concentrations. *Antimicrobial Agents and Chemotherapy*, *18*(5), 699–708. https://doi.org/10.1128/AAC.18.5.699

Perfect, J. R., Ashley, E. D., & Drew, R. (2004). Design of aerosolized amphotericin b formulations for prophylaxis trials among lung transplant recipients. *Clinical Infectious Diseases: An Official Publication of the Infectious Diseases Society of America*, *39 Suppl 4*(SUPPL. 4). https://doi.org/10.1086/421958

Perkhofer, S., Kehrel, B. E., Dierich, M. P., Donnelly, J. P., Nussbaumer, W., Hofmann, J., von Eiff, C., & Lass-Flörl, C. (2008). Human Platelets Attenuate Aspergillus Species via Granule-Dependent Mechanisms. *The Journal of Infectious Diseases*, *198*(8), 1243. https://doi.org/10.1086/591458

Petrosillo, G., Ruggiero, F. M., Pistolese, M., & Paradies, G. (2001). Reactive oxygen species generated from the mitochondrial electron transport chain induce cytochrome c dissociation from beef-heart submitochondrial particles via cardiolipin peroxidation. Possible role in the apoptosis. *FEBS Letters*, *509*(3), 435–438. https://doi.org/10.1016/S0014-5793(01)03206-9

Pewzner-Jung, Y., Tabazavareh, S. T., Grassmé, H., Becker, K. A., Japtok, L., Steinmann, J., Joseph, T., Lang, S., Tuemmler, B., Schuchman, E. H., Lentsch, A. B., Kleuser, B., Edwards, M. J., Futerman, A. H., & Gulbins, E. (2014). Sphingoid long chain bases prevent lung infection by Pseudomonas aeruginosa. *EMBO Molecular Medicine*, *6*(9), 1205–1214. https://doi.org/10.15252/EMMM.201404075

Pfaller, M. A. (2012). Antifungal Drug Resistance: Mechanisms, Epidemiology, and Consequences for Treatment. *The American Journal of Medicine*, *125*(1), S3–S13. https://doi.org/10.1016/J.AMJMED.2011.11.001

Pfaller, M. A., Jones, R. N., Doern, G. v., Sader, H. S., Hollis, R. J., & Messer, S. A. (1998). International Surveillance of Bloodstream Infections Due to Candida Species: Frequency of Occurrence and Antifungal Susceptibilities of Isolates Collected in 1997 in the United States, Canada, and South America for the SENTRY Program. *Journal of Clinical Microbiology*, *36*(7), 1886. https://doi.org/10.1128/JCM.36.7.1886-1889.1998

Philippe, B., Ibrahim-Granet, O., Prévost, M. C., Gougerot-Pocidalo, M. A., Perez, M. S., van der Meeren, A., & Latgé, J. P. (2003). Killing of Aspergillus fumigatus by Alveolar Macrophages Is Mediated by Reactive Oxidant Intermediates. *Infection and Immunity*, *71*(6), 3034. https://doi.org/10.1128/IAI.71.6.3034-3042.2003

Pina-Vaz, C., Sansonetty, F., Rodrigues, A. G., Costa-Oliveira, S., Tavares, C., & Martinez-De-Oliveira, J. (2001). Cytometric approach for a rapid evaluation of susceptibility of Candida strains to antifungals. *Clinical Microbiology and Infection: The Official Publication of the European Society of Clinical Microbiology and Infectious Diseases*, *7*(11), 609–618. https://doi.org/10.1046/J.1198-743X.2001.00307.X

Polak, A., & Scholer, H. J. (1975). Mode of Action of 5-Fluorocytosine and Mechanisms of Resistance. *Chemotherapy*, *21*(3–4), 113–130. https://doi.org/10.1159/000221854

Potera, C. (1999). Forging a Link Between Biofilms and Disease. *Science*, *283*(5409), 1837–1839. https://doi.org/10.1126/SCIENCE.283.5409.1837

Pozniakovsky, A. I., Knorre, D. A., Markova, O. v., Hyman, A. A., Skulachev, V. P., & Severin, F. F. (2005). Role of mitochondria in the pheromone- and amiodarone-induced programmed death of yeast. *The Journal of Cell Biology*, *168*(2), 257. https://doi.org/10.1083/JCB.200408145

Quintin, J., Saeed, S., Martens, J. H. A., Giamarellos-Bourboulis, E. J., Ifrim, D. C., Logie, C., Jacobs, L., Jansen, T., Kullberg, B. J., Wijmenga, C., Joosten, L. A. B., Xavier, R. J., van der Meer, J. W. M., Stunnenberg, H. G., & Netea, M. G. (2012). Candida albicans Infection Affords Protection against Reinfection via Functional Reprogramming of Monocytes. *Cell Host & Microbe*, *12*(2), 223–232. https://doi.org/10.1016/J.CHOM.2012.06.006

Rafferty, P., Biggs, B. A., Crompton, G. K., & Grant, I. W. B. (1983). What happens to patients with pulmonary aspergilloma? Analysis of 23 cases. *Thorax*, *38*(8), 579–583. https://doi.org/10.1136/THX.38.8.579

Ramage, G., Wickes, B. L., & Lopez-Ribot, J. L. (2001). Biofilms of Candida albicans and their associated resistance to antifungal agents. *American Clinical Laboratory*, *20*(7), 42–44.

Ramírez-Labrada, A., Pesini, C., Santiago, L., Hidalgo, S., Calvo-Pérez, A., Oñate, C., Andrés-Tovar, A., Garzón-Tituaña, M., Uranga-Murillo, I., Arias, M. A., Galvez, E. M., & Pardo, J. (2022). All About (NK Cell-Mediated) Death in Two Acts and an Unexpected Encore: Initiation, Execution and Activation of Adaptive Immunity. *Frontiers in Immunology*, *13*, 2307. https://doi.org/10.3389/FIMMU.2022.896228/BIBTEX

Reeves, E. P., Lu, H., Jacobs, H. L., Messina, C. G. M., Bolsover, S., Gabellall, G., Potma, E. O., Warley, A., Roes, J., & Segal, A. W. (2002). Killing activity of neutrophils is mediated through activation of proteases by K+ flux. *Nature 2002 416:6878*, *416*(6878), 291–297. https://doi.org/10.1038/416291a

Ren, J., & Hannun, Y. A. (2016). Metabolism and Roles of Sphingolipids in Yeast Saccharomyces cerevisiae. *Biogenesis of Fatty Acids, Lipids and Membranes*, 1–21. https://doi.org/10.1007/978-3-319-43676-0_21-1

Ricci, J. E., Gottlieb, R. A., & Green, D. R. (2003). Caspase-mediated loss of mitochondrial function and generation of reactive oxygen species during apoptosis. *The Journal of Cell Biology*, *160*(1), 65–75. https://doi.org/10.1083/JCB.200208089

Rice, T. C., Pugh, A. M., Seitz, A. P., Gulbins, E., Nomellini, V., & Caldwell, C. C. (2017). Sphingosine rescues aged mice from pulmonary pseudomonas infection. *The Journal of Surgical Research*, *219*, 354–359. https://doi.org/10.1016/J.JSS.2017.06.042

Rødland, E. K., Ueland, T., Pedersen, T. M., Halvorsen, B., Muller, F., Aukrust, P., & Frøland, S. S. (2010). Activation of platelets by Aspergillus fumigatus and potential role of platelets in the immunopathogenesis of Aspergillosis. *Infection and Immunity*, *78*(3), 1269–1275. https://doi.org/10.1128/IAI.01091-09

Rodriquez-Tudela, J. L., Donnelly, J. P., Arendrup, M. C., Arikan, S., Barchiesi, F., Bille, J., Chryssanthou, E., Cuenca-Estrella, M., Dannaoui, E., Denning, D., Fegeler, W., Gaustad, P., Lass-Flörl, C., Moore, C., Richardson, M., Schmalreck, A., Velegraki, J. A., & Verweij, P. (2008). EUCAST Technical Note on the method for the determination of broth dilution minimum inhibitory concentrations of antifungal agents for conidia-forming moulds. *Clinical Microbiology and Infection: The Official Publication of the European Society of Clinical Microbiology and Infectious Diseases*, *14*(10), 982–984. https://doi.org/10.1111/J.1469-0691.2008.02086.X

Rogers, T. R. (1995). Rogers, T. R. Epidemiology and control of nosocomial fungal infections. *Current Opinion in Infectious Diseases, 8*(4), 287–290.

Roilides, E., Uhlig, K., Venzon, D., Pizzo, P. A., & Walsh, T. J. (1993a). Enhancement of oxidative response and damage caused by human neutrophils to Aspergillus fumigatus hyphae by granulocyte colony-stimulating factor and gamma interferon. *Infection and Immunity*, *61*(4), 1185. https://doi.org/10.1128/IAI.61.4.1185-1193.1993

Roilides, E., Uhlig, K., Venzon, D., Pizzo, P. A., & Walsh, T. J. (1993b). Prevention of corticosteroid-induced suppression of human polymorphonuclear leukocyte-induced damage of Aspergillus fumigatus hyphae by granulocyte colony-stimulating factor and gamma interferon. *Infection and Immunity*, *61*(11), 4870. https://doi.org/10.1128/IAI.61.11.4870-4877.1993

Rollin-Pinheiro, R., Singh, A., Barreto-Bergter, E., & del Poeta, M. (2016). Sphingolipids as targets for treatment of fungal infections. *Future Medicinal Chemistry*, *8*(12), 1469. https://doi.org/10.4155/FMC-2016-0053

Romani, L., Mencacci, A., Cenci, E., del Sero, G., Bistoni, F., & Puccetti, P. (1997). An immunoregulatory role for neutrophils in CD4+ T helper subset selection in mice with candidiasis. *The Journal of Immunology*, *158*(5), 2356–2362. https://doi.org/10.4049/JIMMUNOL.158.5.2356

Roos, D., van Bruggen, R., & Meischl, C. (2003). Oxidative killing of microbes by neutrophils. *Microbes and Infection*, *5*(14), 1307–1315. https://doi.org/10.1016/J.MICINF.2003.09.009

Roscetto, E., Contursi, P., Vollaro, A., Fusco, S., Notomista, E., & Catania, M. R. (2018). Antifungal and anti-biofilm activity of the first cryptic antimicrobial peptide from an archaeal protein against Candida spp. clinical isolates. *Scientific Reports 2018 8:1*, *8*(1), 1–11. https://doi.org/10.1038/s41598-018-35530-0

Sakamoto, H., Okamoto, K., Aoki, M., Kato, H., Katsume, A., Ohta, A., Tsukuda, T., Shimma, N., Aoki, Y., Arisawa, M., Kohara, M., & Sudoh, M. (2005). Host sphingolipid biosynthesis as a target for hepatitis C virus therapy. *Nature Chemical Biology 2005 1:6*, *1*(6), 333–337. https://doi.org/10.1038/nchembio742

Sangalli-Leite, F., Scorzoni, L., Mesa-Arango, A. C., Casas, C., Herrero, E., Soares Mendes Gianinni, M. J., Rodríguez-Tudela, J. L., Cuenca-Estrella, M., & Zaragoza, O. (2011). Amphotericin B mediates killing in Cryptococcus neoformans through the induction of a strong oxidative burst. *Microbes and Infection*, *13*(5), 457–467. https://doi.org/10.1016/J.MICINF.2011.01.015

Sanglard, D., Coste, A., & Ferrari, S. (2009). Antifungal drug resistance mechanisms in fungal pathogens from the perspective of transcriptional gene regulation. *FEMS Yeast Research*, *9*(7), 1029–1050. https://doi.org/10.1111/J.1567-1364.2009.00578.X

Schaffner, A., Douglas, H., & Braude, A. (1982). Selective Protection against Conidia by Mononuclear and against Mycelia by Polymorphonuclear Phagocytes in Resistance to Aspergillus: OBSERVATIONS ON THESE TWO LINES OF DEFENSE IN VIVO AND IN VITRO WITH HUMAN AND MOUSE PHAGOCYTES. *The Journal of Clinical Investigation*, *69*(3), 617–631. https://doi.org/10.1172/JCI110489

Schmidt, S., Tramsen, L., Hanisch, M., Latgé, J. P., Huenecke, S., Koehl, U., & Lehrnbecher, T. (2011). Human natural killer cells exhibit direct activity against Aspergillus fumigatus hyphae, but not against resting conidia. *The Journal of Infectious Diseases*, *203*(3), 430–435. https://doi.org/10.1093/INFDIS/JIQ062

Schorling, S., Vallée, B., Barz, W. P., Riezman, H., & Oesterhelt, D. (2001). Lag1p and Lac1p are essential for the Acyl-CoA-dependent ceramide synthase reaction in Saccharomyces cerevisae. *Molecular Biology of the Cell*, *12*(11), 3417–3427. https://doi.org/10.1091/MBC.12.11.3417/ASSET/IMAGES/LARGE/MK1111657009.JPEG

Scorzoni, L., de Paula e Silva, A. C. A., Marcos, C. M., Assato, P. A., de Melo, W. C. M. A., de Oliveira, H. C., Costa-Orlandi, C. B., Mendes-Giannini, M. J. S., & Fusco-Almeida, A. M. (2017). Antifungal Therapy: New Advances in the Understanding and Treatment of Mycosis. *Frontiers in Microbiology*, *8*(JAN). https://doi.org/10.3389/FMICB.2017.00036

Segal, B. H., Leto, T. L., Gallin, J. I., Malech, H. L., & Holland, S. M. (2000). Genetic, biochemical, and clinical features of chronic granulomatous disease. *Medicine*, *79*(3), 170–200. https://doi.org/10.1097/00005792-200005000-00004

Seitz, A. P., Schumacher, F., Baker, J., Soddemann, M., Wilker, B., Caldwell, C. C., Gobble, R. M., Kamler, M., Becker, K. A., Beck, S., Kleuser, B., Edwards, M. J., & Gulbins, E. (2019). Sphingosine-coating of plastic surfaces prevents ventilator-associated pneumonia. *Journal of Molecular Medicine (Berlin, Germany)*, *97*(8), 1195–1211. https://doi.org/10.1007/S00109-019-01800-1

Serbina, N. v., Cherny, M., Shi, C., Bleau, S. A., Collins, N. H., Young, J. W., & Pamer, E. G. (2009). Distinct Responses of Human Monocyte Subsets to Aspergillus fumigatus Conidia. *Journal of Immunology (Baltimore, Md.: 1950)*, *183*(4), 2678. https://doi.org/10.4049/JIMMUNOL.0803398

Severin, F. F., & Hyman, A. A. (2002). Pheromone induces programmed cell death in S. cerevisiae. *Current Biology: CB*, *12*(7). https://doi.org/10.1016/S0960-9822(02)00776-5

Sheppard, D. C., Marr, K. A., Fredricks, D. N., Chiang, L. Y., Doedt, T., & Filler, S. G. (2006). Comparison of three methodologies for the determination of pulmonary fungal burden in experimental murine aspergillosis. *Clinical Microbiology and Infection: The Official Publication of the European Society of Clinical Microbiology and Infectious Diseases*, *12*(4), 376–380. https://doi.org/10.1111/J.1469-0691.2005.01349.X

Sheppard, D. C., Rieg, G., Chiang, L. Y., Filler, S. G., Edwards, J. E., & Ibrahim, A. S. (2004). Novel inhalational murine model of invasive pulmonary aspergillosis. *Antimicrobial Agents and Chemotherapy*, *48*(5), 1908–1911. https://doi.org/10.1128/AAC.48.5.1908-1911.2004

Shidoji, Y., Hayashi, K., Komura, S., Ohishi, N., & Yagi, K. (1999). Loss of molecular interaction between cytochrome c and cardiolipin due to lipid peroxidation. *Biochemical and Biophysical Research Communications*, *264*(2), 343–347. https://doi.org/10.1006/BBRC.1999.1410

Shintani, T., & Klionsky, D. J. (2004). Autophagy in health and disease: A double-edged sword. *Science*, *306*(5698), 990–995. https://doi.org/10.1126/SCIENCE.1099993/ASSET/53DD8B66-1047-4150-95D3-F30F000975BE/ASSETS/GRAPHIC/306_990_F3.JPEG

Shirazi, F., & Kontoyiannis, D. P. (2015). Micafungin triggers caspase-dependent apoptosis in Candida albicans and Candida parapsilosis biofilms, including caspofungin non-susceptible isolates. *Virulence*, *6*(4), 385–394. https://doi.org/10.1080/21505594.2015.1027479

Shirkhani, K., Teo, I., Armstrong-James, D., & Shaunak, S. (2015). Nebulised amphotericin B-polymethacrylic acid nanoparticle prophylaxis prevents invasive aspergillosis. *Nanomedicine: Nanotechnology, Biology, and Medicine*, *11*(5), 1217–1226. https://doi.org/10.1016/J.NANO.2015.02.012

Shishodia, S. K., Tiwari, S., & Shankar, J. (2019). Resistance mechanism and proteins in Aspergillus species against antifungal agents. *Mycology*, *10*(3), 151. https://doi.org/10.1080/21501203.2019.1574927

Sica, A., Ming Wang, J. I., Colotta, F., Dejana, E., O S T J Oppenheim, J. O., Larsen, C. G., Zachariae, C., & Matsushima, K. (1990). Monocyte chemotactic and activating factor gene expression induced in endothelial cells by IL-1 and tumor necrosis factor. *The Journal of Immunology*, *144*(8), 3034–3038. https://doi.org/10.4049/JIMMUNOL.144.8.3034

Silva, R. D., Sotoca, R., Johansson, B., Ludovico, P., Sansonetty, F., Silva, M. T., Peinado, J. M., & Côrte-Real, M. (2005). Hyperosmotic stress induces metacaspase- and mitochondria-dependent apoptosis in Saccharomyces cerevisiae. *Molecular Microbiology*, *58*(3), 824–834. https://doi.org/10.1111/J.1365-2958.2005.04868.X

Silva, S., Henriques, M., Martins, A., Oliveira, R., Williams, D., & Azeredo, J. (2009). Biofilms of non-Candida albicans Candida species: quantification, structure and matrix composition. *Medical Mycology*, *47*(7), 681–689. https://doi.org/10.3109/13693780802549594

Smith, E. R., Merrill, J., Obeid, L. M., & Hannun, Y. A. (2000). Effects of Sphingosine and Other Sphingolipids on Protein Kinase C. *Methods in Enzymology*, *312*, 361–373. https://doi.org/10.1016/S0076-6879(00)12921-0

Song, J. C., & Stevens, D. A. (2015). Caspofungin: Pharmacodynamics, pharmacokinetics, clinical uses and treatment outcomes.

Http://Dx.Doi.Org.Ejp.Mpip-Mainz.Mpg.de/10.3109/1040841X.2015.1068271, *42*(5), 813–846. https://doi.org/10.3109/1040841X.2015.1068271

Song, J., Zhai, P., Zhang, Y., Zhang, C., Sang, H., Han, G., Keller, N. P., & Lu, L. (2016). The Aspergillus fumigatus Damage Resistance Protein Family Coordinately Regulates Ergosterol Biosynthesis and Azole Susceptibility. *MBio*, *7*(1). https://doi.org/10.1128/MBIO.01919-15

Sorice, M., Misasi, R., Riitano, G., Manganelli, V., Martellucci, S., Longo, A., Garofalo, T., & Mattei, V. (2021). Targeting Lipid Rafts as a Strategy Against Coronavirus. *Frontiers in Cell and Developmental Biology*, *8*, 1848. https://doi.org/10.3389/FCELL.2020.618296/BIBTEX

Soubani, A. O., & Chandrasekar, P. H. (2002). The Clinical Spectrum of Pulmonary Aspergillosis. *Chest*, *121*(6), 1988–1999. https://doi.org/10.1378/CHEST.121.6.1988

Steer, J. H., Vuong, Q., & Joyce, D. A. (1997). Suppression of human monocyte tumour necrosis factor-alpha release by glucocorticoid therapy: relationship to systemic monocytopaenia and cortisol suppression. *British Journal of Clinical Pharmacology*, *43*(4), 383–389. https://doi.org/10.1046/J.1365-2125.1997.00586.X

Stepanović, S., Vuković, D., Hola, V., di Bonaventura, G., Djukić, S., Ćirković, I., & Ruzicka, F. (2007). Quantification of biofilm in microtiter plates: overview of testing conditions and practical recommendations for assessment of biofilm production by staphylococci. *APMIS*, *115*(8), 891–899. https://doi.org/10.1111/J.1600-0463.2007.APM_630.X

Sun, L., Liao, K., Hang, C., & Wang, D. (2017). Honokiol induces reactive oxygen species-mediated apoptosis in Candida albicans through mitochondrial dysfunction. *PloS One*, *12*(2). https://doi.org/10.1371/JOURNAL.PONE.0172228

Tang, Y. Q., Yeaman, M. R., & Selsted, M. E. (2002). Antimicrobial peptides from human platelets. *Infection and Immunity*, *70*(12), 6524–6533. https://doi.org/10.1128/IAI.70.12.6524-6533.2002/ASSET/2748BECF-D2B8-41D3-B733-DF5111AC2350/ASSETS/GRAPHIC/II1220444006.JPEG

Tatsumi, Y., Nagashima, M., Shibanushi, T., Iwata, A., Kangawa, Y., Inui, F., Jo Siu, W. J., Pillai, R., & Nishiyama, Y. (2013). Mechanism of action of efinaconazole, a novel triazole antifungal agent. *Antimicrobial Agents and Chemotherapy*, *57*(5), 2405–2409. https://doi.org/10.1128/AAC.02063-12/ASSET/9D5E99A5-55C4-4998-B7A3-30007DFBD1CA/ASSETS/GRAPHIC/ZAC9991017980003.JPEG

Tavakoli Tabazavareh, S., Seitz, A., Jernigan, P., Sehl, C., Keitsch, S., Lang, S., Kahl, B. C., Edwards, M., Grassmé, H., Gulbins, E., & Becker, K. A. (2016). Lack of Sphingosine Causes Susceptibility to Pulmonary Staphylococcus Aureus Infections in Cystic Fibrosis. *Cellular Physiology and Biochemistry*, *38*(6), 2094–2102. https://doi.org/10.1159/000445567

Teixeira, V., Medeiros, T. C., Vilaça, R., Pereira, A. T., Chaves, S. R., Côrte-Real, M., Moradas-Ferreira, P., & Costa, V. (2015). Ceramide signalling impinges on Sit4p and Hog1p to promote mitochondrial fission and mitophagy in Isc1p-deficient cells. *Cellular Signalling*, *27*(9), 1840–1849. https://doi.org/10.1016/J.CELLSIG.2015.06.001

Tomee, J. F. C., van der Werf, T. S., Latge, J. P., Koeter, G. H., Dubois, A. E. J., & Kauffman, H. F. (2012). Serologic monitoring of disease and treatment in a patient with pulmonary aspergilloma. *Https://Doi.Org/10.1164/Ajrccm.151.1.7812553*, *151*(1), 199–204. https://doi.org/10.1164/AJRCCM.151.1.7812553

Tommasino, C., Marconi, M., Ciarlo, L., Matarrese, P., & Malorni, W. (2015). Autophagic flux and autophagosome morphogenesis require the participation of sphingolipids. *Apoptosis*, *20*(5), 645–657. https://doi.org/10.1007/S10495-015-1102-8/TABLES/1

Uzun, O., Ascioglu, S., Anaissie, E. J., & Rex, J. H. (2001). Risk factors and predictors of outcome in patients with cancer and breakthrough candidemia. *Clinical Infectious Diseases*, *32*(12), 1713–1717. https://doi.org/10.1086/320757/2/32-12-1713-TBL003.GIF

van Hoecke, L., Job, E. R., Saelens, X., & Roose, K. (2017). Bronchoalveolar Lavage of Murine Lungs to Analyze Inflammatory Cell Infiltration. *Journal of Visualized Experiments: JoVE*, *2017*(123). https://doi.org/10.3791/55398

van Laar, V. S., Roy, N., Liu, A., Rajprohat, S., Arnold, B., Dukes, A. A., Holbein, C. D., & Berman, S. B. (2015). Glutamate excitotoxicity in neurons triggers mitochondrial and endoplasmic reticulum accumulation of Parkin, and, in the presence of N-acetyl cysteine, mitophagy. *Neurobiology of Disease*, *74*, 180–193. https://doi.org/10.1016/J.NBD.2014.11.015

Vazquez, J. A., Dembry, L. M., Sanchez, V., Vazquez, M. A., Sobel, J. D., Dmuchowski, C., & Zervos, M. J. (1998). Nosocomial Candida glabrata Colonization: An Epidemiologic Study. *Journal of Clinical Microbiology*, *36*(2), 421. https://doi.org/10.1128/JCM.36.2.421-426.1998

Verhaegh, R., Becker, K. A., Edwards, M. J., & Gulbins, E. (2020). Sphingosine kills bacteria by binding to cardiolipin. *Journal of Biological Chemistry*, *295*(22), 7686–7696. https://doi.org/10.1074/JBC.RA119.012325

Verstrepen, K. J., & Klis, F. M. (2006). Flocculation, adhesion and biofilm formation in yeasts. *Molecular Microbiology*, *60*(1), 5–15. https://doi.org/10.1111/J.1365-2958.2006.05072.X

Verweij, P. E., Zhang, J., Debets, A. J. M., Meis, J. F., van de Veerdonk, F. L., Schoustra, S. E., Zwaan, B. J., & Melchers, W. J. G. (2016). In-host adaptation and acquired triazole resistance in Aspergillus fumigatus: a dilemma for clinical management. *The Lancet Infectious Diseases*, *16*(11), e251–e260. https://doi.org/10.1016/S1473-3099(16)30138-4

Vincent, J. L., Rello, J., Marshall, J., Silva, E., Anzueto, A., Martin, C. D., Moreno, R., Lipman, J., Gomersall, C., Sakr, Y., & Reinhart, K. (2009). International Study of the Prevalence and Outcomes of Infection in Intensive Care Units. *JAMA*, *302*(21), 2323–2329. https://doi.org/10.1001/JAMA.2009.1754

Virgin, H. W. (2014). The Virome in Mammalian Physiology and Disease. *Cell*, *157*(1), 142–150. https://doi.org/10.1016/J.CELL.2014.02.032

Walsh, T. J., Anaissie, E. J., Denning, D. W., Herbrecht, R., Kontoyiannis, D. P., Marr, K. A., Morrison, V. A., Segal, B. H., Steinbach, W. J., Stevens, D. A., van Burik, J. A., Wingard, J. R., & Patterson, T. F. (2008). Treatment of Aspergillosis: Clinical Practice Guidelines of the Infectious Diseases Society of America. *Clinical Infectious Diseases*, *46*(3), 327–360. https://doi.org/10.1086/525258

Walter, D., Wissing, S., Madeo, F., & Fahrenkrog, B. (2006). The inhibitor-of-apoptosis protein Bir1p protects against apoptosis in S. cerevisiae and is a substrate for the yeast homologue of Omi/HtrA2. *Journal of Cell Science*, *119*(Pt 9), 1843–1851. https://doi.org/10.1242/JCS.02902

Wang, Q., Zhang, Y., Wu, L., Niu, S., Song, C., Zhang, Z., Lu, G., Qiao, C., Hu, Y., Yuen, K. Y., Wang, Q., Zhou, H., Yan, J., & Qi, J. (2020). Structural and Functional Basis of SARS-CoV-2 Entry by Using Human ACE2. *Cell*, *181*(4), 894-904.e9. https://doi.org/10.1016/J.CELL.2020.03.045

Washburn, R. G., Hammer, C. H., & Bennett, J. E. (1986). Inhibition of Complement by Culture Supernatants of Aspergillus fumigatus. *The Journal of Infectious Diseases*, *154*(6), 944–951. https://doi.org/10.1093/INFDIS/154.6.944

Wasylnka, J. A., & Moore, M. M. (2003). Aspergillus fumigatus conidia survive and germinate in acidic organelles of A549 epithelial cells. *Journal of Cell Science*, *116*(8), 1579–1587. https://doi.org/10.1242/JCS.00329

Wasylnka, J. A., Simmer, M. I., & Moore, M. M. (2001). Differences in sialic acid density in pathogenic and non-pathogenic Aspergillus species. *Microbiology*, *147*(4), 869–877. https://doi.org/10.1099/00221287-147-4-869/CITE/REFWORKS

Watanabe, R., Funato, K., Venkataraman, K., Futerman, A. H., & Riezman, H. (2002). Sphingolipids Are Required for the Stable Membrane Association of Glycosylphosphatidylinositol-anchored Proteins in Yeast. *Journal of Biological Chemistry*, *277*(51), 49538–49544. https://doi.org/10.1074/JBC.M206209200

Wenisch, C., Linnau, K. F., Parschalk, B., Zedtwitz-Liebenstein, K., & Georgopoulos, A. (1997). Rapid susceptibility testing of fungi by flow cytometry using vital staining. *Journal of Clinical Microbiology*, *35*(1), 5–10. https://doi.org/10.1128/JCM.35.1.5-10.1997

Wilckens, T., & de Rijk, R. (1997). Glucocorticoids and immune function: unknown dimensions and new frontiers. *Immunology Today*, *18*(9), 418–424. https://doi.org/10.1016/S0167-5699(97)01111-0

Wissing, S., Ludovico, P., Herker, E., Büttner, S., Engelhardt, S. M., Decker, T., Link, A., Proksch, A., Rodrigues, F., Corte-Real, M., Fröhlich, K. U., Manns, J., Candé, C., Sigrist, S. J., Kroemer, G., & Madeo, F. (2004). An AIF orthologue regulates apoptosis in yeast. *The Journal of Cell Biology*, *166*(7), 969. https://doi.org/10.1083/JCB.200404138

Wu, X. Z., Chang, W. Q., Cheng, A. X., Sun, L. M., & Lou, H. X. (2010). Plagiochin E, an antifungal active macrocyclic bis(bibenzyl), induced apoptosis in Candida albicans through a metacaspase-dependent apoptotic pathway. *Biochimica et Biophysica Acta*, *1800*(4), 439–447. https://doi.org/10.1016/J.BBAGEN.2010.01.001

Wunder, D., Dong, J., Baev, D., & Edgerton, M. (2004). Human salivary histatin 5 fungicidal action does not induce programmed cell death pathways in Candida albicans. *Antimicrobial Agents and Chemotherapy*, *48*(1), 110–115. https://doi.org/10.1128/AAC.48.1.110-115.2004

Yamauchi, Y., & Greber, U. F. (2016). Principles of Virus Uncoating: Cues and the Snooker Ball. *Traffic*, *17*(6), 569–592. https://doi.org/10.1111/TRA.12387

Zanolari, B., Friant, S., Funato, K., Sütterlin, C., Stevenson, B. J., & Riezman, H. (2000). Sphingoid base synthesis requirement for endocytosis in Saccharomyces cerevisiae. *The EMBO Journal*, *19*(12), 2824–2833. https://doi.org/10.1093/EMBOJ/19.12.2824

Zepelin, M. B. von, Kunz, L., Rüchel, R., Reichard, U., Weig, M., & Groß, U. (2007). Epidemiology and antifungal susceptibilities of Candida spp. to six antifungal agents: results from a surveillance study on fungaemia in Germany from July 2004 to August 2005. *Journal of Antimicrobial Chemotherapy*, *60*(2), 424–428. https://doi.org/10.1093/JAC/DKM145

Zhang, J., Snelders, E., Zwaan, B. J., Schoustra, S. E., Meis, J. F., van Dijk, K., Hagen, F., van der Beek, M. T., Kampinga, G. A., Zoll, J., Melchers, W. J. G., Verweij, P. E., & Debets, A. J. M. (2017). A novel environmental azole resistance mutation in Aspergillus fumigatus and a possible role of sexual reproduction in its emergence. *MBio*, *8*(3). https://doi.org/10.1128/MBIO.00791-17/ASSET/B99EC558-A0EC-4F21-AA6E-61F91A780653/ASSETS/GRAPHIC/MBO0031733610006.JPEG

Zhang, J., van den Heuvel, J., Debets, A. J. M., Verweij, P. E., Melchers, W. J. G., Zwaan, B. J., & Schoustra, S. E. (2017). Evolution of cross-resistance to medical triazoles in Aspergillus fumigatus through selection pressure of environmental

fungicides. *Proceedings. Biological Sciences*, *284*(1863). https://doi.org/10.1098/RSPB.2017.0635

Zhong, W., Jeffries, M. W., & Georgopapadakou, N. H. (2000). Inhibition of Inositol Phosphorylceramide Synthase by Aureobasidin A in Candida and Aspergillus Species. *Antimicrobial Agents and Chemotherapy*, *44*(3), 651. https://doi.org/10.1128/AAC.44.3.651-653.2000

Zhou, P., Yang, X. lou, Wang, X. G., Hu, B., Zhang, L., Zhang, W., Si, H. R., Zhu, Y., Li, B., Huang, C. L., Chen, H. D., Chen, J., Luo, Y., Guo, H., Jiang, R. di, Liu, M. Q., Chen, Y., Shen, X. R., Wang, X., … Shi, Z. L. (2020). A pneumonia outbreak associated with a new coronavirus of probable bat origin. *Nature 2020 579:7798*, *579*(7798), 270–273. https://doi.org/10.1038/s41586-020-2012-7

Ziegler-Heitbrock, L., Ancuta, P., Crowe, S., Dalod, M., Grau, V., Hart, D. N., Leenen, P. J. M., Liu, Y. J., MacPherson, G., Randolph, G. J., Scherberich, J., Schmitz, J., Shortman, K., Sozzani, S., Strobl, H., Zembala, M., Austyn, J. M., & Lutz, M. B. (2010). Nomenclature of monocytes and dendritic cells in blood. *Blood*, *116*(16), e74–e80. https://doi.org/10.1182/BLOOD-2010-02-258558

Appendix

Publication

Hashemi Arani, F.; Kadow, S.; Kramer, M.; Keitsch, S.; Kirchhoff, L.; Schumacher, F.; Kleuser, B.; Rath, P.-M.; Gulbins, E.; Carpinteiro, A. Sphingosine as a New Antifungal Agent against *Candida* and *Aspergillus* spp. *Int. J. Mol. Sci.* 2022, *23*, 15510. https://doi.org/10.3390/ ijms232415510

Acknowledgments

First of all, I would like to thank Priv. Doz. Dr. med. Alexander Carpinteiro and Prof. Dr. Erich Gulbins for giving me the opportunity to work on the lab, studying the projects and most importantly, supporting me with their excellent scientific guidance.

I am very grateful for the academic support from Priv. Doz. Dr. med. Alexander Carpinteiro and Dr. Stephanie Kadow throughout my Ph.D. time. Alex, you have been an amazing mentor and a great supporter through challenges during these years. Your kindness, humility and great leadership skills have taught me a lot. Delicious Korean charismas dinners with your lovely family will never be forgotten. Stephie, I would like to thank you for your support during my study and improving my academic and laboratory skills.

I would like to express my gratitude to Prof. Dr. Peter-Micheal Rath and Prof. Dr. Burkhard Kleuser for their kind help and support.

I would also like to thank my collaboration partners, Dr. Lisa Kirchhoff and Dr. Fabian Schumacher for their technical support, advice and discussions.

I would like to extend my sincere thanks to the graduate school GRK 2098 for the arrangement of the Ph.D. program and meeting so many experienced scientists to enthusiast my study.

I would also like to thank the members of the thesis committee for taking the time to evaluate my Ph.D. thesis.

A huge thank you is to my colleagues at the Department of Molecular Biology, for helping me and creating a kind work environment: Dr. Katrin Becker- Flegler, Dr. Heike Grassmé, Dr. Eyad Naser, Dr. Yuqing Wu, Dr. Rabea Verhaegh, Hannelore Disselhoff, Gabriele Hessler, Claudine Kühn, Carolin Sehl and Andrea Riehle. In particular, I would like to thank Simone Keitsch, Melanie Kramer, Bärbel Pollmeier and Barbara Wilker for supporting me in the lab. Bettina Peter and Kristin Schimank thank you very much for the great support in pharmacy orderings, invoice reimbursements, GRK meeting arrangements and Visa applications. Matthias Soddemann, thank you very much for teaching me to use the Micro- and Cryotome and helping me to cut tissues.

Especially, I would like to say a big thank you to Dr. Peyman Rostami for his endless amount of love, support and encouragement. Thank you Peyman for bringing calmness and harmony back into my life.

Last but not least, I would like to express my heartfelt gratitude to my family, particularly my parents and my sisters. Thank you for your unconditional love and belief in me. Arvin and Aylin, I am so proud to be your auntie. I love you.

Curriculum Vitae

The CV is not included in this online version for reasons of data protection.

Erklärung:

Hiermit erkläre ich, gem. § 6 Abs. (2) g) der Promotionsordnung der Fakultät für Biologie zur Erlangung der Dr. rer. nat., dass ich das Arbeitsgebiet, dem das Thema ***„Rolle von Sphingosin in Pilzinfektion“*** zuzuordnen ist, in Forschung und Lehre vertrete und den Antrag von ***Fahimeh Hashemi Arani*** befürworte und die Betreuung auch im Falle eines Weggangs, wenn nicht wichtige Gründe dem entgegenstehen, weiterführen werde.

PD. Dr. Alexander Carpinteiro

Essen, den _____ _____

Unterschrift des Betreuers (Prof. oder PD) an der Universität Duisburg-Essen

Erklärung:

Hiermit erkläre ich, gem. § 7 Abs. (2) d) + f) der Promotionsordnung der Fakultät für Biologie zur Erlangung des Dr. rer. nat., dass ich die vorliegende Dissertation selbständig verfasst und mich keiner anderen als der angegebenen Hilfsmittel bedient, bei der Abfassung der Dissertation nur die angegeben Hilfsmittel benutzt und alle wörtlich oder inhaltlich übernommenen Stellen als solche gekennzeichnet habe.

Fahimeh Hashemi Arani

Essen, den _____ _____

Unterschrift des/r Doktoranden/in

Erklärung:

Hiermit erkläre ich, gem. § 7 Abs. (2) e) + g) der Promotionsordnung der Fakultät für Biologie zur Erlangung des Dr. rer. nat., dass ich keine anderen Promotionen bzw. Promotionsversuche in der Vergangenheit durchgeführt habe und dass diese Arbeit von keiner anderen Fakultät/Fachbereich abgelehnt worden ist.

Fahimeh Hashemi Arani

Essen, den _____ _____

Unterschrift des/r Doktoranden/in